UNIVERSITY OF
LEADING
THE WAY
WESTMINSTER

WestminsterResearch
http://www.westminster.ac.uk/research/westminsterresearch

Biosynthesis of polyhydroxyalkanoates, their novel blends and composites for biomedical applications

Pooja Basnett

Faculty of Science and Technology

This is an electronic version of a PhD thesis awarded by the University of Westminster. © The Author, 2014.

This is an exact reproduction of the paper copy held by the University of Westminster library.

The WestminsterResearch online digital archive at the University of Westminster aims to make the research output of the University available to a wider audience. Copyright and Moral Rights remain with the authors and/or copyright owners.
Users are permitted to download and/or print one copy for non-commercial private study or research. Further distribution and any use of material from within this archive for profit-making enterprises or for commercial gain is strictly forbidden.

Whilst further distribution of specific materials from within this archive is forbidden, you may freely distribute the URL of WestminsterResearch: (http://westminsterresearch.wmin.ac.uk/).

In case of abuse or copyright appearing without permission e-mail repository@westminster.ac.uk

BIOSYNTHESIS OF POLYHYDROXYALKANOATES, THEIR NOVEL BLENDS AND COMPOSITES FOR BIOMEDICAL APPLICATIONS

Pooja Basnett

A Thesis submitted in partial fulfilment of the requirements of the University of Westminster for the degree of Doctor of Philosophy

June 2014

AUTHOR'S DECLARATION

I declare that the present work was carried out in accordance with the Guidelines and Regulations of the University of Westminster. The work is original except where indicated by special reference in the text.

The submission as a whole or part is not substantially the same as any that I previously or am currently making, whether in published or unpublished form, for a degree, diploma or similar qualification at any university or similar institution.

Until the outcome of the current application to the University of Westminster is known, the work will not be submitted for any such qualification at another university or similar institution.

Any views expressed in this work are those of the author and in no way represent those of the University of Westminster.

Signed: Pooja Basnett Date: 20-06-14

Acknowledgements

First of all, I would like to thank Christ Almighty for His grace and faithfulness. I would also like to thank scholarship committee at the Cavendish for giving me this opportunity to pursue my PhD studies here at the University of Westminster.

I would like to express my heartfelt gratitude to my supervisor Dr. Ipsita Roy. She has been my pillar of strength throughout this journey. Her support and her belief in me has motivated me to work with the best of my ability.

I would like to sincerely thank my co-supervisor Dr. Caroline Smith for her creative inputs, guidance and her kind words of encouragement. I would also like to express my gratitude to Prof. Aldo R. Boccaccini and Prof Taj Keshavarz for their support.

I am indebted to the staff at University College London, particularly Dr. Nicola Mordan, Dr. George Gergiou, Dr. Graham Palmer and Prof. Jonathan Knowles for their assistance with various techniques. I would particularly like to thank Dr. Iban Quintana and Rocio at Tekniker, Spain for helping me with the Laser micropatterning technique.

I would like to thank my friends Andrea, Prachi, Hima, Anju, Geenu, Maryam, Ketki , Ngozi, Monica, Amy, Patience, Rishika, Bijal, Moriom, Rashid, Musa, Kamara, Juliet, Ranjana didi and Anu for their love and support. I would also like to express my gratitude to the technical staff at the University of Westminster particularly, Dr. Thakor Tandel and Neville Antonio for their support.

Finally, I would like to wholeheartedly thank my parents for believing in me, my brother Tapash for his care and affection and my most loving husband Shall for taking care of me and putting up with me through my best and my worst.

Abstract

Polyhydroxyalkanoates (PHAs) are a family of polyhydroxyesters of 3-, 4-, 5- and 6-hydroxyalkanoic acids produced by bacterial fermentation in a nutrient limiting conditions with excess carbon. They can be produced easily using renewable carbon sources. They are biodegradable and biocompatible in nature. Their physical properties are highly tailorable and a range of desired properties can be achieved based on the type of application. Owing to these properties, there has been a considerable interest in the commercial exploitation of PHAs, particularly for biomedical applications.

The main aim of this research project was to produce MCL-PHAs from *Pseudomonas mendocina* and use them for biomedical applications. In this study, an economical production of MCL-PHAs using renewable and cheap carbon sources such as sugarcane molasses, biodiesel waste and pure glycerol was carried out. Maximum PHA yield of 43.2% dcw was obtained in the media containing biodiesel waste. The results demonstrated the successful utilisation of these cheap carbon sources by *P. mendocina* for the economical production of MCL-PHAs.

One of the main objectives of this project was to utilize the PHAs produced for biomedical applications. Multifunctional novel 2D P(3HO)/bacterial cellulose composite films were developed for their potential use in tissue engineering applications. Chemically modified bacterial cellulose microcrystals were used as the reinforcing agent to improve the properties of P(3HO). Mechanical properties such as the Young's modulus and tensile strength values of the P(3HO)/bacterial cellulose composite films were significantly higher in comparison to the neat P(3HO) film. Also, the composite film had a rougher and more hydrophilic surface compared to the neat P(3HO) film. It is known from literature that surface roughness and hydrophilicity affects protein adsorption on the surface of the biomaterial. Protein adsorption, in turn, plays an important role in determining the biocompatibility of a material being used for medical applications (Das *et* al., 2007). In this study, protein adsorption was higher in the P(3HO)/25% bacterial cellulose composite film compared to the neat P(3HO) film. *In vitro* biocompatibility studies using Human microvascular endothelial cells (HMEC-1) was carried out. Both neat and composite films were able to support the proliferation of HMEC-1 cells. However, the biocompatibility of the P(3HO)/25% bacterial cellulose composite

films had increased. The cell proliferation significantly higher on the P(3HO)/25% bacterial cellulose composite film as compared to the neat P(3HO) film on day 7.

In addition, multifunctional 2D P(3HO)/P(3HB) blend films with varying percentages of P(3HO) and P(3HB) were developed and assessed for their suitability in the development of biodegradable stents. Mechanical, thermal and microstructural properties of the P(3HO)/P(3HB) blends were characterised. The results highlighted the role of P(3HB) in enhancing the mechanical properties and thermal stability of the blend films compared to the neat P(3HO) films. However, the results suggested that the mechanical properties of the P(3HO)/P(3HB) had to be further improved to meet the desired values required for the development of a biodegradable stent. The overall protein adsorption and % cell viability was significantly higher in the blend films compared to the neat P(3HO) film. Hydrolytic degradation was faster in the blend films and the degradation rate could potentially be tailored to achieve the optimum rate required for a particular medical application.

From the literature, it is known that the surface topography determines the compatibility of a biomaterial by governing important processes such as wettability, protein adsorption, cell adhesion and proliferation (Duncan *et al*., 2007). In this part of the study, P(3HO)/P(3HB) 50:50 blend films were micropatterned using the laser micropatterning technique to improve their biocompatibility. The results demonstrated an increase in hydrophilicity and protein adsorption on the micropatterned blend films compared to the plain P(3HO)/P(3HB) 50:50 blend films. Cell attachment, proliferation and alignment was significantly higher on the micropatterned blend films compared to the P(3HO)/P(3HB) 50:50 blend films which was a desirable outcome.

Furthermore, an investigation of the P(3HO)/P(3HB) 50:50 2D films as the base material for the development of a drug eluting biodegradable stent was carried out by incorporating aspirin within the film. The percentage viability of the HMEC-1 cells was higher in the blend films with aspirin compared to the blend films without aspirin indicating an increased biocompatibility of the P(3HO)/P(3HB) 50:50 blend film containing aspirin. Controlled release of aspirin was observed without any burst release and 96.6% release was achieved within 25 days, ideal for the development of biodegradable drug eluting stents.

Finally, a drug delivery system for the controlled delivery of aspirin was successfully developed. In this part of the study, 2D solvent cast films and microspheres (average size=30 μm) were developed using P(3HB). Drug release pattern from P(3HB) films as well as P(3HB) microspheres were monitored. The results demonstrated that the P(3HB) films with aspirin were suitable for sustained long term drug release whereas P(3HB) microspheres with aspirin were more suitable for fast release.

In conclusion, this project has led to the successful production of PHAs, and their utilisation in the development of a range of composites, blends and drug elution structures with promising potential medical applications.

Contents

Chapter1 1
1.1 Polyhydroxyalkanoates 1
1.2 Types of PHAs and their properties 3
1.3. Discovery of PHAs 6
1.4 Biosynthesis of PHAs in microorganisms 7
1.4.1 Biosynthesis of SCL-PHAs 7
1.4.2 Biosynthesis of MCL-PHAs 7
1.5 Microbial production of PHAs 11
1.6 Production of PHAs using inexpensive carbon sources 14
1.7 Synthesis of PHA blends 19
1.8 Applications of PHAs 23
1.8.1 Tissue Engineering: 23
1.8.2 Bone tissue engineering 24
1.8.4 Cardiovascular tissue engineering 26
1.9 Endothelial cell micropatterning 28
1.10 Drug Delivery 31
1.10.1 Mechanism of drug release 32
1.11.2 Biodegradable coronary stents: 35
1.12 Other applications of PHAs 39
Aims and Objectives 42
Chapter 2 45
2.1 Chemicals and Reagents 45
2.2 Bacterial strains and cell line 45
2.3 Media 46
2.4 Production of P(3HO) 49
2.4.3 Extraction of PHA by chloroform/ sodium hypochlorite dispersion 50
2.4.4 PHA purification 50
2. 5 Analytical studies 50
2.6 Characterization of the PHAs produced 51
2.6.1 Fourier Transform Infrared Spectroscopy (FTIR) 51
2.6.2 Gas Chromatography – Mass spectroscopy (GC-MS) 51
2.6.3 Nuclear Magnetic Resonance Spectroscopy (NMR) 52

2.6.4 Differential Scanning Calorimetry (DSC) 52
2.7 Production of bacterial cellulose 52
2.8 Production of P(3HB) 53
2.9 Characterization of the composite, blend and films with drugs 54
2.9.1 Scanning Electron Microscopy (SEM) 54
2.9.2 White Light Interferometry 54
2.9.3 Atomic Force Microscopy (AFM) 54
2.9.4 Contact Angle Study 55
2.9.5 Dynamic Mechanical Analyser (DMA) 55
2.9.6 Differential Scanning Calorimetry (DSC) 55
2.9.7 Protein adsorption Test 55
2.9.8 Indirect cytotoxicity testing 56
2.10 *In vitro* degradation study 56
2.10.1 Water uptake, weight loss 56
2.10.2 *In vitro* biocompatibility studies 57
2.10.2.3 Scanning Electron Microscopy (SEM) 58
2.11 *In vitro* release of aspirin using High Performance Liquid Chromatography (HPLC) 58
2.12. Statistical analysis 59
Chapter 3 60
Introduction 60
3. 0 Results 61
3.1.1 PHA production using sugarcane molasses as the carbon source 62
3.1.2 PHA production using biodiesel waste as the carbon source 63
3.1.3 PHA production using pure glycerol as the source of carbon 64
3.2 Characterisation of the polymer produced 65
Discussion 76
Chapter 4 85
INTRODUCTION 83
4.0 Results 84
4.1 P(3HO) Production 84
4.2 Characterisation of the polymer produced 85
4.3 Production of cellulose from Acetobacter xylinum and its chemical modification. 89
4.4 Characterisation of the acetylated cellulose microcrystals using FTIR 91

4.5 X-Ray Diffraction 92
4.7 Characterisation of the P(3HO)/bacterial cellulose composite films 93
4.8.4 *In vitro* degradation study in DMEM and PBS media 99
4.8.4.1 Water uptake, weight loss and pH measurements 99
4.8.4.2 pH measurements 100
4.8.4.3 Mechanical characterisation of the degrading film 100
4.9 *In vitro* biocompatibility study 101
4.10 Scanning Electron Microscopy (SEM) 103
Discussion 105
Chapter 5 117
Introduction ..... 117.
Part I 118
5.0 Results 118
5.1 Production of P(3HB) 118
5.2 Characterisation of the polymer produced 119
5.3 Synthesis of the novel P(3HO)/P(3HB) blends 121
5.11 *In vitro* degradation study 130
5.11.1 Water absorption and weight loss measurements 130
5.12 Surface studies of the degrading films 133
PART II 135
5.13 Picosecond pulse laser technology 135
5.14 Characterization of the micropatterned (3HO)/P(3HB) 50:50 blend film . 136
5.14.6 *In vitro* biocompatibility studies 140
5.14.7 Scanning electron microscopy (SEM) 142
5.14.8 Development of stent prototype 144
PART III 146
Preparation of P(3HO)/P(3HB) 50:50 blend film with aspirin 146
Characterisation of the P(3HO)/P(3HB) 50:50 blend film with aspirin 146
5.15 *In vitro* degradation study in PBS 154
5.15.1 Water absorption and weight loss 154
5.15.2 Scanning Electron microscopy (SEM) 155
5.16 *In vitro* drug release studies 156
Discussion 159
Chapter 6 182

Introduction 182
SECTION I 185
6.0 Results 185
6.1 Preparation of the P(3HB) solvent cast film with and without aspirin and their characterisation 185
6.1.8 *In vitro* degradation study in PBS 192
6.1.8.1 Water absorption 192
6.1.8.2 Weight Loss 194
6.1.9 *In vitro* drug release studies 195
SECTION II 197
6.2 Synthesis of P(3HB) microspheres 197
6.2.1 Characterisation of the P(3HB) microspheres 197
6.2.1.3 Scanning electron Microscopy: 199
6.2.2 *In vitro* degradation study in PBS 203
6.2.2.1 Water absorption 203
6.2.2.2 Weight Loss 204
6.3 *In vitro* drug release studies 206
DISCUSSION 208
7.1 Conclusion 222
References 230

List of Figures

Figure 1.1: The general structure of polyhydroxyalkanoates…….. 2

Figure 1.2: SEM images of discrete granules of P(3HB) in bacteria…….....…...6

Figure 1.3: Biosynthetic pathway of SCL-PHAs.……...…7

Figure 1.4: Biosynthetic pathways of MCL-PHAs…….…….…...9

Figure 1.5: Classification of PHA synthases…….....9

Figure 1.6: Organisation of the genes encoding PHA synthases……...11

Figure 1.7: Structure of cellulose…….....22

Figure 1.8: Abbot's biodegradable vascular scaffold (BVS)……...……37

Figure 1.9: REVA stent with the unique slide and lock design…….…….…….....….38

Figure 2.1: Steps involved in P(3HO) production…….…….....49

Figure 3.1: Fermentation profile of *P. mendocina* using sugarcane molasses as the source of carbon…….....62

Figure 3.2: Fermentation profile of *P. mendocina* using biodiesel waste as the source of carbon……..63

Figure 3.3: Fermentation profile of *P. mendocina* using pure glycerol as the source of carbon……...…...64

Figure 3.4: FTIR spectrum of the polymer produced using sugarcane molasses as the carbon source……...…...65

Figure 3.5: FTIR spectrum of the polymer produced using biodiesel waste as the carbon source…….....66

Figure 3.6: FTIR spectrum of the polymer produced using pure glycerol as the carbon source…….....67

Figure 3.7: GC-MS analysis of the polymer produced by *P. mendocina* using sugarcane molasses as the carbon source……68

Figure 3.8: GC-MS analysis of the polymer produced by *P. mendocina* using biodiesel waste as the carbon source……..……71

Figure 3.9: GC-MS analysis of the polymer produced by *P. mendocina* using pure glycerol as the carbon source……73

Figure 4.1: The fermentation profile for P(3HO) production by *P. mendocina* using sodium octanoate as the sole carbon source ……..…….....84

Figure 4.2: FTIR spectrum of the polymer produced by *P. mendocina* using sodium octanoate. …….....86

Figure 4.3: GC-MS analysis of the polymer produced by *P. mendocina* using sodium octanoate……..……87

Figure 4.4: NMR spectrum of polymer produced by *P. mendocina* using sodium octanoate……88

Figure 4.5: A bacterial cellulose pellicle produced by *Acetobacter xylinum*……90

Figure 4.6: Freeze dried acetylated bacterial cellulose microcrystals ……90

Figure 4.7: Chemical reaction of the bacterial cellulose with acetic anhydride….91

Figure 4.8: The FTIR analysis showing the acetylated bacterial cellulose versus the non-acetylated bacterial cellulose……91

Figure 4.9: XRD patterns of the acetylated bacterial cellulose and the non-acetylated bacterial cellulose……92

Figure 4.10: Static water contact angle measurement of the neat P(3HO) and P(3HO)/ bacterial cellulose composite films……96

Figure 4.11: Surface scans of the neat P(3HO) and P(3HO)/25% bacterial cellulose composite film using White Light Interferometry……97

Figure 4.12: SEM images of the neat P(3HO) and P(3HO)/25% bacterial cellulose composite film……97

Figure 4.13: Protein adsorption of the neat P(3HO) and P(3HO)/25% cellulose composite film……98

Figure 4.14: Water absorption by the neat P(3HO) and P(3HO)/25% bacterial cellulose composite film during the degradation study in (a) DMEM media and (b) PBS media……99

Figure 4.15: Cell proliferation study of the seeded HMEC-1 cells on the neat P(3HO) and P(3HO)/25% bacterial cellulose composite film……101

Figure 4.16: SEM images of the HMEC-1 cells on P(3HO)/25% bacterial cellulose composite film……103

Figure 5.1: The fermentation profile of P(3HB) production using *Bacillus cereus* SPV in Kannan and Rehacek media……118

Figure 5.2: FTIR spectrum of the polymer produced by *Bacillus cereus* SPV using Kannan and Rehacek media……120

Figure 5.3: The Gas chromatogram of the methyl esters of 3-hydroxybutyric acid……120

Figure 5.4: SEM images of the P(3HO)/P(3HB) blend films……122

Figure 5.5: The AFM images of the (a) P(3HO)/P(3HB) 80:20 (b) P(3HO)/P(3HB) 50:50 blend film……123

Figure 5.6: Static water contact angle measurements of the neat P(3HO) and P(3HO)/P(3HB) blend films……124

.

Figure 5.7: Protein adsorption of the neat P(3HO) and P(3HO)/P(3HB) blend films……..…….....126

Figure 5.8: Indirect toxicity assessment of P(3HB)/P(3HO) blend films……..….127

Figure 5.9: Water absorption by the neat P(3HO) and P(3HO)/P(3HB) blend films during the *in vitro* degradation study in (a) DMEM media and (b) PBS media……..……..130

Figure 5.10: Water absorption by the neat P(3HO) and P(3HO)/P(3HB) blend films during the *in vitro* degradation study in (a) DMEM media and (b) PBS media……..132

Figure 5.11: SEM images of the P(3HB)/P(3HO) blend films after of one month of incubation exhibiting different states of degradation……..134

Figure 5.12: SEM images of the plain P(3HO)/P(3HB) 50:50 blend film and surface micropatterned P(3HO)/P(3HB) 50:50 blend film AFM……..136

Figure 5.13: Surface roughness of the plain P(3HO)/P(3HB) 50:50 blend film and the micropatterned blend film measured using ……..…..137

Figure 5.14: Static water contact angle measurements of the plain P(3HO)/P(3HB) 50:50 blend film and micropatterned blend film……138

Figure 5.15: Total protein adsorption on the plain P(3HO)/P(3HB) 50:50 blend film and the micropatterned blend film……....139

Figure 5.16: Cell proliferation study of the HMEC-1 cells on the plain and micropatterned blend film……....141

Figure 5.17: SEM images of the HMEC-1 cells on plain as well as micropatterned films ……....142

Figure 5.18: Dimensions of a laser cut film for stent prototype development……144

Figure 5.19: A stent prototype made up of P(3HO)/P(3HB) 50:50 blend film……....145

Figure 5.20: FTIR spectra of the (a) commericial aspirin (-) and (b) P(3HO)/P(3HB) 50:50 blend film with aspirin ……..……....147

Figure 5.21:.SEM images of the P(3HO)/P(3HB) 50:50 blend film with and without aspirin ….……..……....148

Figure 5.22: Surface roughness of the P(3HO)/P(3HB) 50:50 blend films with and without aspirin……..……....149

Figure 5.23: Static water contact angle measurements of P(3HO)/P(3HB) 50:50 blend films with and without aspirin……..150

Figure 5.24: Protein adsorption on the P(3HO)/P(3HB) 50:50 blend films with and without aspirin……151

Figure 5.25: Indirect toxicity testing of the P(3HO)/P(3HB) 50:50 blend films with and without aspirin…….. ……..……152

Figure 5.26: Water absorption (%WA) and Weight loss (%WL) in P(3HO)/P(3HB) 50:50 blend films with and without aspirin……..154

Figure 5.27: SEM images of the P(3HO)/P(3HB) 50:50 blend film with and without aspirin after being immersed in PBS for one month……..155

Figure 5.28: *In vitro* release profile of aspirin from P(3HO)/P(3HB) 50:50 blend film for a period of 30 days……....156

Figure 5.29: : *In vitro* release profile of chemically stable aspirin from (a)P(3HO)/P(3HB) 50:50 blend film and control aspirin standard (b) for a period of 30 days…….....157

Figure 6.1: Solvent cast P(3HB) film and the P(3HB) film with aspirin……..….185

Figure 6.2: The FTIR spectra of the (a) P(3HB) film with aspirin and the (b) P(3HB) film. …….....186

Figure 6.3: SEM images of the P(3HB) film and P(3HB) film with aspirin……187

Figure 6.4: The AFM images of the (a)P(3HB) film (b)P(3HB) film with aspirin..188

Figure 6.5: Static water contact angle measurements of the P(3HB) film and the P(3HB) film with aspirin……..……..189

Figure 6.6: Protein adsorption on the P(3HB) film and the P(3HB) film with aspirin……..……..190

Figure 6.7: Indirect toxicity testing of the P(3HB) film and P(3HB) film with aspirin……..……....191

Figure 6.8: Water absorption (%WA) by the P(3HB) film and P(3HB) film with aspirin ……..……193

Figure 6.9: % Weight Loss (WL) in the P(3HB) film and P(3HB) film with aspirin……..……..……....194

Figure 6.10: *In vitro* release profile of aspirin from P(3HB) film containing aspirin for a period of 30 days……..……195

Figure 6.11: *In vitro* release profile of chemically stable aspirin in the released samples from the (a) P(3HB) film with aspirin and (b) control aspirin standard for a period of 30 days……..……..……196

Figure 6.12: The FTIR spectra of the (a)P(3HB) microspheres and the (b) P(3HB) microspheres with aspirin ……..…….....198

Figure 6.13: SEM images of the (a) P(3HB) microspheres and the (b) P(3HB) microspheres with aspirin……..199

Figure 6.14: Porosity measurements of the P(3HB) microspheres and P(3HB) microspheres with aspirin ……..200

Figure 6.15: The amount of the Rose Bengal dye adsorbed onto the surface of the P(3HB) microspheres and P(3HB) microspheres aspirin……..201

Figure 6.16: Protein adsorption on the P(3HB) microspheres and P(3HB) microspheres with aspirin ……...202

Figure 6.17 : Water absorption (%WA) by the P(3HB) microspheres and P(3HB) microspheres with aspirin ……...203

Figure 6.18: % Weight Loss (WL) in the P(3HB) microspheres and P(3HB) microspheres with aspirin ……...205

Figure 6.19: *In vitro* release profile of aspirin from the P(3HB) microspheres with aspirin for a period of 30 days……...206

Figure 6.20: *In vitro* release profile of chemically stable aspirin in the released samples from the (a) P(3HB) microspheres with aspirin and (b) control aspirin standard for a period of 30 days……..207

List of Tables

Table 1.1: Physical properties of P(3HB)……..4

Table 1.2: Physical properties of P(4HB) ……..5

Table 1.3: Physical properties of P(3HO) ……..5

Table 2.1: Composition of seed culture medium……..……..45

Table 2.2: Composition of the second stage MSM. ……..…...46

Table 2.3: Composition of the production stage MSM……..46

Table 2.4: Composition of the trace element solution ……..……..47

Table 2.6: Composition of the Kannan and Rehacek media……...48

Table 3.1: Thermal Analysis of the polymer produced using cheap carbon sources……75

Table 4.1: Thermal Analysis of the neat P(3HO)/bacterial cellulose composite films……94

Table 4.2: Mechanical properties of the P(3HO)/bacterial cellulose composite films ……..95

Table 5.1: Thermal Analysis of the neat P(3HO) and P(3HO)/P(3HB) blend films……128

Table 5.2: Mechanical analysis of the neat P(3HO) and P(3HO)/P(3HB) blend films……129

Table 5.3: Mechanical characterisation of the plain and surface micropatterned P(3HO)/P(3HB) 50:50 blend film……140

Table 5.4: Thermal properties of P(3HO)/P(3HB) 50:50 blend film with and without aspirin ……153

Table 5.5: Mechanical characterisation of the P(3HO)/P(3HB) 50:50 blend film with and without aspirin……154

Table 6.1: Thermal properties of the P(3HB) films with and without aspirin……..192

Table 6.2: Thermal properties of the P(3HB) microspheres with and without aspirin……203

List of Abbreviations

PHA	Polyhydroxyalkanoates
SCL-PHA	short chain length polyhydroxyalkanoate
MCL-PHA	medium chain length polyhydroxyalkanoate
P(3HB)	poly(3-hydroxybutyrate)
P(3HHx)	poly(3-hydroxyhexanoate)
P(3HO)	poly(3-hydroxyoctanoate)
P(3HB-co-3HV)	poly(3-hydroxybutyrate-co-3-hydroxyvalerate)
P(4HB)	poly(4-hydroxybutyrate)
P(3HB-co-4HB)	poly(3-hydroxybutyrate-co-4-hydroxybutyrate)
P(3HB-co-3HHx)	poly(3-hydroxybutyrate-co-3-hydroxyhexanoate)
P(3HO-co-3HHx)	poly(3-hydroxyoctanoate-co-3-hydroxyhexanoate)
P(3HB-co-3HO)	poly(3-hydroxybutyrate-co-3-hydroxyoctanoate)
3HB	3-hydroxybutyrate
3HV	3-hydroxyvalerate
3HD	3-hydroxydecanoate
3HHp	3-hydroxyheptanoate
CoA	coenzyme A
MSM	mineral salt medium
O.D.	optical density
DOT	dissolved oxygen tension
rpm	revolutions per minute
GC	Gas Chromatography
GC-MS	Gas Chromatography- Mass Spectrometry
MS	Mass Spectrometry
SEM	Scanning Electron Microscopy
XRD	X-ray diffraction
FTIR	Fourier Transform Infrared
NMR	Nuclear Magnetic Resonance
DSC	Differential Scanning Calorimetry
DMA	Dynamic Mechanical analysis
HPLC	High Performance Liquid Chromatography

AFM	Atomic Force Microscopy
PDI	polydispersity index
T_g	glass transition temperature
T_m	melting temperature
T_C	crystallisation temperature
PDI	polydispersity index
SD	standard deviation
wt%	weight percentage
dcw	dry cell weight
µm	micrometre
RMS	root mean square
LPS	lipopolysaccharides
PBS	phosphate buffer saline
DMEM	Dulbecco's modified Eagle's medium
FBS	foetal bovine serum
SDS	sodium dodecyl sulphate
MTT	(3-(4,5-Dimethylthiazol-2-yl)-2,5 diphenyltetrazolium bromide
PVA	polyvinyl alcohol
PIP	poly(cis-1,4-isoprene)
PCL	poly(e-caprolactone)
PEG	polyethylene glycol
PGA	poly(glycolic acid)
PLA	poly(lactic acid)
PLGA	poly(lactic-co-glycolic)acid
PDLLA	poly(DL-lactic acid)
PLLA	poly(L-lactic acid)
PEO	poly(ethylene oxide)
PVA-g-PLGA	polyvinyl alcohol grafted poly(lactic-co-glycolactic)
PET	polyethylene terephthalate
PEO	polyethylene oxide

PTFE	poly(tetrafluroethylene)
PDMS	poly(dimethylsiloxane)
HA	hydroxyapatite
SGBG	sol-gel bioactive glass
nBG	nanobioglass particles
PDMS	polydimethylsiloxane
UV	ultraviolet
HEK-293	Human embryonic kidney cells
CHO-K1	Chinese Hamster Ovary cells
HUVEC	Human umbilical vein endothelial cells
HMEC-1	Human dermal microvascular endothelial cells
HAEC	Human aortic endothelial cells
PTFE	polytetrafluroethylene
CAD	coronary artery disease
PTCA	percutaneous transluminal coronary angioplasty
CABG	coronary artery bypasses graft
BVS	biodegradable vascular scaffold
Mn	average molecular weight
M_W	weight average molecular weight
%WA	water absorption
% WL	weight loss
C/N	carbon to nitrogen ratio
R_t	retention time

Chapter 1

INTRODUCTION

1.0 INTRODUCTION

Plastics have become a part of our daily lives. They are cheap, durable, resistant to corrosion, lightweight and can be readily moulded into various products. They are widely used for several applications ranging from packaging to the manufacture of medical devices. The production of plastics has increased significantly over the last 60 years to meet their ever increasing demand. However, there are two major drawbacks of using plastics. Firstly, plastics are made up of petrochemicals derived from non-renewable sources. Production of plastics account for the usage of 4% of petroleum reserves produced annually. Secondly, most of the plastics are non-degradable in nature (Hopewell *et al*., 2009). They accumulate in the environment causing contamination to the terrestrial and marine habitat. It is a known fact that the chemicals that are used in the production of plastics are toxic in nature. Biomonitoring data has revealed that these toxic chemicals are present within the human body posing a threat to human health. Dwindling petroleum reserves and the environmental threat posed by the traditional plastics have resulted in an extensive research to find an alternative. Biodegradable polymers have emerged as a potential substitute. They have several advantages over traditional plastics. They are degraded by a variety of microorganisms eliminating any kind of threat to the environment and the human population. The economical production of these biodegradable polymers could provide potential solutions to the problems created by these traditional plastics (Hopewell *et al*., 2009; Thomson *et al*., 2009).

1.1 Polyhydroxyalkanoates (PHAs)

Polyhydroxyalkanoates (PHAs), also referred to as bacterial or microbial polyesters, are produced by the bacteria in an environment where one of the essential nutrients such as nitrogen, phosphorus or potassium is limited, whereas the carbon source is present in excess. PHAs are accumulated as intracellular storage compounds within the bacteria (Khanna and Srivastava, 2005; Hazer and Steinbuchel, 2007). They are biodegradable, biocompatible, hydrophobic and also exhibit thermoplastic properties. They can be produced readily from renewable carbon sources.

The molecular weight of PHAs produced is determined by the type of the microorganism and the culture conditions used. It ranges between 2×10^5 to 3×10^6 Da (Byrom, 1987; Lee, 1996). The general structure of PHAs is shown in **Figure 1.1**.

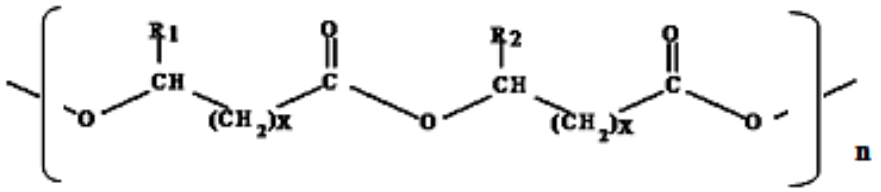

Figure 1.1: The general structure of polyhydroxyalkanoate (x = 1, 2, 3; n = 100-30000; R_1, R_2 = alkyl groups, C_1-C_{13}) (Philip *et al*., 2007)

The presence of PHAs within bacterial cells was identified for the first time by Lemoigne in 1926. Around 300 different species of PHA producing bacteria have been identified so far (Lee, 1996). Staining methods using Sudan Black and Nile Blue A have been used in the past to detect the presence of PHAs accumulated within bacterial cells. The PHAs produced by the bacteria can be chemically characterized using gas chromatography techniques (Lee, 1996). The properties of PHAs have been found to be similar to that of the traditional plastics such as polypropylene.

Previous studies have established that PHAs are biocompatible in nature and are well tolerated by the mammalian system, therefore, they have been considered for tissue engineering applications (Reddy *et al*., 2003). PHAs are biodegradable in nature. Under aerobic conditions, PHAs are degraded into carbon dioxide and water whereas under anaerobic conditions, PHAs are degraded into carbon dioxide and methane. They are also degraded within the human body. In recent years, PHAs have been used in the manufacture of several medical devices such as sutures, surgical mesh, tendon repair devices, ocular cell implants, skin substitutes, vein valves, orthopaedic pins, bone plates and bone plating system. PHAs have some fascinating physical properties such as piezoelectricity activity which broadens their area of application (Chen and Wu, 2005).

1.2 Types of PHAs and their properties

Depending on the number of carbon atoms present in their monomer units, PHAs can be classified into two main types, short chain length PHAs (SCL-PHAs) that have 3-5 carbon atoms and medium chain length PHAs (MCL-PHAs) that have 6-14 carbon atoms in their monomers (Khanna and Srivastava, 2005). Apart from the number of carbon atoms, PHAs can also be classified based on the type of the monomer units present. PHAs containing a single type of monomer unit are called homopolymers such as Poly(3-hydroxybutyrate) or P(3HB), Poly(3-hydroxyhexanoate) or P(3HHx) and Poly(3-hydroxyoctanoate) or P(3HO) whereas PHAs containing more than one type of monomer unit are called heteropolymers such as Poly(3-hydroxybutyrate-co-3-hydroxyvalerate) or P(3HB-co-3HV), and Poly(3-hydroxyhexanoate-co-3-hydroxyoctanoate) or P(3HHx-co-3HO)(Byrom, 1987; Asrar *et al.*, 2002).

The physical properties of PHAs are greatly influenced by the length of the side chain and the functional group present. Therefore, SCL-PHAs are generally brittle in nature with a very high melting point and crystallinity (with the exception of poly(4-hydroxybutyrate), P(4HB), whereas MCL-PHAs have a low melting temperature, crystallinity, tensile strength and are extremely elastomeric in nature (Martin and William, 2003). SCL-PHAs are produced by numerous bacteria such as *Cuprivadus necator*, *Alcaligenes latus, Bacillus megaterium and Bacillus cereus* while MCL-PHAs are synthesized by bacteria such as *Pseudomonas putida, Pseudomonas mendocina* and *Pseudomonas oleovorans.* Examples of SCL-PHAs include P(3HB), P(4HB) and P(3HB-co-3HV). The examples of MCL-PHAs include P(3HHx) and P(3HO) (Lee, 1996; Khanna and Srivastava, 2005).

1.2.1 P(3HB)

P(3HB) is a type of SCL-PHA which has been extensively studied since its discovery in 1926 by Lemoigne. From literature, it is known that low molecular weight P(3HB) is a component of human blood and is degraded within the body into 3-hydroxybutyric acid. Therefore, P(3HB) is biocompatible and biodegradable in nature (Misra *et al*., 2006). P(3HB) is crystalline with a crystallinity percentage ranging between 60-80%. However, it exists in an amorphous form within the cells. P(3HB) is rigid, brittle and highly crystalline due to the presence of a short methyl side chain within its structure (Kawaguchi and Doi, 1992). Mechanical properties of

P(3HB) such as its tensile strength is comparable to that of the synthetic polymer such as polypropylene (Engelberg and Kohn, 1991). P(3HB) also possesses properties such as piezoelectricity and optical activity (Ha and Cho, 2002). Thermal and mechanical properties of P(3HB) is shown in **Table 1.1**.

Properties	Values
T_m (˚C) T_g (˚C)	175-179
Crystallinity (%)	4
Tensile strength (MPa)	60– 80
Young's Modulus (GPa)	40
% Elongation at break	1.1 – 3.5
	5-6

Table 1.1: Physical properties of P(3HB)(Misra *et al.,* 2006)

Properties of P(3HB) differ depending on various factors such as the type of the organism used for the production, the method used for the extraction and the preparation of the sample, molecular weight and polydispersity index. Based upon the type of application, properties of P(3HB) can be controlled by blending or making composites with natural or synthetic polymers (Misra *et al*., 2006).

1.2.2 P(4HB)

P(4HB) is also a type of SCL-PHA. Its physical properties are different compared to that of the other SCL-PHAs. This has a semi-crystalline nature with a crystallinity percentage of around 35%. P(4HB) has a low melting and glass transition temperature but a very high tensile strength and elongation at break value. The physical properties of P(4HB) is very similar to that of the traditional plastics. P(4HB) has gained a lot of attention in recent times and has been used for a variety of medical applications such as heart valves, vascular grafts and sutures due to its unique properties (Martin and Williams, 2003). The physical properties of P(4HB) are shown in **Table 1.2.**

Properties	Values
T_m (˚C) T_g (˚C)	54
Crystallinity (%)	-48
Tensile strength (MPa)	34
% Elongation at break	104
	1000

Table1.2: Physical properties of P(4HB) (Tsuge, 2002; Martin and Williams, 2003; Khanna and Srivastava, 2005).

1.2.3 P(3HO)

P(3HO) is a type of MCL-PHA. It has a low crystallinity percentage of around 37.5% due to the presence of an uneven pendant side chain within its structure. P(3HO) is elastomeric in nature and has a low melting temperature, low crystallinity and a high elongation at break value (Rai *et al.,* 2011). The properties of P(3HO) is shown in **Table 1.3**.

Properties	Values
T_m (˚C) T_g (˚C)	39 - 50
Crystallinity (%)	-35 to -36
Tensile strength (MPa)	37.5
Young's Modulus (MPa)	1.8
% Elongation at break	11.4
	278

Table 1.3: Physical properties of P(3HO)(Rai *et al.,* 2011)

The mechanical properties such as tensile strength and Young's modulus of P(3HO) is very low compared to P(3HB)(Rai *et al.,* 2011). Based on the desired application, the mechanical properties of P(3HO) can be manipulated by blending, forming composites with natural and synthetic polymers as well as by chemical modification.

1.3. Discovery of PHAs

Intracellular granules within bacterial cells were first observed by Beijerinck in 1888. These intracellular granules were identified to be P(3HB) by Lemoigne in 1926 (Lee, 1996).

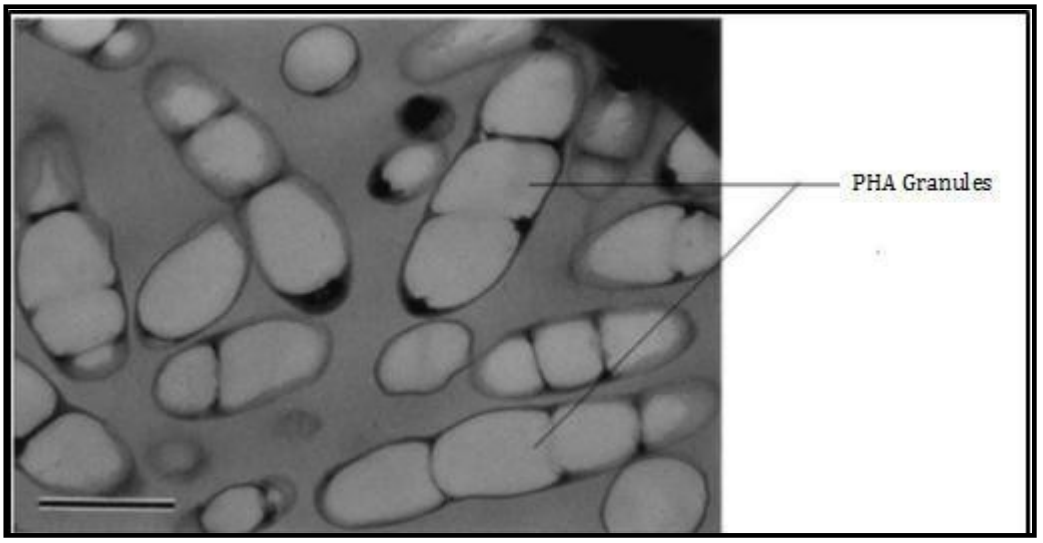

Figure 1.2: SEM images of synthesized and intracellularly accumulated discrete granules of P(3HB) in bacteria (Sudesh *et al.*, 2000).

PHAs did not attract any attention until 1958, when Macrae and Wilkinson reported the biodegradable nature of the P(3HB) (Macrae and Wilkinson, 1958). In 1974, Wallen and Rohwedder reported the presence of other 3-hydroxyacids such as 3-hydroxyvalerate (3HV), 3-hydroxyhexanoate (3HHx) and 3-hydroxyheptanoate (3HHp) along with 3-hydroxybutyrate (3HB) in the chloroform extracts of activated sewage sludge (Wallen and Rohwedder, 1974). Similar reports of the presence of other 3-hydroxyacids along with 3HB were made by Findlay and White in 1983. They stated that the Gas chromatographic (GC) analysis of the PHAs extracted from marine sediments showed the presence of 11 different 3-hydroxyacids. However, the major constituents were 3HB and 3HV. From literature, it is now known that around 150 different types of PHA constituents have been identified (Anderson and Dawes, 1990; Braunegg *et al.*, 1998).

1.4 Biosynthesis of PHAs in microorganisms

1.4.1 Biosynthesis of SCL-PHAs

PHAs produced by a wide variety of bacterial species are chemically diverse. However, P(3HB) is commonly produced and most extensively studied. The biosynthetic pathway for the production of P(3HB) involves three main enzymes and the respective genes encoding these enzymes. These enzymes involved are present in the cytosol of the cell. Biosynthesis of P(3HB) involves three key steps. (1) The condensation of two acetyl CoA molecules to form acetoacetyl CoA. This step is catalysed by β- ketothiolase which is coded by the *phaA* gene. (2) The reduction of acetoacetyl CoA to (R)- 3-hydroxybutyryl CoA. This step is catalysed by acetoacetyl-CoA-reductase which is in turn coded by the *phaB* gene. (3) The polymerisation of (R)- 3-hydroxybutyryl CoA to form P(3HB). This key step is catalysed by PHA synthase which is coded by *phaC* gene (Huisman *et al*., 1989; Reddy *et al*., 2003; Khanna and Srivastava, 2005). The biosynthetic pathway of SCL-PHA in *C. necator* is shown in **Figure 1.3**.

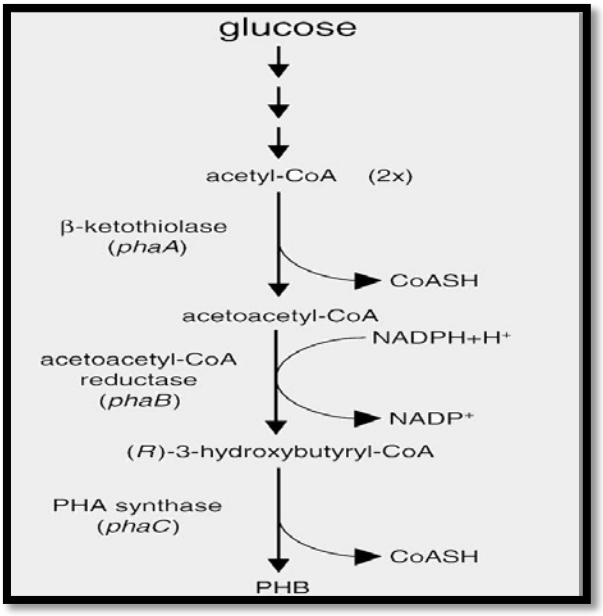

Figure 1.3: Biosynthetic pathway of SCL-PHAs production in *C. necator* (Khanna and Srivastava, 2005).

1.4.2 Biosynthesis of MCL-PHAs

Synthesis of MCL-PHAs involves three different pathways namely: (1) *de novo* fatty acid biosynthesis, (2) β-oxidation pathway and (3) chain elongation pathway.

(1) **de novo fatty acid biosynthesis**: This is the metabolic route by which non related carbon sources such as glucose generate (R)-3-hydroxyacyl-CoA precursors. In this pathway, (R)-3-hydroxyacyl-ACP is converted to (R)-3-hydroxyacyl CoA. This reaction is catalysed by the enzyme (R)-3-hydroxyacyl-CoA-ACP transferase which is encoded by the *phaG* gene (Taguchi *et al.,* 1999; Sudesh *et al.,* 2000). (2) **β-oxidation pathway** produces MCL-PHA precursor molecules from fatty acids. The three key enzymes involved in this pathway include 3-hydroxyacyl-CoA epimerase which converts (S)-3-hydroxyacyl-CoA into (R)-3-hydroxyacyl CoA, enoyl-CoA hydratase which converts 2-trans-enoyl-CoA into (R)-3-hydroxyacyl CoA and finally 3-ketoacyl-CoA reductase which converts 3-ketoacyl-CoA to (R)-3-hydroxyacyl CoA (Huisman *et al.,* 1989). (3) **Chain elongation pathway** also produces MCL-PHA precursor from non-related carbon sources by extending the acetyl CoA to acyl CoA. The contribution of this pathway in generating MCL-PHA precursors by the elongation of acyl CoA derived from fatty acids is significant, however, it only forms a very small fraction of the total PHA accumulated within the bacterial cells. The final step which involves the polymerization of the (R)-3-hydroxyacyl CoA into poly-(R)-3-hydroxyacyl CoA is catalysed by the PHA synthase enzyme with the release of CoA (Dawes and Senior, 1973; Zinn *et al*., 2001). The biosynthetic pathway of MCL-PHAs is shown in **Figure 1.4.**

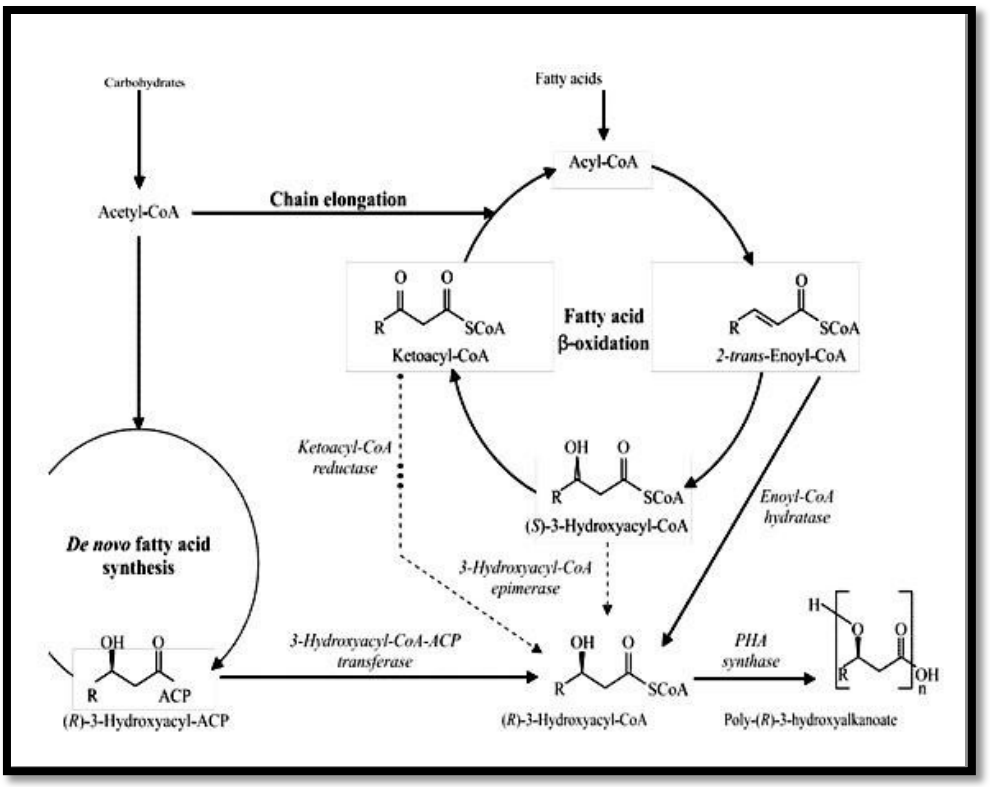

Figure 1.4: Biosynthetic pathways of MCL-PHAs (Kim *et al.*, 2007).

1.4.3 Polyhydroxyalkanoate synthases or PHA synthases and the PHA biosynthetic genes

The enzyme that catalyses the final polymerization of the (R)-3-hydroxyacyl CoA into poly-(R)-3-hydroxyacyl CoA is the PHA synthase (Rehm, 2003). Based on their subunit composition and substrate specificity, the PHA synthase enzyme can be classified into four different classes as shown in **Figure 1.5**.

Class	Subunits	Species	Substrate
I	PhaC ~60-73 kDa	*Ralstonia eutropha*	$3HA_{SCL}$-CoA (~C3-C5) $4HA_{SCL}$-CoA, $5HA_{SCL}$-CoA, $3MA_{SCL}$-CoA
II	PhaC ~60-65 kDa	*Pseudomonas aeruginosa*	$3HA_{MCL}$-CoA (~C5)
III	PhaC ~40 kDa, PhaE ~40 kDa	*Allochromatium vinosum*	$3HA_{SCL}$-CoA ($3HA_{MCL}$-CoA [~C6-C8], 4HA-CoA, 5HA-CoA)
IV	PhaC ~40 kDa, PhaR ~22 kDa	*Bacillus megaterium*	$3HA_{SCL}$-CoA

Figure 1.5: Classification of PHA synthases based on their subunit composition and substrate specificity (Adapted from Rehm, 2003).

Class I and II PHA synthase enzymes consist of the *PhaC* subunit and are represented by the PHA synthase of *C. necator* and *P. aeroginosa* respectively. Molecular masses of these *PhaC* subunits range between 61 to 73 KDa (Qi and Rehm, 2001). Class I PHA synthase prefers thioesters of (R)-3-hydroxy fatty acids made up of 3 to 5 carbon atoms. Class II PHA synthases, however prefers CoA thioesters of (R)-3- hydroxy fatty acids made up of 6 to 14 carbon atoms (Peoples and Sinskey, 1989; Rehm, 2003).

The Class III PHA synthase enzyme comprises of *PhaC* and *PhaE* subunits. This class of PHA synthase is represented by the PHA synthases of *Allochromatium vinosum*. The *PhaC* subunit present in this class of PHA synthase has a molecular mass of 40 kDa and exhibits 21-28% similarity in their amino acid sequence with the *PhaC* subunit present in Class I and II PHA synthases. They prefer to utilize CoA thioesters of (R)-3-hydroxy fatty acids made up of 3 to 5 carbon atoms (Stubbe and Tian, 2003). Finally, Class IV PHA synthases include the *PhaC* and *PhaR* subunits and are represented by the PHA synthase of *Bacillus megaterium.* Molecular masses of the *PhaC* and *PhaR* subunits are 40 and 22 kDa respectively. Class IV PHA synthases also have substrate specificity towards the CoA thioesters of (R)-3-hydroxy fatty acids made up of 3 to 5 carbon atoms (McCool and Cannon, 2001). The organization of the genes encoding different classes of PHA synthases is shown in **Figure 1.6**:

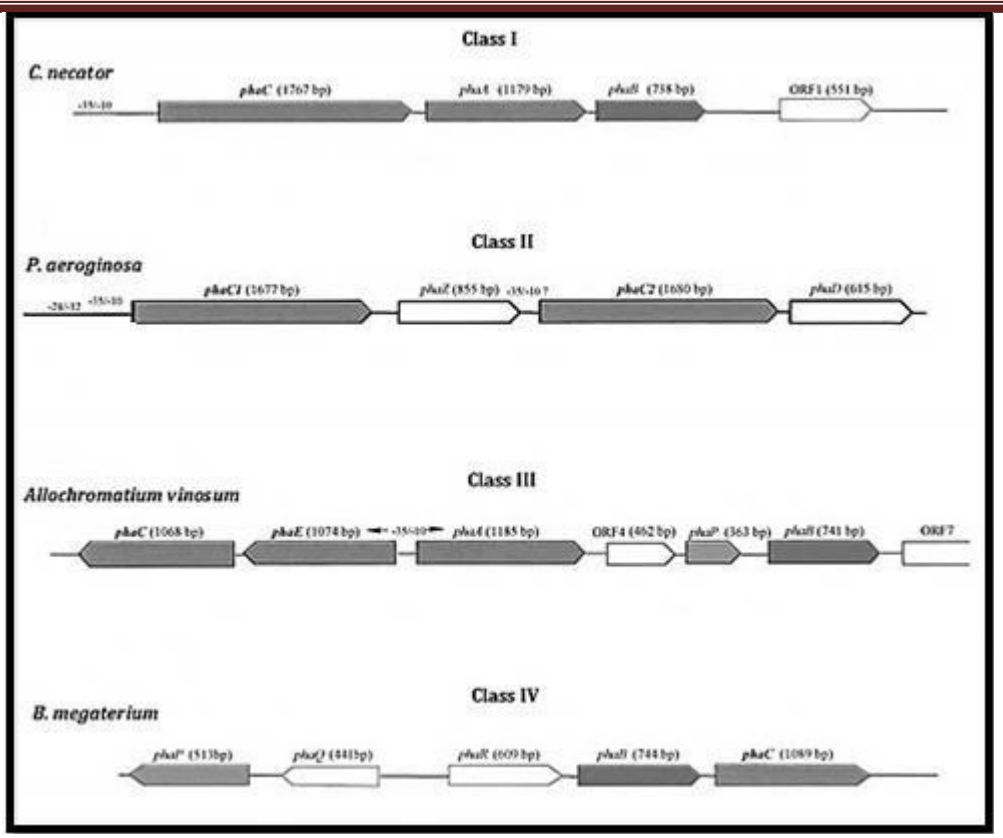

Figure 1.6: Organisation of the genes encoding different classes of PHA synthases (Adapted from Rehm, 2003)

1.5 Microbial production of PHAs

Based on the culture condition requirements, PHA producing microorganisms can be classified into two groups. Organisms such as *B. cereus*, *C. necator,* and *Methylobacterium organophilum* that require a nutrient limiting condition for the production of PHAs belong to the first group whereas organisms such as *Alcaligenes latus* and recombinant *E. coli* that produce PHAs during their growth in the cultivation medium belong to the second group (Lee, 1996). Most commonly used organisms for the production of PHAs include *C. necator, Pseudomonas* spp*, A. latus* and *Bacillus* spp.

C. necator is the most widely studied organism for the production of PHAs. It has the ability to utilize a wide range of carbon sources and produce a significant amount of P(3HB) (Ryu *et al*., 1997). A metabolically engineered glucose utilizing mutant of *C. necator* produces 80% (wt/wt) of P(3HB) using glucose as the sole carbon source. The addition of propionic acid along with the glucose resulted in the production of Poly(hydroxybutyrate-co-hydroxyvalerate), a copolymer of 3HB and 3HV (Anderson and Dawes, 1990). The ratio of propionic acid to glucose determined the 3HV content in the accumulated PHA. It has been reported that *C.*

necator are also able to utilize a wide range of plant oils such as olive oil, corn oil and palm oil to produce 80% (wt/wt) of P(3HB) (Fukui and Doi, 1998).

***Bacillus* spp** have been extensively investigated for the production of PHAs. Various characteristics that make these bacteria ideal candidates for the production of PHAs include lack of endotoxin and the presence of enzymes such as amylase and proteinase that helps them to utilize agricultural waste as the carbon source for the production of PHAs (Law and Slepecky, 1961). This helps in the economical production of PHAs. P(3HB) production by *Bacillus megaterium* was first reported by Findlay and White in 1983. This finding was followed by the production of P(3HB) by the *Bacillus* sp IPCB-403. Approximately, 70% (wt/wt) of P(3HB) was produced. *Bacillus* spp also accumulate copolymers such as P(3HB-co-3HV), P(3HB-co-3HHx) and terpolymer of 3-hydroxybutyrate, 6-hydroxyhexanoate and 3-hydroxyhexanoate or P(3HB-co-6HHx-co-3HHx) when grown using carbon sources such as butyrate, valerate, hexanoate, octanoate, decanoate and caprolactone (Tajima *et al.,* 2003). Valappil *et al.,* reported the production of P(3HB) by *Bacillus cereus* SPV when grown in Kannan and Rehacek media. *B. cereus* SPV when grown in odd chain fatty acids such as propionate, heptanoate and nonanoate resulted in the production of P(3HB-co-HV). The highest yield of 45.5% (wt/wt) of P(3HB-co-HV) was produced when the bacteria was grown in nonanoate. *B. cereus* SPV when grown in even chain fatty acids such as acetate, hexanoate, decanoate and dodecanoate resulted in the production of P(3HB). The highest yield of 74.5% (wt/wt) of P(3HB) was produced when grown in dodecanoate (Valappil *et al.,* 2007). Other strains of *Bacillus* spp that are involved in the production of PHAs include *B. cereus* INT005, *B. mycoides* RLJB-017 and *B. cereus* UW85.

Alcaligenes latus is a fast growing bacterium that has been widely studied for the production of PHAs. They are able to utilize sucrose as well as the cheap carbon sources such as the sugarcane and beet molasses to produce PHAs. 50% of P(3HB) was obtained using these cheap carbon sources. To improve the yield, *A. latus* was grown in a nutrient limiting medium. Wang and Lee in 1997 carried out an extensive study by allowing *A. latus* to grow in various nutrient limiting conditions such as nitrogen, phosphorus, magnesium and sulphur. They reported that P(3HB) production increased when grown in nutrient limiting condition. A fed batch culture of *A. latus* under nutrient limiting conditions resulted in the accumulation of 88% (wt/wt) of P(3HB) content (Wang and Lee, 1997).

***Pseudomonas* spp** have been used extensively for the production of MCL-PHAs (Diard *et al.*, 2002). They utilize both structurally related and unrelated carbon sources and accumulate diverse MCL-PHA monomer units. *P. putida* produced a copolymer of 3-hydroxydecanoate (3HD), 3-hydroxydodecanoate (3HDD), (3HHx) and (3HO) using glucose as the sole carbon source (Kim *et al.,* 2007). It was reported by Kim *et al.,* that *Pseudomonas* spp produced 3HO as the main monomer unit when grown on fatty acids with even number of carbon atoms. They also reported that *Pseudomonas* spp produced 3-hydroxynonanoate, 3HNN as the main monomer unit when grown on carbon sources with odd number of carbon atoms (Kim *et al.,* 2007). Chen *et al.*, reported that *Pseudomonas* sp DSY-82, *P. stutzeri*, *Pseudomonas* sp. 61-3, and *Pseudomonas* spp A33 accumulated SCL monomer units alongside the MCL monomer units such as P(3HB-co-3HHx) (Chen *et al.*, 2004). This was confirmed when Hang *et al.,* reported that *Pseudomonas* spp such as *P. nitroreducens* produced a copolymer containing SCL and MCL monomer units such as P(3HB-co-3HO) when grown using octanoic acid as the sole carbon source (Hang *et al.,* 2002). A similar observation was made when *P. pseudoalkaligenus* was cultured using octanoic acid as the only carbon source where P(3HB-co-3HO-co-3HD) was produced. This observation suggested that *Pseudomonas* spp were able to accumulate copolymers and terpolymers when grown on structurally related carbon sources. However, this finding was challenged when *Pseudomonas* sp. 61-3 produced copolymers of SCL and MCL monomers when cultured using carbon sources such as glucanoate and other alkanoic acids (Kato *et al.,*, 1996). It has been reported that the organisms producing SCL-MCL copolymers and terpolymers are rare in nature (Kim *et al.,* 2007). Apart from producing copolymers and terpolymers, these *Pseudomonas* spp are also known to produce aliphatic as well as aromatic PHAs when grown on aromatic hydrocarbons (Tobin and O'Connor, 2005). The examples of aromatic and aliphatic PHAs producing *Pseudomonas* spp include *P. putida, P. oleovorans P. citronellolis, P. fluorescens* and *P. jessenii*. In another experiment, *phaC1* and *phaC2* genes from *P. putida* were expressed in *E. coli* for the production of MCL-PHAs. The authors observed that a high level of expression of *phaC* genes were required for a significant production of PHAs. Therefore, they developed a system comprising of a strong heterologous promoter combined with a low copy number plasmid within the *E. coli* which resulted in the production of MCL-PHAs (Ren *et al*., 2005).

1.6 Production of PHAs using inexpensive carbon sources

There has been a great interest in the commercial exploitation of PHAs. However, their high production cost has been the limiting factor. It is a known fact that the expensive carbon sources used for the production of PHAs account for 50% of the total production costs and therefore, reduction in the cost of carbon would automatically lower the cost of production and enhance the commercial viability of PHAs (Kim *et al*., 2000a). The use of inexpensive carbon substrates such as waste by products from the agriculture or food based industry for the production of PHAs has been considered to be the best approach in reducing the production cost. Apart from bringing down the production costs, the utilization of waste material for PHA production would also help in waste management. Previous studies have shown that the use of inexpensive carbon sources for PHA production reduced the overall production cost by approximately 50% (Marangoni *et al*., 2001; Marangoni *et al*., 2002).

1.6.1 SCL-PHA production using vegetable oils as the carbon source

The production of SCL-PHA using inexpensive carbon substrates was first reported by Shimamura and his colleagues in 1994. They observed that *Aeromonas caviae* when grown in unsaponified olive oil resulted in the production of P(3HB-co-3HHx) with an HHx content of less than 20% (Shimamura *et al*., 1994). Fukui and Doi in 1998 reported the production of P(3HB) and P(3HB-co- 3HHx) when the wild type strain of *C. necator* H16 and a recombinant strain of *C. necator* containing the PHA synthase gene of *A. caviae* were cultured in the presence of olive oil, corn and palm oil (Fukui and Doi, 1998). Taniguchi *et al*., utilised waste edible oils and tallow as the carbon source for the production of SCL-PHAs. They observed that *C. necator* when grown in a media containing edible oil produced P(3HB) whereas in a media containing tallow, P(3HB-co-3HV) was produced (Taniguchi *et al*., 2003). Kahar *et al*., demonstrated that the wild type strain of *C. necator* H16 gave higher yield of P(3HB) compared to the recombinant *C. necator* when grown in soybean oil as the sole carbon source (Kahar *et al*., 2004). Furthermore, Loo *et al*., investigated the utilisation of palm kernel oil, palm olein oil, crude palm oil and palm acid oil for the production of PHAs by the recombinant strain of *C. necator* containing the PHA synthase gene of *A. caviae.* They reported the production of P(3HB-co-HHx) containing 5% of the HHx content (Loo *et al*., 2005). Alias and Tan in 2005 isolated a palm oil utilizing Gram negative bacteria named FLP1 from the waste materials of

a palm oil mill. They reported the production of P(3HB) when FLP1 was grown in crude palm oil and palm kernel oil. They also observed that the addition of odd chain fatty acids such as valerate and propionate alongside crude palm oil and palm kernel oil led to the production of copolymers such as P(3HB-co-3HV) (Alias and Tan, 2005). Akiyama *et al*., in 2003, carried out a comparative study to demonstrate that the P(3HB) production by the recombinant strain of *C. necator* containing the PHA synthase gene of *A. caviae* using soybean oil as the sole carbon source. They demonstrated that less energy was required for the production of P(3HB) and a low level of carbon dioxide was emitted compared to the production of P(3HB) using glucose as the main carbon source (Akiyama *et al*., 2003). From these studies, it was evident that a variety of microorganisms were able to utilize vegetable oil as the main carbon source and produce SCL-PHAs. Optimisation of the media, physical parameters and the mode of fermentation for the production of PHAs using vegetable oils as the main carbon source would enhance the economical production of SCL-PHAs.

1.6.2 SCL-PHA production using whey as the carbon source

Whey is a by-product which is generated in large quantities during the manufacture of dairy products such as cheese. It is considered to be a rich substrate for fermentation process. It contains nutrients such as lactose, lipids and proteins (Athanasiadis *et al.,* 2002). Utilisation of whey for the production of PHAs would not only decrease the production cost but also solve the problem of its disposal which is currently a huge environmental concern.

Lee *et al*., reported the production of P(3HB) by the recombinant strain of *E. coli* GCSC 4401 and *E. coli* GCSC 6576 containing the PHA synthase genes of *C. necator* using whey as the carbon substrate (Lee *et al*., 1997). The P(3HB) yield of 4.5 g/L and 5.2 g/L was obtained respectively. Ahn *et al*., demonstrated an increase in the P(3HB) yield obtaining a value of 96.2 g/L. They reported a high P(3HB) yield by the recombinant strain of *E. coli* GCSC 4401, containing the PHA synthase genes of *A. latus,* when grown in whey, under high cell density conditions. This was further improved when these recombinant *E. coli* GCSC 4401 cells were cultured in a cell recycle fed batch mode. The P(3HB) yield of 168 g/L was reported (Ahn *et al*., 2000). Yellore and Desai in 1998, isolated a whey utilising methylbacterium which produced P(3HB), the yield obtained was 1.1 g/L. but the addition of ammonium

sulphate to the whey medium increased the P(3HB) yield from 1.1g/L to 3 g/L. (Yellore and Desai, 1998). Marangoni *et al*., reported the production of P(3HB-co-3HV) by *C. necator* when grown in whey media containing equal proportions of glucose and fructose and the addition of propionic acid at specific intervals. The yield however was 0.17g/L which was quite low (Marangoni *et al*., 2002). Several other organisms such as *Sinorhizobium meliloti* 41, *Hydrogenophaga pseudoflava* DSM 1034, *Azotobacter vinelandii* and *P. cepacia* have been explored for the production of PHAs using whey as the carbon substrate (Povolo and Casella, 2003; Dhanasekar and Viruthagiri, 2005).

1.6.3 SCL-PHA production using molasses

Sucrose rich molasses are generated as a by-product from the crop refining industries such as sugar beet and sugar cane refining industries. Large volume of sugar rich molasses generated at these refining plants has been used as a carbon feedstock for the production of PHAs. Apart from sugar molasses, soy molasses which is a by-product released from the soy processing plants, are rich in sucrose, raffinose and stachyose. Soy molasses can be utilized by the microorganisms containing enzymes such as α-galactosidases and β-furanosidases. The use of molasses as the cheap carbon source for the production of PHAs could also help in their disposal (Solaiman *et al.,* 2006).

Production of a copolymer such as P(3HB-co-HV) was first reported by Page in 1992, when *A. vinelandii* was grown in beet molasses with the addition of valerate (Page, 1992). Bonatto *et al*., 2004 isolated the *Rastolnia pickettii* 61A6 from the subtropical rainforest which produced P(3HB) in a medium containing sugarcane molasses supplemented with vitamins and minerals. However, the polymer yield was very low (Bonatto *et al*., 2004). Jiang *et al*., isolated the strain *P. fluorescens* and cultivated the bacteria in a medium containing sucrose rich sugarcane liquor for the production of P(3HB) (Jiang *et al*., 2008a). The results of the use of molasses as the carbon feedstock for the production of SCL-PHAs have been very encouraging. The optimisation of the fermentation strategy for the increased production of PHAs could help in the commercialization of SCL- PHAs.

1.6.4 SCL-PHA production using biodiesel waste

The waste by product generated during the production of biodiesel or ethanol is rich in glycerol content. This glycerol rich waste effluent is generated in a significant amount and their utilisation as a carbon source for the production of PHA could enhance the market value of the biodiesel production.

Organisms such as *Methylobacterium rhodesianum* and *C. necator* have been reported to have utilised glycerol rich biodiesel waste for the production of P(3HB) (Bormann and Roth, 1999). Ashby *et al.*, demonstrated the production of a low molecular weight P(3HB) by an SCL-PHA producing strain of *Pseudomonas oleovorans* NRRL B-14682 in a basal medium containing biodiesel waste with 30% glycerol content. They reported that the molecular weight of the P(3HB) produced decreased with the increase in the glycerol content in the medium (Ashby *et al.*, 2004). The use of biodiesel waste as the carbon feedstock for fermentation purposes has gained momentum in the last few years. Their use in the production of PHAs has not yet been fully exploited. The increased SCL-PHA production using biodiesel waste would be a huge boost to the economic viability of SCL-PHAs.

1.6.5 MCL-PHA production using triacylglycerols

Apart from the production of SCL-PHAs, the cheap sources of carbon have also been investigated for the production of MCL-PHAs. From literature, it is known that fatty acids are the ideal substrates for the production of MCL-PHAs (Solaiman *et al.*, 2006). Therefore, the use of triacylglycerols directly without the saponification would lead to an economical production of MCL-PHAs.

Cromwick *et al.,* demonstrated that *P. resinovorans* was able to utilise triacylglycerols for the production of MCL-PHAs (Cromwick *et al.,* 1996). Subsequently, the production of MCL-PHAs by *P. resinovorans* using unsaponified fats and oils as the carbon source was carried out by Ashby and Foglia in 1998. They observed that the monomer composition of the polymer produced corresponded to the fatty acid composition of the oil used as the carbon source (Ashby and Foglia, 1998). He *et al.*, reported the production of MCL-PHAs by *P. stutzeri* when grown using soybean oil as the main carbon source (He *et al.*, 1998). Several *Pseudomonas* species such as *P. putida*, *P. oleovorans* and *P. corrugata* were metabolically engineered to utilise triacylglycerols for the production of MCL-PHAs (Solaiman *et al.,* 2006). Fuchtenbusch *et al.*, investigated the use of residual oil

generated during rhamnose production as a carbon feedstock for the production of PHAs. They observed that *P. oleovorans* was able to utilise this residual oil for the production of a heteropolymer comprising of (3HD), (3HO) and (3HDD) units (Fuchtenbusch *et al.*, 2000). These studies confirmed that *Pseudomonas* spp which is commonly used for MCL-PHA production was able to utilize a wide variety of triacylglycerols as the carbon source for the production of MCL-PHAs.

1.6.6 MCL-PHA production using biodiesel waste

Biodiesel waste which is rich in glycerol content have been utilised previously for the production of SCL-PHAs. Similarly, Ashby *et al.*, reported the production of MCL-PHAs by *P. corrugata* using biodiesel waste as the carbon source (Ashby *et al.*, 2004). *P. oleovorans* NRRL B-14682 which produced a low molecular weight SCL-PHA when grown in biodiesel waste was also used for the production of MCL-PHAs. MCL-PHAs produced by *P. oleovorans* NRRL B-14682 using biodiesel waste did not show the trend of decrease in the molecular weight with increase in the glycerol content of the biodiesel waste observed in the case of SCL-PHA production (Ashby *et al.*, 2004). Not many investigations have been carried out to study the use of biodiesel waste as the source of carbon for MCL-PHA production. However, the results obtained have been very encouraging.

1.6.7 MCL-PHA production using molasses

Molasses which is a waste by product generated in the crop refining industries have been explored extensively for the production of SCL-PHAs. However, molasses have not been commonly used as a carbon source for the production of MCL-PHAs. Solaiman *et al.*, identified *P. corrugata* as a molasses utilising strain of *Pseudomonas* for the production of PHAs (Solaiman *et al.*, 2006). The use of molasses as the source of carbon for the MCL-PHA production has not yet been fully exploited. The results of the investigations so far have demonstrated that molasses have a great potential to be used as a carbon source for the increased production of MCL-PHAs.

Several strategies have been employed to bring down the cost of the production of the PHAs. Apart from using the cheap carbon sources, some of the other effective strategies include the use of efficient polymer extraction processes, metabolically

engineered strains, the use of efficient mode of fermentation and the optimisation of the operating conditions using statistical analysis method (Lee and Gilmore, 2005; Follonier *et al*., 2011; Hong *et al*., 2009).

1.7 Synthesis of PHA blends

As discussed earlier, PHAs are biocompatible and biodegradable in nature and therefore, they have been used for various biomedical applications. Due to the differences in their structure, the properties of PHAs vary, with SCL-PHAs such as P(3HB) being highly crystalline, rigid and brittle in nature, whereas MCL-PHAs such as P(3HO) and P(3HHx) being elastomeric in nature with low crystallinity and poor mechanical properties (Misra *et al*., 2006). Inspite of being biodegradable and biocompatible, the brittle nature of P(3HB) and the poor mechanical and thermal properties of the MCL-PHAs limit their potential in the field of regenerative medicine (Wang *et al*., 2002). Therefore, synthesis of blends has generated biomaterials with novel properties to suit various biomedical applications (Yu *et al.,* 2006).

Satoh *et al*., studied the hydrolytic degradation pattern of the P(3HB)/P(3HB-co-3HV) blends. They observed that the presence of P(3HB-co-3HV) influenced the degradation behaviour of P(3HB). They concluded that the degradation rate of the blend films exhibited a linear correlation with the crystallinity (Satoh *et al*., 1994). Chen and Wu in 2005, synthesised a blend of P(3HB) and P(3HB-co-HHx) for tissue engineering applications. They investigated the biocompatibility of the P(3HB)/P(3HB-co-HHx) blends by growing L929 cells on these novel blend films. They observed that there was a significant improvement in the growth of the cells on these blend films compared to neat P(3HB). They also demonstrated that chondrocytes flourished on these blend films compared to neat P(3HB) films (Chen and Wu, 2005). The outcome of these experiments made it evident that intermediate properties suitable for desired applications could be achieved by blending different types of PHAs.

1.7.1 Synthesis of PHA blends with synthetic polymers

Apart from synthesizing blends within the PHA family, several novel blends of PHAs with synthetic biodegradable, non-biodegradable polymers and natural polymers have been created. A lot of research has been done to obtain miscible, low

cost, biocompatible and biodegradable blends and composites with optimum properties suitable for various biomedical applications (Yang and Hu, 2008). Zhang *et al*., synthesized blends of P(3HB) and PLA and studied their miscibility and mechanical properties. They observed that both P(3HB) and PLA were miscible when the sample was melt blended at a high temperature. They concluded that there was a significant enhancement in the mechanical properties of the P(3HB)/PLA blends compared to the neat P(3HB) (Zhang *et al*., 1996). Yoon *et al*., reported a blend of P(3HB) and poly(cis-1,4-isoprene)(PIP) which is a synthetic polymer of amorphous nature. This blend was created to enhance the mechanical properties of P(3HB). However, they found out that P(3HB) and PIP were immiscible. In order to overcome this issue, they grafted poly(vinyl acetate)(PVC) which has a good compatibility with P(3HB), onto PIP which was in turn blended with P(3HB). Mechanical property such as the tensile strength of the PHB/PIP-g-PVC blend was found to be higher compared to the P(3HB)/PIP blends (Yoon *et al*., 1999).

Ikejima *et al*., investigated the hydrolytic degradation properties of P(3HB) and polyvinyl alcohol (PVA). They demonstrated that the degradation rate of the blends was influenced by their surface properties. They also demonstrated that the degradation rate of the P(3HB)/PLA blend was higher compared to the degradation rate of the neat P(3HB) and neat PVA (Ikejima *et al*., 1998). Huang *et al*., studied the miscibility of the blends of P(3HB) and 80% hydrolyzed PVA. P(3HB)/PVA blend was created to improve the mechanical properties of P(3HB) by reducing the brittleness, crystallinity and high melting temperature which limits the use of P(3HB). PVA is hydrophilic and biodegradable in nature. They observed that P(3HB) and PVA were miscible when the concentration of P(3HB) in the blend was less that 20 wt% (Huang *et al*., 2005).

Blends of P(3HB) with non-biodegradable poly(ethylene oxide)(PEO) has also been studied. They have been found to have excellent compatibility with P(3HB) (Park *et al*., 2001). Duarte *et al*., blended P(3HB) with poly(ε-caprolactone) (PCL), a semi crystalline polymer with a glass transition temperature of -70℃. Their aim was to synthesize a novel blend with high flexibility, ideal for use in the packaging industry. They demonstrated that the P(3HB)/PCL blends had a low crystallinity and high elongation at break values confirming that P(3HB)/PCL blends were highly flexible (Duarte *et al*., 2006). P(3HB-co-3HHx) with the HHx content of 11 mol% was blended with PEO to improve the mechanical properties of P(3HB-co-3HHx). It was

found that the blend was miscible in the amorphous state when the concentration of PEO in the blend was lesser than 20 wt%. The mechanical properties of the P(3HB-co-3HHx)/PEO was significantly improved when the concentration of PEO in the blend was within the range of 5-17% (Yu *et al*., 2009). P(3HO) is a type of MCL-PHA. It is elastomeric in nature with low crystallinity, low melting temperature and poor mechanical properties. From literature, it is known that PHAs are hydrophobic in nature and therefore, the hydrolytic degradation of P(3HO) is very slow. In order to improve the physical properties and the degradation rate of P(3HO), it was blended with PLA. Novel blends with increased degradation rates were obtained (Takagi *et al*., 2004).

In another study, P(3HB-co-3HV) was combined with PLA via bicomponent melt spinning to obtain fibres with enhanced functional properties relevant for various applications. The authors successfully spun fibres with P(3HB-co-3HV) core and PLA sheath which demonstrated enhanced mechanical properties as well as cytocompatibility (Hufenus *et al*., 2012).

1.7.2 Synthesis of PHA blends with natural polymers

Natural polymers such as starch, cellulose and protein based polymers such as collagen, are biodegradable and renewable in nature. The formation of blends and composites of PHAs with these natural polymers has attracted a lot of attention in the recent times.

Parulekar and Mohanty in 2007 developed a novel flexible biomaterial by blending plasticized starch derived from the plant source and P(3HB-co-3HV). The most common plasticizer used for starch is glycerol. Amylose rich starch plasticized with glycerol was blended with P(3HB-co-3HV) using a process engineering technique and cast into films by extrusion (Parulekar and Mohanty, 2007). Reis *et al*., studied the blends of PHBV with varying percentages of corn starch. They characterised the microstructural, mechanical and chemical properties of the resulting P(3HB-co-3HV)/starch blends. Chemical analysis using Fourier Transform Infrared Spectroscopy (FTIR) confirmed that there was no chemical interaction between the P(3HB-co-3HV) and the starch and hence, the blend was considered to be immiscible in nature. The blends exhibited poor crystalline properties. The mechanical properties such as the tensile strength and the Young's Modulus decreased with the increase in the content of starch within the blend (Reis *et al*.,

2008). Rubber is another type of a natural polymer which is biodegradable, highly elastomeric and has a high melting point. It was blended with varying concentrations of MCL-PHAs which is known to have a low melting temperature and crystallinity. These blends were synthesized to obtain biomaterials with desired properties such has high melting temperature, high ductility and a low crystallinity. The resulting MCL-PHA/rubber blend had a high melting temperature. The mechanical properties of these blends were not characterised (Bhatt *et al.,* 2008).

1.7.3 Cellulose

In recent times, there has been a great interest in utilising natural fibres as the reinforcement material to enhance the mechanical properties of the biodegradable polymers. One of the most commonly used reinforcing elements is cellulose. It is a major component of the plant biomass and an extracellular polymer in microorganisms belonging to the genera *Acetobacter, Rhizobium, Agrobacterium,* and *Sarcina.* The major difference between plant and bacterial cellulose is the absence of hemicelluloses and lignin residues in the latter which makes them highly pure (Soykeabkaew *et al*., 2009). Cellulose is a naturally occurring polymer made up of glucose monomer units. The glucose molecules are linked with each other by β (1-4) glycosidic linkages. They possess excellent mechanical properties such as modulus ranging around 16.9 GPa and the tensile strength around 2 GPa.

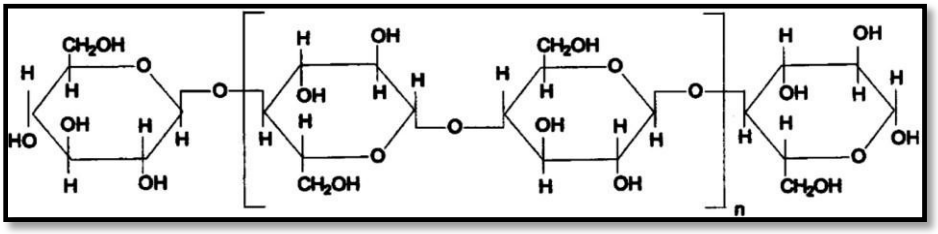

Figure 1.7: Structure of cellulose (Soykeabkaew *et al*., 2009)

Due to its excellent mechanical properties, hydrophilic nature and most importantly, its biodegradability, bacterial cellulose has been widely used as a reinforcement material in the synthesis of novel composite materials (Klemm *et al*., 2001). Grunert and Winter in 2000, synthesized novel nanocomposites with polydimethylsiloxane and bacterial cellulose where the storage modulus of pure polydimethylsiloxane was increased two times with the addition of bacterial cellulose (Grunert and Winter, 2000). Similarly, bacterial cellulose reinforced epoxy

resin composite also exhibited dramatic improvement in its mechanical properties (Gabr *et al*., 2010). Jiang *et al.,* synthesized novel poly(3-hydroxybutyrate-*co*-3-hydroxyvalerate)/cellulose nanowhisker composites where there was an increase in the tensile strength as well as the Young's modulus (Jiang *et al*., 2008b). Polylactic acid reinforced with cellulose nanowhiskers obtained by acid hydrolysis showed an improvement in the Young's modulus and tensile strength (Bondeson *et al*., 2006). Cellulose has therefore, proven to be one of the finest natural fibres to be used for reinforcements.

1.8 Applications of PHAs

1.8.1 Tissue Engineering:

Tissue engineering is an emerging field that combines the principles of engineering and life sciences to address the issues related with the currently available therapeutic treatments. There are several restorative options available to treat the incidence of tissue loss and organ failure. The most promising ones include organ transplantation from a healthy donor, tissue transfer from the healthy site to replace the diseased and the use of prosthetics or other mechanical devices such as dialysis machine or a pacemaker. There have been major advances in the healthcare system since the introduction of these therapeutic treatments. However, there are several issues related with these treatments. The major issues have been the shortage of the organ donors, the lifelong dependency of the patients on immunosuppressant, organ rejection, donor-site issues, infection, lack of biocompatibility and the durability of the mechanical devices. In recent times, tissue engineering has emerged as a potential solution to these issues (Nugent and Edelman, 2003). The basic concept of tissue engineering is to facilitate the growth of the isolated cells on the scaffolds that enhance the proliferation of these cells and allows them to develop into desired tissues and organs prior to the implantation (Shieh and Vacanti, 2005).

The function of the scaffold is to provide the cells with an anchorage by mimicking the biomechanical profile of the replacement tissue. There are several synthetic and non synthetic biodegradable polymers that have been used for the development of scaffolds. Characteristics of an ideal scaffold used for tissue regeneration include biocompatibility, controllable degradation rate, microstructural and material

properties that enhance cell growth, proliferation and differentiation. PHAs have been used to produce scaffolds for tissue engineering due to their excellent biocompatibility and biodegradability (Shieh and Vacanti, 2005; Martina and Hutmacher, 2007; Ravichandran *et al*., 2012).

1.8.2 Bone tissue engineering

Bone tissue engineering is an emerging field of research that has come forward with an idea of generating new bone tissue to be used for the treatment of diseases such as osteoarthritis, osteomyelitis, osteoporosis and spine arthrodesis. There is a huge economic and clinical impact of the success of bone tissue engineering. It is a known fact that defective bone over the critical size is unable to heal on its own, therefore, a substitute material is filled in place of the defective bone to restore normal function. The options available for the treatment of bone defects include autogenous bone grafting, use of allografts and xenotransplantation. However, they are associated with high risk of infection, donor site morbidity, toxicity and pain. Bone tissue engineering merges engineering principles with the body's mechanism of response to tissue damage. This has led to the development of synthetic bioactive scaffolds with excellent mechanical properties, accurate architecture to promote vascularisation, biocompatibility, biodegradability and most importantly, the ability to promote osteogenic differentiation (Nugent and Edelman,, 2003; Vara *et al*., 2005).

1.8.3 PHAs in bone tissue engineering

As mentioned previously, Poly 3-hydroxybutyrate P(3HB) is one of the most extensively studied polyhydroxyalkanoate. P(3HB) has excellent mechanical properties for bone tissue engineering, with high crystallinity and tensile strength. It is biodegradable and biocompatible in nature. In another experiment, P(3HB) composites with hydroxyapatite (HA) were synthesized and implanted for a period of 12 months. During the implantation period, it was established that P(3HB) based materials produced constructive bone tissue adaptation response. As a result, a layer of apatite surface was formed demonstrating the bioactivity of the HA/P(3HB) composites. There was no indication of inflammatory response during the implantation period (Doyle *et al*., 1991). Knowles *et al*., performed extensive studies on composite implants composed of P(3HB)/HA in the femur of Japanese

white rabbits to evaluate the interaction between the tissues and the implants. Histological evidence showed an increased bone growth (Knowles *et al*., 1992). Similar experiments using copolymers of 3-hydroxybutyrate and 3-hydroxyvalerate P(3HB-co-3HV) and tricalcium phosphate (TCP) were carried out. A bone like layer of HA crystallites was formed on the implant interface after implantation, indicating bone regeneration (Shishatskaya *et al*., 2002). Galego *et al*., reported that the mechanical strength of P(3HB)/HA and P(3HB-co-3HV)/HA was equivalent to the human bones and therefore could play a key role in fracture fixation (Galego *et al*., 2000).

Zheng *et al*., reported that porous composites of P(3HB-co-3HV) and sol-gel bioactive glass (SGBG) when immersed in simulated body fluid(SBF) for 12 hours indicated the formation of hydroxyl carbonate apatite layer on the surface of P(3HB-co-3HV)/SGBG scaffold (Zheng *et al*., 2003). Similarly, Al-Salihi and Samsudin in 2004, tested the composites of P(3HB) with coral powder for bone tissue engineering. They concluded that the P(3HB)/coral composites had excellent pore sizes that facilitated the vascular invasion and bone development. They also established that the materials based on P(3HB) had higher biocompatibility compared to the HA and coral (Al-Salihi and Samsudin, 2004).

Misra *et al*., tested the multifunctional composite scaffold made up of P(3HB) and nanobioglass particles (nBG) to evaluate their bioactivity and biocompatibility. These P(3HB)/nBG scaffolds were implanted into the rats subcutaneously for a period of seven days. There was no evidence of inflammatory response and in addition, these composite scaffolds also demonstrated bactericidal properties when tested for the growth of *Staphylococcus aureus* (Misra *et al*., 2008).

In another study, composites of P(3HB) and HA were synthesized and implanted into the rabbit bone for a period of 90 days. They were monitored for osteoconduction, osteointegration and biocompatibility. The results of the experiment demonstrated that there was no evidence of inflammation throughout the period of implantation, the composites were osteoconductive and they also showed signs of biodegradability (Carlo *et al*., 2009). Composites of P(3HB-co-3HV) with violacein, which is an antitumor agent was synthesized and implanted in to the femur of Wister rats for a period of 60 days. The histological evidence demonstrated that there was no inflammatory response and there was new bone regeneration on the implants (Rambo *et al*., 2012).

Apart from, P(3HB) and P(3HB-co-3HV), a copolymer of 3-hydroxybutyrate and 3-hydroxyhexanoate P(3HB-co-3HHx) has also been investigated for bone tissue engineering applications. P(3HB-co-3HHx) scaffold was found to be an excellent biomaterial for the proliferation of bone marrow cells. The cell viability rate on the P3HB-co-3HHx scaffolds was 40% higher than on P(3HB) and 60% higher than on PLA, after an incubation period of 10 days (Wang *et al*., 2004). However, one of the problems associated with P(3HB-co-3HHx) was that the incorporation of HA particles into P(3HB-co-3HHx) scaffold using salt leaching technique did not lead to the enhancement of the mechanical properties. By varying the HHx content in P(3HB-co-3HHx), a range of polymer surface properties can be achieved. Better proliferation of chondrocytes was achieved on the P(3HB-co-3HHx) /P(3HB) scaffold compared to the P(3HB) scaffold on its own (Deng *et al*., 2002).

Results of the investigations carried out by various researchers have shown that PHAs such as P(3HB), P(3HB-co-3HV) and P(3HB-co-3HHx), their composites and blends have properties that are relevant for bone tissue engineering.

1.8.4 Cardiovascular tissue engineering

Loss of cardiovascular function can be restored by surgical restoration, organ transplantation, the use of advanced drugs and mechanical devices. These treatments have improved the quality of human health. However, cardiovascular dysfunction continues to be fatal. Shortage of the organ donors and the compatibility issues related with transplantation has made these procedures very rare. Cardiovascular tissue engineering has emerged as a potential solution to treat the injured cardiac muscle or a blocked artery to restore the cardiovascular function. Development of tissue engineered conduits, replacement heart valves and cellular cardiomyoplasty to heal the injured myocardium has been promising. Apart from being used widely for bone tissue engineering, PHAs have also been used in several cardiovascular applications such as in the development of cardiac stents, pericardial patches, vascular grafts, artery augments and implants. The extensive range of applications of PHAs is due to diverse physical properties within the PHA family (Nerem and Seliktar, 2001; Vara *et al*., 2005; Grabow *et al*., 2007).

1.8.5 PHAs in cardiovascular tissue engineering

P(4HB) or poly(4-hydroxybutyrate) which has elastomeric properties was one of the first PHAs to be used in cardiovascular tissue engineering for myocardial repair. However, its rapid degradation in *in vivo* conditions made it an unlikely choice for this application (Chen and Wu, 2005). Another such PHA to be used in cardiovascular application was poly(3-hydroxybutyrate-co-3-hydroxyvalerate) or P(3HB-co-3HV). It was used along side polylactic acid and polyglycerol sebacate to form electrospun fibre materials to form a pericardial patch for myocardium repair. They were successful in making macroporous tubing to create a pericardial patch using these electrospun fibres (Kenar *et al*., 2010).

Stock *et al*., carried out a successful experiment where he implanted a P(3HO) polymer implant in the pulmonary artery of the sheep to replace the native pulmonary valve and the artery. They concluded that there was no thrombosis or stenosis at the end of the experimental period of 24 weeks. The P(3HO) patch seeded with autologous cells had an organized cell accumulation at the end of the experiment (Stock *et al*., 2000). Sodian *et al.,* designed a biocompatible and biodegradable trileaflet heart valve made up of porous P(3HO) seeded with an endothelial cell line. They utilised the salt leaching technique to synthesise these three dimensional porous scaffolds. They synthesised around ten heart valve scaffolds and seeded them with vascular cells for *in vitro* testing. They observed a confluent layer of cells on the scaffold. One of the unique characteristics of the P(3HO) trileaflet heart valve was that it was able to mould itself without being sutured to the conduit. They demonstrated that P(3HO) was an ideal candidate to be used for the development of heart valves (Sodian *et al.,* 2000).

Cheng *et al.,* carried out an experiment using a PHA scaffold for smooth muscle proliferation to evaluate its use in the development of artificial blood vessels. Poly(3-hydroxybutyrate-co-4-hydroxybutyrate) was the chosen material for the formation of elastin in rabbit blood vessel smooth muscle cells. They concluded that poly(3-hydroxybutyrate-co-4-hydroxybutyrate) with 20mol% 4HB showed an increase of 160% elastin compared to poly(3-hydroxybutyrate-co-hydroxyhexanoate) which has been extensively studied for this application and they could be potential materials for the development of artificial blood vessels (Cheng *et al.,* 2008).

Long term degrading elastomeric PHAs have been proven to be used widely in cardiovascular applications and have proven to be the best suited material due to their long term *in vivo* degradation property.

1.9 Endothelial cell micropatterning

Endothelial cells form the inner lining of the blood vessel wall. They act as an interface between blood and the vessel wall. It is very crucial to maintain a healthy endothelium layer to avoid any kind of vascular dysfunction. Extensive studies have been carried out to understand the function and the behaviour of the endothelial cells. Recent studies have shown that the endothelial cells alter their morphology and phenotype in response to the blood flow. Endothelial cells demonstrated healthy elongated morphology under unidirectional smooth flow whereas under disturbed flow, endothelial cells exhibited thrombogenic cobblestone morphology (Uttayarat *et* al., 2008; Anderson and Hinds, 2011). In the last few years, micropatterning techniques have been utilised to alter the morphology of the endothelial cells under *in vitro* conditions. This technique involves the fabrication of the scaffold or the cell-substrate by creating definite microtopographical features on the surface that allows the cells to adhere and migrate in an aligned pattern (Thery, 2010). From literature, it is known that the surface topography determines the biocompatibility of a biomaterial. Surface topography and chemistry govern various important processes such as protein adsorption, cell adhesion and migration (Duncan *et al*., 2007). The micropatterning technique creates a tissue like environment within the *in vitro* culture. It has made it easier for the researchers to study the interaction between cells and the surface topography which acts as the microenvironmental cue. Apart from causing a change in the morphology of the endothelial cells, micropatterning technique can also modify other cell processes such as their adhesion, proliferation, and their function. This technique has been very useful in studying the interaction between the cells and their method of proliferation. The use of this technique in the development of tissue engineered constructs is still in its initial phase (Thery, 2010; Anderson and Hinds, 2011). At present, there are several micropatterning techniques that are being utilised to understand the morphology of the cells such as microcontact printing, photopatterning and laser micropatterning.

- **Microcontact printing**: This is one of the most commonly used micropatterning technique. It utilises cytophobic and cytophilic adsorbed coatings to direct the attachment of the cells on the substrate. Microcontact printing involves the use of polydimethylsiloxane (PDMS) with the desired surface features as a stamp. This patterned PDMS stamp is then pressed against scaffold or the cell substrate to transfer the pattern. The endothelial cells are then cultured on these patterned substrates. Even though this technique has been widely used, it has several drawbacks such as its inconsistency in the quality of the protein transfer and the requirement of an additional step of fabricating the stamp prior to the final printing step (Thery, 2010; Anderson and Hinds, 2011).

- **Photopatterning**: This method uses Ultraviolet (UV) light to fabricate the surface of the scaffold used for cell culture. UV irradiation causes the polymerization or the detachment of different molecules present on the surface of the substrate. In order to control the UV exposure spatially, a photo mask is placed on top of the substrate. This photo mask is also used to filter the UV light to prevent over exposure of the sample to UV light. This technique is often very flexible, reproducible and a large area of the substrate can be fabricated at a time. However, it also has some drawbacks such as the requirement of specialized equipment which are not available readily and the requirement of photosensitisers which are highly incompatible (Thery, 2010; Anderson and Hinds, 2011).

- **Laser micropatterning**: This technique has gained popularity in the recent years. It involves the use of UV light with a wavelength around 200nm from the laser source. One of the greatest advantages of this technique is that it does not require any photosensitisers and hence allows direct patterning of the biomaterials. The only disadvantage of using this technique is the requirement of expensive specialized equipment (Thery, 2010; Anderson and Hinds, 2011).

1.9.1 Use of laser micropatterning for medical applications

Laser micropatterning is one of the well established techniques used for surface fabrication. It has been used to fabricate different vascular grafts, stents and tissue engineering scaffolds. The use of this technique in medical research has gained momentum in the last few years due to its ease of handling, time efficiency and its ability to produce various micropatterns. Several investigations have been made to determine the role of laser micropatterning technique in understanding the cell-substrate relationship.

Li *et al*., used laser micropatterning to fabricate the thermanox film for their potential application in the development of small diameter vessels. Grooves of width 1.2 μm – 9.7 μm, groove depth and the ridge depth of 0.4 μm – 1.3 μm were created. Mouse fibroblast cell line L929 was grown on these laser modified surface. They observed that the cells exhibited elongated morphology in narrow grooves compared to the cells in wider grooves that exhibited triangular morphology. They concluded that the microstructures on the surface of the film had an effect on the morphology and the orientation of the cells (Li *et al*., 2003). In another similar experiment, Rebollar *et al*., used KrF laser of 248 nm wavelength to fabricate the surface of polystyrene. The laser modified surface was analysed using Atomic force microscopy. They cultured Human embryonic kidney cells (HEK-293) on the modified as well as the unmodified polystyrene surface. They observed that cell adhesion on the micropatterned surface was significantly higher compared to the unmodified surface. Along with this, they also carried out an experiment on cell alignment by culturing Chinese Hamster Ovary cells (CHO-K1) as well as skeletal myoblast cells. They observed that the cells aligned themselves following the micropattern on the polystyrene surface. They concluded that the micropatterns on the cell substrate affect the adhesion, proliferation and alignment (Rebollar *et al*., 2008).

Mikulikova *et al*., carried out an experiment where they modified the surface of polytetrafluroethylene (PTFE) using a laser beam of the wavelength 172 nm. They cultured Human embryonic kidney cells (HEK) on these laser modified surfaces to study the behaviour of the cells on the micropatterned substrate. The cell proliferation was measured using the Neutral Red Assay. They observed that the cells adhered on the micropatterned surfaces and proliferated. They stated that the

increase in hydrophilicity of the laser modified surface resulted in an increase in the protein adsorption, hence lead to increased cell proliferation (Mikulikova *et al*., 2005). Yu *et al*., studied the interaction of the cells with a micropatterned surface. They altered the surface of the polycarbonate substrate using the Laser ablation technique. They generated two different types of the micropatterns, line micropatterns and the point micropatterns. On these micropatterned surfaces they cultured Human pulmonary fibroblast cells. They made an interesting observation that cells cultured on the line micropatterns exhibited alignment following the micropatterns whereas the cells cultured on the point micropatterns had no definite orientation (Yu *et al*., 2005). Similar observation was made by Duncan *et al*., when they carried out an experiment where they modified the surface of PTFE disks using computer controlled cold laser KrF beam coupled with a microlithographic projection technique. They designed parallel microgrooves of 3--30 μm deep, 1-10 μm wide and 3-30 μm apart. They cultured Human umbilical vein endothelial cells (HUVEC) on these laser modified PTFE surfaces to determine their potential for applications such as biosensors, tissue engineering scaffolds and vascular grafts. They observed that the cells aligned themselves based on the microgrooves on the modified surface (Duncan *et al*., 2007).

Isenberg *et al*., used micropatterned polystyrene substrates to generate cell sheets with definite extracellular matrix and cellular organization. They cultured vascular smooth muscle cells on the micropatterned substrate to generate intact cell sheets. They observed that the cells demonstrated strong alignment based on the micropattern and successfully generated cell sheets (Isenberg *et al*., 2008).

Laser micropatterning has thus proven to be a valuable technique for various biomedical applications. This technique has not yet been fully exploited and has a great potential.

1.10 Drug Delivery

New and innovative local drug delivery systems have been developed in recent times to replace the conventional mode of drug administration. One of the major issues associated with the conventional dosage system is a requirement of higher dosage of drug to elicit a pharmacological response causing a number of side effects (Pouton and Akhtar, 1996).

The basic concept of a local drug delivery system includes the encapsulation of a drug or an active ingredient within a material and its delivery to the target cells or tissues within the body. This method prevents the healthy cells and tissue being exposed to the drug and also maintains lower incidence of toxicity in the plasma. An ideal drug carrier protects the drug from being degraded, delivers the drug to the site of action, reduces the toxicity and degrades away after the delivery into non toxic degradation products. Several synthetic and non synthetic biodegradable polymers have been used as drug carriers (Pouton and Akhtar, 1996).

1.10.1 Mechanism of drug release

The drug encapsulated within the carrier is released via three different mechanisms namely:

1. Osmosis
2. Diffusion
3. Degradation

Osmotic release: This type of release occurs when the drug or the active pharmaceutical ingredient is present within the core of the carrier. The drug is released from within the core by osmosis. Osmotic release is usually appropriate for the conventional oral administration where the drug is in a tablet form and is covered by another layer of a semi-permeable membrane. This semi permeable membrane is usually made up of cellulosic material. When the tablet comes in contact with the water, it absorbs the water through the pores building a hydrostatic force. This force causes the drug to be released through the membrane. Burst release phenomenon is observed in this type of release which is followed by slow release (Dash and Suryanarayanan, 1992).

Diffusion: Concentration gradient is the main force driving this kind of release. The drug present within the carrier is released in the body by dissolution which is followed by diffusion. Solubility of the drug in the aqueous environment also plays an important role. In this case hydrophilic drugs are released via burst release phenomenon whereas hydrophobic drugs or a drug with very low water solubility is not released at all (Dash and Suryanarayanan, 1992).

Degradation: In this kind of release, the drug is released in the body when the carrier is degraded via hydrolysis. The degradation occurs in two different ways

such as bulk and surface erosion. Bulk degradation occurs when the rate of water absorption is faster than the rate of degradation while surface erosion occurs when the rate of degradation is faster than the rate of water absorption within the bulk of the polymer (Dash and Suryanarayanan, 1992).

1.10.2 PHAs in drug delivery

Naturally derived polymers such as polyhydroxyalkanoates (PHAs) are attractive for the development of drug delivery systems for a number of reasons. Primarily, they are readily available and relatively inexpensive. In addition, they are biocompatible in nature (Chasin and Langer, 1990). Akhtar and Pouton in 1996, reviewing the potential of using PHAs as drug delivery systems highlighted the possible benefits of using a biosynthetic rather than a chemically synthesised polymer. They argued that a biosynthetic PHA, devoid of chemical catalysts and initiators is more likely to make a safer pharmaceutical product than their synthetic counterparts. Furthermore, the involvement of microbial enzymes in the production of PHAs is likely to result in more reliable consistent polymer, from a stereochemical point of view, thus ensuring highly reproducible physical properties (Pouton and Akhtar, 1996).

Of all the properties that make PHAs a preferred material for drug delivery systems, their slow biodegradability and high biocompatibility are the main characteristics that give them an edge over other polymers. With respect to the *in vivo* degradation, available data to explain this process is quite limited. Gogolewski *et al*., compared the fate of poly-lactides to PHAs such as P(3HB) and P (3HB-co-3HV). They recorded 50% degradation for the poly-lactides compared to less than 1.6% degradation in the PHAs over a period of 6 months. The slow degradation rate of PHAs *in vivo* is the basis for current exploitation of PHAs for the design of long acting drug formulations (Gogolewski *et al*., 1993). Biocompatibility has been defined as the effects of the physiological environment on the polymer and the effect of the polymer on that same environment. Several studies have confirmed the toxicological acceptability and biocompatibility of PHAs. Lafferty *et al*., demonstrated that P(3HB) did not affect cell metabolism or growth by measuring glucose consumption and lactate production when compressed P(3HB) tablets were exposed to mice fibroblast cells in a culture (Lafferty *et al*., 1988).

The efficacy of PHAs in designing drug delivery systems would most likely be seen in parenterally administered polymeric carrier systems, where the active drug is usually encapsulated in or conjugated onto a polymeric device. This is because most of the barriers to drug delivery presented by such phenomena such as poor solubility, rapid breakdown of drug *in vivo*, unfavourable pharmacokinetics and lack of selectivity for target tissues, to a large extent are surmounted when carrier delivery systems are employed (Allen and Cullis, 2004).

Another interesting aspect of PHAs as materials for drug delivery is their drug targeting potential. Yao *et al*., attached $PhaP_{Re}$ originally expressed from *C. necator* fused with cell specific receptor proteins to the hydrophobic surface of PHA nanoparticles for targeted drug delivery. Both *in vivo* and *in vitro* studies demonstrated a preferential uptake of drug within this delivery system by hepatocellular carcinoma cells highlighting the targeting potential of these biopolymers (Yao *et al*., 2008).

Besides parenterally administered drugs, PHAs could also be used to enhance the performance of other dosage forms such as oral suspensions for paediatric use. There are presently many paediatric oral dosage forms that are faced with significant stability issues. An example is the artemisinin-based oral suspension which is vital for treating malaria in children (Gabriels and Plaizier-Vercammen, 2004). Oral suspensions containing drug encapsulated in PHA microspheres, when thoroughly studied, could greatly improve the stability of these vital dosage forms.

Finally, transdermal drug delivery systems made of PHAs is another area with future potential. PHAs have been shown to provide suitable adhesiveness and drug permeation required for optimal performance of patches as drug delivery systems (Wang *et al*, 2003). Wang *et al*., suggested the possibility of exploiting interaction between active drug and various functional groups in the side chains of PHA for the construction of clinically useful transdermal drug delivery system (TDDS). Since the production conditions such as carbon sources utilised, to a large extent determine the functional groups present in the side chains of these polymer, the prospect of clinically useful PHA patches look very promising (Wang *et al*., 2003).

1.11 Coronary Artery disease (CAD)

Coronary artery disease is a type of a cardiovascular disease where the artery gets narrowed or blocked obstructing the normal blood flow. The blockage in the artery occurs due to the accumulation of lipids and cholesterol within the arterial wall. Due to this, the lumen of the artery becomes narrow restricting the blood flow to the other parts of the heart. This leads to the inadequate supply of oxygen resulting in coronary occlusion or myocardial infarction. CAD is still considered to be one of the major causes of death in the developed world. There are several treatment options that are available to restore the arterial function such as the intake of therapeutic agents coupled with lifestyle changes, invasive treatments such as coronary artery bypass graft (CABG) and minimally invasive techniques such as percutaneous transluminal coronary angioplasty (PTCA). Balloon angioplasty is the most common type of PTCA used to treat CAD. However, the main drawback of using PTCA is the renarrowing of the vessel wall. These narrowed arteries are widened by using a stent (Libby *et al*., 2002; Grabow *et al*., 2007; Basnett and Roy, 2010).

1.11.1 Coronary stent: A stent is a scaffold that is inserted or placed within the diseased or narrowed coronary artery to restore its function. The stent is guided into the artery using a catheter. The major function of a stent is to broaden the blocked or narrowed artery so that normal blood flow is restored. The desirable properties of an ideal stent include

- Biodegradability to avoid its lifelong presence within the body
- Flexibility to ease the insertion into the artery
- High tensile strength, ductility and radial strength to prevent stent recoiling after placement
- Ability to encapsulate and release drugs to prevent restenosis or the reoccurrence of the blockage.

In recent years, stents have undergone a rapid evolution from the bare metal stents to polymer coated, drug eluting, biodegradable metallic stents, to the biodegradable polymeric stents. Biodegradable stents have several advantages over the commercially available metal stents. They are less obtrusive compared to the metal stents that is known to rupture the artery during its placement that later results in restenosis. As the name suggests, biodegradable stents degrade into non toxic

degradation products after completing their function and therefore do not remain in the body for a lifetime like the metal stents. Biodegradable stents have an added advantage over the metal stents, which is their ability to encapsulate and deliver drugs. However, a major disadvantage that has hindered the commercialization of these biodegradable stents is their poor mechanical properties (Basnett and Roy, 2010; Cantor *et al*., 2000).

1.11.2 Biodegradable coronary stents*:* Researchers have stated that a stent is no longer required within the artery after complete vascular healing is achieved. In the case of bare metal stents and the polymer coated metal stents, they remain in the body for a lifetime interfering with the patient's wellbeing. Biodegradable stents on the other hand could be completely degraded into nontoxic degradation products after completing their function. Biodegradable stents are designed to provide support to the injured artery for a short period of time, therefore the long-term structural stability of these stents is not a huge concern. However, it is still a challenge to design a stent with an ideal geometry using complex polymeric materials. Apart from the inferior mechanical properties, the limited number of design tools available for stent design, also hinders the success of these biodegradable stents (Moore *et al*., 2010).

1.11.2.1 History

The development of the first biodegradable stent was reported by Stack *et al*., 1988 at Duke University. They constructed a self-expanding open mesh stent structure using Polylactic acid (PLA) which is a synthetic biodegradable polymer. This was designed to withstand high pressure in order to prevent the loss of its radial strength after implantation. The implantation of this stent into an animal model led to an inflammatory response. There was an evidence of minimal thrombosis and neointimal growth and no further clinical tests were carried out (Stack *et al*., 1988). Agrawal and Clark, 1992 successfully deployed a PLA stent into the femoral arteries of dogs. The stent was able to withstand the pressure and maintain its structural stability. However, there was evidence of inflammatory response (Agrawal and Clark, 1992). Bier *et al*., 1992 developed a self–expanding stent made up of Type I collagen which is a naturally occurring polymer. However, this attempt was unsuccessful due to poor stent design, which failed to maintain its structural stability, and collapsed upon implantation (Bier *et al*., 1992). Tamai *et al*., successfully designed a zig-zag, balloon expandable biodegradable stent made up of

PLA which required heat setting to install the geometry. The results of the trials conducted in animals were successful. This was the first biodegradable stent that was deployed in humans and was able to provide a substantial follow up data upon its implantation in the human coronary artery. At the end of one year, the results showed that there was 10.5% restenosis. This stent failed to commercialize due to the issues over heat setting that was required during the deployment (Tamai *et al.*, 2000). These attempts of developing a commercially viable stent were unsuccessful which has led to extensive research to find the ideal biodegradable stent.

1.11.2.2 Abbot's biodegradable vascular scaffold (BVS)

Currently, there are several medical companies that are working on the development of an ideal biodegradable polymeric stents. The most promising effort has been by the Abbot vascular, USA that developed Everolimus eluting biodegradable polymeric stent made up of polylactide called Abbot's biodegradable vascular scaffold (BVS). Their first phase of clinical trials involved the implantation of BVS into 30 patients. The results of their 2 year follow up were encouraging even though the 6 month follow up results showed that there was 16% reduction in the size of the lumen due to stent recoil. It was claimed that the success rate of the BVS deployment into the patients was 94%. BVS was fully degraded at the end of 2 years after implantation. Their second phase of clinical trials involved the implantation of BVS into 101 patients in Europe, Australia and New Zealand. The results of their three years follow up were positive (Moore *et al.*, 2010). This led to their third phase of clinical trials involving 1000 patients. Abbot's BVS was used in the UK for the first time at the Royal Brompton hospital to treat a patient with coronary artery disease in October 2012.

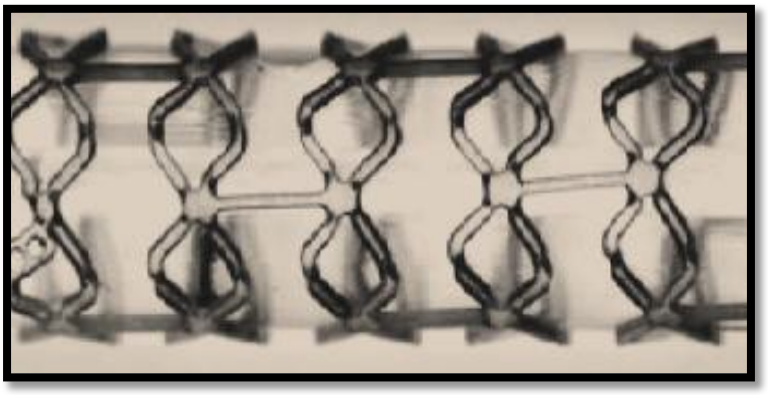

Figure 1.8: Abbot's biodegradable vascular scaffold (BVS) (Moore *et al.*, 2010)

1.11.2.3 REVA stent

REVA medical Inc. has developed a biodegradable polymeric stent made up of L-tyrosine. They have stated that this stent is biocompatible and is completely absorbed within 18 months of implantation into non-toxic degradation products which is eliminated from the body through a metabolic pathway. Preliminary trial results showed that there was there were no signs of inflammatory response or in stent restenosis. The novelty of the REVA stent is their unique slide and lock design that allows them to maintain their structural stability. Since, the acquisition of REVA Medical Inc. by the Boston Scientific, active work on the manufacture of paclitaxel releasing REVA stent has been on going (Moore *et al*., 2010).

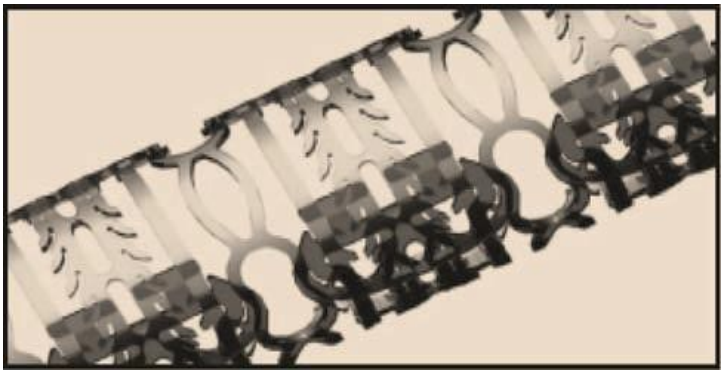

Figure 1.9: REVA stent with the unique slide and lock design (Moore *et al*., 2010)

Researchers at the University of Texas, Arlington developed a stent impregnated with recombinant adenovirus vectors carrying nuclear localizing βGal reporter gene. The stent was made up of the polymer fibres. However, this stent has only been tested in the animal models and has not yet been implanted in humans (Moore *et al*., 2010).

1.11.2.4 PHAs in stent development

P(3HB) was used in the development of a biodegradable stent. Unverdorben *et al*., developed a biodegradable P(3HB) stent and implanted it into the iliac arteries of the rabbits. The follow up results demonstrated inflammatory reactions (Unverdorben *et al*., 2002). Grabow *et al*., developed a laser machined biodegradable, balloon expandable slotted tube stent. The stent was made up of a blend of Poly(L-lactide) or PLLA and P(4HB). They stated that the PLLA/P(4HB) stents exhibited high radial strength comparable to the metallic stainless steel and had the ability for rapid expansion. The physical characterisation of these PLLA/P(4HB) stents demonstrated suitable properties for several peripheral

vascular applications. They implanted the stents into iliac arteries of the porcine model for the preliminary trials. The six week follow up results showed that there were evidence of inflammatory reaction and neointimal response. This was caused due to the presence of large spaces within the strut allowing the tissues to proliferate within the stent struts. They are currently working actively on addressing this design limitation (Grabow *et al*., 2007). With the ideal design and mechanical properties, PHAs could prove to be an ideal candidate to be used as the platform or the base material for the development of a drug eluting biodegradable stent.

1.12 Other applications of PHAs

There are several other uses of PHAs apart from those discussed above. Some of these are briefly described below.

1.12.1 Active Drug Compounds

In recent times, the demand for the use of chiral compounds as drugs has inspired research into industrial production of enantiomerically pure compounds from PHAs. Being a family of polyesters consisting of over 140 chiral R-Hydroxycarboxylic acids (R-HAs), PHAs are considered a promising renewable source of obtaining chiral compounds that may be used in the synthesis of active drug compounds. P(3HB) is among the few commercially available PHAs. At present P(3HB) is known to be well tolerated due to their biocompatibility and hence have recently been employed as chiral products in the treatment of traumatic injuries like haemorrhagic shock, severe burns, myocardial damage and ischemia, anoxia and cerebral hypoxia (Massieu *et al*., 2003). Kashiwaya *et al*., further reported that these compounds were capable of reducing the death rate associated with human neuronal cell model culture for Alzheimer's and Parkinson's disease and also reduce apoptosis that brings about corneal epithelial erosion (Kashiwaya *et al*., 2000). The antimicrobial activities of R-3HB are also well documented (Sandoval *et al*., 2005; Chen and Wu, 2005; Shiraki *et al*., 2006; Ruth *et al*., 2007).

1.12.2 Health food and Nutrition

3HB oligomers are known to have a good penetration and rapid diffusion into peripheral tissues and hence could be utilised as emergency energy substrates for injured patients (Tasaki *et al*., 1999). These oligomers, when evaluated *in vivo* were found to release ketone bodies over prolonged periods. For this reason, several potential uses of these compounds including parenteral nutrition, management of diabetes and insulin resistance states, seizure control, reduction of protein catabolism, appetite suppression and control of some metabolic diseases (Williams *et al*., 2003)

1.12.3 Orthopaedics

Some studies have shown that scaffolds made up of PHAs result in consistent and favourable bone tissue adaptation response without any undesirable chronic inflammatory evidence after implantation periods of up to 12 months (Doyle *et al*., 1991). PHA compression-moulded T-plates prepared from P(3HB) reinforced with 7% carbon fibre were used to fix osteotomies of tibial diaphysis in rabbits. The implants, fixed to the tibia by absorbable sutures were compared to implants made from vicryl. After 12 weeks, better results were obtained from the reinforced PHA implants whereas implants from the vicryl plates resulted in frequent breakages and angulation (Bostman *et al*., 1987). The possibility of manufacturing several composite materials from among different PHAs and with other polymers underlines the potential of designing materials with superior qualities such as suitable mechanical strength, biocompatibility and optimal degradation time for use as implants in orthopaedics (Vainionpaa *et al*., 1986).

1.12.4 Uses in urology

The possibility of PHAs being used to repair a ureter was first proposed by Baptist and Ziegler in 1965. Another study in this area was carried out by Bowald and Johansson in 1990 where a vicryl tube coated with a solution of P(3HB-co-3HV) copolymer were implanted to replace the ureter in dogs. A fully functional ureter was claimed to have been formed within all model animals within a period of nine months (Baptist and Ziegler, 1965; Bowald and Johansson, 1990).

1.12.5 Wound management

The use of PHAs in the manufacture of sutures with superior quality has been suggested as far back as 1965 (Baptist and Ziegler, 1965). The biocompatibility and biodegradability of these materials, among other suitable qualities could explain the use of PHAs as clinical sutures. Looking into the wider context of controlled drug delivery by PHA materials, the prospects of designing wound dressings with these biological polymers to deliver such agents as antibiotics, minerals and vitamins, proteins and other wound healing mediators, in a controlled manner, would be worth considering.

1.12.6 Dusting powders

Small particle powders from P(3HB) have been produced and have been proposed to be used as dusting powders, particularly on surgical gloves (Holmes, 1985)

Indeed, several other medical and pharmaceutical applications of PHAs have been suggested, especially in recent times. Williams *et al.,* have listed ligament and tendon grafts, spinal fusion cages, surgical mesh and repair patches, ocular cell implants, bulking and filling agents, vein valves and haemostats are among the many possible medical uses of PHAs (Williams *et al*., 2003).

AIMS AND OBJECTIVES

The aim of this research project was to carry out the production of PHAs from *Pseudomonas mendocina* and use the PHAs produced for biomedical applications.

Specific objectives of this project are:

1. **Investigation of the use of various renewable non-expensive carbon sources such as sugarcane molasses, biodiesel waste and glycerol for the economical production of MCL-PHAs by *P. mendocina*.** The polymer produced will be characterised for their chemical properties using Gas Chromatography Mass Spectrometry (GC-MS), structural properties using Fourier Transform Infrared Spectroscopy (FTIR) and thermal properties using Differential Scanning Calorimetry (DSC).

2. **Development of novel, biocompatible and biodegradable P(3HO)/bacterial cellulose composites.** These composites will be characterised with respect to their mechanical properties using a Dynamic Mechanical Analyser (DMA), microstructural properties using Scanning Electron Microscopy (SEM) and thermal properties using DSC. In addition, the effect of the addition of cellulose microcrystals on the degradability of P(3HO) will be investigated, focusing on their potential use as scaffolds for tissue engineering. Biocompatibility of these P(3HO)/bacterial cellulose composites will be tested using Human dermal microvascular endothelial cells (HMEC-1).

3. **Development of novel, biocompatible and biodegradable multifunctional 2D P(3HO)/P(3HB) blend films with varying percentages of P(3HO) and P(3HB) such as P(3HO)/P(3HB) 80:20, P(3HO)/P(3HB) 50:50 and P(3HO)/P(3HB) 20:80**. These blend films will be characterised with respect to their mechanical properties using DMA, thermal properties using DSC and microstructural properties using SEM, White Light Interferometry and contact angle measurements. They will also be characterised for their bioactivity using HMEC-1 cells and their

degradation properties to assess their suitability in the development of biodegradable stents and scaffolds in tissue engineering.

4. **(1) Surface micropatterning of the P(3HO)/P(3HB) 50:50 blend films using the laser micropatterning technique**. Bearing in mind, the potential application of the P(3HO)/P(3HB) 50:50 blend films as a platform material for the development of a biodegradable stent and as a tissue engineering scaffold, HMEC-1 will be grown on the micropatterned P(3HO)/P(3HB) 50:50 blend films to assess the influence of micropatterning on cell growth and proliferation. The effect of the laser micropatterning on the surface and mechanical properties of the P(3HO)/P(3HB) 50:50 blend films will be examined using SEM, AFM and water contact angle measurements and DMA respectively**. (2) Development of micropatterned and non-micropatterned stent prototypes.**

5. **Investigation of the use of P(3HO)/P(3HB) 50:50 2D blend films with aspirin as the base material for the development of a drug eluting biodegradable stent and as a drug delivery vehicle for the controlled release of aspirin.** P(3HO)/P(3HB) 50:50 blend film with aspirin will be characterised for its mechanical properties using DMA, thermal properties using DSC and surface properties using SEM, AFM and water contact angle measurements to investigate the effect of the incorporation of aspirin on the blend film. Biocompatibility of these blend films containing aspirin will be investigated using HMEC-1 and their degradation properties will also be characterised to determine the effect of drug loading. Drug release studies will be carried out using High performance Liquid Chromatography (HPLC).

6. **Microbial production of P(3HB) and their utilisation in the synthesis of microspheres and films to investigate their potential as a drug delivery tool for the controlled delivery of aspirin**. P(3HB) microspheres and films containing aspirin will be characterised. Drug release rates from the microspheres and the films will be measured using HPLC.

The ultimate aim of this research project is to use PHAs, their composites and blends for various biomedical applications such as scaffolds for tissue engineering, development of biodegradable stents and drug delivery.

CHAPTER 2

Materials and Methods

2.1 Chemicals and Reagents

All the chemicals were purchased from Sigma-Aldrich or BDH Ltd. (Dorset, UK) or VWR (Leicestershire, UK). For analytical studies, analytical grade reagents were used. For chromatography analysis such as GC-MS and Nuclear Magnetic Resonance (NMR), chromatography grade reagents were used. Distilled and HPLC grade water were used for the experiments. Bicinchoninic acid assay kit used for protein estimation was purchased from Thermo-Scientific, UK. Aspirin (acetyl salicylic acid ≥ 99.0% crystalline) which was used as the model drug for drug delivery studies was purchased from Sigma-Aldrich, UK. Cell culture studies were carried out using cell culture grade media and reagents from Sigma-Aldrich, UK, and Lonza, UK.

2.2 Bacterial strains and cell line

P(3HO) was produced using the Gram-negative bacterium *P. mendocina,* which was obtained from the National Collection of Industrial and Marine Bacteria (NCIMB 10542), Aberdeen, UK. Bacterial cellulose (BC) was produced by growing *Acetobacter xylinum* (JCM10150) obtained from the culture collection, University of Westminster, UK. P(3HB) was produced using Gram-positive bacterium *Bacillus cereus* SPV which was also obtained from the culture collection, University of Westminster, UK. Human dermal microvascular endothelial cells (HMEC-1) were obtained from the University of Westminster, cell line collection.

2.3 Media

Various media compositions used during this study has been listed as follows:

2.3.1 Seed culture medium

Chemicals	Composition (g/L)
'Lab-Lemco' powder	1.0
Yeast Extract	2.0
Peptone	5.0
Sodium chloride	5.0

Table 2.1: Composition of the seed culture medium (Rai *et al.*, 2011)

2.3.2 P(3HO) production media

P. mendocina was grown in the second stage mineral salt medium (MSM) and the production stage MSM using sodium octanoate as the carbon source for the production of P(3HO).

2.3.2.1 Composition of the second stage MSM (g/L)

Chemicals	Composition (g/L)
$(NH_4)_2SO_4$	0.45
Mg SO_4	0.40
Na_2HPO_4	3.42
KH_2PO_4	2.38
Trace element solution	1 ml/L

Table 2.2: Composition of the second stage MSM (Rai *et al.*, 2011)

2.3.2.2. Composition of the production stage MSM (g/L)

Chemicals	Composition (g/L)
$(NH_4)_2SO_4$	0.50
Mg SO_4	0.40
Na_2HPO_4	3.80
KH_2PO_4	2.65
Trace element solution	1 ml/L

Table 2.3: Composition of the production stage MSM (Tian *et al.*, 2000)

2.3.2.3 Trace element solution (TE)

Chemicals	Composition (g/L)
$CoCl_2$	0.22
$FeCl_3$	9.70
$CaCl_2$	7.80
$NiCl_3$	0.12
$CrCl_6$. H_2O	0.11
$CuSO_4$. $6H_2O$	0.16

Table 2.4: Composition of the trace element solution (Rai *et al.*, 2011)

Mineral salts were sterilised by autoclaving at 121°C for 15 minutes (min). Sodium octanoate and magnesium sulphate were sterilised separately. Trace element solution was prepared by dissolving all the chemicals in 1N HCL. The TE solution was filter sterilised before use. The pH of the media, sodium octanoate and magnesium sulphate was adjusted to 7.15 using 1N HCL or 1M NaOH before autoclaving. Prior to the inoculation, the mineral salts, sodium octanoate, magnesium sulphate and the trace element solution were mixed together in a sterile condition.

2.3.3 Bacterial cellulose production media

A. xylinum was grown in the production media containing following nutrients:

Chemicals	Composition (g/L)
Yeast extract	5
Calcium carbonate	12
Glucose	50

Table 2.5: Composition of the media for bacterial cellulose production (Kim *et al.*, 2002).

Glucose solution were sterilised separately at 110°C for 10 min while the rest of the chemicals were autoclaved at 121°C for 15 min. Before the inoculation, pH of the production media was adjusted to 6.6, using 1N HCL and 1M NaOH.

2.3.4 P(3HB) production media

B. cereus SPV was grown in Kannan and Rehacek media for the production of P(3HB).

2.3.4.1 Media composition (Kannan and Rehacek media)

Chemicals	Composition (g/L)
Glucose Yeast extract	20.0
Potassium chloride	2.5
Ammonium sulphate	3.0
Defatted soybean dialysate	5.0
	100 mL

Table 2.6: Composition of the Kannan and Rehacek media (Valappil *et al*., 2007)

Kannan and Rehacek media was prepared by dissolving all the components in distilled water. Soybean dialysate was prepared by dissolving 10 g of defatted soybean flour in 1000 mL of water for 24 hours at 4°C. Soybean dialysate and the glucose solution were sterilised separately at 110°C for 10 min while the rest of the chemicals were autoclaved at 121°C for 15 min. The final pH of the production medium was adjusted to 6.8 by using 1N HCL or 1M NaOH. Prior to the inoculation, the soybean dialysate, glucose and the salts were mixed together in a sterile condition.

2.4 Production of P(3HO)

The production of P(3HO) can be divided into four phases. These include:

- Culturing of the *P. mendocina* in nutrient broth, the second stage MSM and then in the production stage MSM.
- Harvesting the cells and their lyophilisation
- Extraction and precipitation
- Characterisation of the PHA produced

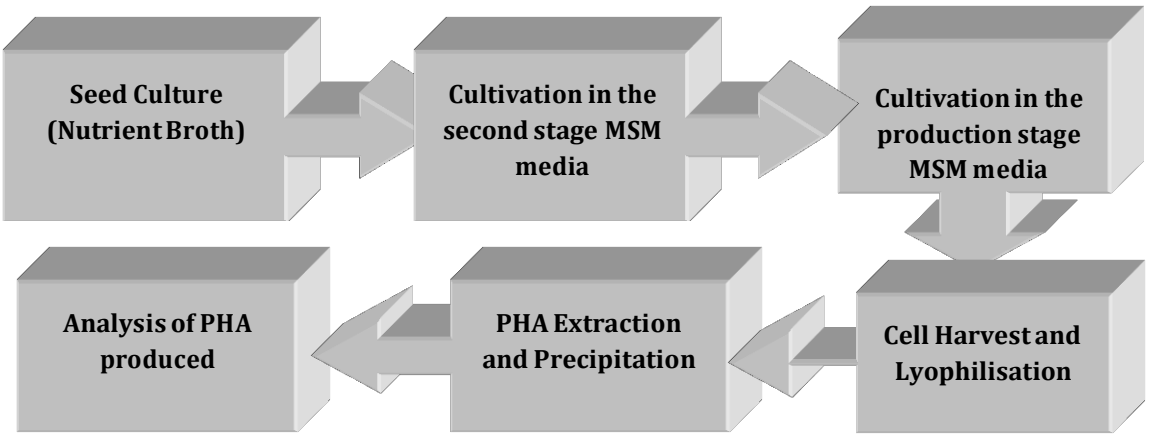

Figure 2.1: Diagrammatic representation of the steps involved in P(3HO) production.

2.4.1 Seed culture preparation in nutrient broth

A single colony of *P. mendocina* was used to inoculate the nutrient broth. The culture was incubated at 30°C at 200 rev/min for 24 hours.

2.4.2 Cultivation of *P. mendocina* cells in the second stage and the production stage MSM

The seed culture that was prepared as described in **section 2.3.1** was used to inoculate the second stage MSM. The cells were cultured in this medium for 18 hours at 30°C at 200 rev/min. 10% of the total volume of this culture was then used to inoculate the production stage MSM. Sodium octanoate was used as the carbon source at both the stages. The culture was grown for a period of 48 hours before being harvested (Rai *et al*., 2011).

2.4.3 Extraction of PHA by chloroform/ sodium hypochlorite dispersion

After 48 hours of growth, the cells were harvested by centrifuging the cultures at 4600 rev/min for 30 min. The cell pellet obtained was then lyophilised. The polymer was then extracted using chloroform/sodium hypochlorite dispersion method. In this method, the lyophilised cell biomass was incubated in a dispersion containing 80% of sodium hypochlorite and chloroform in 1:4 ratio at 30°C, for two hours at 150 rev/min. The slurry was then subjected to centrifugation at 4600 rpm for 20 min. This resulted in the formation of three layers of which the first layer was that of the sodium hypochlorite solution, the middle layer was that of the cell debris and the bottom most layer was that of the chloroform containing the dissolved polymer. This layer of chloroform containing the dissolved polymer was then concentrated using the rotary vacuum evaporator in which the chloroform solution was evaporated, the polymer was precipitated using ten volumes of ice cold methanol under continuous stirring (Rai *et al*., 2011).

2.4.4 PHA purification

The polymer obtained using the chloroform/sodium hypochlorite dispersion method was then subjected to purification to reduce the contaminating lipopolysaccharide (LPS). The polymer was precipitated using ice cold 50% methanol/ethanol mixture in an equal volume. The precipitated polymer was then dissolved in acetone and then precipitated using the same mixture. This procedure was repeated several times to obtain purified polymer.

2. 5 Analytical studies

2. 5.1 Biomass estimation

Estimation of the biomass was carried out by centrifuging 1 ml of the culture sample at 12,000g for 10 min. The cell pellets obtained were freeze dried and weighed.

2.5.2 Estimation of nitrogen concentration

The reagents required for this analysis was prepared as follows:

- Phenol nitroprusside buffer: Sodium phosphate tribasic (3 g), sodium citrate (3 g) and ethylene tetraacetic acid (EDTA) (0.3 g) were dissolved in HPLC water. pH was adjusted to 12. To this, 6 g of phenol and 20 mg of sodium nitroprusside were added.

- Alkaline hypochlorite reagent: This reagent was prepared by mixing 2.5 ml of sodium hypochlorite solution containing 4% chlorine and 40 ml of 1M sodium hydroxide solution.

The estimation of ammonium in the medium was done using the phenol hypochlorite reaction method. The sample was prepared by centrifuging the culture at 12,000 g for 10 min. The supernatant obtained was used for the analysis by performing a dilution of 1:100 in Millipore water. To this, 1 ml of phenol nitroprusside buffer was added to the 2.5 ml of diluted sample and mixed by swirling. After this, 1.5 ml of the hypochlorite reagent was added rapidly and mixed by inversion. The sample was then incubated for 45 min. The absorbance was measured at 635 nm. This method was used to determine the concentration of inorganic nitrogen present in the sample (Rai *et al*., 2011).

2.6 Characterization of the PHAs produced

2.6.1 Fourier Transform Infrared Spectroscopy (FTIR)

Initial confirmation of the polymer produced was done by FTIR. The conditions under which this analysis was performed were as follows: spectral range 4000 to 400 cm^{-1}; window material, CsI: 10 scans and resolution 4 cm^{-1}. Polymer sample (2 mg) was used to carry out this analysis at the Department of Biomaterials and Tissue Engineering, Eastman Dental institute, University College London, UK.

2.6.2 Gas Chromatography – Mass spectroscopy (GC-MS)

Identification of the polymer produced was done using GC-MS analysis of the methanolysed polymer. Furrer *et al*., developed the method such as methanolysis used for making methyl esters of the polymer extracted from *P. mendocina*. Methylene chloride (2 ml) and 2–ethyl-2-hydroxybutyric acid (10 mg/ml) were added to 20 mg of polymer. This reaction mixture containing the polymer was allowed to stand at the room temperature for 1 hour. After this, 2 ml of boron trifluoride in methanol (0.65M) was added to the mixture and tightly sealed followed by vigorous shaking. This reaction mixture was then refluxed for 16 hours after which the reaction tubes were cooled on ice for 5 min. HPLC (2 ml) water was added to the reaction mixture and it was vortexed thoroughly for 1 min. This led to the phase separation after which the bottom organic phase containing the polymer was collected and dried using the mixture of anhydrous sodium sulphate and

sodium carbonate (Furrer *et al*., 2007). This was then filtered and sent for GC-MS analysis to the School of Chemistry, University of Southampton, U.K.

2.6.3 Nuclear Magnetic Resonance Spectroscopy (NMR)

Structural characterisation of the polymer produced by *P. mendocina* was carried out using ^{13}C and ^{1}H NMR. For this analysis, 20 mg of the purified polymer were dissolved in 1 ml of deuterated chloroform. These samples were sent to the Department of Chemistry, University College London, UK for NMR analysis. Chemical shifts were referenced against the residual solvent signal (7.26 ppm and 77.0 ppm for ^{1}H and ^{13}C respectively). Spectra were analysed using MestRec software package.

2.6.4 Differential Scanning Calorimetry (DSC)

Thermal properties of the polymer sample such as melting temperature (T_m) and glass transition temperature (T_g) were measured by DSC using a Perkin Elmer Pyris Diamond (Perkin Elmer Instrument). 5 mg of the polymer sample was used for the analysis. Prior to the analysis, these samples were placed in the standard aluminium pans and the tests were performed under nitrogen atmosphere. The sample was heated and then cooled and then heated again at the rate of 20 ^{o}C/min between -50°C to 200°C. This investigation was carried out at the Department of Biomaterials and Tissue engineering, Eastman Dental Institute, University College London, UK.

2.7 Production of bacterial cellulose

2.7.1 Inoculum preparation

A. xylinum was grown in a universal bottle containing 10 ml of the production medium, for 24 hours, at 27°C, under static conditions. This inoculum was used to inoculate 300 mL of production media in a 1L Erlenmeyer flask.

2.7.2 Production of bacterial cellulose

Bacterial cellulose was produced at the flask level by inoculating the production media as described in **section 2.3.3**. Before the inoculation, pH of the production media was adjusted to 6.6, using 1N HCL and 1M NaOH and autoclaved separately.

After the inoculation, culture was grown under static conditions at 26°C for about 7 days. To preserve the integrity of the cellulose pellicles, no samplings were carried out and the culture was left undisturbed.

2.7.3 Extraction of cellulose pellicles

After 7 days of incubation, cellulose pellicles were harvested, washed with deionised water several times and then bleached using 70% sodium hypochlorite solution for 30 min. After this, the pellicles were washed several times with water and then stored in deionised water at 4°C.

2.7.4 Synthesis of cellulose microcrystals

Bacterial cellulose pellicles were homogenised into microcrystals using the blender and then freeze dried. After this, 1 g of freeze dried cellulose microcrystals were treated with sulphuric acid at 80°C to obtain shorter microfibrils before being subjected to the acetylation reaction. Cellulose microcrystals were recovered by centrifuging them at 4000 g for 10 min.

2.7.5 Acetylation of the bacterial cellulose microcrystals

Before the reaction, bacterial cellulose microcrystals were soaked in anhydrous acetic acid. This was repeated three times in order to remove the water completely. After this, the microcrystals were added into a stoppered glass bottle containing a mixture of acetic acid, toluene and 60% perchloric acid. This mixture was then vigorously shaken for about 1 min. After this, acetic anhydride was added to the reaction mixture and again shaken vigorously for about 1 min. The reaction was allowed to stand overnight at the room temperature with continuous stirring. After this reaction, the cellulose microcrystals were recovered by centrifuging at 4000 g for about 10 min. They were then washed with methanol and then with deionised water (Kim *et al.,* 2002).

2.8 Production of P(3HB)

P(3HB) was produced by *B. cereus* SPV using Kannan and Rehacek medium at pH 6.8, in shaken flasks (Valappil *et al.*, 2007). Glucose was used as the sole carbon source at a concentration of 20 g/L. The pH of the media was adjusted to 6.8 using 1N HCL or 1M NaOH in order to allow cell growth and facilitate polymer

accumulation by avoiding extreme pH conditions. The production medium, which was inoculated using the 10% inoculum, was grown for 72 hours at 30°C, with a stirrer speed of 200 rev/min. The cells were harvested by centrifuging the culture at 4600 rev/min for 30 min. The cell pellet obtained was then lyophilised. The polymer was then extracted using chloroform/sodium hypochlorite dispersion method. The polymer was precipitated using ten volumes of ice cold methanol under continuous stirring.

2.9 Characterization of the composites, blends and films containing aspirin

2.9.1 Scanning Electron Microscopy (SEM)

Surface characterisation of the films were carried out using a JOEL 5610LV-scanning electron microscope (JOEL). The polymer samples were placed on the 8mm diameter aluminium stubs and gold coated for 2 min using the gold spluttering device (EMITECH-K550). Images were then recorded at different magnifications and acceleration voltages to study the surface topography of the sample (Misra *et al.,* 2008). The operating pressure of 7 x 10^{-2} bar and deposition current of 20 mA, for 2 min, was used. The SEM analysis was carried out at the department of Biomaterials and Tissue Engineering, Eastman Dental Institute, University College London, UK.

2.9.2 White Light Interferometry

This technique was used to study the surface roughness of the film samples. This was done by measuring the surface roughness of the samples by obtaining a 3D image of the surface using the analyzer ZYGO (New view 200 OMP 0407C) at the Department of Biomaterials, Imperial College, UK.

2.9.3 Atomic Force Microscopy (AFM)

This technique was also used to study the surface roughness of the film samples. The surface of the film exposed to air was used for analysis. All the samples were run with scan size: 50µm x 50 µm using Cantilever type AC200TS-R3 and a spring constant of 10 N/m; AFM MFP3D; scan rate 0.50 Hz; Tapping mode. The films samples were sent to the University of Southampton, UK for this analysis.

2.9.4 Contact Angle Study

Static contact angle study was carried out by measuring the hydrophilicity of the film samples by using KSV Cam 200 optical contact angle meter (KSV instruments Ltd) as described in Misra *et al.,* 2008. This experiment was done at the Department of Biomaterials and Tissue Engineering, Eastman Dental Institute, University College London, UK.

2.9.5 Dynamic Mechanical Analyser (DMA)

Mechanical properties of the films were carried out using the Perkin–Elmer Dynamic Mechanical Analyser (DMA) as described in Misra *et al.,* 2008. This test was carried out to measure the Young's modulus, tensile strength and the elongation at break values. This investigation was carried out at the Department of Biomaterials and Tissue engineering, Eastman Dental Institute, University College London, UK.

2.9.6 Differential Scanning Calorimetry (DSC)

Thermal properties of the films such as melting temperature (T_m) and the glass transition temperature (T_g) were measured by DSC using a Perkin Elmer Pyris Diamond (Perkin Elmer Instrument). Film samples were used for the analysis. Prior to the analysis, these samples were encapsulated in the standard aluminium pans and the tests were performed under nitrogen atmosphere. The sample was heated and then cooled and then heated again at the rate of 20 ^{o}C/min between 60 ^{o}C to 200 ^{o}C. This investigation was carried out at the Department of Biomaterials and Tissue engineering, Eastman Dental Institute, University College London, UK.

2.9.7 Protein adsorption Test

Protein adsorption assay was carried out by incubating 1 cm^2 film samples in 400 µL of undiluted foetal bovine serum (FBS) at 37^{0}C for 24 hours. After incubation, the samples were washed three times with phosphate buffer saline (PBS). The samples were then incubated in 1 mL of 2% sodium dodecyl sulphate (SDS) in PBS to extract the adsorbed proteins on the film surface. This was done for 24 hours at room temperature under vigorous shaking. The overall protein adsorbed on the P(3HO)/P(3HB) blend film samples was quantified using the Bicinchoninic acid assay (Walker, 2009). The absorbance was measured spectrophotometrically at

562 nm against a calibration curve using bovine serum albumin. The assay was carried out in triplicates.

2.9.8 Indirect cytotoxicity testing

Indirect cytotoxicity assessment using HMEC was carried out on the film samples to establish their biocompatibility. Prior to the assessment, the films were sterilised with UV rays using two UV lamps of 15W, separated by a distance of 3 cm, for a period of 30 min on each side. The samples were incubated in 1 mL of DMEM medium for 24 hours at 37^0C. Simultaneously, HMEC-1 cells (100, 000 cells/mL) were cultured for 24 hours in 24 well plates. The DMEM medium from step 1 was then added to the cells and cultured for a further 24 hours. Cell viability was measured using MTT assay (Gerlier and Thomasset, 1986). 4% hydrogen peroxide was used as the positive control.

2.10 *In vitro* degradation study

Degradation study was carried out by incubating film samples in phosphate buffered saline solution (PBS) and Dulbeccos Modified Eagle medium (DMEM) at 37^0C. The choice of the media used for this study was based on the fact that DMEM is the optimum media used for the growth of HMEC-1, which was seeded on the P(3HO) neat, composite and blend film samples, to carry out the biocompatibility studies. Phosphate buffered saline (PBS) is an isotonic solution containing: NaCl 8 g/L, KCL 0.2 g/L, Na_2HPO_4 1.44 g/L and KH_2PO_4 0.24 g/L. DMEM media contained 4.5 g/L of glucose supplemented with 10% foetal calf serum, 2mM glutamine and 1% penicillin and streptomycin. The cells were kept in the incubator at 37^0C in a humidified atmosphere (5% CO_2) and cultured as described by Misra *et al.,* 2008.

2.10.1 Water uptake, weight loss

Prior to the incubation, the samples were weighed M_o dry (M_o, the initial weight of the sample). After this, the samples were immersed in PBS as well DMEM media under static conditions, at 37^0C, for a period of one and four months. Fresh medium was added to these samples every four days. At the end of the incubation period, the samples were withdrawn from the media and their weight loss (%WL) and water uptake (%WA) behaviour was analysed as described in Misra *et al.,* 2008.

The following equations were used to calculate water uptake and weight loss of the samples:

$$\text{Water uptake (\% WA)} = [(M_w \text{ wet}-M_t \text{ dry})/M_t \text{ dry}]\ 100$$

$$\text{Weight loss (\% WL)} = [(M_o \text{ dry}-M_t \text{ dry})/M_o \text{ dry}]\ 100$$

Where,

M_o dry = M_o, the initial weight of the sample.

M_w, wet = M_w, the weight of the samples after the immersion in the respective media

M_t, dry = M_t, the dry weight of the samples after the incubation in the respective media followed by drying (Misra *et al.,* 2008).

2.10.2 *In vitro* biocompatibility studies

2.10.2.1 Cell seeding on the samples

The samples were cut to a size of 1cm^2 in area and were exposed to UV rays for 30 min on each side. This was done to sterilise the samples. Prior to the seeding, the samples were incubated in the DMEM media for about 12 hours at 37^{0}C. The confluent cells were subjected to trypsinisation and recovered by centrifugation at 1000 rev/min for 10 min. The fresh medium was then added to the cell pellet and then transferred to 75 cm^2 tissue culture flask for further passages. Using the haemocytometer, the cells were counted. A cell density of 20,000 cells was used to seed the samples that were placed in 24 well plates. The cells were cultured by incubation at 37^{0}C in a humidified atmosphere (5% CO_2) for a period of 7 days, as in complete media. Standard tissue culture plastic was used as the control for this experiment (Misra *et al.,* 2008).

2.10.2.2 Cell proliferation assay

Neutral Red (NR) assay was carried out for cell adhesion and cell proliferation studies. DMEM media containing 40 mg/ml of Neutral Red (NR) dye was added to the samples placed in 24 well plates. The cells were incubated for 3 hours. This was to allow the viable cells to take up the dye. At the end of the incubation period, the samples were then transferred to a new 24 well plate. Solution A (2 ml) containing 1 % $CaCl_2$, 0.5 % formaldehyde was used to wash the sample twice. After this, 300

µl of solution B containing 1% acetic acid and 50% ethanol solution were added to each sample to extract the dye. The samples were then incubated at the room temperature for about 10 min. This was followed by vigorous agitation of the microtitre plate shaker. The absorbance was measured at 540 nm using a microtitre plate from Thermomax using Softmax Pro version 4.8 software. To measure the cell viability, total Neutral Red (NR) uptake was measured since % NR is directly proportional to the number of viable cells. Therefore, the following equation was used to calculate the % cell proliferation:

$$\% \text{ viability} = \frac{\text{Mean absorbance of samples X 100}}{\text{Mean absorbance of control}}$$

DMEM medium containing the cells in the tissue culture plastic was used as the positive control, whereas samples incubated in the medium without the cells was used as the negative control. This was to measure the absorption of the NR dye by the samples on their own (Misra *et al.,* 2008).

2.10.2.3 Scanning Electron Microscopy (SEM)

P(3HO)/bacterial cellulose composite films with HMEC-1 cells were examined using SEM to analyse the proliferation of HMEC-1 cells on the surface. The samples were fixed in 0.1M phosphate buffer containing 4% glutaraldehyde for 12 hours at 4^0C. Before being observed under the SEM, the samples with the cells were subjected to dehydration in a sequence of graded ethyl alcohol such as 25%, 50%, 70%, 80%, and 100% for 10 min each. The samples were allowed to dry for 30 min in the fume hood. These dried samples containing cells were then mounted on aluminium stubs, gold coated and observed under SEM, using the conditions described in **section 2.9.1**

2.11 In vitro release of aspirin using High Performance Liquid Chromatography (HPLC)

1 cm^2 of the films with aspirin were immersed in PBS release medium in triplicates. The tubes containing films with aspirin in PBS were kept in a shaking incubator at 37^0C with 35 rpm. A sample volume of 1 ml was collected at predetermined time points and each aliquot was replaced with fresh buffer throughout the entire release study. The drug content in the sample was analysed using HPLC. From

literature, it is known that aspirin is hydrolysed into salicylic acid and acetic acid (Tang and Singh, 2008). A HPLC system containing C_{18} column was used to measure both salicylic acid and acetic acid. A methanol and water solution containing 0.5% (v/v) of acetic acid was used as the mobile phase at a flow rate of 1 ml/min. Samples injected into the HPLC system were detected at 240nm. Aspirin control samples were prepared in PBS. They were also kept in a shaking incubator at 37^0C with 35 rpm for the same period of time as the film samples containing aspirin. These aspirin control samples were prepared in order to compare the chemical stability of the aspirin released from the blend film samples to that of free aspirin. The amount of aspirin hydrolysed was calculated using the following formula:

Hydrolysed aspirin (mg) = [salicylic acid (mg)/molecular weight of salicylic acid x molecular weight of aspirin]

2.12. Statistical analysis

Data sets have been expressed along with their mean standard deviation. The data, where appropriate, were compared using the student's t-test and ANOVA. The differences were considered significant when $*p<0.05$. p value greater than 0.05 ($p > 0.05$) was interpreted as indicating no significant difference.

CHAPTER 3

Production of PHAs using inexpensive carbon sources

INTRODUCTION

Plastics are one of the most exploited materials in the modern world. Their applications range from being used in the packaging industry and in the medical industry. These plastics are mostly used for short term applications such as packaging and disposable items and therefore contribute to about 15% of the domestic and industrial waste. It has been predicted that the use of these plastics would continue to increase until the 2020 (Castilho *et al*., 2009). These plastics are derived from non-renewable source such as petroleum reserves. According to literature, these petroleum derived plastics remain in the environment for an average of 100 years. Due to the slow degradation rates in the landfills and extremely high costs involved in incineration, it is challenging to find an adequate method of disposal of these plastics. Disposal of conventional plastics has a negative impact on the environment and this has motivated progress in biotechnology research on biodegradable and biocompatible polymers (Akiyama *et al.*, 2003). Dwindling petroleum reserves and the environmental hazard caused by the petroleum derived plastics have led to the search for a potential alternative. Biodegradable polymers have emerged as the one of the potential alternatives. They have several advantages over the traditional plastics that are being used at present. They are sustainable, biodegradable and biocompatible in nature. One such biodegradable polymer that has gained fresh impetus in the recent years is polyhydroxyalkanoates. Polyhydroxyalkanoates (PHAs) are polyesters of 3-, 4-, 5- and 6 hydroxyalkanoic acids produced by a variety of bacterial species, under nutrient-limiting conditions for e.g. with excess carbon source and limiting nitrogen. PHAs are accumulated as intracellular storage compounds within the bacteria. These polymers are biodegradable, biocompatible and exhibit thermoplastic properties. However, they can be degraded into carbon dioxide and water by several microorganisms producing extracellular PHA depolymerases (Valappil *et al.,* 2007). There has been a great interest in the commercial utilization of these biodegradable polyesters for industrial as well as biomedical applications. One of the hindrances in the commercialization of PHAs is its high production costs. Statistics revealed that in Europe, biodegradable polymers constituted of only 0.1% of the total polymer market due to its high production cost (Kim *et al*., 2000a). Different strategies have been used to lower the PHA production costs. Some of these include the use of metabolic engineering, efficient downstream processing

and fermentation methods such as two stage fermentation and the use of transgenic plants for PHA production. At present, PHAs are produced using pure carbon sources which contribute to a major fraction of the total production costs. The use of inexpensive renewable carbon sources such as industrial, agricultural and domestic waste reduces the costs of production as well as adds to the environmental significance by easing the disposal. This has been considered to be a potential alternative for the economical production of PHAs (Marangoni *et al*., 2002; Lee and Gilmore, 2005).

The main objective of this study was to produce PHAs using inexpensive renewable carbon sources such as biodiesel waste, pure glycerol and sugarcane molasses. The chosen organism used for the production of PHAs was *P. mendocina.*

3. 0 Results

3.1 PHA production by *P. mendocina* using sugarcane molasses, biodiesel waste and glycerol as the carbon source

In order to investigate the potential of cheap renewable carbon sources such as sugarcane molasses, biodiesel waste and pure glycerol as a replacement of expensive carbon sources for the production of PHAs, *P. mendocina* was cultivated in the production stage MSM for 48 hours using these three different carbon sources. The samples were withdrawn every 3 hours during the fermentation process. The O.D. and the pH of the culture were measured during the course of the fermentation, whereas biomass estimation and nitrogen concentration measurements were carried out at the end of the fermentation as described in **section 2.5.**

3.1.1 PHA production using sugarcane molasses as the carbon source

A single colony of *P. mendocina* was used to inoculate the production stage MSM media containing 20 g/L of sugarcane molasses. From literature, it is known that the sugarcane molasses is composed of a mixture of sugars such as glucose, fructose and raffinose that form 62% of the total composition. It also contains 10% of nitrogenous compounds, 8% of inorganic constituents and 20% of water (Olbrich, 1963). The production was carried out in 5L shaken flasks in a batch mode. The cells were harvested at the end of the fermentation to extract the polymer produced. The growth profile of the *P. mendocina* using sugarcane molasses as the source of carbon is shown in **Figure 3.1**.

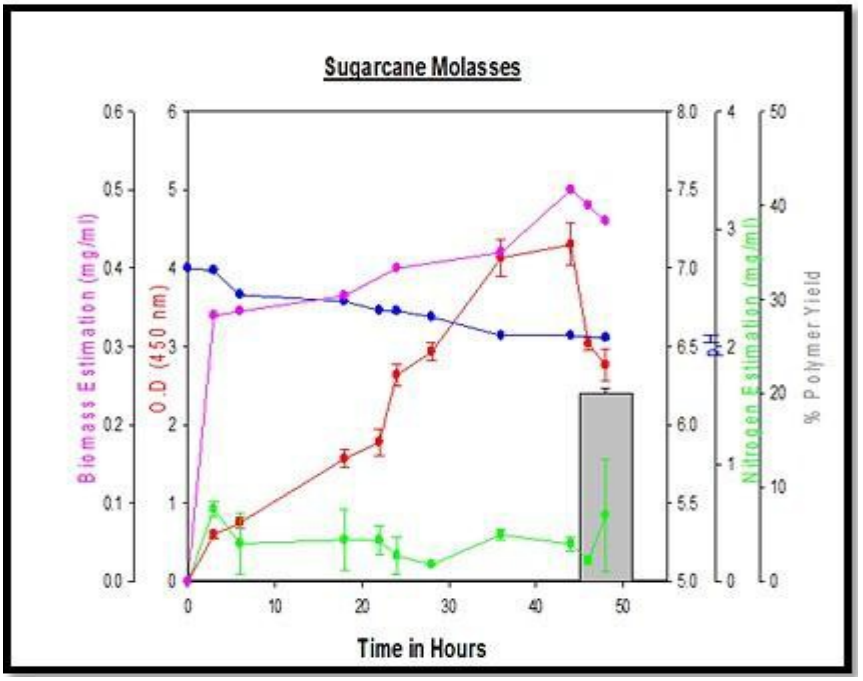

Figure 3.1: Fermentation profile of *P. mendocina* using sugarcane molasses as the source of carbon.

As the fermentation started, the $O.D._{450}$ and the biomass values increased exponentially until 45 hours after which it decreased dramatically. The maximum O.D. value obtained was 4.1 at 45 hours. pH was not controlled during the course of the fermentation. The starting pH of the media was set to 7. The pH of media decreased slightly from its initial value of 7 reaching around 6.5 at the end of the fermentation. The nitrogen concentration decreased initially but remained constant until 23 hours after which there was a decrease. However, there was an unexpected

increase in the nitrogen concentration at 36 hours of fermentation. This could indicate the release of a nitrogenous compound by the organism during the fermentation. The cells entered log phase within 3 hours of the fermentation, reaching stationary phase at around 45 hours. The maximum dry cell weight values observed was 9 g/L at 45 hours. The % polymer yield obtained at the end of the fermentation was 20% dcw.

3.1.2 PHA production using biodiesel waste as the carbon source

A single colony of *P. mendocina* was used to inoculate the MSM media containing 20 g/L of biodiesel waste under nitrogen limiting conditions. The production was carried out in 5L shaken flasks in a batch mode. The cells were harvested at the end of the fermentation to extract the polymer produced. The growth profile of the *P. mendocina* using biodiesel waste as the carbon source is shown in **Figure 3.2**.

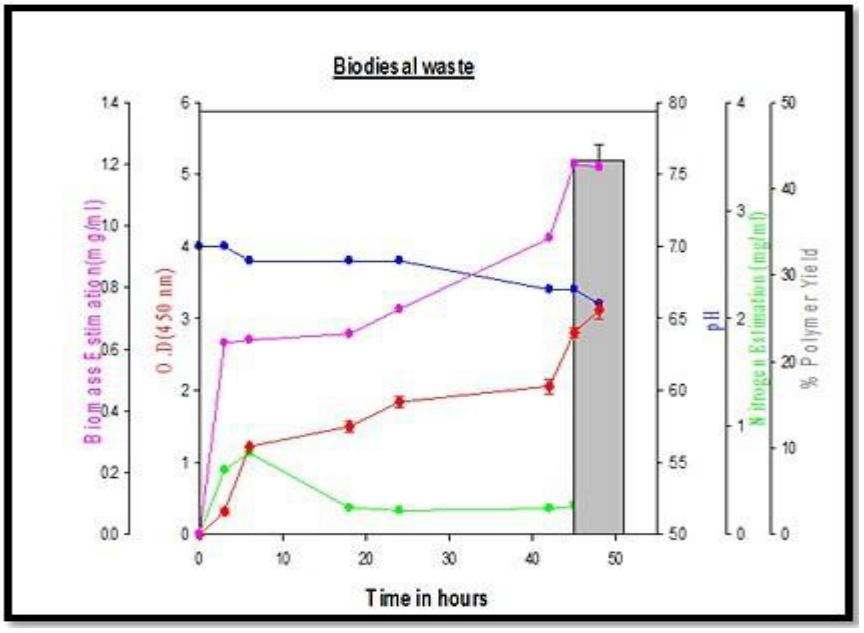

Figure 3.2: Fermentation profile of *P. mendocina* using biodiesel waste as the source of carbon.

As the fermentation started, the O.D.$_{450}$ and the biomass values increased gradually, until the end of the fermentation. The O.D.$_{450}$ values were lower compared to the cells grown in sugarcane molasses. This could be due to the inability of the organism to utilise crude biodiesel waste easily or the presence of a toxic substance. The maximum O.D.$_{450}$ value obtained was 2.9 at 48 hours. Nitrogen was used as the limiting factor. The nitrogen concentration gradually decreased during

the course of the fermentation. The pH of culture medium decreased slightly from its initial value of 7 to around 6.5 at the end of the fermentation. The maximum dry cell weight (dcw) obtained was 7.4 g/L at 48 hours of cultivation. The % polymer yield obtained at the end of the fermentation was 43.2% dcw.

3.1.3 PHA production using pure glycerol as the source of carbon

A single colony of *P. mendocina* was used to inoculate the MSM media containing 20 g/L of pure glycerol under a nitrogen limiting condition. This was carried out to compare the growth of *P. mendocina* and the production of PHAs in the biodiesel waste containing crude glycerol and pure glycerol. The production was carried out in 5L shaken flasks in a batch mode. The cells were harvested at the end of the fermentation to extract the polymer produced. The growth profile of *P. mendocina* using pure glycerol as the source of carbon is shown in **Figure 3.3**.

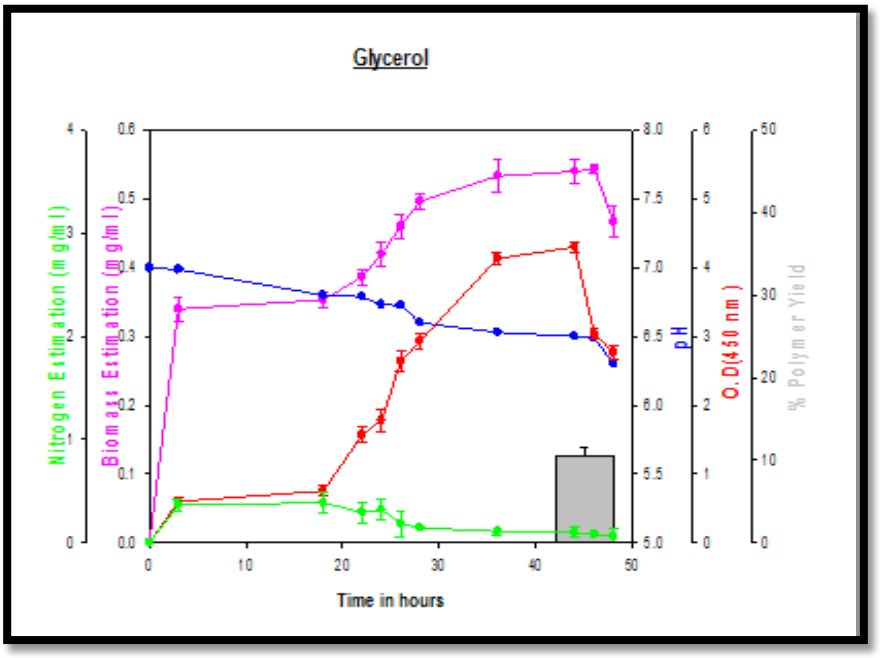

Figure 3.3: Fermentation profile of *P. mendocina* using pure glycerol as the source of carbon.

As the fermentation process started, the O.D.$_{450}$ and the biomass values increased gradually, within 3 hours of the fermentation, after which it increased exponentially until 30 hours. The cells entered stationary phase after 30 hours. Maximum O.D.$_{450}$ value obtained was 4.1 at 45 hours. Nitrogen was used as the limiting factor. The nitrogen concentration gradually decreased during the course of the fermentation and maintained the limiting condition. The pH of the culture

medium decreased slightly from its initial value of 7 to around 6.3. The maximum dry cell weight value obtained was 8.6 g/L at 45 hours. The polymer yield obtained at the end of the fermentation was 10.5% dcw.

3.2 Characterisation of the polymer produced

3.2.1 Fourier Transform Infrared Spectroscopy (FTIR)

The polymer produced using these cheap carbon sources were characterised using FTIR as described in **section 2.6.1**. From literature, it is known that the absorption bands at 1720 cm^{-1} and 1282 cm^{-1} corresponding to the ester carbonyl group and –CH_2 groups respectively are the principal bands found in SCL-PHAs, whereas the absorption bands at 1742 cm^{-1} and 1165 cm^{-1} corresponding to the ester carbonyl group and C-O stretching are the signature bands found in MCL-PHAs (Randriamahefa *et al.*, 2003).

3.2.1.1 FTIR analysis of the polymer produced using sugarcane molasses as the carbon source.

The absorption spectrum of the polymer produced using sugarcane molasses as the carbon source, as shown in **Figure 3.4**.

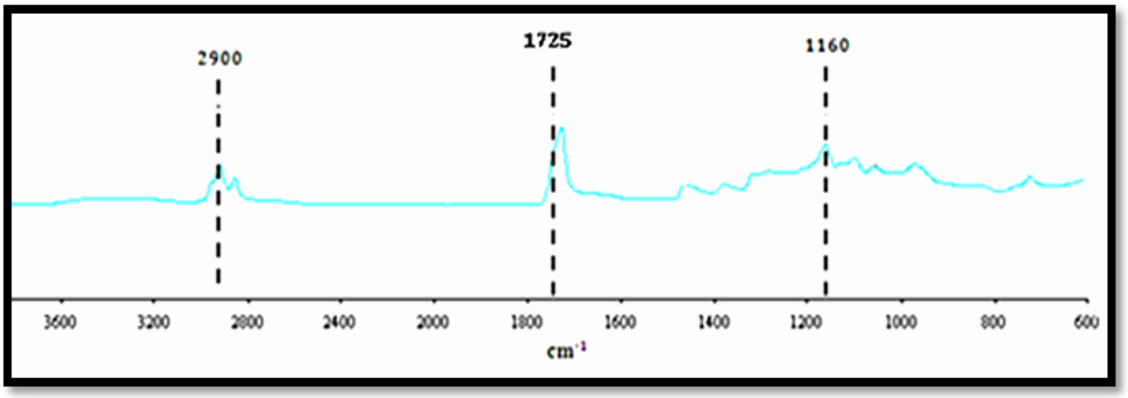

Figure 3.4: FTIR spectrum of the polymer produced using sugarcane molasses as the carbon source.

The absorption spectrum showed the presence of a peak at 2900 cm^{-1} corresponding to the aliphatic –CH group of the polymer backbone. The absorption spectrum of the polymer confirmed the presence of the characteristic marker ester carbonyl band for MCL-PHAs, which occurs around 1725 cm^{-1} and the band at 1160 cm^{-1} that occurs due to C-O stretching. Preliminary characterisation using FTIR suggested that the polymer produced was an MCL-PHA.

3.2.1.2 FTIR analysis of the polymer produced using biodiesel waste as the carbon source.

The absorption spectrum of the polymer produced using biodiesel waste as the carbon source is shown in **Figure 3.5**.

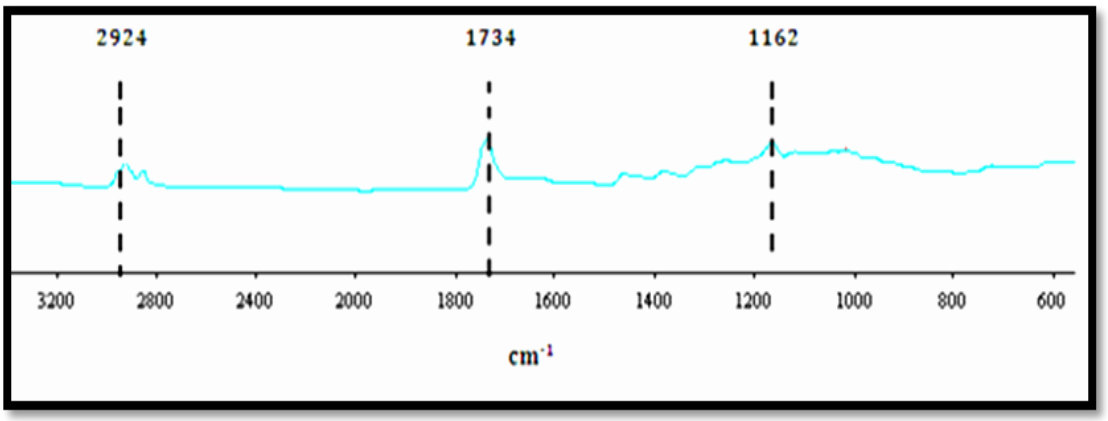

Figure 3.5: FTIR spectrum of the polymer produced using biodiesel waste as the carbon source.

The absorption spectrum showed the presence of a peak at 2924 cm^{-1} corresponding to the aliphatic –CH group of the polymer backbone. The absorption spectrum of the polymer confirmed the presence of the characteristic marker ester carbonyl band for MCL-PHAs that occurs around 1734 cm^{-1} and the band at 1162 cm^{-1} that occurs due to C-O stretching. Preliminary characterisation using FTIR suggested that the polymer produced was an MCL-PHA.

3.2.1.3 FTIR analysis of the polymer produced using pure glycerol as the carbon source.

The absorption spectrum of the polymer produced using pure glycerol as the carbon source is shown in **Figure 3.6**.

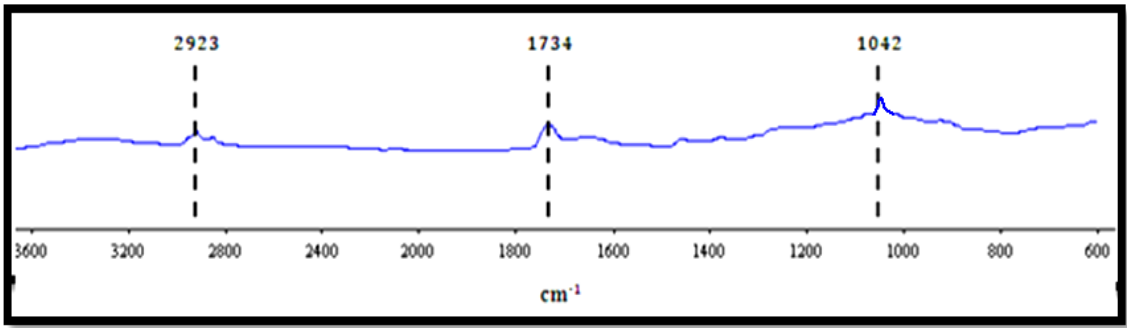

3.6: FTIR spectrum of the polymer produced using pure glycerol as the carbon source.

The absorption spectrum showed the presence of a peak at 2923 cm^{-1} corresponding to the aliphatic –CH group of the polymer backbone. The absorption spectrum of the polymer confirmed the presence of the characteristic marker ester carbonyl band for MCL-PHAs which occurs around 1734 cm^{-1} and the band at 1042 cm^{-1} which occurs due to C-O stretching. Preliminary characterisation using FTIR suggested that the polymer produced was an MCL-PHA. These polymers produced were further characterised using Gas chromatography Mass Spectrometry (GC-MS***).***

3.2.2 Gas chromatography Mass Spectrometry (GC-MS)

3.2.2.1 GC-MS analysis of the polymer produced using sugarcane molasses as the carbon source.

The polymer produced was further characterised using Gas chromatography-mass spectrometry. Prior to this analysis, the polymer was methanolysed to obtain a methyl ester as described in **section 2.6.2.** The GC-MS spectrum of the polymer is shown in **Figure 3.7.**

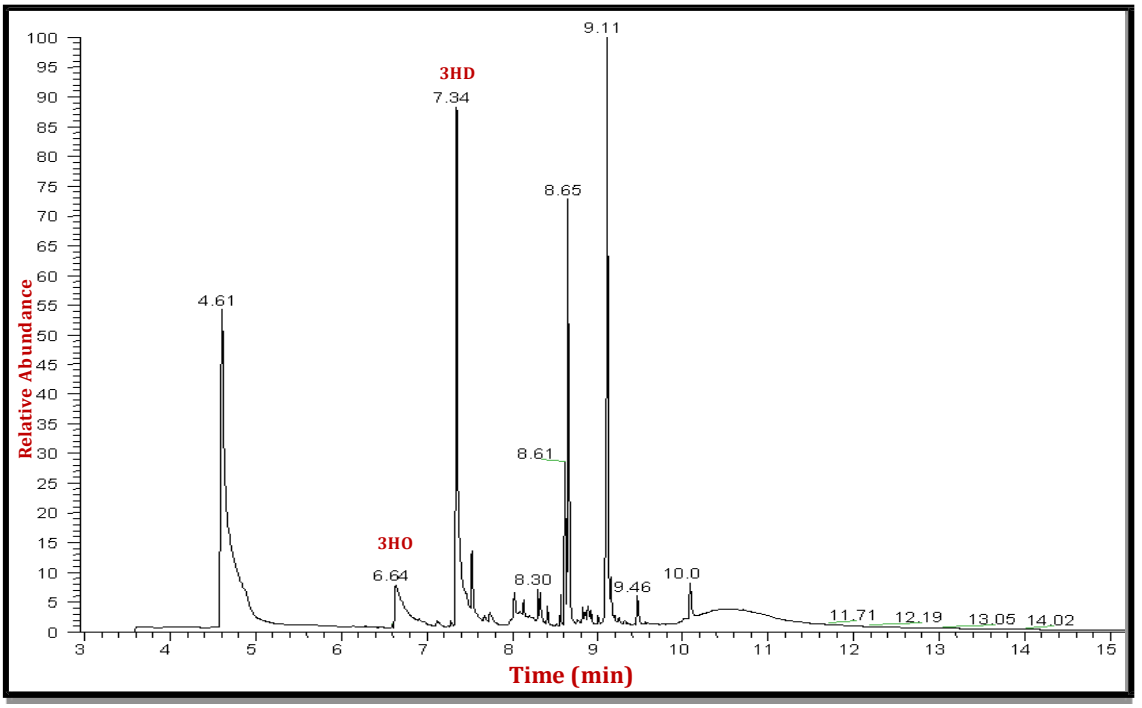
Relative Abundance
Time (min)
3HD
3HO
9.11
7.34
8.65
4.61
8.61
6.64
8.30
9.46
10.0
11.71
12.19
13.05
14.02

(a)

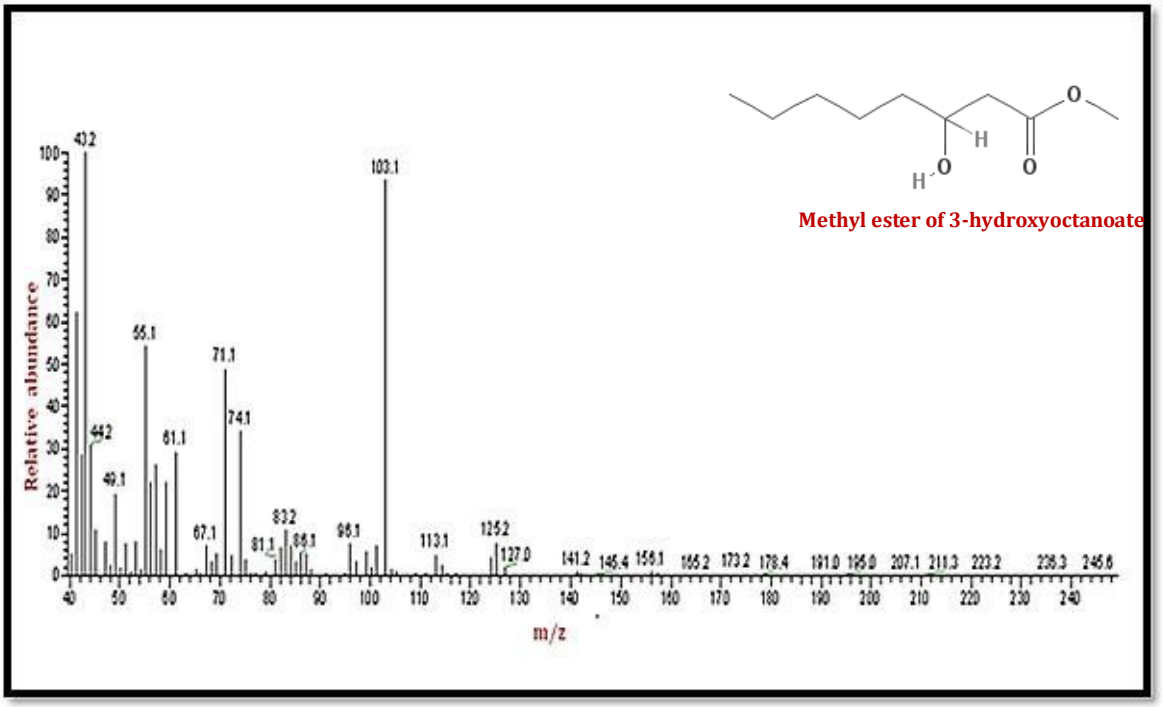
Relative abundance
m/z
Methyl ester of 3-hydroxyoctanoate
43.2
103.1
55.1
71.1
74.1
44.2
61.1
49.1
83.2
67.1
96.1
113.1
125.2
127.0

(b)

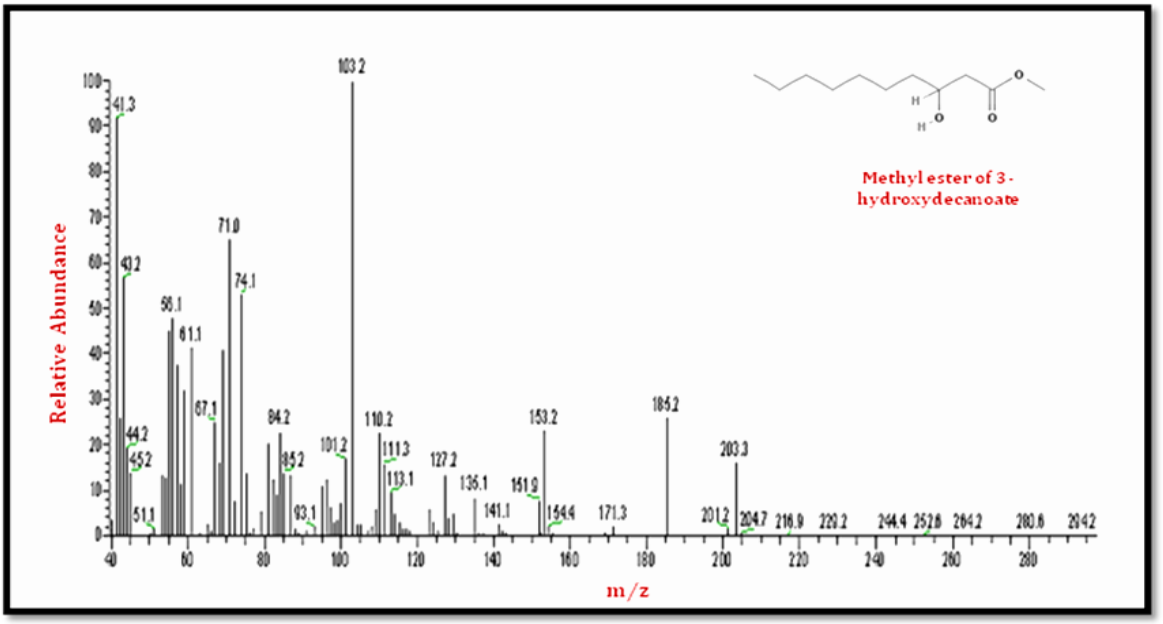

(c)

Figure 3.7: GC-MS analysis of the polymer produced by *P. mendocina* using sugarcane molasses as the carbon source**.** (a) A total ion gas chromatogram of the polymer showing peaks at 6.64 (3HO) and 7.34 (3HD) min (b) The MS fragmentation pattern of the GC peak at a retention time 6.64 min showing 3HO. (c) The MS fragmentation pattern of the GC peak at retention time 7.34 min showing 3HD.

2-ethyl-2-hydroxybutyric acid was used as an internal standard and showed a peak at a retention time of 4.61 min. The mass spectrum of the molecular ion related mass fragment peak at a retention time (R_t) of 6.64 min was identical to the mass spectrum of the methyl ester of 3-hydroxyoctanoate in the MS (NIST) library, confirming that the polymer produced contained monomer units of the 3-hydroxyoctanoate. The mass spectrum of the molecular ion related mass fragment peak at a retention time (R_t) of 7.34 min was identical to the mass spectrum of the methyl ester of 3-hydroxydecanoate in the MS (NIST) library, confirming that the polymer produced also contained monomer units of 3-hydroxydecanoate. 3HD was the major monomer unit present in this copolymer at 87 mol% while 3HO was a minor constituent at 7 mol% approximately.

The MS fragmentation pattern of 3HO in **Figure 3.7** (b) showed m/z peaks at 43.2, 71.1, 74.1 and 103.1. The peak at m/z 43.2 corresponded to the alkyl end of the molecule formed due to the cleavage between the C_5 and C_6 carbon atoms**.** The peak at m/z 71.1 represented the alkyl end of the molecule occurring due to the cleavage

between C_3 and C_4 carbon atoms. The peak at m/z 74.1 represented the carbonyl end of the molecule occurring due to the cleavage between C_3 and C_4 carbon atoms. The peak at 103.1 corresponded to the hydroxyl end of the molecule occurring due to the cleavage between C_3 and C_4 atoms. This fragmentation pattern followed the McLafferty rearrangement (McLafferty, 1956).

The MS fragmentation pattern of 3HD in **Figure 3.7** (c) showed m/z peaks at 43.2, 71.0, 74.1 and 103.2. The peak at m/z 43.2 corresponded to the alkyl end of the molecule originated due to the cleavage between C_7 and C_8 carbon atoms. The peak at m/z 71.1 represented the alkyl end of the molecule formed due to the cleavage between C_3 and C_4 carbon atoms. The peak at m/z 74.1 represented the carbonyl end of the molecule formed due to the cleavage between C_3 and C_4 carbon atoms. The peak at 103.2 corresponded to the hydroxyl end of the molecule occurring due to the cleavage between C_3 and C_4 atoms. This fragmentation pattern followed the McLafferty rearrangement (McLafferty, 1956).

The fragment peaks at a retention time (R_t) of 7.52 and 8.65 min were identical to the mass spectrum of the methyl ester of dodecanoic acid and pentadecanoic acid in the MS (NIST) library. These are saturated fatty acids. The other fragment peaks at a retention time (R_t) of 8.61 and 9.11 min were identical to the mass spectrum of the methyl ester of hexadecenoic acid and 13-octadecenoic acid, also known as oleic acid respectively in the MS (NIST) library. These are monounsaturated fatty acids. They could be removed by the further purification of the polymer (Rai *et al.*, 2011).

3.2.2.2 GC-MS analysis of the polymer produced using biodiesel waste as the carbon source.

The GC-MS result of the methanolysed polymer produced using biodiesel waste as the carbon source is shown in **Figure 3.8.**

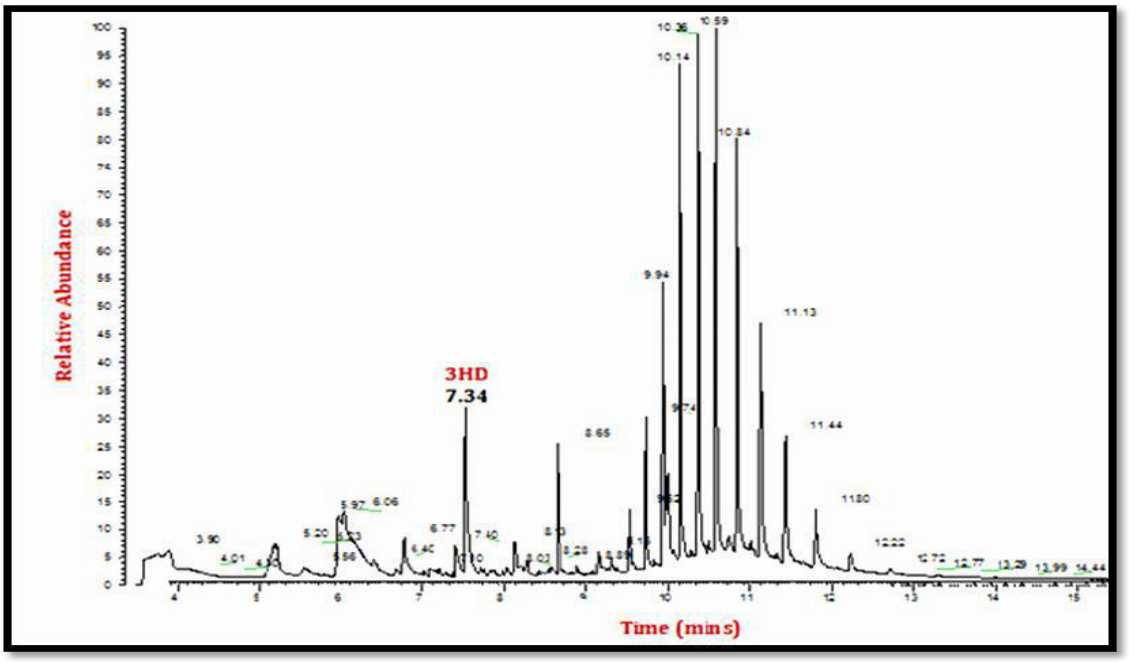

(a)

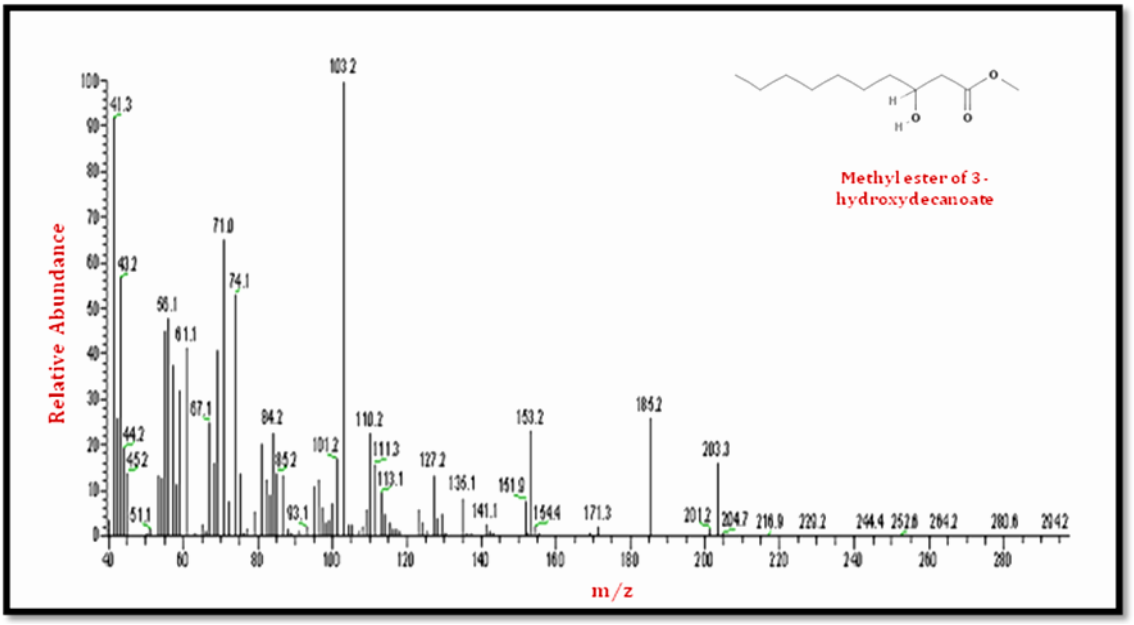

(b)

Figure 3.8: GC-MS analysis of the polymer produced by *P. mendocina* using biodiesel waste as the carbon source**.** (a) A total ion gas chromatogram of the

polymer produced showing peaks at 7.34 min. (b) The MS fragmentation pattern of the GC peak at a retention time of 7.34 min showing 3HD.

The mass spectrum of the peak at a retention time (R_t) of 7.34 min was identical to that of the methyl ester of 3-hydroxydecanoic acid in the MS (NIST) library, confirming that the polymer produced was the polymer of 3-hydroxydecanoate. 3HD was the main monomer unit at 33 mol% approximately. 2-ethyl-2-hydroxybutyric acid was used as an internal standard and was represented by the peak at a retention time of 5.20 min.

The MS fragmentation pattern of 3HD in **Figure 3.8** (b) showed m/z peaks at 43.2, 71.0, 74.1 and 103.2. The peak at m/z 43.2 corresponded to the alkyl end of the molecule formed due to the cleavage between C_7 and C_8 carbon atoms. The peak at m/z 71.1 represented the alkyl end of the molecule formed due to the cleavage between C_3 and C_4 carbon atoms. The peak at m/z 74.1 represented the carbonyl end of the molecule formed due to the cleavage between C_3 and C_4 carbon atoms. The peak at 103.2 corresponded to the hydroxyl end of the molecule occurring due to the cleavage between C_3 and C_4 atoms. This fragmentation pattern followed the McLafferty rearrangement (McLafferty, 1956).

Apart from the above mentioned peaks, there were other fragment peaks that were detected during this analysis. The peak at a retention time (R_t) of 8.65 was identical to the mass spectrum of the methyl ester of pentadecanoic acid in the MS (NIST) library. The peaks at 9.52, 9.74 and 10.36 min were identical to the mass spectrum of heptacosane in the MS (NIST) library. Another peak at 9.94 min was identical to the mass spectrum of pentacosane in the MS (NIST) library. Other peaks at 10.59, 10.84 and 11.13 min were identical to the mass spectrum of octacosone in the MS (NIST) library. Heptacosane, octacosone and pentacosane belong to the hydrocarbon family of alkanes and are known to form major constituents of diesel and aviation fuel. By further purification of the polymer, these non-relevant compounds can be removed.

3.2.2.3 GC-MS analysis of the polymer produced using pure glycerol as the carbon source.

GC-MS result of the methanolysed polymer produced using pure glycerol as the carbon source is shown in **Figure 3.9.**

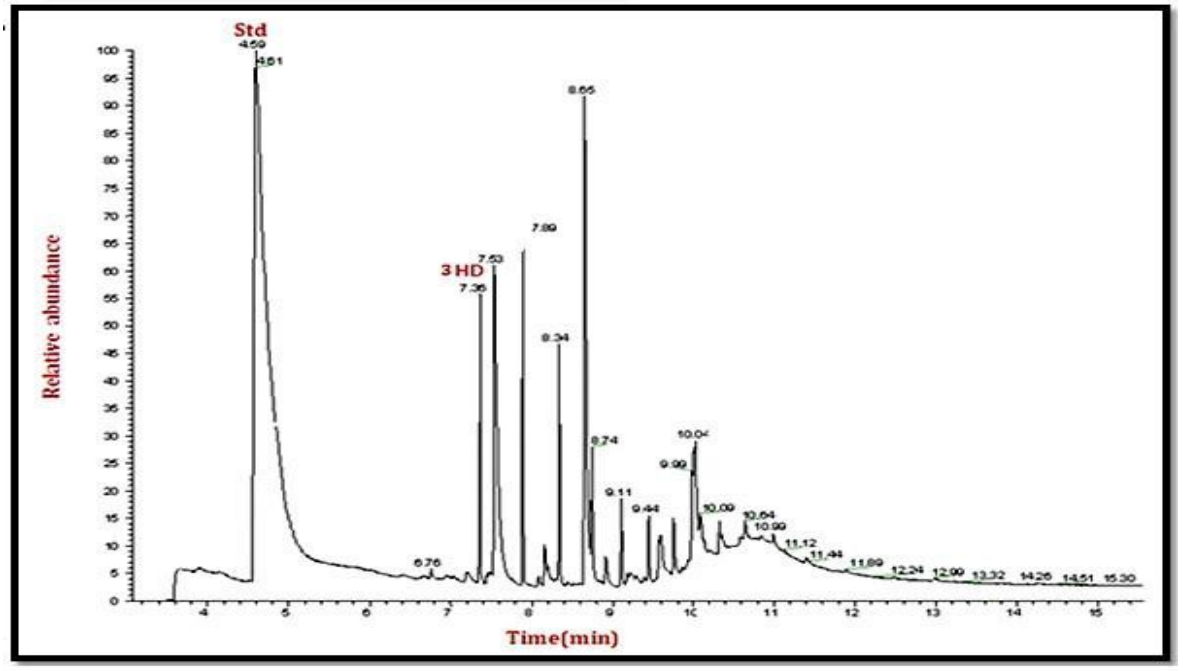

(a)

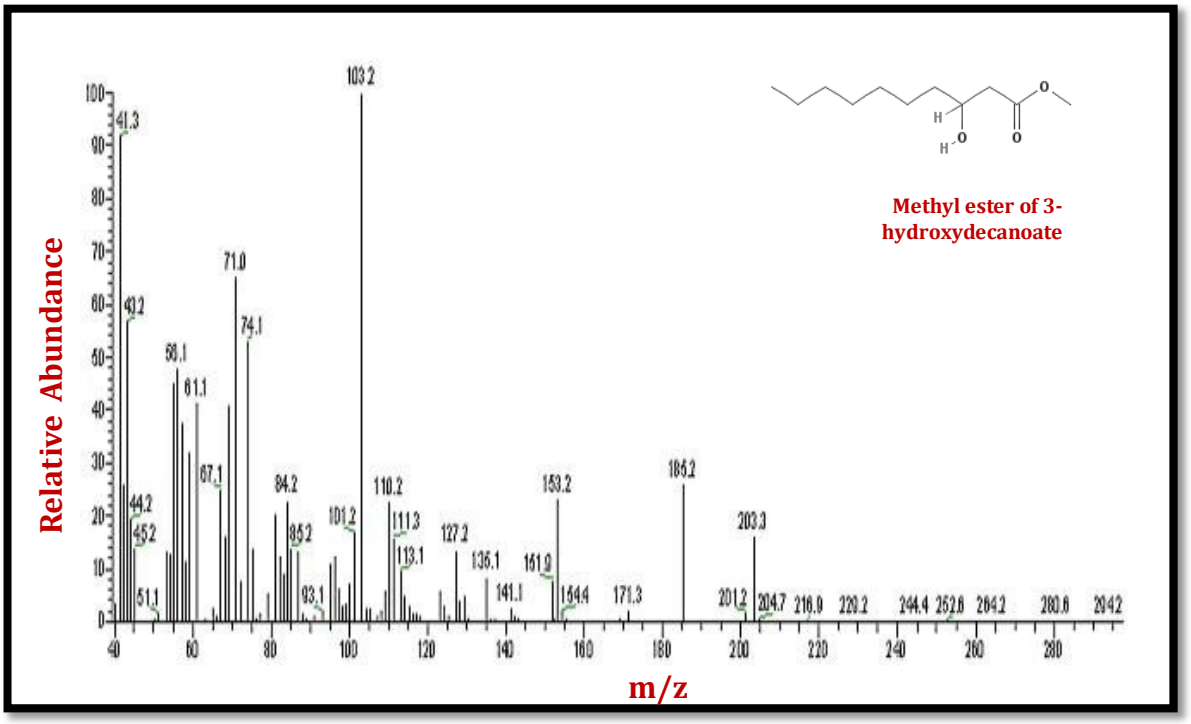

(b)

Figure 3.9: GC-MS analysis of the polymer produced by *P. mendocina* using glycerol as the carbon source**.** (a) A total ion gas chromatogram of the polymer produced

showing peaks at 7.34 min. (b)The MS fragmentation pattern of the GC peak at a retention time 7.36 min showing 3HD.

The mass spectrum of the peak at a retention time (R_t) of 7.36 min was identical to that of the methyl ester of 3-hydroxydecanoic acid in the MS (NIST) library, confirming that the polymer produced was the polymer of 3-hydroxydecanoate. 2-ethyl-2-hydroxybutyric acid was used as an internal standard and showed as a peak at a retention time of 4.59 min.

The MS fragmentation pattern of 3HD in **Figure 3.9** (b) showed m/z peaks at 43.2, 71.0, 74.1 and 103.2. The peak at m/z 43.2 corresponded to the alkyl end of the molecule originated due to the cleavage between C_7 and C_8 carbon atoms. The peak at m/z 71.1 represented the alkyl end of the molecule occurring due to the cleavage between C_3 and C_4 carbon atoms. The peak at m/z 74.1 represented the carbonyl end of the molecule occurring due to the cleavage between C_3 and C_4 carbon atoms. The peak at 103.2 corresponded to the hydroxyl end of the molecule occurring due to the cleavage between C_3 and C_4 atoms. This fragmentation pattern followed the McLafferty rearrangement.

There were other fragment peaks that were detected during this analysis peak at a retention time (R_t) of 8.65 and 10.04 min that were identical to the mass spectrum of the methyl ester of hexadecanoic acid and octadecanoic acid in the MS (NIST) library. These are saturated fatty acids. The polymer produced can be further purified by solvent extraction to remove these impurities.

3.2.3 Molecular weight analysis

The weight average molecular weight (M_w) of the polymer produced by *P. mendocina* using sugarcane molasses, biodiesel waste and pure glycerol was determined using gel permeation chromatography (GPC). Two Polar Gel-M columns (30 cm) in series (Varian Inc) were calibrated to 380994 – 590 Da using narrow molecular weight polystyrene standards. Tetrahydrofuran was the eluent used in this analysis and the flow rate was adjusted to be 1 ml/min. The polymer that was eluted was detected using a differential refractometer. Viscotek 'Trisec 2000' and 'Trisec 3.0' software was then used to collect and analyse the data. This analysis was carried out at the Department of Chemistry, University of Nottingham, UK.

According to literature it is known that the relative M_w (weight average molecular weight) of the MCL-PHAs fall within the range of 60,000 and 412,000. Similarly, the M_w of the SCL-PHAs fall within the range of 5,30,000 to 1,100,000 (Valappil *et al.*, 2007).

The GPC analysis of the polymer produced by *P. mendocina* using sugarcane molasses was carried out. The weight average molecular weight of the Poly(3-hydroxydecanoate-3-hydroxyoctanoate) was found to be 1.4 x 10^5. Polydispersity index (PDI), which is a measure of the distribution of molecular masses in a polymer, was calculated to be 1.9, indicating that the molecular mass distribution of the polymer sample was within a small range, a desirable property. The GPC analysis of the polymer produced by *P. mendocina* using biodiesel waste was also carried out. The weight average molecular weight of the Poly(3-hydroxydecanoate) was found to be 6.5 x 10^4. The PDI was calculated to be 2.0. The GPC analysis of the polymer produced by *P. mendocina* using pure glycerol was carried out. The weight average molecular weight of Poly(3-hydroxydecanoate) was found to be 4.6 x 10^4. The PDI was calculated to be 2.6.

3.2.4 Thermal characterisation

Thermal characterisation of the polymer was carried out using Differential Scanning Calorimetry (DSC) as described in **section 2.6.4**. DSC was used to determine the melting temperature (T_m) and the glass transition temperature (T_g) of the polymer produced using cheap carbon sources. The results of the thermal analyses are summarised in **Table 3.1**.

Samples	T_m (°C)	T_g (°C)
Sugarcane molasses	**53.9 ± 0.2**	**-37.9 ± 0.4**
Biodiesel waste	**42.3 ± 0.7**	**-29.8 ± 0.3**
Pure glycerol	**44.5 ± 1.0**	**-22.8 ± 0.7**

Table 3.1: Thermal analysis of the polymer produced using cheap carbon sources

Sugarcane molasses: The T_m and the T_g of the polymer produced using sugarcane molasses as the carbon source were found to be 53.9 ± 0.2 and -37.9 ± 0.4 °C

respectively. The FTIR and the GC-MS results have confirmed that the polymer produced is a copolymer of P(3HD-co-3HO) which is a type of a medium chain length (MCL) PHA. According to the literature, it is known that MCL-PHAs have a low melting temperature and glass transition temperature. The melting temperature ranges within 40 – 60°C and the glass transition temperature ranges within -50 and -25°C (Rai *et al.*, 2011). The thermal properties of this polymer produced using sugarcane molasses falls within this range.

Biodiesel Waste: The T_m and the T_g of the polymer produced using biodiesel waste as the carbon source were found to be 42.3 ± 0.7 °C and -29.8 ± 0.3 °C respectively. The FTIR and the GC-MS results have confirmed that the polymer produced is P(3HD) which is a type of a medium chain length (MCL) PHA containing 10 carbon atoms within a monomer unit. The thermal properties of this polymer produced using biodiesel waste also falls within the range of the thermal properties of the MCL-PHAs (Rai *et al.*, 2011).

Pure Glycerol: The T_m and the T_g of the polymer produced using pure glycerol as the carbon source were found to be 44.5 ± 1 and -22.8 ± 0.7 °C respectively. The FTIR and the GC-MS results have confirmed that the polymer produced is a P(3HD) which is a type of a medium chain length (MCL) PHA containing 10 carbon atoms within a monomer unit. Thermal properties of this polymer produced using pure glycerol falls within the range thermal properties of the MCL-PHAs (Rai *et al.*, 2011).

Discussion

Recent studies have shown that the production of PHAs could become commercially viable with the utilisation of cheap and renewable carbon sources. This could bring down the cost of production of PHAs by about 50% (Chaudhry *et al.*, 2011). Therefore, in this study, the production of PHAs by *P. mendocina* using cheap carbon sources such as sugarcane molasses, biodiesel waste and pure glycerol have been investigated. The results of these studies have been discussed in detail. *P. mendocina* was the chosen organism used for the production of PHAs during this study. *P. mendocina* is a Gram negative bacteria which was first isolated from the soil and water samples by N.J. Palleroni in 1970 (Palleroni *et al.*, 1970). They belong to the rRNA homology group I and are known to produce MCL-PHAs from both structurally related and unrelated carbon sources, under nutrient

limiting conditions (Tian *et al.,* 2000; Rai *et al.,* 2011). *P. mendocina* was grown in MSM medium containing 20 g/L of the cheap renewable carbon source in 5L shaken flasks.

Sugarcane molasses is rich in sugar such as sucrose, stachyose, raffinose and vitamins such as thiamine, riboflavin, pyridoxine and niacinamide, therefore sugarcane molasses has been widely used as the energy source for the production of PHAs. Previous studies have shown that sugarcane molasses enhances the growth of the organism and also causes the accumulation of PHAs within the cells (Gouda *et al*., 2001; Chaudhry *et al*., 2011; Akaraonye *et al*., 2012). In this study, an MCL copolymer containing 3HO and 3HD monomer units were produced by *P. mendocina* using sugarcane molasses as the carbon source. This was confirmed by carrying out FTIR and GC-MS analysis. A similar experiment was carried out by Solaiman *et al*., where they screened and identified *P. corrugata* as the organism that was able to utilise 5% of soy molasses and produce 0.6 g/L of the MCL-PHAs containing repeating units of 3HDD, 3HO and 3-hydroxytetradodecanoate (Solaiman *et al*., 2006). However, in an experiment carried out by Jiang *et al*., 2008, they observed that *P. fluorescens* when cultured in sugarcane liquor produced P(3HB). The P(3HB) yield obtained was around 70% dcw. This proved that *P. fluorescens,* which is commonly known to be an MCL-PHA producer was able to synthesize P(3HB) (Jiang *et al*., 2008a). In this work, the maximum dry cell weight obtained using sugarcane molasses as the sole carbon source was 9 g/L at 45 hours. However, the PHA yield at 48 hours was 20% dcw which was low in comparison to the amount of the biomass obtained. This suggested that under the specific conditions used, maximum energy was utilised in growth instead of PHA biosynthesis. The finding of this study was in agreement with the results obtained by Gouda *et al*., 2001 where they cultivated *Bacillus megaterium* in a medium containing sugarcane molasses as the carbon source. They stated that PHA yield is not dependent on cell growth (Gouda *et al*., 2001). Nitrogen was the limiting nutrient in this study. The concentration of nitrogen decreased gradually. However, there was an unexpected increase in the concentration of nitrogen at 36 hours. The cells had a prolonged log phase and entered stationary phase at 45 hours. According to literature, the presence of nitrogen is crucial for cell growth. It is also known that the depletion of the nitrogen concentration in the media guides the cells into the stationary phase and causes the accumulation of PHA (Lageveen *et al*.,

1988; Kim *et al.,* 1994; Wang and Lee, 1997; Choi and Lee, 1999). In another experiment carried out by Tian *et al.,* 2000, they cultivated *P. mendocina* strain 0806 in glucose media. They observed that the ratio of carbon source to nitrogen source (C/N) affected the accumulation of PHA. They concluded that nitrogen limitation was a major factor for the triggering of the polymer synthesis (Tian *et al*., 2000). Sugarcane molasses have been used widely for the production of SCL-PHAs such as P(3HB) by various organisms such as *Bacillus* spp JMa5, *R. picketti*, *B. megaterium* and *B. cereus* SPV (Gouda *et al*., 2001; Bonatto *et al*., 2004; Akaraonye *et al.,* 2012). However, sugarcane molasses remain fairly unexplored for the production of MCL-PHAs.

The waste product generated during the production of biodiesel is rich in glycerol, fatty acids and fatty acid methyl esters. Under appropriate conditions, they can be used as the feedstock for various industrial processes (Ashby *et al*., 2004). In this study, an MCL polymer containing 3HD monomer units were produced by *P. mendocina* using biodiesel waste as the sole carbon source. This was confirmed by carrying out FTIR and GC-MS analysis. Maximum dry cell weight obtained was 7.4 g/L at 48 hours. The polymer yield at 48 hours was 43.2% of the dry cell weight which was the highest yield obtained in this study. In an experiment carried out by Ashby *et al*., 2004, they cultivated *P. corrugata* in a medium containing 1 to 5 % of the biodiesel waste that was rich in glycerol, free fatty acids and fatty acid methyl esters. They observed that the increase in the concentration of the biodiesel waste in the production media had a negative effect on the growth of the cells. Maximum cell growth was attained when the biodiesel waste concentration was 1% in the medium. In this study, the concentration of the biodiesel waste in the media was 20% which is much higher compared to 5% used in the study carried out by Ashby *et al*., 2004. Poor growth of *P. mendocina* in this study could be due to a very high concentration of biodiesel waste in the media. Highest PHA yield obtained by Ashby *et al*., 2004 was 42% of the dry cell weight when the concentration of biodiesel waste was 3% in the media. GC-MS analysis confirmed that the polymer produced contained 3-hydroxyoctanoic acid, 3-hydroxydecanoic acid and 3-hydroxytetradodecanoic acid as monomers (Ashby *et al*., 2004). These results were in agreement with the outcome of this study that the crude biodiesel waste could be utilized as the carbon source for the production of PHAs. In the same experiment, Ashby *et al*., cultivated another *Pseudomonas* strain such as *P. oleovorans* NRRL

B14682 in a medium containing 5% biodiesel waste. They observed the production of a homopolymer of P(3HB) (Ashby *et al*., 2004). This suggested that the type of the polymer produced using the biodiesel waste as the carbon source is dependent on the type of the organism used. They also added that the growth of *P. oleovorans* was not affected by the increase in the concentration of the biodiesel waste in the media. This indicated that the effect of the biodiesel waste on the growth of the organism was dependant on the type of organism (Ashby *et al*., 2004). The maximum P(3HB) yield obtained was 27% dcw at 5% of biodiesel waste concentration (Ashby *et al*., 2004).

Future studies involving cultivation of *P. mendocina* in various concentrations of biodiesel waste could shed light on the effect of the biodiesel waste on cell growth and PHA accumulation within the *P. mendocina* cells. In a similar experiment carried out by Koller *et al*., 2004, they cultivated an osmophilic wild strain of bacteria, in a medium containing biodiesel waste rich in glycerol content. They observed the production of poly(3-hydroxybutyrate-co-hydroxyvalerate) (Koller *et al*., 2005). Organisms such as *Methylobacterium rhodesianum* and *C. necator* have been reported to have utilised glycerol rich biodiesel waste for the production of P(3HB) (Bormann and Roth, 1999).

In this study, *P. mendocina* was also cultivated in a medium containing pure glycerol for the production of PHAs. The results obtained were compared to that of the glycerol rich biodiesel waste. In this study, MCL polymer containing 3HD units were produced by *P. mendocina* using pure glycerol as the sole carbon source. This was confirmed by carrying out FTIR and GCMS analysis. The maximum dry cell weight obtained was 8.6 g/L at 45 hours. This showed that cell growth was better in the medium containing glycerol compared to the biodiesel waste. However, the polymer yield at 48 hours was 10.5% of the dry cell weight which was much lower compared to the polymer yield in the biodiesel waste. In an experiment carried out by Ashby *et al.,* 2005, a mixed culture containing P(3HB) producing *P. oleovorans* NRRL B14682 and the MCL-PHA producing *P. corrugata* was cultivated in a medium containing pure glycerol as the carbon source. They observed that *P. corrugata* was not capable of producing MCL-PHAs when the glycerol concentration was higher than 3% whereas *P. oleovorans* NRRL B14682 was able to accumulate P(3HB) at 5% glycerol concentration in the media. *P. oleovorans* NRRL B14682 produced a homopolymer of P(3HB) while *P. corrugata* produced the MCL

copolymer containing 3HD and 3HDD monomer units at 2% glycerol concentration (Ashby *et al.,* 2005). Ashby *et al.,* 2005 obtained maximum P(3HB) yield of 40% dcw by *P. oleovorans* NRRL B14682 and a maximum MCL-PHA yield of 20% dcw by *P. corrugata*. The MCL-PHA yield was lower in the pure glycerol medium compared to the medium containing biodiesel waste (Ashby *et al.,* 2005). As mentioned earlier, nitrogen limitation triggers the accumulation of PHAs (Lageveen *et al*., 1988). Nitrogen was the limiting nutrient in both biodiesel waste and the pure glycerol containing media. The concentration of the nitrogen in the biodiesel waste medium decreased during the early hours of fermentation maintaining a nitrogen limiting condition throughout the course of the fermentation. In the case of the pure glycerol, there was an unexpected increase in the concentration of nitrogen at 36 hours. This could most likely be a nitrogenous compound which forms the part of the chemical composition of the carbon source. These results suggested that *P. mendocina* was capable of utilising both crude as well as pure glycerol as the sole carbon source for the production of PHAs. However, in future, analysis to determine PHA yield at regular intervals during the course of the fermentation would point towards an optimum time for the polymer extraction. It would also determine the degradation of the accumulated PHA. Apart from this, the estimation of the carbon in the media would give an understanding of the utilization of the carbon source by *P. mendocina*. Depending on the percentage of the unused carbon in the media at the end of the fermentation, one would be able to determine the optimum carbon concentration for the increased PHA production.

GPC analysis was carried out to determine the molecular weight of the polymers produced. The molecular weight of the PHAs produced using sugarcane molasses, biodiesel waste and pure glycerol were within the known range for the MCL-PHAs which is 60,000 – 412,000. However, P(3HD) produced using pure glycerol as the carbon source has a lower molecular weight compared to the P(3HD) produced using biodiesel waste as the carbon source. PHAs are produced intracellularly within the organism (Rai *et al.,* 2011). In this study, the polymer produced within the cells was extracted using chloroform and hypochlorite dispersion method. Furrer *et al*., 2007 stated that the sodium hypochlorite used for the extraction of the polymer is responsible for the degradation of the polymer by causing chain scission. This was confirmed by carrying out GPC analysis (Furrer *et al*., 2007). Previous studies have shown that hypochlorite degradation can cause upto 50%

decrease in the molecular weight of the polymer produced (Yasotha *et al*., 2006). Apart from this, it has also been reported that the polymer is degraded due to the repeated washing after the hypochlorite extraction (Rai *et al.,* 2011). This could be one of the reasons for the decrease in the molecular weight of the polymer produced. The effect of the hypochlorite on the molecular weight of the polymer depends on the type of the organism used. There was a 75% reduction in the molecular weight of the polymer produced by *A. eutrophus* due to the chain scission caused by hypochlorite, whereas there was 15% reduction in the molecular weight of the polymer produced by recombinant *E. coli* (Rai *et al*., 2011). The decrease in molecular weight of the polymer produced using glycerol rich biodiesel waste and the pure glycerol have been previously observed by Koller *et al*., 2005, Ashby *et al.,*2004 and Ashby *et al*., 2005. Koller *et al*., stated that the presence of glycerol in the medium terminated the chain elongation by covalently binding to the carboxyl end of the PHA (Koller *et al*., 2005). Ashby *et al*., reported that there was 72% decrease in the molecular weight of the MCL-PHAs produced by *P. corrugata* using pure glycerol. However, they stated that there was no evidence of the termination of chain propagation. They speculated that this decrease in the molecular weight of the MCL-PHAs could be due to osmotic stress caused by the increase in the concentration of glycerol in the media resulting in low biomass yield, low polymer synthesis and molecular weight (Ashby *et al*., 2005).

Thermal properties of the polymer were studied using DSC. The results have been summarised in **Table 3.1**. The T_m and the T_g values of the polymer produced corresponded to the T_m of MCL-PHAs which ranges between 40°C and 60°C and the T_g values which ranges between -50 and -25°C (Rai *et al*., 2011). MCL-PHAs in general, have a low melting and glass transition temperature. According to the literature, they have a low crystallinity and therefore exhibit poor mechanical properties. However, their elastomeric nature makes them highly suitable for biomedical applications such as soft tissue engineering (Rai *et al*., 2011).

In conclusion, this study has demonstrated the utilization of cheap carbon sources such as the sugarcane molasses, glycerol rich biodiesel waste and pure glycerol by *P. mendocina* for the production of PHAs. MCL-PHAs were produced and characterised. A maximum PHA yield of 43.2% dcw was obtained in the media containing biodiesel waste. Utilisation of these inexpensive carbon sources for the

production of MCL-PHAs could bring down the cost of PHA production and help in moving a step closer towards their commercialisation.

CHAPTER 4

Novel Poly (3-hydroxyoctanoate)/ Bacterial Cellulose Composites

INTRODUCTION

Medium chain length PHAs (MCL-PHAs) are structurally diverse and their properties can be tailored for specific applications (Philip *et al*., 2007). Due to their elastomeric properties, MCL-PHAs have been explored for their application in soft tissue engineering, biological implants such as the heart valves, cartilage tissue engineering and in wound healing (Kim *et al*., 2007). P(3HO) is a type of MCL-PHA which has a % elongation at break value of 278. It has a low melting temperature (T_m) and a low glass transition temperature (T_g) of 30-50°C and -35 to -36°C respectively. P(3HO) has relatively low tensile strength and Young's Modulus value of around 1.8 and 11.4 MPa respectively (Rai *et al.,* 2011). However, previous studies have shown that the MCL-PHAs can be modified to obtain optimum properties such as high mechanical strength by making composites and blends with inorganic and organic additives (Kim *et al*., 2007).

In recent times, there has been a great interest in using natural fibres as reinforcement agents to enhance the mechanical properties of biodegradable polymers. One of the most commonly used reinforcing element is cellulose. It is a major component of the plant biomass and an extracellular polymer in microorganisms belonging to the genera *Acetobacter, Rhizobium, Agrobacterium,* and *Sarcina.* The major difference between plant and bacterial cellulose is the absence of hemicelluloses and lignin residues in the latter which makes them highly pure compared to the plant cellulose (Soykeabkaew *et al*., 2009). Bacterial cellulose has excellent mechanical properties such as a Young's modulus value of 16.9 GPa and tensile strength of 256 MPa. It is highly hydrophilic in nature. Due to its excellent mechanical properties and hydrophilic nature, bacterial cellulose has been widely used as a reinforcement material in the synthesis of novel composite materials (Klemm *et al*., 2001).

Therefore in this study, P(3HO), a type of MCL-PHA produced by *P. mendocina*, a Gram negative bacteria was reinforced using bacterial cellulose to produce P(3HO)/bacterial cellulose composite film. It is a known fact that bacterial cellulose is extremely hydrophilic in nature with a very high water retention capacity whereas P(3HO) is very hydrophobic in nature. In order to achieve a significant level of compatibility between bacterial cellulose and P(3HO), bacterial

cellulose was chemically modified using an acetylation reaction in which the water retaining cellulose hydroxyl groups were replaced by acetyl groups. This would decrease the hydrophilic properties of bacterial cellulose and hence make them compatible with the P(3HO) matrix. P(3HO)/5% bacterial cellulose, P(3HO)/15% bacterial cellulose and P(3HO)/25% bacterial cellulose composite films were characterised with respect to their mechanical, thermal and microstructural properties. In addition, the effect of the addition of cellulose microcrystals on the degradability as well as biocompatibility of P(3HO) were also investigated.

4.0 Results

4.1 P(3HO) Production

P(3HO) production by *P. mendocina* using sodium octanoate as the sole carbon source was carried out as described in **section 2.4**. The carbon to nitrogen (C/N) ratio used in this study was 15:1. The fermentation profile is shown in Figure 4.1.

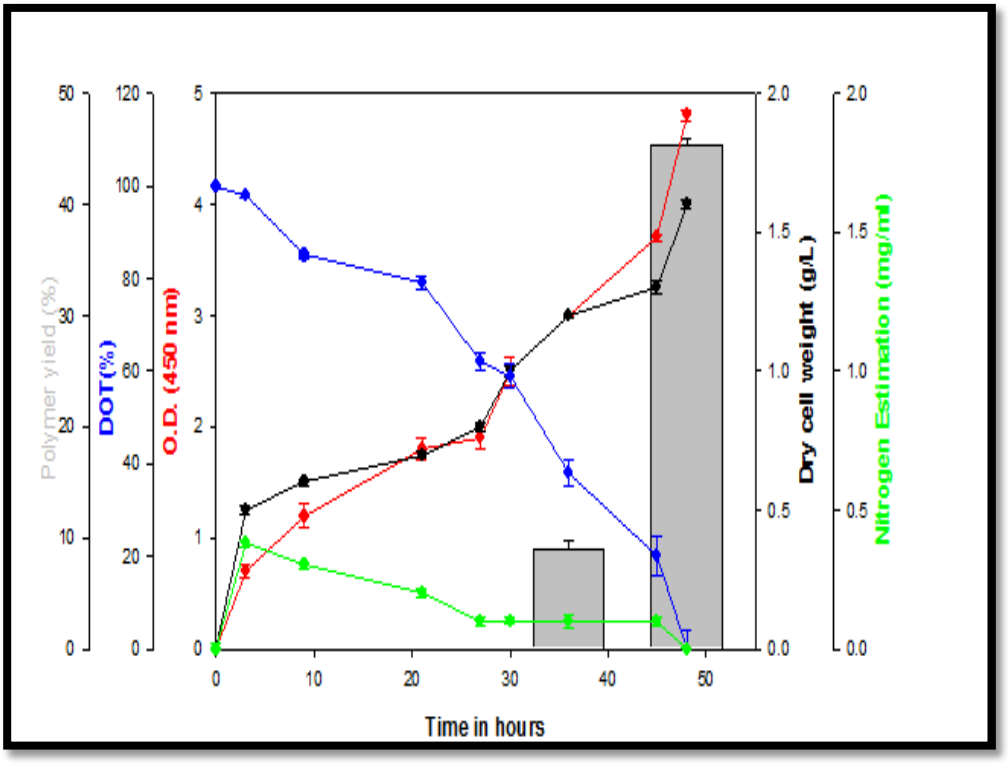

Figure 4.1: The fermentation profile for P(3HO) production by *P. mendocina* using sodium octanoate as the sole carbon source.

The $O.D._{450}$ and the dry cell weight (dcw) values increased exponentially reaching a value of 4.8 and 1.6 g/L respectively, at 48 hours, showing a steady growth of the organism throughout the 48 hour fermentation period. The nitrogen concentration reduced rapidly through the fermentation process, indicating usage of nitrogen by the organism. After about 32 hours, nitrogen concentration had reduced from its initial value of 0.5 mg/ml to 0.1 mg/ml, becoming a limiting condition. The % DOT

values also reduced from its initial value of 100%, through the fermentation, reaching a value of 0%. After 48 hours of fermentation, the *P. mendocina* cells were harvested for the extraction of the polymer. In this study, NaOCl/chloroform mixture was used to rupture the cells followed by dissolution of the PHA inclusions in the chloroform solution as described in **section 2.4.3**. A polymer yield of 45.3% dcw was observed at 48 hours while 9% dcw polymer yield was observed at 36 hours of the fermentation. Polymer produced was purified using the method described in **section 2.4.4**. Elbahloul and Steinbüchel, 2009 were able to achieve 95% (wt/wt) of 99% pure polymer from the freeze dried cells using this method. This was followed by an additional purification step using acetone as the polymer has a higher solubility in acetone than the lipolysaccharide (an endotoxin present on the cell wall of the Gram negative bacteria such as in *Pseudomonas* species) (Elbahloul and Steinbuchel, 2009). Therefore, in this study, this procedure was repeated several times to ensure that the polymer produced were of high purity. This purified polymer was then further characterised.

4.2 Characterisation of the polymer produced

4.2.1 Fourier Transform Infrared Spectroscopy (FTIR)

The polymer produced was characterised using FTIR as described in **section 2.6.1.** The absorption spectrum of the polymer confirmed the presence of the characteristic marker ester carbonyl band for MCL-PHAs which occurs around 1742 cm^{-1} and the band at 1162 cm^{-1} which occurs due to C-O stretching (Randriamahefa *et al.*, 2003) as shown in **Figure 4.2.**

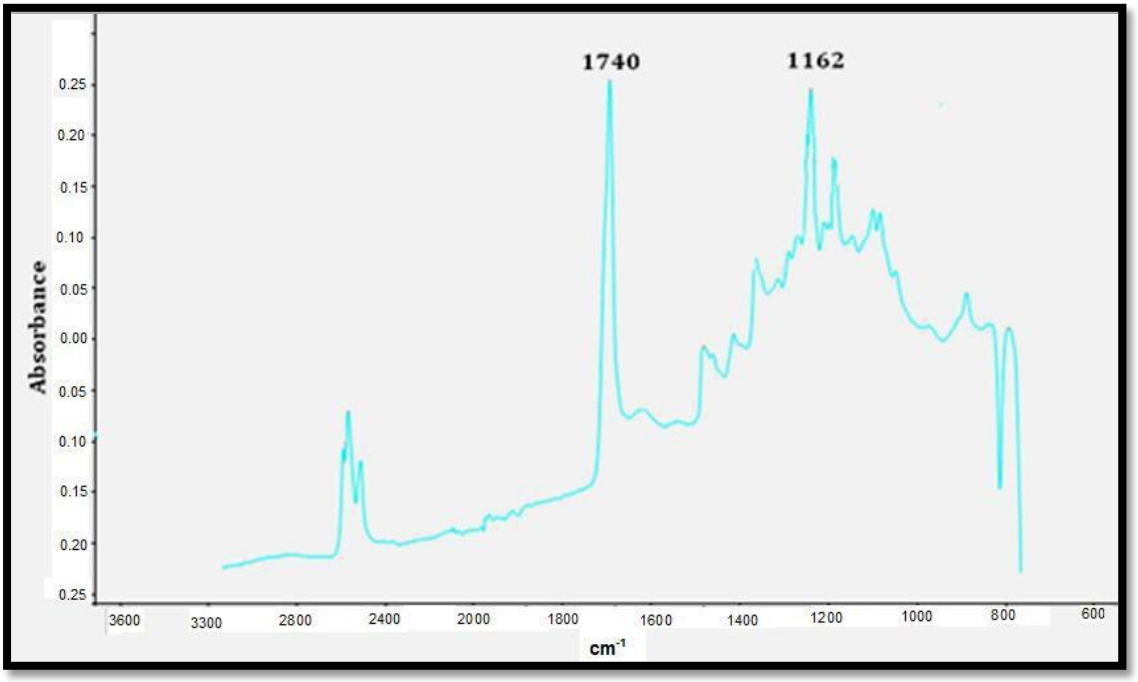

Figure 4.2: FTIR spectrum of the polymer indicating the presence of absorption peak at 1740 cm^{-1} and 1162 cm^{-1}.

Preliminary characterisation using FTIR suggested that the polymer produced was an MCL-PHA.

4.2.2 Gas Chromatography Mass Spectrometry (GC-MS)

The polymer produced was further characterised using Gas chromatography mass spectrometry. Prior to this analysis, the polymer was methanolysed to obtain methyl esters as described in **section 2.6.2.**

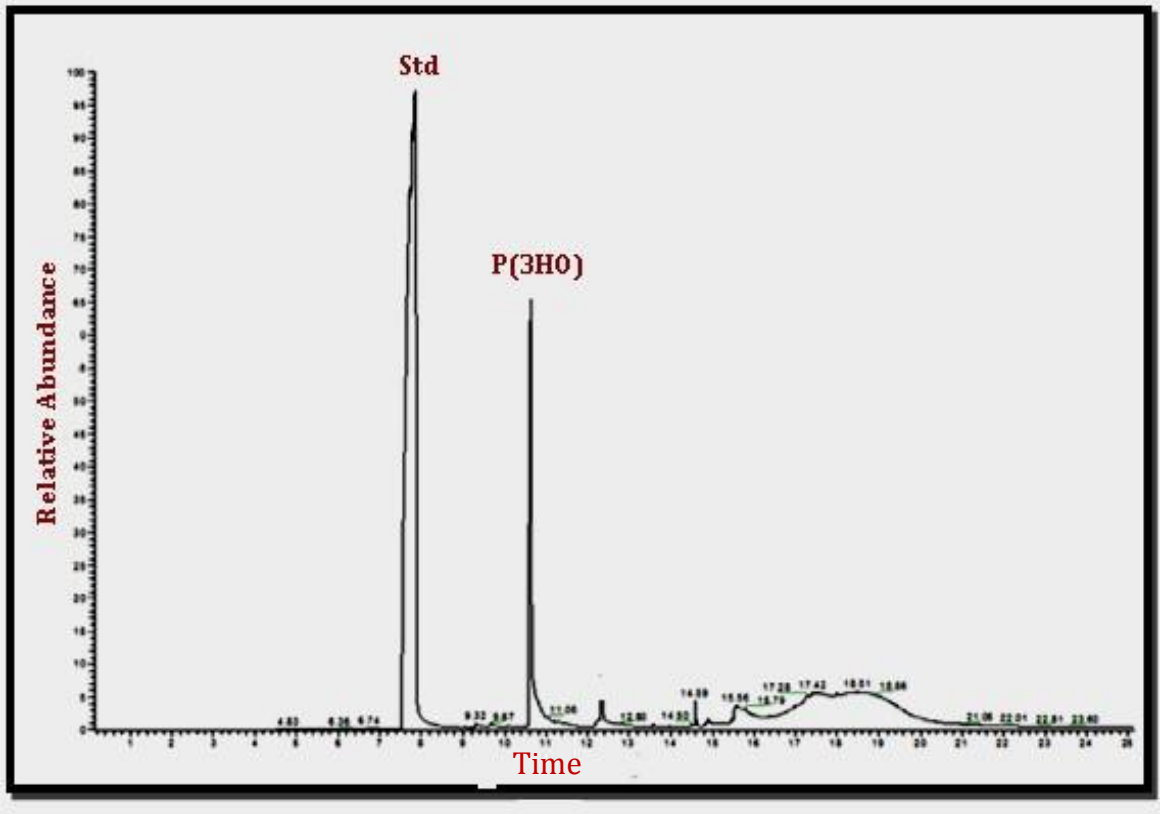

(a)

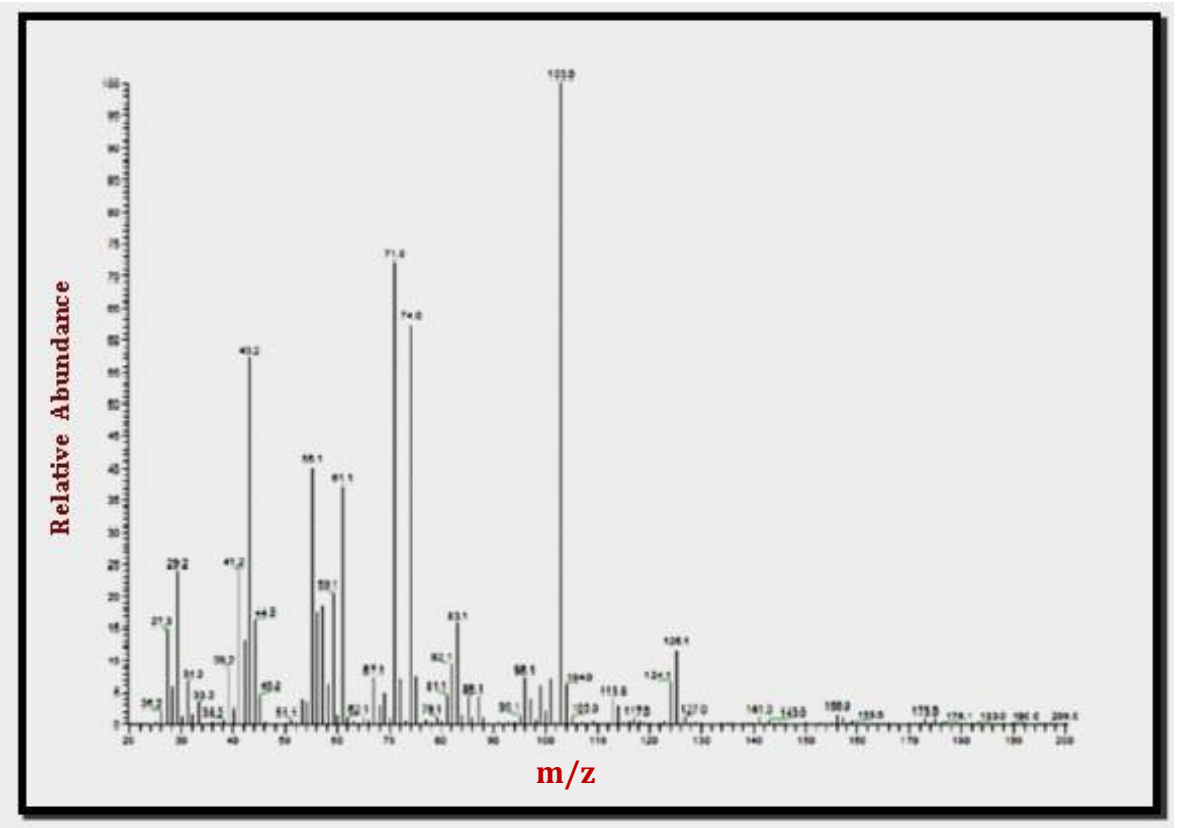

(b)

Figure 4.3: GC-MS analysis of the polymer produced by *P. mendocina* using sodium octanoate as the sole carbon source**.** (a) A total ion gas chromatogram of the

polymer produced using sodium octanoate as the carbon source. (b) The MS fragmentation pattern of the GC peak at a retention time 10.63 min.

The mass spectrum of the peak at a retention time (R_t) of 10.63 min was identical to that of the methyl ester of 3-hydroxyoctanoate (M_w = 174) in the MS (NIST) library, confirming that the polymer produced was Poly(3-hydroxyoctanoic acid). 2-ethyl-2-hydroxybutyric acid was used as an internal standard and showed as a peak at a retention time of 7.86 min as shown in **Figure 4.3.**

4.2.3 Nuclear Magnetic resonance (NMR)

Final characterisation of the polymer produced by *P. mendocina* was carried out using ^{13}C and ^{1}H NMR as described in **section 2.6.3**. ^{1}H and ^{13}C spectra of the polymer are represented in **Figure 4.4 (A)** and **(B)**.

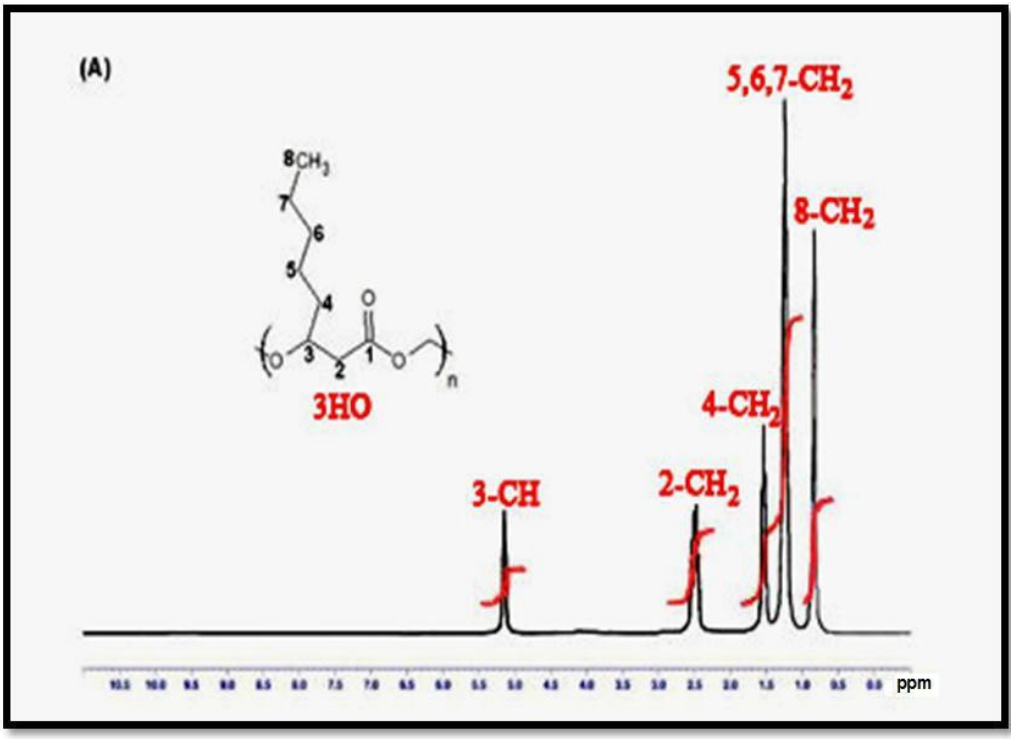

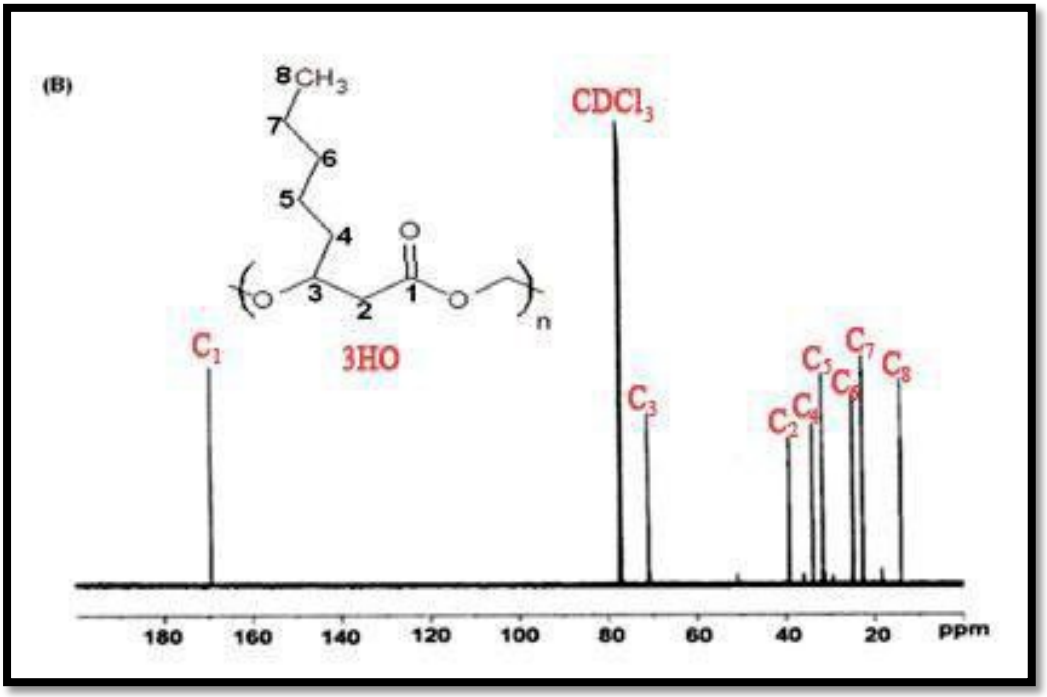

Figure 4.4: NMR spectrum of polymer produced by *P. mendocina* using using sodium octanoate as the sole carbon source (A) ^{1}H spectrum; (B) ^{13}C spectrum.

In the ^{13}C spectrum, eight peaks have been observed. This corresponds to the eight different environments for the carbon in the molecule. The chemical shift at 169.53 ppm corresponds to C_1 (C=O group), 70.94 ppm to C_3 (-CH), 39.18 ppm to C_2 ($-CH_2$), 23 – 35 ppm to C_4, C_5, C_6, C_7 ($-CH_2$) and 13.93 ppm to C_8 ($-CH_3$). Similarly, in ^{1}H spectrum, five different peaks were observed owing to the five different environments for the proton in the molecule. The chemical shifts of 2.5, 5.1, 1.5, 1.2 and 0.8 ppm demonstrated the presence of protons bonded to C_2 ($-CH_2$), C_3 (-CH), C_4 ($-CH_2$), C_5, C_6, C_7 ($-CH_2$) and C_8 ($-CH_3$) respectively. Hence, the ^{13}C and ^{1}H NMR analysis further confirmed the GC-MS result, i.e. that the polymer produced by *P. mendocina,* using sodium octanoate as the sole carbon source, is the homopolymer of 3-hydroxyoctanoic acid.

4.3 Production of cellulose from *Acetobacter xylinum* and its chemical modification.

In this study, bacterial cellulose was used as a reinforcing agent to improve the mechanical properties of P(3HO). It was produced by *A. xylinum* at the conical flask level as described in **section 2.7.2**. In this study, *A. xylinum* was cultured in a static mode and the bacterial cellulose was produced in the form of a gel like pellicle as shown in **Figure 4.5**

Figure 4.5: A bacterial cellulose pellicle produced by *Acetobacter xylinum* in a hydrated state.

These bacterial cellulose pellicles were then washed with 2% sodium hydroxide at 96°C for an hour. They were then subjected to homogenisation followed by acid hydrolysis as described in **section 2.7.4.** This was carried out to generate shorter microfibrils referred to as cellulose microcrystals as shown in **Figure 4.6**

Figure 4.6: Freeze dried acetylated bacterial cellulose microcrystals used for composite production.

The bacterial cellulose microcrystals were then subjected to an acetylation reaction as described in **section 2.7.5.** This was carried out to increase the compatibility of the hydrophilic bacterial cellulose with the hydrophobic P(3HO). Acetic anhydride was used as the catalyst for this acetylation reaction as shown in **Figure 4.8.**

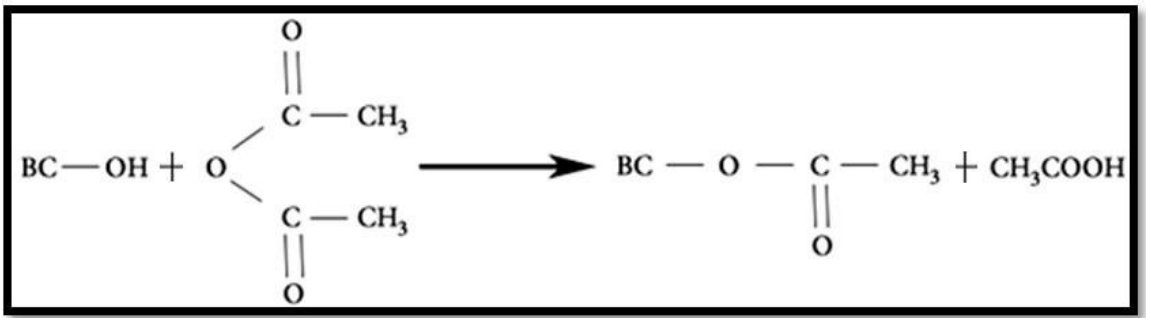

Figure 4.7: Chemical reaction of the bacterial cellulose with acetic anhydride (Jonoobi *et al.*, 2010).

4.4 Characterisation of the acetylated cellulose microcrystals using FTIR

After the acetylation reaction, bacterial cellulose microcrystals were characterised using FTIR in order to confirm their chemical modification as described in **section 2.6.1**. The FTIR spectrum of the acetylated bacterial cellulose microcrystals was compared with the spectrum of the native cellulose as shown in **Figure 4.8.**

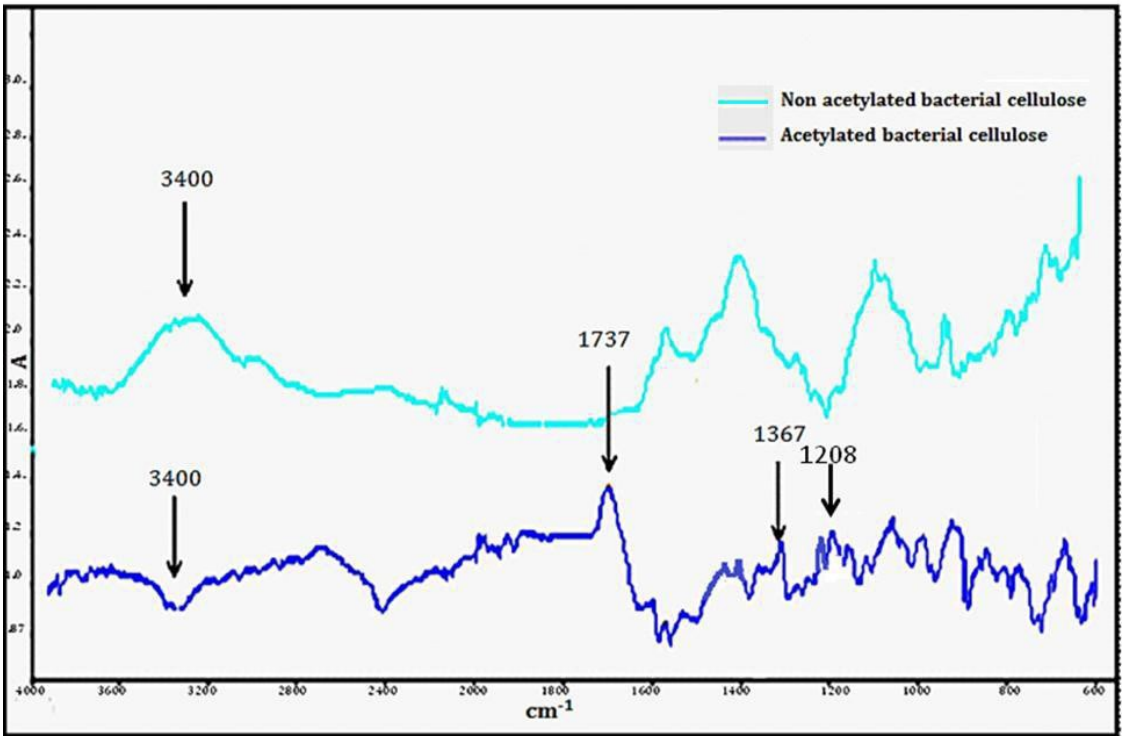

Figure 4.8: The FTIR analysis showing the acetylated bacterial cellulose versus the non-acetylated bacterial cellulose.

A sharp peak at 3400 cm^{-1} corresponding to hydroxyl groups was observed in the FTIR spectrum of the native bacterial cellulose. As expected there was a decrease in the intensity of this absorption peak in the acetylated bacterial cellulose

microcrystals. This decrease in the absorption intensity confirmed the substitution of the hydroxyl groups by the acetyl groups. The acetylation of the cellulose was further confirmed by the presence of the absorption band at 1737 cm^{-1} corresponding to C=O ester stretching, at 1208 cm^{-1} corresponding to C-O stretching of the acetyl group and 1367 cm^{-1} corresponding to the CH_3 group, which were not present in the spectrum of native bacterial cellulose.

4.5 X-Ray Diffraction

To investigate the effect of acetylation on the crystallinity of the bacterial cellulose, XRD studies were carried out. This test was carried out on the acetylated and the non-acetylated bacterial cellulose. The cellulose samples were analysed on a Brüker D8 Advance diffractometer in flat plate geometry, using Ni filtered Cu Ka, radiation. Data was collected from 10 to 100° with a primary beam slit size of 0.6 mm. A Brüker Lynx Eye silicon strip detector was used and a step size of 0.02° and a count time of 0.1 s per step. The XRD pattern of the acetylated bacterial cellulose was compared with the non-acetylated bacterial cellulose microcrystals as shown in **Figure 4.9.**

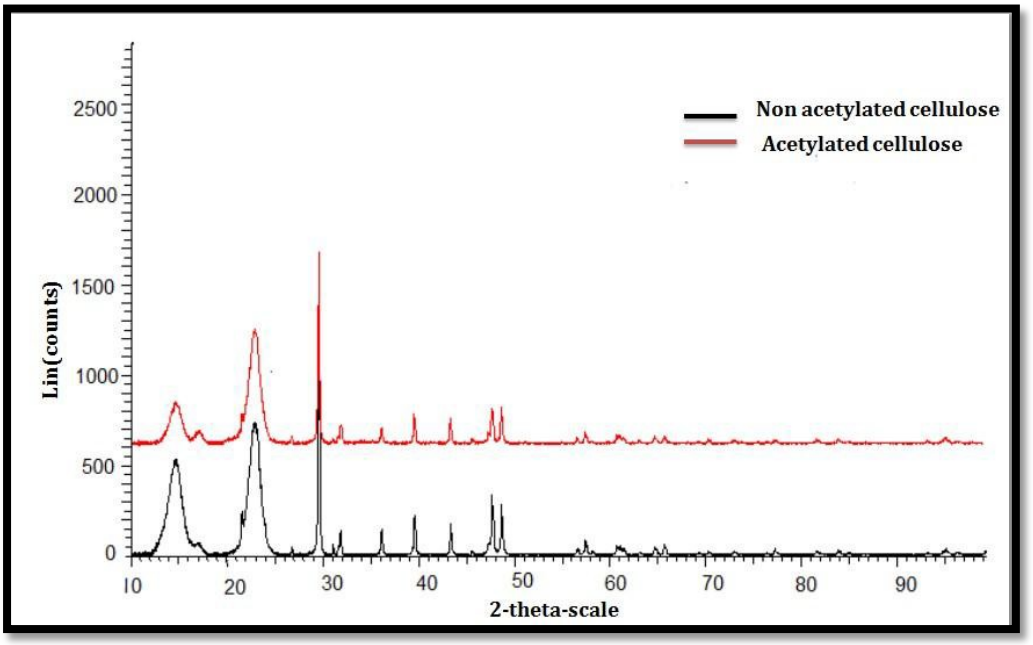

Figure 4.9: XRD patterns of the acetylated bacterial cellulose and the non-acetylated bacterial cellulose.

There was a decrease in the intensity of the absorption peaks of the acetylated bacterial cellulose compared to the non-acetylated bacterial cellulose indicating a decrease in the crystallinity.

4.6 Preparation of neat P(3HO) and P(3HO)/5% bacterial cellulose, P(3HO)/ 15% bacterial cellulose and P(3HO)/25% bacterial cellulose composite films using the solvent cast method.

Acetylated bacterial cellulose microcrystals were incorporated into the P(3HO) matrix to produce 2D composite films containing 5%, 15%, 25% of acetylated bacterial cellulose microcrystals using the solvent casting method. This was done by dissolving the P(3HO) polymer and acetylated cellulose microcrystals in chloroform, casting the solution onto a glass petri dish. The film was then air dried for one week before being freeze dried for another two weeks.

4.7 Characterisation of the P(3HO)/bacterial cellulose composite films

4.7.1 Mechanical properties

The mechanical properties of the neat and the composite films were measured using the Perkin–Elmer Dynamic Mechanical Analyser (DMA) as described in **section 2.9.5**. This was carried out in order to investigate the effect of the bacterial cellulose microcrystals on the mechanical properties of the composite films. The results are summarised in **Table 4.1**.

Samples	Young's Modulus (MPa) E values	Tensile strength (MPa)	Elongation break (%)
P(3HO)	1.5 ± 0.1	1.8 ± 0.5	204.0 ± 0.2
P(3HO)/5% cellulose	7.0 ± 0.1	5.0 ± 0.8	145.0 ± 0.3
P(3HO)/15% cellulose	11.3 ± 0.9	4.3 ± 1.0	65.0 ± 0.7
P(3HO)/25% cellulose	18.4 ± 0.7	4.2 ± 0.9	35.0 ± 3.0

Table 4.1: Mechanical properties of the neat P(3HO) as well as P(3HO)/ bacterial cellulose composite films (n = 3).

The Young's modulus value, which is a measure of the stiffness of the materials was higher for the composite films compared to the neat P(3HO) film. With the increasing concentration of modified cellulose microcrystals in the P(3HO), there was an increase in the 'E' values of the composite films. The tensile strength of the P(3HO)/ bacterial cellulose composite films were also higher than the neat P(3HO) films. However, there was a decrease in the tensile strength of the P(3HO)/cellulose composite films with the increase in the concentration of the bacterial cellulose microcrystals in the P(3HO) film. Therefore, the composite production method needed improvement in order to suitably exploit the properties of the acetylated bacterial cellulose microcrystals for enhancement of the tensile strength of the composites.

From the literature, it is established that the % elongation at break values for MCL-PHAs range between 6.5 to 350 % (Asrar *et al.*, 2002). The values obtained in this study were within this range. There was a decrease in the elastomeric properties with the increase in the concentration of modified cellulose microcrystals in the films indicating that the presence of bacterial cellulose microcrystals had a significant effect on the elastomeric properties of the composite films.

4.7.2 Thermal Characterisation

Thermal characterisations were carried out to investigate the thermal stability of the composite films as a function of the temperature, as described in **section 2.9.6.** The results of the thermal analysis are summarised in **Table 4.2.**

Samples	T_g (°C)	T_m (°C)
P(3HO)	-34.0 ± 0.8	51.8 ± 0.2
P(3HO)/5% cellulose	-32.4 ± 0.3	47.0 ± 0.5
P(3HO)/15% cellulose	-31.4 ± 1.0	46.3 ± 0.7
P(3HO)/ 25 % bacterial cellulose	-33.8 ± 1.2	44.3 ± 0.9

Table 4.2: Thermal analysis of the neat P(3HO) and P(3HO)/bacterial cellulose composite films (n = 3).

There was a decrease in the melting temperature (T_m) of the P(3HO)/bacterial cellulose composite films compared to the neat P(3HO) film due to the addition of the modified bacterial cellulose microcrystals. On the other hand, there was an increase in the glass transition temperature (T_g) on addition of the modified cellulose microcrystals to the P(3HO) matrix.

4.7.3 Contact Angle Study

Static contact angle measurement was carried out in order to determine the effect of bacterial cellulose microcrystals on the hydrophilicity or wettability of P(3HO)/bacterial cellulose composite films as described in **section 2.9.4.** According to the literature, it is known that the polymer film with the contact angle (θ) values less than 70° are considered to be hydrophilic whereas θ values greater than 70° are considered to be hydrophobic in nature (Peschel *et al.,* 2008). Static contact angle measurements of the P(3HO) neat and P(3HO)/bacterial cellulose composites films are shown in **Figure 4.10.**

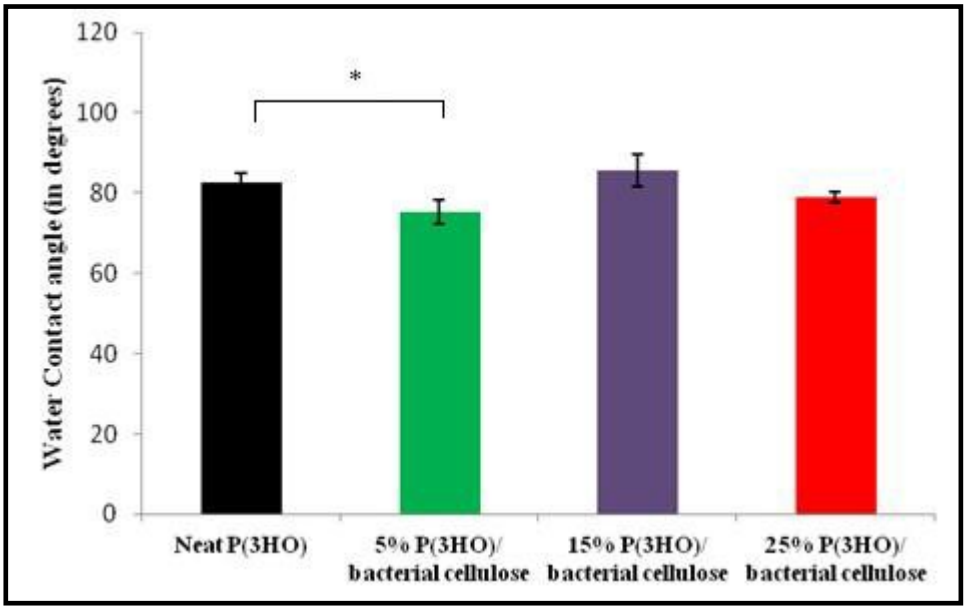

Figure 4.10: Static water contact angle measurement of the neat P(3HO) and P(3HO)/ bacterial cellulose composite films (n = 3). The data were compared using ANOVA and the difference were considered significant when *p<0. 05.

P(3HO)/5% and P(3HO)/25% bacterial cellulose composite films had a more hydrophilic surface compared to the neat P(3HO) film. While P(3HO)/15% cellulose composite film had a more hydrophobic surface compared to the neat P(3HO) neat film.

Based on these preliminary data, P(3HO)/25% bacterial cellulose composite films with the highest Young's modulus value and a relatively higher hydrophilicity, known to favour cell adhesion, was chosen for further characterisation.

4.8 Microstructural studies of the neat P(3HO) and P(3HO)/25% bacterial cellulose film.

4.8.1 Scanning Electron Microscopy (SEM)

Surface topography of the P(3HO)/25% bacterial cellulose film was studied using SEM as described in **section 2.9.1** in order to study the effect of bacterial cellulose on the surface properties of the composite film. The surface topography of the P(3HO)/25% bacterial cellulose composite film was compared to the neat P(3HO) film as shown in **Figure 4.11**.

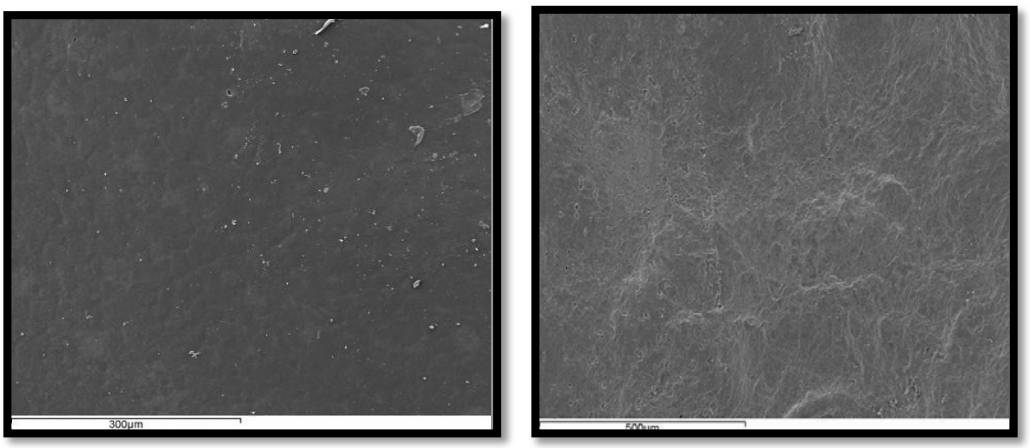

(a) **(b)**

Figure 4.11: SEM images of the neat P(3HO) and P(3HO)/ 25% bacterial cellulose composite films. (a) Surface of the neat P(3HO) film (b) Surface of the P(3HO)/25% bacterial cellulose composite film.

A new topography was introduced when modified bacterial cellulose microcrystals were included within the P(3HO) matrix. This change in the surface topography of the composite film was further confirmed using White Light Interferometry.

4.8.2 White Light interferometry

Surface roughness of the neat P(3HO) and P(3HO)/25% bacterial cellulose composite films was measured using White light interferometer as described in **section 2.9.2**. As shown in **Figure 4.12**, the root mean square (RMS) roughness of the (a) neat P(3HO) film was calculated to be 0.272 µm (b) whereas the RMS roughness of the P(3HO)/25wt% bacterial cellulose composite film was found to be 0.884 µm.

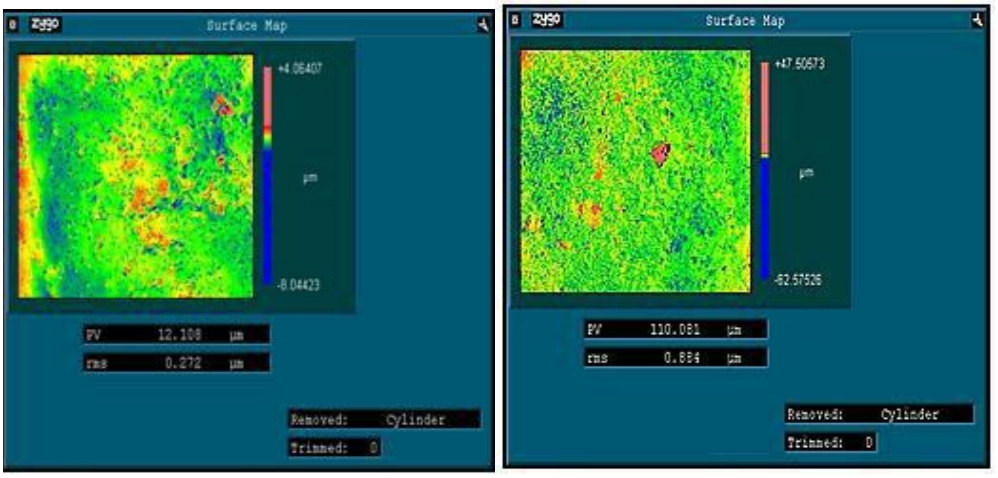

(a) **(b)**

Figure 4.12: Surface scans of the (a) P(3HO) neat and (b) P(3HO)/25% bacterial cellulose composite films using White Light Interferometry.

Hence, the addition of modified bacterial cellulose microcrystals to the neat P(3HO) film resulted in a rougher topography. Surface roughness of the P(3HO)/25% bacterial cellulose composite film was 226% higher compared to the neat P(3HO) film.

4.8.3 Protein Adsorption Test

Previous results in this study have shown that the presence of acetylated cellulose within the P(3HO) matrix resulted in the change of surface topography as well as the water contact angle. In order to evaluate the effect of these changes on the total protein adsorption on the composite film, an assay was carried to quantify the total protein adsorption as described in **section 2.9.7.** The results of the total protein adsorption is shown in **Figure 4.13.**

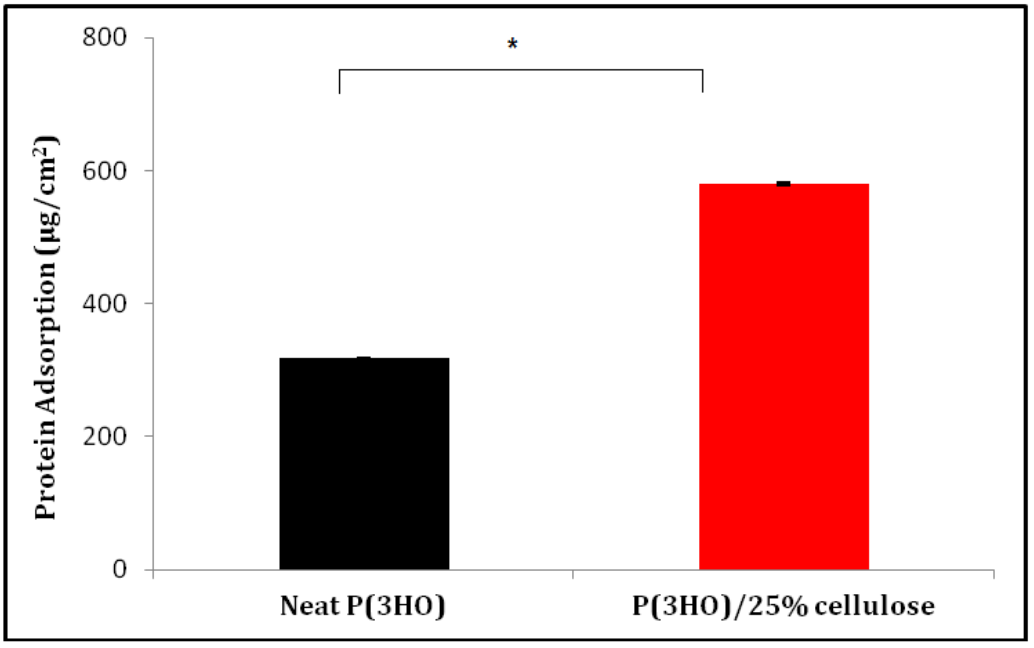

Figure 4.13: Protein adsorption of the neat P(3HO) and P(3HO)/25% cellulose composite film (n = 3). The data were compared using t-test and the difference were considered significant when *p<0. 05.

The overall protein adsorbed on the neat P(3HO) film was 318±1.0 µg/cm^2 which was lower as expected, compared to the total protein adsorbed on the surface of the P(3HO)/25% bacterial cellulose which was 580±1.6 µg/cm^2. The protein adsorption was significantly higher in the composite film in comparison to the neat P(3HO) film (*p<0. 05).

4.8.4 *In vitro* degradation study in DMEM and PBS media

A short, one month, *in vitro* degradation study was carried out using phosphate buffered saline solution (PBS) and Dulbeccos Modified Eagle Medium (DMEM) to investigate the effect of bacterial cellulose microcrystals on the degradation behaviour of the composite film, as described in **section 2.10.**

4.8.4.1 Water uptake, weight loss and pH measurements

Percentage of water absorbed (%WA) and weight loss (%WL) during the degradation of the neat as well as the composite film were measured and are presented in **Figure 4.14** (a), (b), (c) and (d).

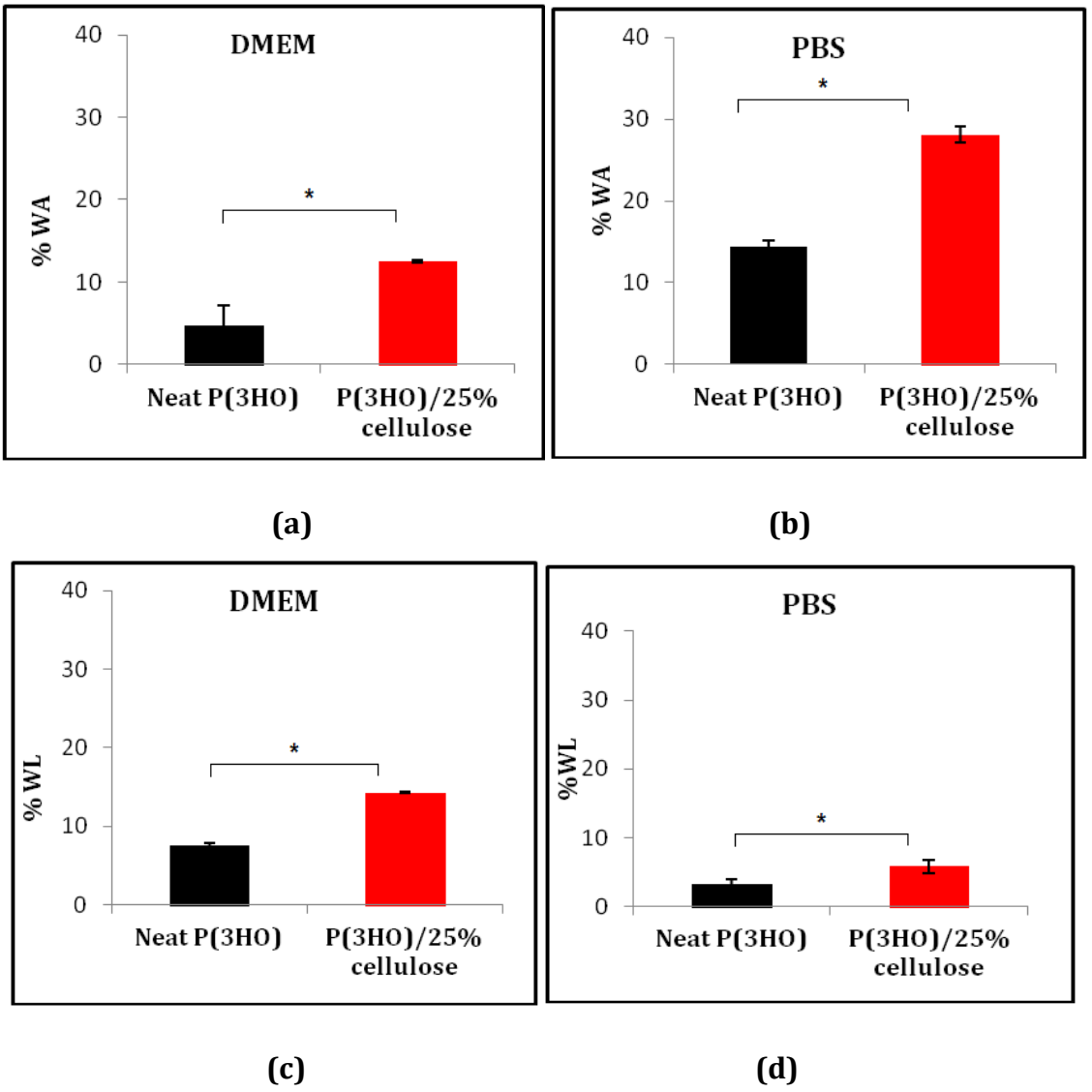

Figure 4.14: Water absorption by the neat P(3HO) and P(3HO)/25% bacterial cellulose composite films during the degradation study in (a) DMEM media and (b) PBS media. Weight loss by the degrading neat P(3HO) and P(3HO)/25% bacterial

cellulose composite film during the degradation study in (c) DMEM media and (d) PBS media (n = 3). The data were compared using t-test and the difference were considered significant when *p<0. 05.

Water absorption (%WA) was significantly higher in the composite film compared to the neat film both in DMEM and PBS media (*p<0.05). The %WA by the neat P(3HO) film in DMEM media during this one month study was 4.6±2.5%, whereas it was 12.5±0.1% in the P(3H0)/25% bacterial cellulose. In the PBS media, the %WA in the neat P(3HO) film was 14.4±0.7% compared to 28.1±1.0% in the P(3HO)/25% bacterial cellulose respectively.

The weight loss by the composite film was significantly higher compared to the neat film in both DMEM and PBS media (*p<0. 05). The % weight loss (%WL) by the neat P(3HO) film in DMEM media during this one month study was 7.5±0.2% whereas it was 14.2±1.0% for P(3H0)/25% bacterial cellulose. Similarly, in the PBS media, the %WL in the neat P(3HO) film was 3.3±0.6% compared to 5.8±1.0% in P(3H0)/25% bacterial cellulose. Hence, the P(3HO)/25% cellulose composite film had increased water absorption and weight loss in comparison to the neat P(3HO) film.

4.8.4.2 pH measurements

During the study, the neat P(3HO) and P(3HO)/25% bacterial cellulose composite film were incubated in DMEM and PBS media for a period of 30 days as described in **section 2.10**. pH measurements were carried out to analyse any change in the media due to the degradation of the film. There was an increase in the pH of both DMEM and PBS media after the completion of the study**.** The pH value of the DMEM media increased from a value of 7 to 8.4. Similarly, there was an increase in the pH of PBS media from 7.4 to 8.1.

4.8.4.3 Mechanical characterisation of the degrading film

At the end of the incubation period of the film samples in DMEM and PBS media, the Young's moduli of the degrading samples were measured to investigate the effect of degradation on the mechanical properties of the neat as well as the composite film. The Young's modulus values of the degrading samples had increased in both DMEM and PBS media as compared to the non-degraded samples. The 'E' values of the neat P(3HO) film incubated in the DMEM increased from 1.5±1.0 MPa to 7.3±0.8 MPa. A

similar trend was observed in the P(3HO)/25% bacterial cellulose composite film with an increase in the 'E' values of P(3HO)/25% bacterial cellulose composite film from 18.4±0.4 MPa to 25.1±0.3 MPa, upon incubation in the DMEM media, for a period of one month. Similar increase in the 'E' values of the neat P(3HO) and P(3HO)/bacterial cellulose composite film was observed in the PBS where the 'E' values of the neat P(3HO) film incubated in the PBS increased from 1.5±0.2 MPa to 1.8±0.5 MPa and the 'E' values of P(3HO)/25% bacterial cellulose composite film from 18.4±1.2 MPa to 27.1±2.0 MPa.

4.9 *In vitro* biocompatibility study

Preliminary *in vitro* cell culture studies were carried out on neat P(3HO) and P(3HO)/25% bacterial cellulose composite film using Human dermal microvascular endothelial cell line (HMEC-1) as described in **section 2.10.2**. HMEC-1, which is an endothelial cell line, was chosen for this study due to the potential application of these novel P(3HO)/bacterial cellulose microcrystal composites for tissue engineering applications. The Neutral red (NR) assay was carried out for cell adhesion and cell proliferation studies. Attachment and proliferation of HMEC-1 cells on the film were analysed over a period of 1, 4 and 7 days. The standard tissue culture plate was used as the positive control for this experiment. The results of these biocompatibility tests have been summarised in **Figure 4.15.**

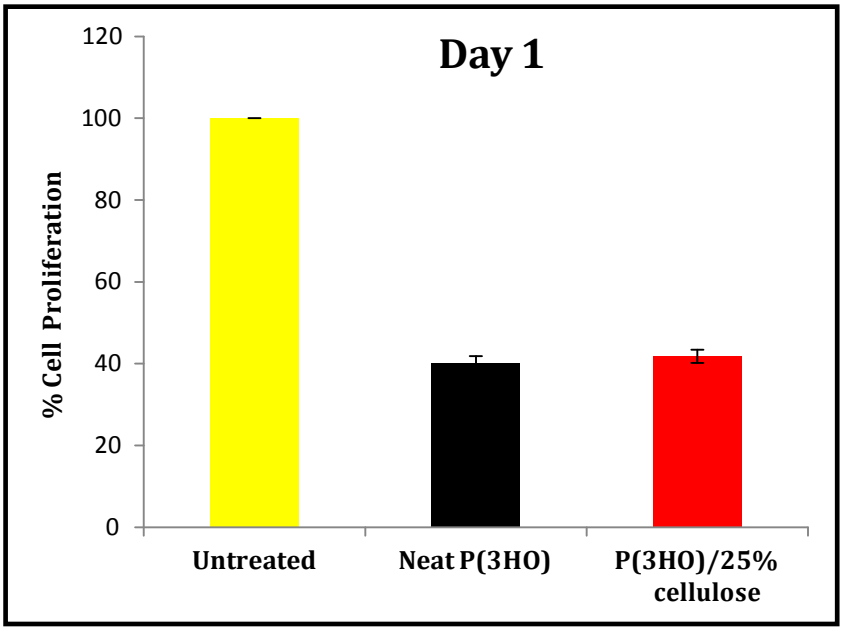

(a)

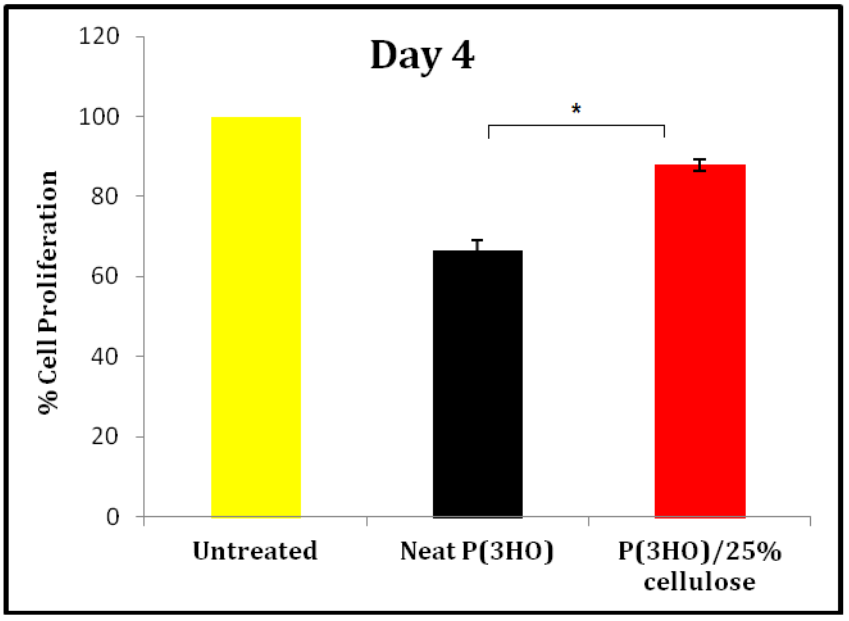

(b)

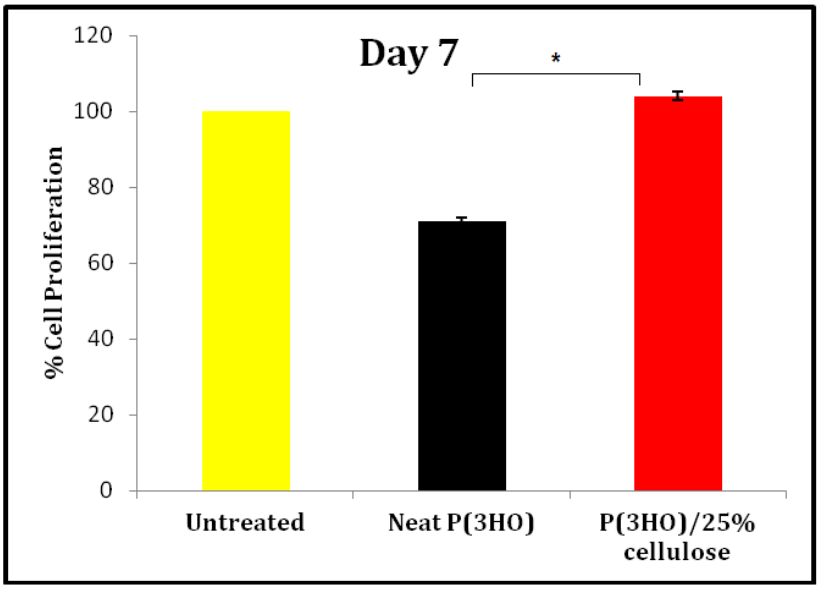

(c)

Figure 4.15: Cell proliferation study of the seeded HMEC-1 cells on the neat P(3HO) and P(3HO)/25% bacterial cellulose composite film on (a) day 1, (b) 4 and (c) 7 using Neutral Red assay. The data were compared using t-test and the difference were considered significant when *$p<0.05$. All the tested samples were measured relative to the untreated cells on the tissue culture plate. Untreated cells were set to 100% control (n = 3).

There was a better growth and proliferation of the cells on the composite film as compared to the neat film. At the end of the 1st day, the growth of the cells on the neat P(3HO) film and the P(3HO)/25% bacterial cellulose composite film was comparable. The growth of HMEC-1 on the P(3HO)/25% bacterial cellulose film

and P(3HO) neat film was 40±1.8% and 41±1.6% respectively as compared to tissue culture plastic. However, there was a significant increase in the growth of the cells on the P(3HO)/25% bacterial cellulose composite film as compared to the P(3HO) neat film when analysed at the end of the 4th day (*p<0.05). The growth of HMEC-1 cells on the P(3HO)/
25% bacterial cellulose film was 87±1.5% respectively as compared to the neat P(3HO) film which had 66±2.4 % growth.

At the end of the 7th day, there was a further significant increase in the growth of the cells on the P(3HO)/ bacterial cellulose composite film as opposed to the cells on the neat P(3HO) film (*p<0.05). The growth of HMEC-1 cells on the P(3HO)/25% bacterial cellulose film was measured to be 104±1.1% as compared to the 71±0.9% of cell growth on the neat P(3HO) film. The cell growth and proliferation on the composite film was 33% higher compared to the neat P(3HO) film at day 7.

4.10 Scanning Electron Microscopy (SEM)

In this study, the HMEC-1 cells seeded onto the P(3HO)/25% bacterial cellulose composite film was analysed using SEM as described in **section 2.11.9.4.** The HMEC-1 cells fixed on the composite film at day 4 and 7 are shown in **Figure 5.12.**

Day 1

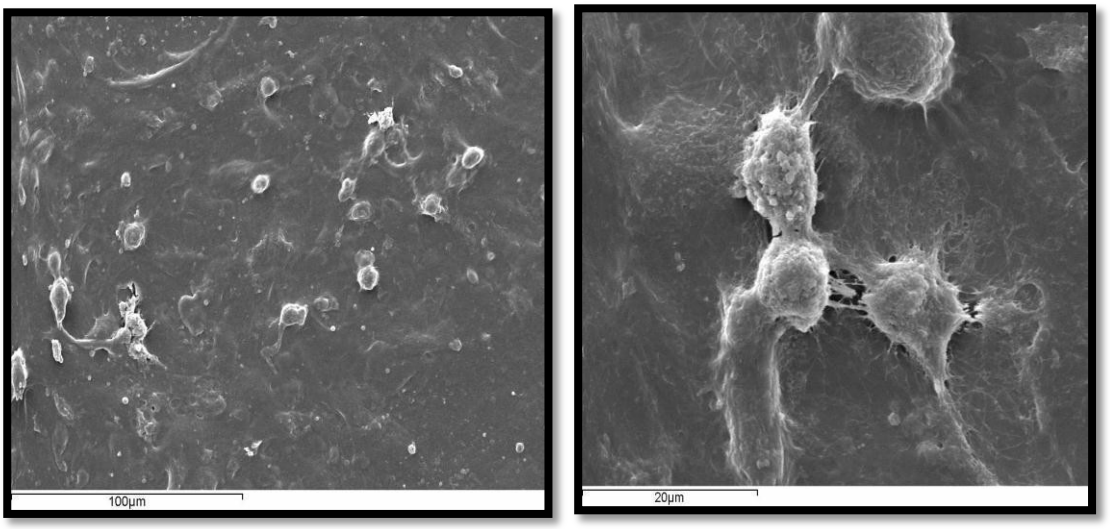

A1 **A2**

Day 4

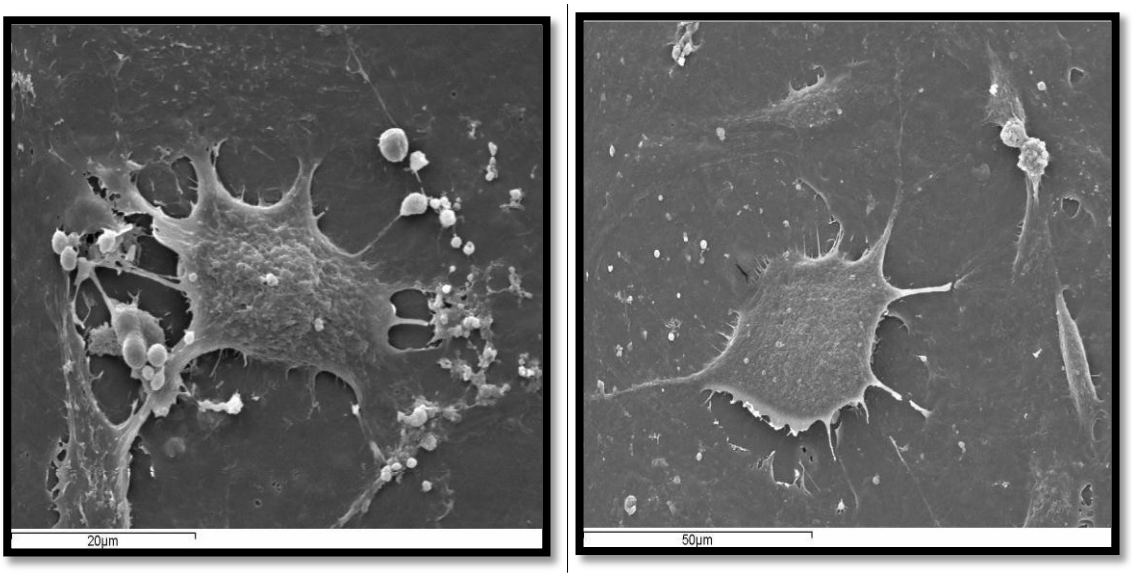

A3 **A4**

Day 7

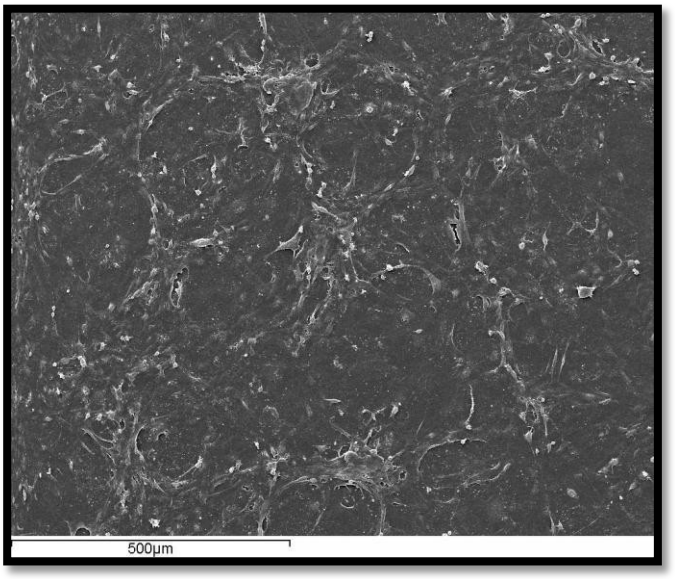

A5

Figure 4.16: SEM images of the HMEC-1 cells on P(3HO)/25% bacterial cellulose composite film on day 1 (A1-A2), day 4(A3-A4) and day 7(A5).

The SEM images revealed the adhesion and proliferation of HMEC-1 cells on the surface of P(3HO)/25% bacterial cellulose composite film.

Discussion

MCL-PHA was produced by *P. mendocina,* using sodium octanoate as the sole carbon source. The %PHA yield at 48 hours obtained in this study was 45.3% which was about 10% higher than the 35% yield reported in the literature (Rai *et al*., 2011). Higher PHA yield of 62% was achieved by Kim *et al.,* (2002) when *P. oleovorans* was grown on octanoic acid in a fed batch mode versus the batch mode of fermentation used in this study. This finding suggested that the mode of fermentation played a very important role in PHA accumulation (Kim *et al*., 20007). Organisms are capable of utilising the PHAs produced during carbon limiting conditions in order to sustain growth. This occurs usually in the batch mode when carbon in the media is insufficient unlike the fed batch or continuous fermentation where the media is continually replenished (Rai *et al*., 2011). Extraction of the polymer from the cells plays a very important role in determining the yield as well as the purity of the polymer (Rai *et al*., 2011). Studies on different extraction methods and their effect on the yield and purity of the PHA produced were carried out by Rai *et al.,* which revealed that the dispersion method utilising 80% sodium hypochlorite solution (NaOCl) and chloroform solution ($CHCl_3$) was the most effective in the efficient recovery of the polymer (Rai *et al*., 2011). PHA produced in this study was confirmed to be P(3HO), which is a homopolymer of 3-hydroxyoctanoic acid using GC-MS and NMR analysis.

Bacterial cellulose was also successfully produced by culturing *A. xylinum* in a static mode. It is known from the literature that the morphology and the mechanical properties of bacterial cellulose is highly dependent on the mode of culturing. Bacterial cellulose pellicles produced via static mode exhibited better mechanical properties compared to that produced using agitated cultures (Ciechanska, 2004). Therefore, in this study, cellulose pellicles were produced on the surface of the production media via static culturing.

The bacterial cellulose pellicles were homogenised and subjected to the acetylation reaction to increase its compatibility with the hydrophobic P(3HO) matrix. Previous studies have shown that the modification of bacterial cellulose pellicles by carrying out acetylation reaction makes it increasingly compatible with the other hydrophobic materials. During acetylation, the hydrophilic hydroxyl groups present in the bacterial cellulose are replaced by the hydrophobic acetyl groups (Kim *et al*., 2002). Usually, acetyl chloride along with a solvent such as acetic acid is

used in the presence of a catalyst to speed up the acetylation reaction, as reported by Bledzki *et al.,* 2008. In this study, acetic anhydride was added in the presence of acetic acid and perchloric acid as the catalyst. Chemical modification of the bacterial cellulose microcrystals using acetic anhydride was chosen for this study due to the ease of the methodology. There are several other methods that can be employed to modify natural fibres which include physical methods such as electric discharge method, mercerization and chemical methods such propionylation, treatment with isocyanates and the use of organosilanes as coupling agents (Bledzki and Gassan, 1999).

The FTIR analysis was used to confirm the acetylation reaction was successful. The hydroxyl groups in bacterial cellulose were replaced with the acetyl groups. The X ray diffraction patterns indicated that there was a decrease in the overall crystallinity of the bacterial cellulose microcrystals due to the acetylation reaction. It is known from literature that chemical modification of bacterial cellulose leads to the disruption of the crystalline regions causing degradation as well as a decrease in the crystallinity (Barud *et al*., 2008).

Mechanical characterisation of the P(3HO)/bacterial cellulose composite films were done to investigate the effect of acetylated bacterial cellulose microcrystals on the mechanical properties of the composite films. Previous studies have shown that MCL-PHAs exhibited Young's modulus values in a range of 3.6 MPa to 600 MPa depending upon the thickness and the monomeric composition of the polymer film (Rai *et al*., 2011). The 'E' values of the neat P(3HO) film obtained in this study were within this range. With the increasing concentration of modified cellulose microcrystals in the P(3HO), there was an in increase in the 'E' values of the composite films. However, the increase was not very high indicating that the stiffness enhancement properties of cellulose were not fully exploited. Soykeabkaew *et al*., demonstrated that the incorporation of the cellulose microfibrils within the polymer matrix increased the stiffness of the composite material (Soykeabkaew *et al*., 2009). This increase would be due to the restricted mobility of the polymer in the presence of modified bacterial cellulose microcrystals (Shumigin *et al*., 2011). Polycaprolactone (PCL) when reinforced with 3% of modified microfibrilliated cellulose (MFC) exhibited an increase in the Young's modulus value up to 60%. The authors attributed this drastic increase to the excellent interaction between the polymer matrix and the cellulose fibrils at 3%

concentration of MFC (Siqueiria *et al*., 2010). Cheng *et al.,* demonstrated that there was an increase in the Young's modulus of the polyvinyl alcohol (PVA) and propylene when reinforced with fibril aggregates isolated from cellulose fibres. However, the increase was not very high. They hypothesized that this could be due to several factors such as poor adhesion between the fibrils and the polymer matrix, poor dispersion of the fibrils in the matrix or the aspect ratio of the polymer (Cheng *et al.,* 2007). There was an increase in the tensile strength of the P(3HO)/bacterial cellulose composite films compared to the neat P(3HO) film. However, the increase was not as high as expected. Therefore, it can be concluded that the tensile properties of the acetylated bacterial cellulose microcrystals were not fully exploited in the composites. This could be due to the heterogeneous dispersion of the modified bacterial cellulose microcrystals in the P(3HO) matrix which led to the formation of weak points (Siqueiria *et al*., 2010). This may be improved in future, by better modification of the bacterial cellulose microcrystals to achieve uniform dispersion of the bacterial cellulose within the P(3HO) matrix. Shumigin *et al.,* demonstrated that there was a decrease in the tensile strength of the PLA/cellulose composites with the increase in the concentration of bacterial cellulose within the composite film. They stated that this decrease in the tensile strength was due to the irregular aligning of the cellulose composites in the PLA matrix and poor adhesion between the filler and the matrix leading to formation of numerous microflaws in the composite structure, thereby causing inefficient stress transfer between the matrix and the cellulose fillers (Shumigin *et al.,* 2011). Similarly when styrene–butadiene rubber (SBR)/α-cellulose composite were tested for their mechanical properties, there was a decrease in the tensile strength with increase in the filler concentration (Haghighat *et al*., 2005). These results indicate that the filler-polymer interaction is crucial to achieve good mechanical properties in composites. This can be achieved by good processing methodology.

According to the literature, it is known that the % elongation at break values for MCL-PHAs range between 6.5 to 350% (Asrar *et al*., 2002). The value obtained for the neat P(3HO) film in this study was within this range. The elongation at break values of the P(3HO)/bacterial cellulose composites were lower compared to the neat P(3HO) film. Hence, as expected, there was a decrease in the elastomeric properties of the composite film due to the addition of the acetylated cellulose microcrystals. There was a similar decrease in the % elongation at break value of the PCL/modified cellulose nanocrystals composite film with the addition of 12 wt%

of modified cellulose nanocrystals within the PCL matrix (Siqueiria *et al.*, 2010). Another study also similarly demonstrated a decrease in the % elongation at break values of the poly(styrene-co-butyl acrylate)/MFC composites with the addition of MFC as a reinforcing agent. The authors attributed this decrease to the filler/filler entanglement causing poor dispersion of the filler in the polymer matrix (Dalmas *et al.,* 2006).

Hence, overall, the results in the context of mechanical properties suggested that the interaction of the acetylated bacterial cellulose microcrystals with P(3HO) has led to some improvement in mechanical properties but in future, further work would be needed to achieve even better improved mechanical properties by modification of the processing methodology and ensuring higher degree of acetylation of the cellulose.

Thermal characterisation was carried out on the P(3HO)/bacterial cellulose composite films as well as on the neat P(3HO) film to determine the effect of the acetylated bacterial cellulose microcrystals on the thermal properties of the composite film. There was a decrease in the T_m values of the composite films compared to the neat P(3HO) film. This decrease in the T_m could also be due to the disruption of the crystalline region of the polymer by the acetylated bacterial cellulose microcrystals (Siqueiria *et al.*, 2010).

There was an increase in the T_g values of the of the composite films compared to the neat P(3HO) film. The increase was not statistically significant. However, the presence of the acetylated bacterial cellulose microcrystals would restrict the mobility of the amorphous region in the polymer increasing the T_g values. A similar observation was made when modified fibrillated cellulose nanoparticles were used to reinforce PCL. The authors stated that this increase in the T_g occurred when the molecular mobility of the amorphous region of the polymer matrix was restricted due to the addition of the fillers (Siqueiria *et al.*, 2010).

Water contact angle studies were carried out to investigate the effect of acetylated bacterial cellulose microcrystals on the wettability of the composite films. The presence of acetylated bacterial cellulose microcrystals lowered the contact angle of the P(3HO)/5% cellulose and P(3HO)/25% cellulose composite films compared to the neat P(3HO) film. Also, the higher hydrophobicity of the P(3HO)/15% cellulose composite film as compared to the neat P(3HO) film was quite an unusual result. This was possibly due to the fact that at this specific concentration (15%), the cellulose remains within the interior of the 2D-film as compared to the 5%

and 25% cellulose composites, resulting in higher hydrophobicity of the surface of the 2D film.

Based on these preliminary data, P(3HO)/25% bacterial cellulose composite films with the highest Young's modulus value and a relatively higher hydrophilicity, known to favour cell adhesion, was chosen for further characterisation.

Microstructural studies were carried out to investigate the effect of bacterial cellulose microcrystals on the surface topography of the composite film. SEM studies revealed a rough topography of the P(3HO)/25% bacterial cellulose composite film compared to the smooth surface of the neat P(3HO) film. This could be most likely due to the presence of acetylated bacterial cellulose microcrystals dispersed on the surface of the P(3HO) film. It is known from literature that the arrangement of the crystalline and amorphous domain on the surface of the composite film determines its morphology (Luo *et al*., 2009).

Rai *et al.,* demonstrated that there was a change in the surface topography of the P(3HO)/n-BG composite film due to the addition nanobioactive glass (n-BG) particles within the P(3HO) matrix. The authors attributed the rough topography of the P(3HO)/n-BG composite film to the presence of n-BG particles on the film-air interface (Rai *et al.,* 2011).

In order to confirm the change in the surface topography, the surface roughness of the composite film were measured using the White Light Interferometry. The result was compared with the surface roughness values of the neat P(3HO) film. The increase in the surface roughness of the composite film was due to the presence of acetylated bacterial cellulose microcrystals on the surface. This could be due to the exposure of the modified cellulose microcrystals on the surface of the P(3HO) matrix due to heterogeneous distribution of the former within the P(3HO) matrix. The finding of this study is supported by the results demonstrated in the previous studies. Siqueiria *et al*., observed that there was no change in the surface roughness of the cellulose/polycaprolactone composite film when modified cellulose whiskers were uniformly or homogenously dispersed within the polycaprolactone matrix, (Siqueiria *et al*., 2010). Previous studies have shown that surface roughness, hydrophilicity and total protein adsorption, which is crucial for cell adhesion, are interrelated. Therefore, surface roughness is known to play a significant role in cell adhesion and proliferation process (Hao and Lawrence, 2004). The increase in the surface roughness of the P(3HO)/25% bacterial cellulose composite film is

therefore an encouraging result for the use of the composite films as tissue engineering scaffolds.

Another characterisation that was carried out on the composite as well as the neat P(3HO) film were total protein adsorption assay. This was carried out in order to assess the effect of the bacterial cellulose microcrystals on the total protein adsorption. The increase in protein adsorption on the composite film compared to the neat P(3HO) film could be due to the increase in the surface roughness of the composite film. Previous studies have shown that there is increased protein adsorption on a rough surface compared to the smooth, flat surface (Chen *et al.*, 2009). Protein adsorption plays a key role in determining the biocompatibility of a biological implant. Failure of protein adsorption on the implant could lead to inflammatory responses (Das *et al.*, 2007). Therefore, this increase in the total protein adsorption on the P(3HO)/25% bacterial cellulose composite film would make these film highly suitable for biomedical applications.

Cell culture studies were carried out to determine the effect of the presence of the acetylated cellulose microcrystals on the adhesion and the proliferation of the HMEC-1 cells on the P(3HO)/25% bacterial cellulose composite film compared to the neat P(3HO) film. According to literature, it is known that increased protein adsorption enhances cell adhesion and proliferation processes (Das *et al.*, 2007). Gentile *et al.,* demonstrated an increase in the cell growth when grown on rough topography compared to the smooth surface. This could also be another reason for the increased cell proliferation in the P(3HO)/25% bacterial cellulose microcrystals composite as compared to the neat P(3HO) film (Gentile *et al.,* 2010). Similar observations were made by other researchers where there was an increased cell proliferation on the P(3HO)/n-BG and P(3HB)/n-BG composites respectively, in comparison to the neat polymer film. The authors attributed this increase in the % cell proliferation on the composite film to the increase in the surface roughness (Rai *et al.,* 2010; Misra *et al.,* 2008; Gentile *et al.*, 2010). Hence, the rough topography followed by increased protein adsorption due to the addition of bacterial cellulose resulted in enhanced biocompatibility of the P(3HO)/25% bacterial cellulose composites. SEM images of the HMEC-1 cells on the P(3HO)/25% bacterial cellulose composite film confirmed the biocompatibility of these composite film. These results suggested the fact that these P(3HO)/25% bacterial cellulose composites were suited for biomedical applications.

Another important characterisation that was carried out on the composite film was the *in vitro* degradation study. Biodegradability is considered to be a significant feature of a biomaterial with potential medical application (Li and Shimizu, 2007). It was found that the inclusion of the acetylated bacterial cellulose microcrystals in the P(3HO) film increased the degradation rate of the composite film in comparison to the neat P(3HO) film in both PBS and DMEM media. Previous studies have shown that there is a correlation between the water absorption and the progressive degradation of the polymer film (Holland *et al*., 1987). This was in agreement with the finding in this study where highest %WL in the P(3HO)/25% cellulose microcrystals had the highest % WA compared to the neat P(3HO) film in both DMEM and in the PBS media. Rai *et al*., demonstrated an increase in the %WL for the P(3HO)/nBG composite film compared to the neat P(3HO) film due to the addition of nBG particles within the matrix at the end of 4 month degradation study. Considering the fact that these composite as well as the neat P(3HO) film were incubated in the non- enzymatic media, the degradation occurred via hydrolysis. It is known from the literature that during hydrolytic degradation, water molecules initially attack the amorphous region of the polymer followed by the crystalline regions of the polymer which then gets degraded forming monomers and dimers (Volova and Volova, 2004). This was confirmed by measuring the pH of the DMEM and the PBS at the end of the one month degradation study. There was an increase in the pH which could possibly be due to the degradation of the amorphous regions of the P(3HO) resulting in the production of 3-hydroxyoctanoic acid or 3-hydroxyoctanoate. The pKa for 3-hydroxyoctanoic acid, which is the degradation product of the P(3HO) is 4.89 which is lower than the pH of DMEM and PBS media (pH 7.0), therefore 3-hydroxyoctanoic acid exists as 3-hydroxyoctanoate in these media, which is a base, causing an increase in the pH of the media (Rai *et al.,* 2011). These results indicated that the weight loss of the samples was due to the hydrolytic degradation of the amorphous region of P(3HO).

The mechanical characterisation of the degrading composite film was carried out to investigate the effect of the degradation on their mechanical properties. The results were quite unexpected. The Young's modulus values of the degrading samples were higher than the non-degraded samples. This was possibly due to the ageing process of the PHAs during which the amorphous region of the polymer becomes crystallised thereby causing an increase in the E values or the stiffness of the degrading film (Hutchinson *et al*., 1995).

In conclusion, P(3HO)/bacterial cellulose composites with improved mechanical microstructural and biodegradability properties were successfully produced. Further improvement in the method of fabrication of this composite film, better mechanical properties can be achieved. The cell culture data obtained from this study revealed promising results by demonstrating good cell growth and proliferation on the composites making them suitable for medical applications such as scaffolds for tissue engineering.

CHAPTER 5

Poly (3-hydroxyoctanoate)/Poly (3-hydroxybutyrate) homopolymer blends: a potential material for biodegradable stents

INTRODUCTION

Cardiovascular disease is responsible for a significant number of deaths in the developed world (Kurowska-Nouyrigat and Szumbarski, 2009). According to the estimates of the World Health Organization (WHO), cardiovascular disease will be responsible for the highest rate of morbidity and death by the year 2020 (Bogaert and Dymarkowski, 2005). Coronary artery disease (CAD) is a type of cardiovascular disease where a coronary artery is blocked or narrowed due to the plaque formation within the vessel affecting the normal blood flow. This in turn causes inadequate supply of oxygen to other parts of the heart leading to heart attack (Kurowska-Nouyrigat and Szumbarski, 2009). Percutaneous Transluminal Coronary Angioplasty (PTCA) has been widely used to treat the patients suffering from CAD (Kastrati *et al*., 2000). PTCA is a minimally invasive procedure where a catheter mounted with a balloon at its tip is directed into the blocked artery. The balloon is inflated at the site of blockage to widen the narrowed artery (Basnett and Roy, 2010). A major breakthrough was achieved with the use of coronary stent in 1986 to address the limitations of conventional PTCA such as vessel renarrowing (Kastrati *et al*., 2000). A stent is an implant that is guided using a catheter into the diseased or narrowed coronary artery to restore its function. In the recent years, stents have undergone a rapid evolution from the bare metal stents to polymer coated, drug eluting, biodegradable metallic stents, to the fully biodegradable polymeric stents.

Studies have shown that biodegradable stents are less obtrusive compared to metal stents that are known to cause injury to the artery during its placement that later result in restenosis. Restenosis is the reoccurrence of the blockage after the stent is placed within the artery. Three factors that lead to restenosis include (a) stent injury which could occur during the implantation (b) incompatibility of the stent material with the blood components causing inflammatory response followed by a cascade of events leading to neointimal thickening and (c) smooth muscle cell proliferation caused due to local wall shear stress (Basnett and Roy, 2010). Biodegradable stents have several advantages compared to these metal stents. They are made up of biocompatible polymers which degrade in to non-toxic degradation products. However, a major disadvantage that has hindered the commercialization of these biodegradable stents is their poor mechanical properties (Basnett and Roy, 2010; Cantor *et al*., 2000).

PHAs are attractive materials for biomedical applications because of their natural origin, enhanced biocompatibility and biodegradability. They can be classified as short chain length (SCL) and medium chain length (MCL) PHAs depending on the total number of carbon atoms present in their monomeric units. Their properties vary depending on the type. SCL-PHAs are brittle, have high melting temperature and crystallinity whereas MCL-PHAs are elastomeric in nature and have a low melting temperature and low crystallinity (Valappil *et al.,* 2007). Based on the nature of the application, desired characteristics can be attained by making blends of PHAs and composites with various organic and inorganic additives (Kim *et al*., 2007). It is known that polymer blends are developed to tailor the bulk as well as the surface properties of the individual polymers based on the desired application (Zhang, 1999). Blending has several advantages over co-polymerization techniques. The main advantage of the blending approach is the ease of the processability, reduced costs and optimum properties (Ha and Cho, 2002).

This study is divided into three parts. In the first part of this study, P(3HB) was successfully produced by *B. cereus* using Kannan and Rehacek media. P(3HO) and P(3HB) blends with intermediate properties were developed and characterised. The production of these novel blends with tailored desirable properties was aimed for their use as a base material in the development of a biodegradable coronary stent. These blend films were characterised with respect to their mechanical, thermal, surface and microstructural properties. Degradation and biocompatibility studies were carried out on the blend films containing various ratios of P(3HO) and P(3HB)

In the second part of this study, surface micropatterning of the P(3HO)/P(3HB) 50:50 blend film using Laser microcutting technique was carried out. Surface topography of a biomaterial plays an important role in their biocompatibility. It strongly affects the nature of the interaction between the biomaterial and the biological host. Surface topography dictates cell adhesion, differentiation and cell morphology. From literature, it is known that medical applications require a biomaterial to have a positive interaction with the cells. Therefore, biodegradable stents would require the chosen biomaterials to be compatible with the vascular endothelial cells (Li *et al.,* 2001; Duncan *et al*., 2007; Anderson and Hinds, 2011). Endothelial cells form the inner lining of the blood vessel wall. They act as an interface between the components of blood and the vessel wall. Endothelial cell

dysfunction leads to vascular diseases such as atherosclerosis (Kidd *et al*., 2003). Previous studies have shown that the shape and the orientation of the endothelial cells within the artery were regulated by blood flow. It was observed that the endothelial cells within the arteries were aligned along the axis of the vessel maintaining their function (Langille and Adamson, 1981). It is known that the shape and the alignment of the endothelial cells play a key role in the occurrence of artherosclerotic lesions. The development of artherosclerotic lesions occurs in the arterial region where the endothelial cells display a round morphology. No such occurrence was recorded in the arterial region with elongated and aligned endothelial cells. It is known that the function of endothelial cells is regulated by the cell shape (Gray *et al*., 2002). Endothelial cells, when cultured in a static mode or in an environment with a multi directional or disturbed flow reveal cobblestone morphology which is attributed to a thrombogenic phenotype. On the contrary, the endothelial cells when cultured under oriented or unidirectional flow exhibit elongated morphology with a healthy phenotype (Anderson and Hinds, 2011). In order to improve biocompatibility, it is crucial for the cells to grow in an oriented manner to form tissues of specific architecture (Li *et al.,* 2001). Therefore, surface modification or fabrication of the biomaterials to encourage the cells to grow in an aligned manner has been investigated for several years.

One of the most promising technologies used in the surface fabrication of the biomaterials is micropatterning. Most commonly used micropatterning techniques include microcontact printing, photo patterning and most recently laser micropatterning (Thery, 2010). Micropatterning allows the cells to be exposed to a physiologically relevant environment compared to the traditional cell culture conditions. It also makes it possible to interfere or control cell behaviour in the absence of the flow which is a great step forward in regenerative medicine. The response of the cells to the engineered surface of the biomaterial enables one to understand cell behaviour during its growth and differentiation. Using micropatterning, one could guide the attachment, proliferation and alignment, thereby controlling the phenotypic characteristics of the cells (Anderson and Hinds, 2011). Bearing in mind, the potential application of the P(3HO)/P(3HB) 50:50 blend films as a platform material for the development of biodegradable stents, Human microvascular endothelial cells (HMEC-1) were grown on the micropatterned P(3HO)/P(3HB) 50:50 blend films under static conditions. The

influence of the laser micropatterning on the microstructural and the mechanical properties of the P(3HO)/P(3HB) 50:50 blend films were examined. The % cell proliferation and the orientation of the HMEC-1 cells on the micropatterned P(3HO)/P(3HB) 50:50 blend films were compared with that on plain P(3HO)/P(3HB) 50:50 blend films.

In the final part of this study, the potential of the P(3HO)/P(3HB) 50:50 blend films as the base material for the development of drug eluting biodegradable stents with controlled delivery of aspirin was investigated. One of the most desirable characteristics of an ideal biodegradable stent is its ability to deliver drugs (Moore *et al*., 2010).

Numerous attempts have been made to develop an efficient drug delivery system to prevent restenosis (Faxon, 2002). One of the major difficulties in developing an efficient pharmacotherapeutic regime to prevent restenosis via systemic administration is their inability to deliver a drug concentration that triggers a pharmacological response. Local drug delivery has been considered to be key in addressing the limitations of systemic drug administration. With local drug delivery, there would be no systemic toxicity and the drug would be delivered locally at a concentration to evoke a pharmacological response combined with drug release kinetics required for the vascular healing process (Basnett and Roy, 2010).

For this particular study, aspirin was chosen as the model drug. Aspirin is commonly used to achieve relief from pain and fever. However, the most significant property of aspirin is its antithrombotic activity. Previous studies have shown that thrombus formation plays an important role in the initial stages of neointimal thickening leading to restenosis (Basnett and Roy, 2010). The principle behind the anti-thrombotic effect of aspirin is that it inhibits thrombooxygenase A_2, a strong inducer of thrombus formation, thereby reducing platelet aggregation. Because of its anti-thrombotic property, aspirin is an important drug used to prevent cardiovascular events such as myocardial infarction. One of the problems associated with the conventional oral dosage of aspirin is that it has a poor oral bioavailability. This makes it extremely challenging to deliver a concentration that triggers a pharmacological response. Studies have shown that the prolonged use of aspirin in the form of oral dosage leads to a number of side effects such as gastrointestinal (GI) mucosa ulcer and GI haemorrhage. Clinical trials have

established that a low dose local delivery of aspirin would strongly improve the therapeutic efficacy of the drug (Tang and Singh, 2008).

Therefore, the main focus of this part of the study was to investigate the potential of the P(3HO)/P(3HB) 50:50 blend films as the base material for the development of drug eluting biodegradable stents with controlled delivery of aspirin.

Part I

Production of P(3HO)/P(3HB) blends for the development of biodegradable stents

5.0 Results

5.1 Production of P(3HB)

P(3HB) production was carried out using *B. cereus* SPV in Kannan and Rehacek media, as described in **section 2.8.** Analytical studies such as O.D. and pH measurements, nitrogen and biomass estimation were done using samples withdrawn at an interval of 3 hours, as described in **section 2.5**. The growth profile of *Bacillus cereus* SPV in Kannan and Rehacek media for the production of P(3HB) is shown in **Figure 5.1**.

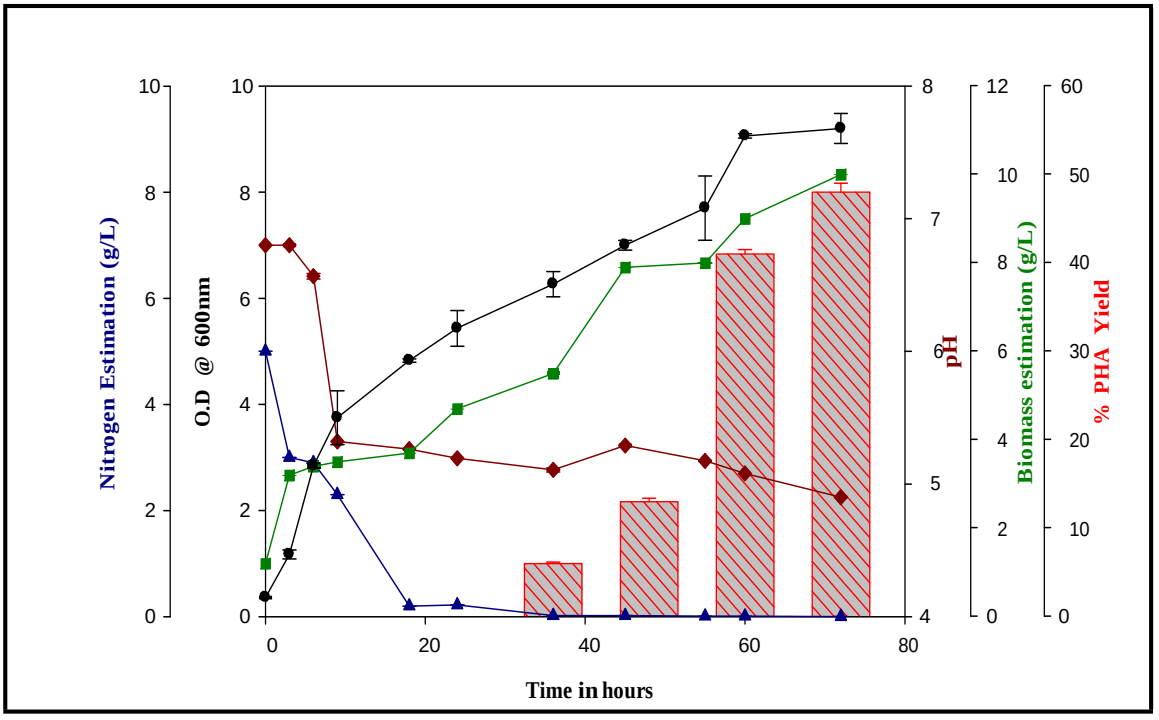

Figure 5.1: The fermentation profile of P(3HB) production using *Bacillus cereus* SPV in Kannan and Rehacek media.

Optical density (O.D.), pH, nitrogen concentration and biomass estimation was carried out for the samples withdrawn at intervals of every 3 hours. From the O.D. values measured at 600 nm, there was a steady increase in cell growth from the initial hours of fermentation indicating that there was no lag phase. The O.D. values increased exponentially, reaching a value of 8.9 at 60 hours of fermentation. This

was considered to be the log phase. After this, the cells entered stationary phase where there was no further increase in the O.D. Dry cell weight of the cells increased progressively reaching a maximum value of 9 g/L at 60 hours after which there was no further increase. This could be explained in relation to the O.D. values which increased until 60 hours after which there was no increase as the cells had entered stationary phase. Nitrogen concentration decreased throughout the fermentation reaching a value of 0.0009 g/L at 57 hours. pH was not controlled during fermentation and the values were observed to decrease progressively from the 6th hour of fermentation reaching a pH value of 4.9 at the end of the fermentation. A maximum PHA yield of 48% dry cell weight was obtained at 72 hours. In this study, P(3HB) production was carried out in a nitrogen limiting condition. The decrease in pH, reaching acidic levels, during P(3HB) production has been previously observed by Philip *et al.,* 2007. This acidic pH is known to protect the degradation of P(3HB). Since, P(3HB) is degraded to 3-hydroxybutyric acid, its degradation under acidic pH conditions is inhibited according to the law of mass action. Apart from preventing the degradation of P(3HB), this low pH environment also prevents spore formation in *B. cereus* (Kominek and Halvorson, 1965). According to a study conducted by Browne and Dowds, 2002, *B. cereus* cells in their log phase are more sensitive to the acidic stress and become increasingly resistant as they enter stationary phase. Hence, the pH adjusted to 6.8 at the start of the fermentation promotes cell growth during log phase, when the cells are sensitive to acidic stress. The polymer produced during fermentation was analysed using FTIR and Gas Chromatography.

5.2 Characterisation of the polymer produced

5.2.1 Fourier Transform Infrared Spectroscopy (FTIR)

The polymer that was produced by *B. cereus* SPV using Kannan and Rehacek media was characterised using FTIR, as described in **section2.6.1.** The IR spectrum of the polymer produced is shown in **Figure 5.2.**

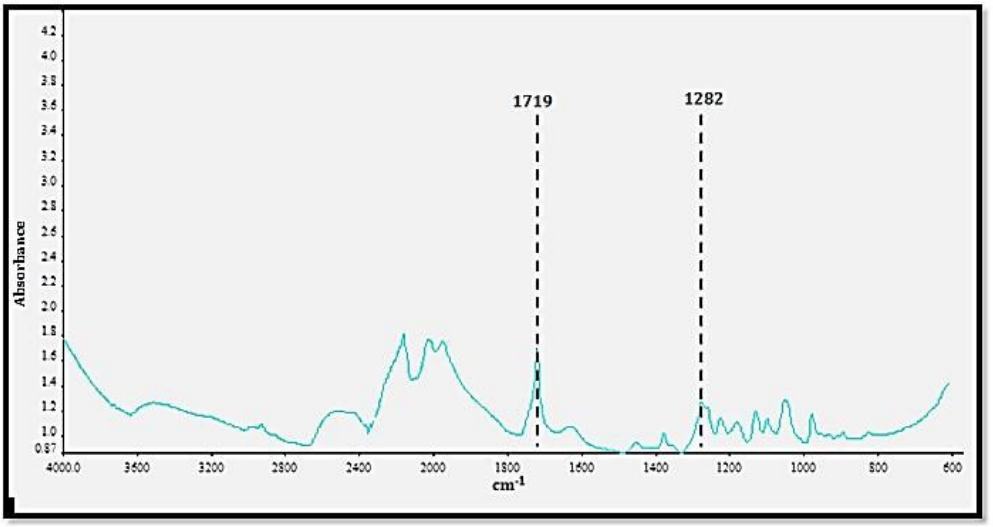

Figure 5.2: FTIR spectrum of the polymer produced by *Bacillus cereus* SPV using Kannan and Rehacek media.

The IR spectrum of the polymer showed the presence of two characteristic absorption peaks present in the SCL-PHAs such as 1719 cm^{-1} corresponding to the ester carbonyl group and the absorption peak at 1282 cm^{-1} corresponding to the $-CH_2$ group. This confirmed that the polymer produced was a type of SCL-PHA. The polymer was further characterised using GC.

5.2.2 Gas Chromatography (GC)

The SCL-PHA produced was further analysed using the Gas chromatography. The polymer was methanolysed to obtain methyl esters as described in **section 2.6.2.** The gas chromatogram of the methanolysed polymer is shown in **Figure 5.3**.

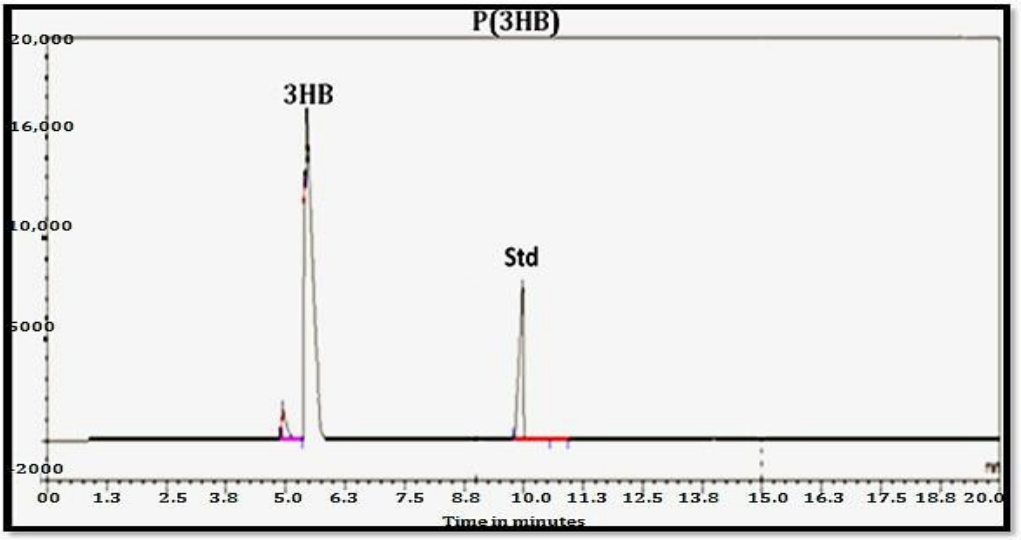

Figure 5.3: The Gas chromatogram of the methyl esters of 3-hydroxybutyric acid.

A peak with the retention time (R_t) of 5.47 corresponded to the methyl ester of 3-hydroxybutyric acid (3HB) while the peak with retention time (R_t) of 9.9 corresponded to methyl benzoate which was added as the internal standard (Rai *et al.,* 2011). This confirmed that the polymer produced by *B. cereus* SPV using Kannan and Rehacek media was P(3HB).

5.3 Synthesis of the novel P(3HO)/P(3HB) blends

P(3HO)/P(3HB) blends with varying compositions such as 20:80, 50:50, 80:20 and neat P(3HB) films were synthesized using the solvent cast technique. P(3HO) and P(3HB) were dissolved in chloroform in order to obtain a polymer concentration of 5wt% in ratios of 80:20, 50:50 and 20:80. The polymer solution was mixed well by sonication and then cast in a glass petri dish. The film was air dried for one week. Films of 0.18mm thickness were produced. The surface of the film exposed to air was used for analysis. These blend films were then characterised with respect to their microstructural, thermal and mechanical properties and compared with the properties of the neat P(3HO) film.

Characterisation of the P(3HO)/P(3HB) blend films

5.4 Scanning Electron Microscopy:

Microstructural studies of these P(3HO)/P(3HB) blend films were carried out using SEM as described in **section 2.9.1**. This study was carried out to investigate the effect of the varying proportions of P(3HB) on the surface properties of the blend films. The surface properties of these blend films were then compared to the surface of the neat P(3HO) film as shown in **Figure 5.4.**

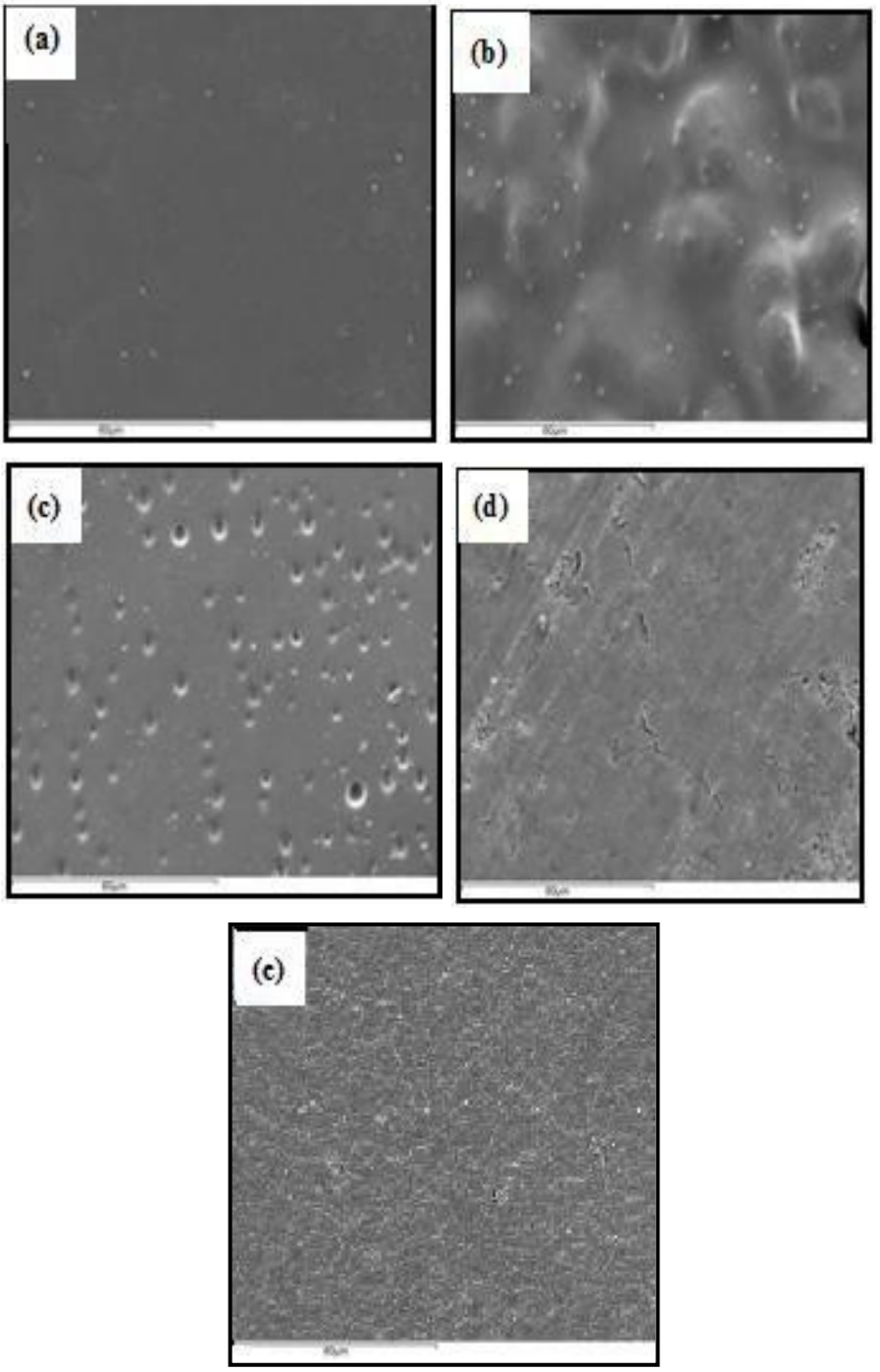

Figure 5.4: SEM images of the P(3HO)/P(3HB) blend films revealing a change in their surface topography with the addition of P(3HB) in comparison to the neat P(3HO) film. (a) neat P(3HO) film, (b) P(3HO)/P(3HB) 20:80 (c)

P(3HO)/P(3HB) 50:50 (d) P(3HO)/P(3HB) 80:20 blend films (e) P(3HB) film. Scale bars = 60 µm.

The surface properties of the blend film changed with the varying proportions of P(3HB). The SEM images of the neat P(3HO) film revealed a smooth surface while the blend films with increasing concentration of P(3HB) revealed a rough

topography. P(3HO)/P(3HB) 80:20 blend film which had the highest concentation of P(3HO) and the P(3HO)/P(3HB) 50:50 blend film appeared to have a relatively smoother surface whereas P(3HO)/P(3HB) 20:80 blend which had the highest concentration of P(3HB) appeared to have a rough topography. Overall, the SEM images revealed that a new level of surface topography was introduced with the incorporation of P(3HB) in the P(3HO) matrix. These blend films were further characterised using Atomic Force Microscopy (AFM).

5.5 Atomic Force Microscopy (AFM)

To evaluate the effect of varying proportions of P(3HB) on the surface roughness of the blend films, AFM was used to measure their surface roughness values as described in **section 2.9.3.** The surface roughness of these blend films were then compared with the neat P(3HO) film. Typical root mean square (rms) values were calculated to determine the surface roughness of these blend films as shown in **Figure 5.5**.

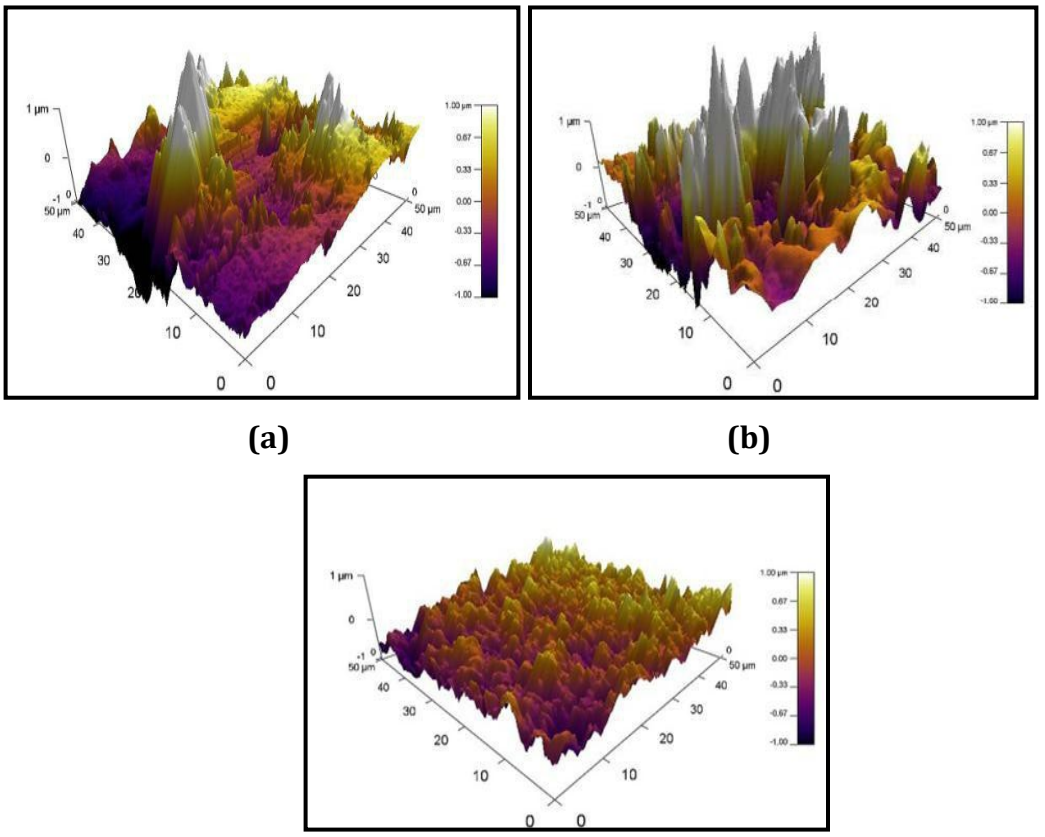

Figure 5.5: The AFM images of the (a) P(3HO)/P(3HB) 80:20 (b) P(3HO)/P(3HB) 50:50 blend film and (c) neat P(3HB) film. Scan size: 50 µm. The surface of the film exposed to air was used for the analysis.

AFM images of the P(3HO)/P(3HB) blend films confirm the increase in the surface roughness with the increase in the P(3HB) content. From previous studies, it has been found that the roughness value of the neat P(3HO) film is 0.272 µm. The rms value of the P(3HB) film was calculated to be 0.24 ± 0.10 µm. The rms values of the P(3HO)/P(3HB) 50:50 blend were found to be 0.59 ± 0.02 µm and the rms values of P(3HO)/P(3HB) 80:20 blend were found to be 0.58 ± 0.04 µm. The surface roughness of the P(3HO)/P(3HB) 50:50 and P(3HO)/P(3HB) 80:20 blend films were found to be 118% and 114% higher respectively compared to the neat P(3HO) film. Due to highly increased roughness of the P(3HO)/P(3HB) 20:80 blend film, it was not feasible to measure its roughness values using the AFM. In future, White Light Interferometry studies could be carried out to measure its surface roughness. These results confirmed that there was an increase in the surface roughness of the blend films compared to the neat P(3HO) film.

5.6 Water contact angle

Water contact angle studies were carried out to study the effect of the different concentrations of P(3HB) on the wettability of the blend films as described in **section 2.9.4.** The results were compared to the wettability properties of the neat P(3HO) films are shown in **Figure 5.6**.

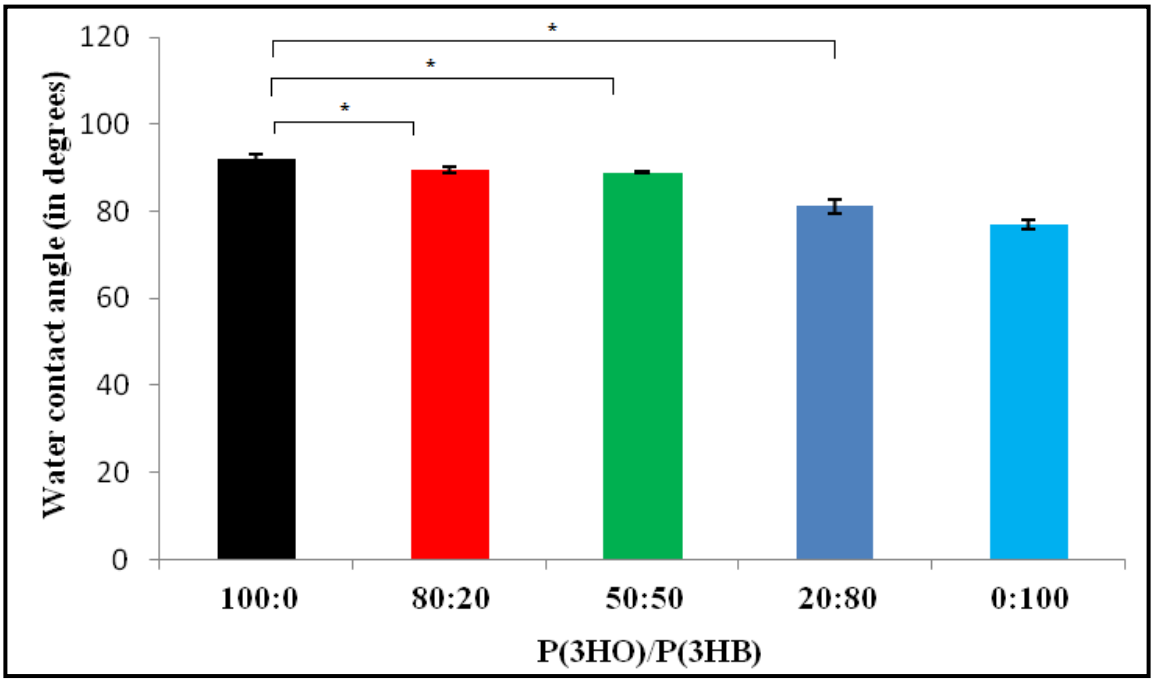

Figure 5.6: Static water contact angle measurements of the neat P(3HO),P(3HO)/P(3HB) blend films and neat P(3HB) film(n = 3; error bars = ± SD).

The data were compared using ANOVA and the difference were considered significant when *p<0.05.

Hydrophobicity was significantly decreased in P(3HO)/P(3HB) blend films in comparison to the neat P(3HO) film (*p<0.05). The water contact angle of the P(3HO)/P(3HB) 80:20, P(3HO)/P(3HB) 50:50 and P(3HO)/P(3HB) 20:80 blend films were 88.9±0.3, 89.5±0.8, and 81.1±1.5 respectively compared to the water contact angle of the neat P(3HO) film which was measured to be 92.0±1.0. The neat P(3HO) film as well as the blend films were hydrophobic in nature. There was a decrease in the hydrophobicity of the blend films with the increase in the concentration of the P(3HB) within the film. However, there was a surprising result where P(3HO)/P(3HB) 50:50 had a higher contact angle compared to the P(3HO)/P(3HB) 80:20. The results confirmed that the blend films were comparatively hydrophilic cpompared to the neat P(3HO) film.

5.7 Protein Adsorption Test

Surface characterisation of these blend films confirmed the change in the surface topography, roughness and the wettability properties due to the addition of varying proportions of P(3HB) in the film. In order to evaluate the effect of these changes on the total protein adsorption on the blend films, an assay was carried out to quantify the total protein adsorption as described in **section2.9.7.** The results of the total protein adsorption is shown in **Figure 5.7**.

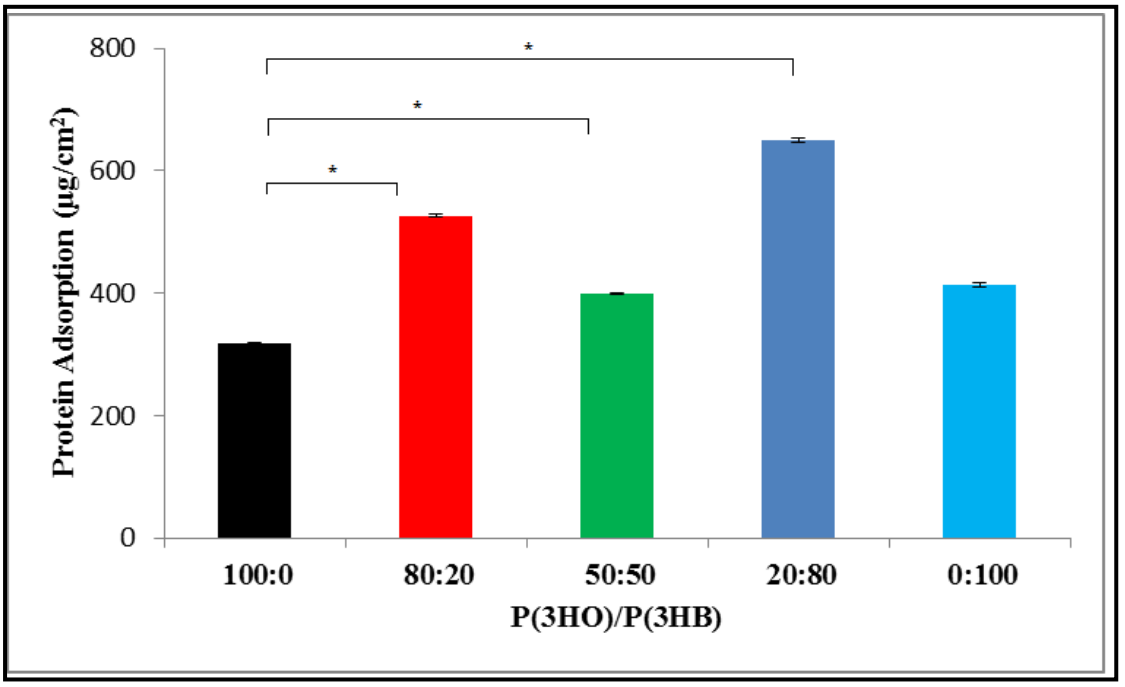

Figure 5.7: Protein adsorption of the neat P(3HO), P(3HO)/P(3HB) blend films and neat P(3HB) film (n = 3; error bars = ± SD). P(3HO)/P(3HB) 20:80 which has the highest P(3HB) content exhibits highest protein adsorption compared to the neat P(3HO) film. The data were compared using ANOVA and the difference were considered significant when *p<0. 05.

The overall protein adsorbed on to the neat P(3HO) film was 318 ± 1.0 µg/cm^2 which was lower compared to the total protein adsorbed on to the P(3HO)/P(3HB) 80:20, P(3HO)/P(3HB) 50:50 and P(3HO)/P(3HB) 20:80 blend films which were 527±2 µg/cm^2, 400±1 µg/cm^2 and 650±4 µg/cm^2 respectively. Protein adsorption on the neat P(3HB) film was 414±3 µg/cm^2 . The protein adsorption was 65%, 25% and 104% higher in the P(3HO)/P(3HB) 80:20, P(3HO)/P(3HB) 50:50 and P(3HO)/P(3HB) 20:80 blend films respectively in comparison to the neat P(3HO) film. The increase in protein adsorption was statistically significant (*p<0. 05)

5.8 Indirect Cytotoxicity Assessment

To investigate the effect of the substances released from the blend films on the HMEC-1 cells, indirect cytotoxicity assessment was carried out as described in **section 2.9.8**. Bearing in mind, the potential application of these P(3HO)/P(3HB) blend films as the base material for the development of biodegradable stents, an endothelial cell line was selected for this study. The negative control for this experiment was the cells grown in DMEM in the absence of polymer and the positive control was the cells grown in the presence of 4% hydrogen peroxide,

which is known to induce cell death as shown in **Figure 5.8**.

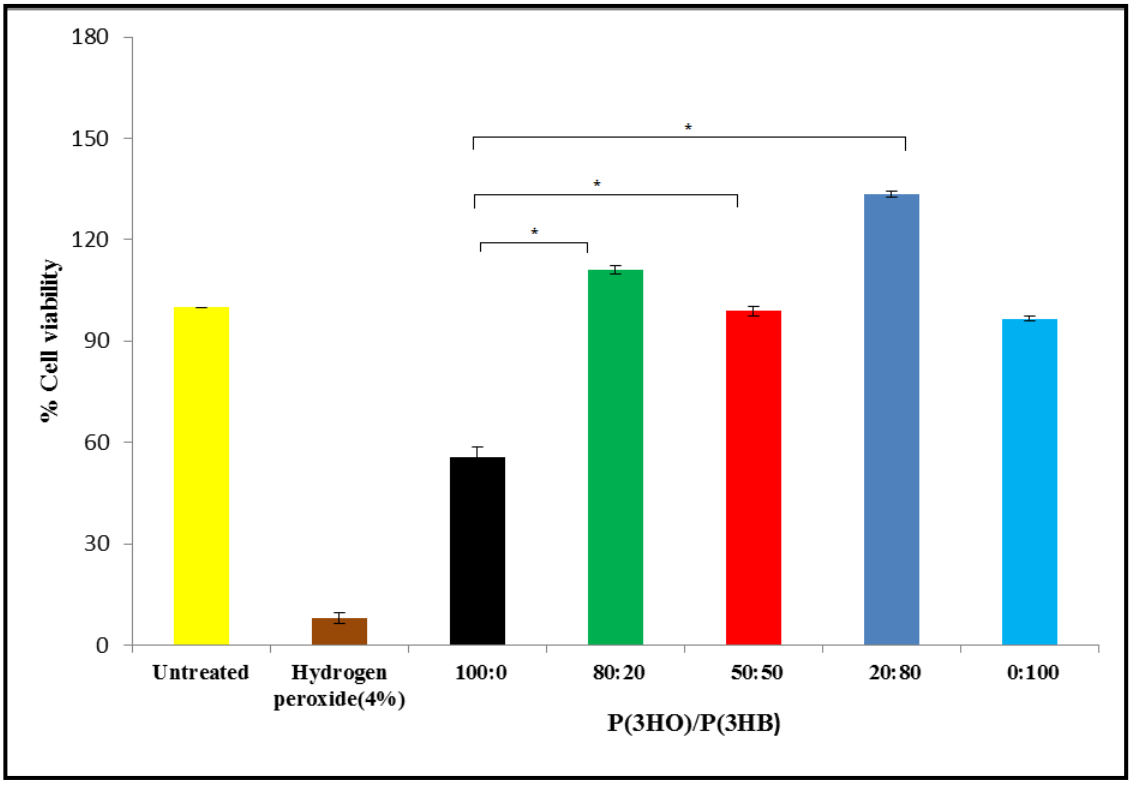

Figure 5.8: Indirect toxicity assessment of P(3HB)/P(3HO) blend films (n = 3; error bars = ± SD). All the tested samples were measured relative to the untreated cells on the tissue culture plate and the untreated were set to 100%. The data were compared using ANOVA and the difference were considered significant when *p<0. 05.

The % cell viability observed in the P(3HO)/P(3HB) 80:20, P(HO)/P(3HB) 50:50 and P(3HO)/P(3HB) 20:80 blend films were 111.1±1.3%, 98.9±1.5%, 133.3±0.9% compared to the % cell viability of 55.5±3.1% in the neat P(3HO) film The % cell viability in the positive control was 8±1.6% and in the neat P(3HB) film was 96.6±0.8%. The highest percentage of cell viability was observed with the P(3HO)/P(3HB) 20:80 blend film containing the highest amount of P(3HB). The increase in the % cell viability in the P(3HO)/P(3HB) compared to the neat P(3HO) film were statistically significant (*p<0. 05). The assessment suggested that no cytotoxic degradation products were released from the blend films.

5.9 Thermal properties

Thermal characterisations of the blend films were carried out to investigate the thermal stability of the blend films as a function of the temperature. Thermal properties such as melting temperature (T_m), glass transition temperature (T_g) and crystallization temperature (T_c) were measured using Differential Scanning

Calorimetry (DSC) as described in **section 2.9.6**. The results of the thermal analysis are summarised in **Table 5.1**.

Samples	T_m (°C)	T_g (°C)	T_c (°C)
P(3HO)	51.8 ± 0.2	-34.0 ± 0.8	-
P(3HB)/P(3HO) 20:80	150.3 ± 0.1	-13.3 ± 0.3	61.0 ± 0.1
P(3HB)/P(3HO) 50:50	159.5 ± 0.1	11.9 ± 0.1	98.5 ± 0.3
P(3HB)/P(3HO) 80:20	166.4 ± 0.3	16.3 ± 0.1	102.7 ± 0.3
P(3HB)	170.3 ± 0.0	10.0 ± 0.0	109.5 ± 0.0

Table 5.1: Thermal Analysis of the neat P(3HO), P(3HO)/P(3HB) blend films and neat P(3HB) film (n = 3).

There was an increase in the glass transition temperature (T_g) with the increase in the amount of P(3HB) in the blend films. A similar trend was observed in the melting temperature (T_m) of the blend films. There was an increase in the T_m of the blend films with the increase in the amount of P(3HB) in the blend film. The crystallization temperature (T_c) also increased with increasing P(3HB) content in the film. P(3HB)/P(3HO) 80:20 blend film with the highest amount of P(3HB) concentration had the highest value of T_g, T_m and T_c. The results demonstrated that the presence of P(3HB) increased the thermal stability of the blend films.

5.10 Dynamic Mechanical Analysis

Mechanical properties of the blend films such as tensile strength, Young's modulus (E values) and elongation at break values were measured using Dynamic Mechanical Analysis (DMA) as described in **section 2.9.5**.

Samples	Young's Modulus (MPa) E values	Tensile strength (MPa)	Elongation break (%)
P(3HO)	1.50 ± 0.01	1.80 ± 0.05	204.05 ± 0.02
P(3HB)/P(3HO) 20:80	28.03 ± 0.75	6.01 ± 0.01	58.70 ± 0.15
P(3HB)/P(3HO) 50:50	78.50 ± 0.01	7.80 ± 0.03	22.90 ± 0.05
P(3HB)/P(3HO) 80:20	84.60 ± 0.40	7.50 ± 0.03	10.10 ± 0.01

Table 5.2: Mechanical analysis of the neat P(3HO) and P(3HO)/P(3HB) blend films (n = 3).

This was carried out to understand the effect of P(3HB) on the mechanical properties of the blend films. The results have been summarised in **Table 5.2**. The Young's Modulus values increased with the increase in the concentration of P(3HB) in the blend film. The E values of the blend films were higher than the E values of the neat P(3HO) which is 1.5 MPa. The Young's modulus value of the P(3HB)/P(3HO) 80:20 blend film which has the highest concentration of P(3HB) was 5540% higher compared to the neat P(3HO) film. The Young's Modulus of values of the other blend films such as P(3HB)/P(3HO) 50:50 and P(3HB)/P(3HO) 20:80 were 5133% and 1766% higher compared to the neat P(3HO) film.

The tensile strength of the P(3HO)/P(3HB) blend films were higher compared to the neat P(3HO) film. The tensile strength of blend films such as P(3HB)/P(3HO) 20:80 blend film, P(3HB)/P(3HO) 50:50 and P(3HB)/P(3HO) 80:20 were 300%, 420% and 400% higher than the neat P(3HO) film respectively. However, the tensile strength of the P(3HB)/P(3HO) 80:20 blend film which has the highest concentration of the P(3HB) content was slightly lower compared to the P(3HO)/P(3HB) 50:50 blend film. Elongation at break value, which is the measure of the elastomeric properties of the films was also measured using DMA. The results obtained showed, as expected, a drastic decrease in the elastomeric

properties of the blend films with an increase in the concentration of P(3HB) when compared to the neat P(3HO) film. The elongation at break value of the P(3HB)/P(3HO) 80:20 blend film which has the highest concentration of the P(3HB) content was 95% lower compared to the neat P(3HO) film. The elongation at break values of the other blend films such as P(3HB)/P(3HO) 50:50 and P(3HB)/P(3HO) 20:80 were 88% and 71% lower than the elongation at break value of the neat P(3HO) film. The mechanical properties of the neat P(3HB) film could not be measured using DMA due to its high Young's Modulus value which

5.11 *In vitro* degradation study

The film samples incubated in DMEM and PBS were characterised as described below to find out the changes that occurred during degradation.

5.11.1 Water absorption and weight loss measurements

Percentage of water absorbed (%WA) and weight loss (%WL) during the degradation of the films were measured for one and four months as described in **section 2.10**. The result of the one month study is presented in **Figure 5.9** (a), (b), (c) and (d).

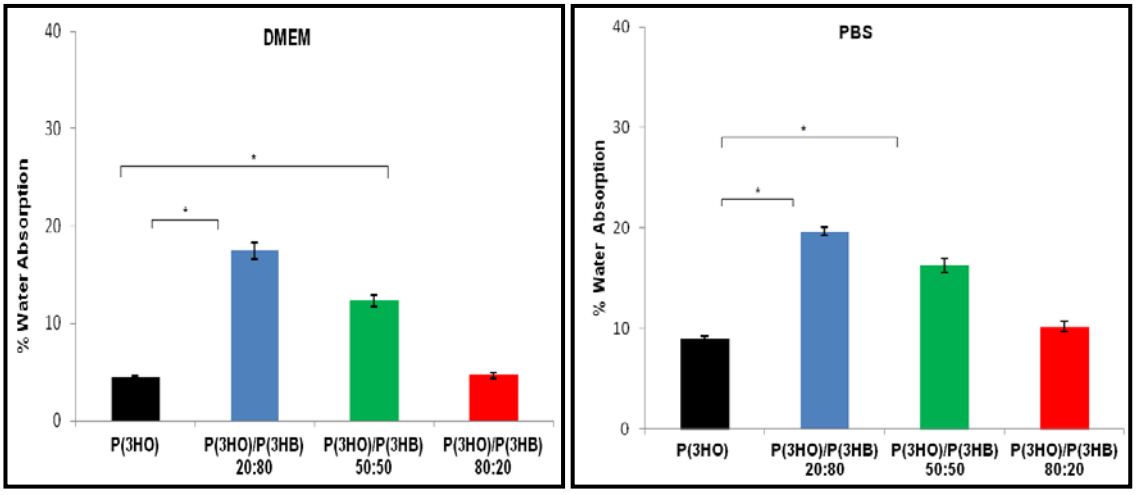

(a) **(b)**

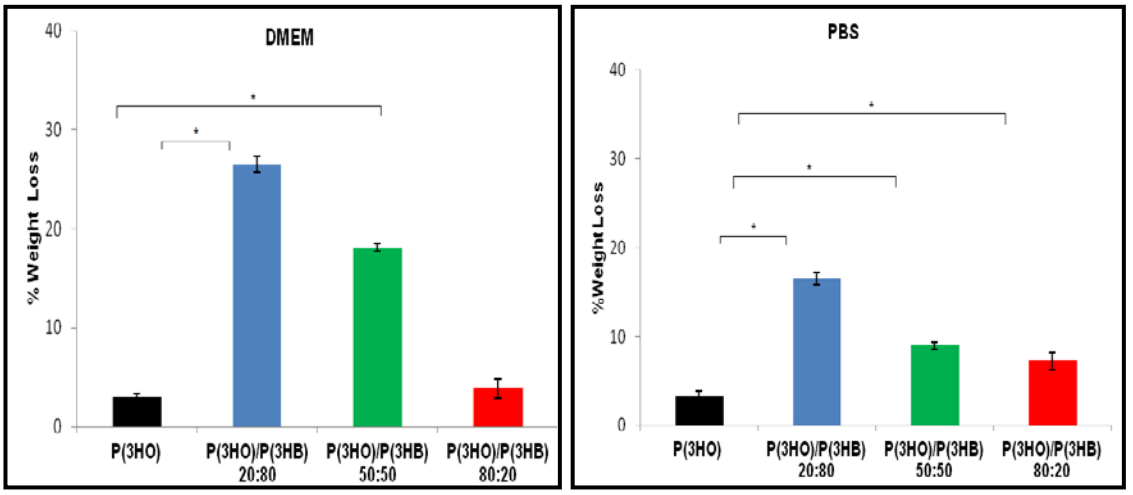

(c) **(d)**

Figure 5.9: Water absorption by the neat P(3HO) and P(3HO)/P(3HB) blend films during the *in vitro* degradation study in (a) DMEM media and (b) PBS media. Weight loss by the degrading neat P(3HO) and P(3HO)/P(3HB) blend films during one month *in vitro* degradation study in (c) DMEM media and (c) PBS media (n = 3). The data were compared using ANOVA and the difference were considered significant when *p<0. 05.

The water absorption was higher in the blend films compared to the neat P(3HO) film in both DMEM and PBS medium. The percentage water absorption (% WA) by the neat P(3HO) film in DMEM media was measured to be 4.5±0.1% at the end of a one month degradation study as compared to the blend films which were 17.4±0.8%, 12.3±0.6% and 4.6±0.3% in P(3HO)/P(3HB) 20:80 blend film, P(3HO)/P(3HB) 50:50 blend film and P(3HO)/P(3HB) 80:20 blend film respectively. The water absorption was significantly higher in P(3HO)/P(3HB) 20:80 and P(3HO)/P(3HB) 50:50 blend films compared to the neat P(3HO) film (*p<0. 05). Similarly in the PBS media, the % WA by the neat P(3HO) film was 9.1±0.2% in comparison to the 19.6±0.4%, 16.3±0.7% and 10.2±0.5% in P(3HO)/P(3HB) 20:80, P(3HO)/P(3HB) 50:50 and P(3HO)/P(3HB) 80:20 blend films respectively.

It was also found that the weight loss was significantly greater in P(3HO)/P(3HB) 20:80 and P(3HO)/P(3HB) 50:50 blend films compared to the neat P(3HO) films in both DMEM and PBS media (*p<0. 05). The % WL in the neat P(3HO) film in DMEM was 3.1±0.3% at the end of one month degradation study as compared to the blend films which was 26.5±0.8%, 18.1±0.4% and 3.8±0.9% in the P(3HO)/P(3HB) 20:80,

P(3HO)/P(3HB) 50:50 and P(3HO)/P(3HB) 80:20 blend films respectively. Similarly, in the PBS media, the % WL in the neat P(3HO) film was 3.3±0.5% in comparison to 16.4±0.7%, 9.1±0.4% and 7.2±1.0% in P(3HO)/P(3HB) 20:80, P(3HO)/P(3HB) 50:50 and P(3HO)/P(3HB) 80:20 blend films respectively.

The result of the four month study is presented in **Figure 5.10** (a), (b), (c) and (d).

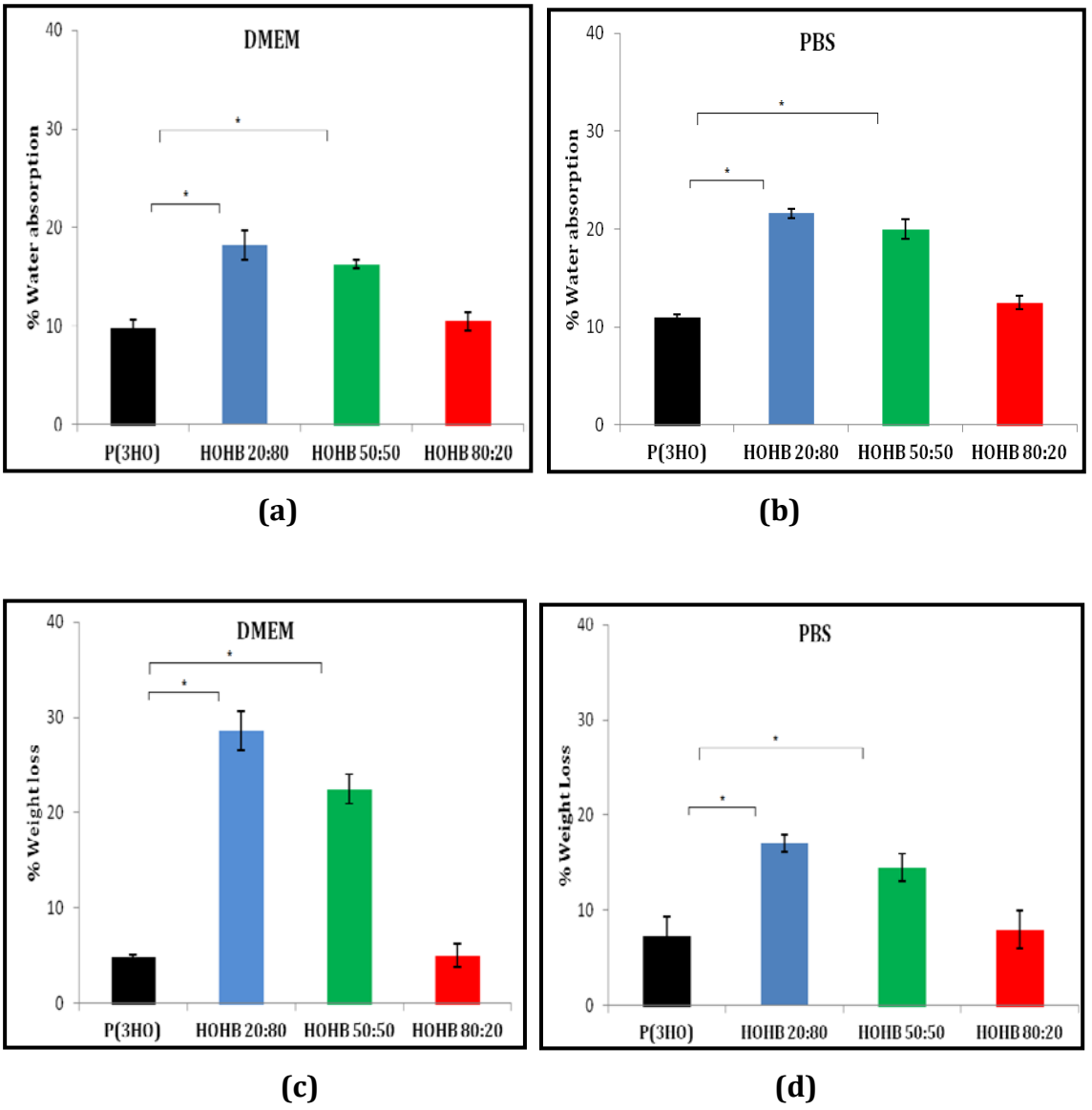

Figure 5.10: Water absorption by the neat P(3HO) and P(3HO)/P(3HB) blend films during the *in vitro* degradation study in (a) DMEM media and (b) PBS media. Weight loss by the degrading neat P(3HO) and P(3HO)/ P(3HB) blend films during the *in vitro* degradation study in (c) DMEM media and (d) PBS media (n = 3). The data were compared using ANOVA and the difference were considered significant when *p<0. 05.

The water absorption was significantly higher in P(3HO)/P(3HB) 20:80 and P(3HO)/P(3HB) 50:50 blend films compared to the neat P(3HO) film in both DMEM

and PBS medium at the end of the four month study (*p<0. 05). The percentage water absorption (% WA) by the neat P(3HO) film in DMEM media was measured to be 9.8±0.8% at the end of a four month degradation study as compared to the blend films which were 18.2±1.5%, 16.2±0.4% and 10.5±0.9% in P(3HO)/P(3HB) 20:80 blend film, P(3HO)/P(3HB) 50:50 blend film and P(3HO)/P(3HB) 80:20 blend film respectively. Similarly in the PBS media, %WA by the neat P(3HO) film was 11±0.3% in comparison to 21.6±0.5%, 20.2±1.1% and 12.5±0.7% in P(3HO)/P(3HB) 20:80, P(3HO)/P(3HB) 50:50 and P(3HO)/P(3HB) 80:20 blend films respectively.

It was also found that the weight loss was significantly greater in P(3HO)/P(3HB) 20:80 and P(3HO)/P(3HB) 50:50 blend films compared to the neat P(3HO) film in both DMEM and PBS medium at the end of the four month study (*p<0. 05). The % WL for the neat P(3HO) film in DMEM was 4.4±1.3% at the end of one month degradation study as compared to the blend films which was 28.6±2.1%, 22.5±1.5% and 5.0±0.9% in the P(3HO)/P(3HB) 20:80, P(3HO)/P(3HB) 50:50 and P(3HO)/P(3HB) 80:20 blend films respectively. Similarly, in the PBS media, %WL in the neat P(3HO) film was 7.3±0.5% in comparison to 17.1±0.7%, 14.5±1.4% and 8.0±2.0% in P(3HO)/P(3HB) 20:80, P(3HO)/P(3HB) 50:50 and P(3HO)/P(3HB) 80:20 blend films respectively.

5.12 Surface studies of the degrading films

At the end of the one month degradation study, the neat P(3HO) film and P(3HO)/P(3HB) blend films were rinsed in HPLC grade water. The surface morphology of the degrading films were studied using Scanning electron microscopy (SEM) as described in **section 2.9.1**. SEM images confirmed that there was higher level of degradation in the P(3HO)/P(3HB) blend films as compared to the neat (P3HO) film (**Figure 5.11**). Biodegradability of the blend films is affected by various factors such as the blend composition and the surface properties of the blend components.

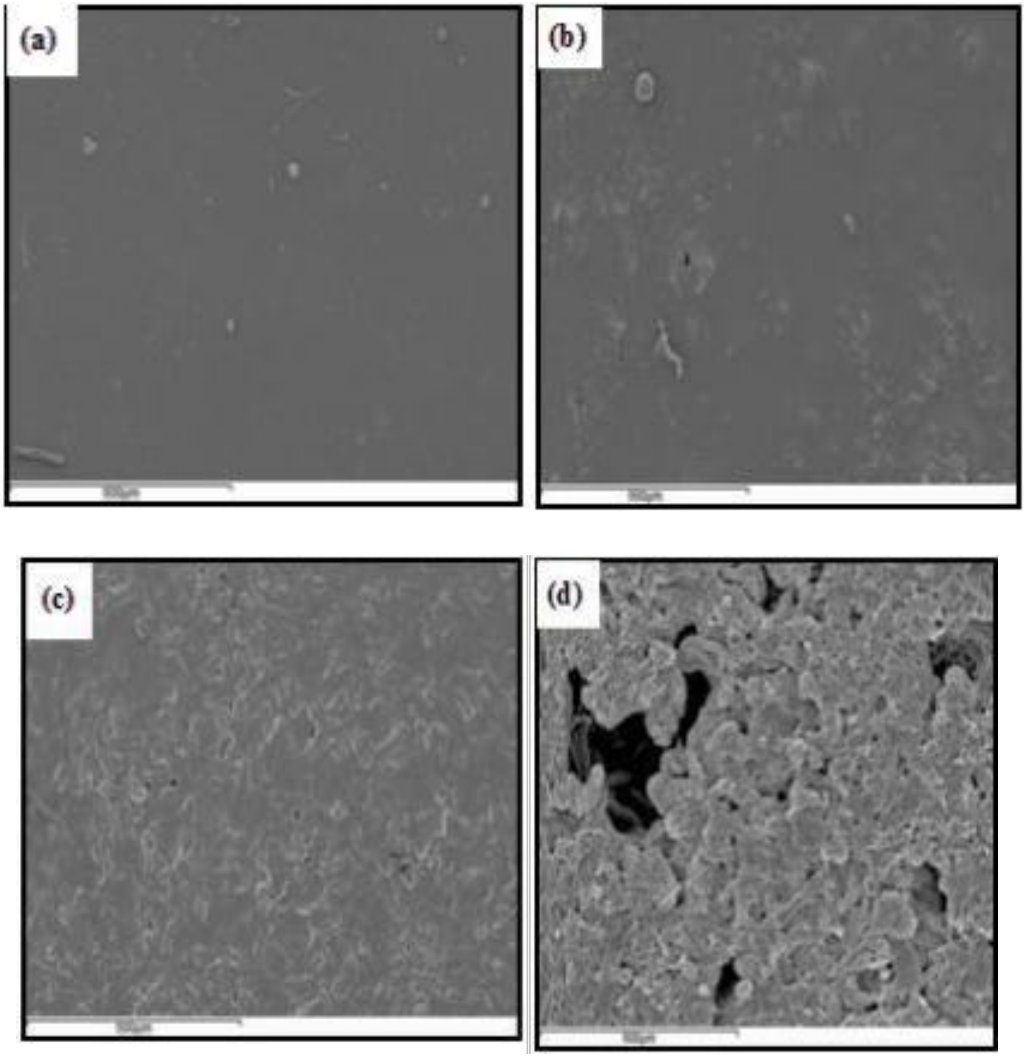

Figure 5.11: SEM images of the P(3HB)/P(3HO) blend films after of one month of incubation exhibiting different states of degradation: (a) neat P(3HO) film, (b) P(3HO)/P(3HB) 80:20 (c) P(3HO)/P(3HB) 50:50 (d) P(3HO)/P(3HB) 20:80 blend film in DMEM. Scale bars = 100μm.

The degradation rate was higher in the all the P(3HO)/P(3HB) blend films compared to the neat P(3HO) film. The highest percentage of degradability was found to be associated with the P(3HO)/P(3HB) 20:80 blend film as confirmed by SEM. The SEM image showed the degraded surface of the the P(3HO)/P(3HB) 20:80 film compared to the relatively non-degraded neat P(3HO) film.

Based on these results, P(3HO)/P(3HB) 50:50 blend with intermediate properties were chosen for further studies.

PART II

Surface micropatterning of the P(3HO)/P(3HB) 50:50 blend films using laser micropatterning technique. This work was led by Dr. Iban Quintana at Tekniker Institute in Bilbao, Spain.

5.13 Picosecond pulse laser technology

A pico-second pulse Nd:YVO_4 laser (RAPID: Lumera Laser) integrated in a micromachining workstation by a 3D-Micromac was used to micropattern P(3HO)/P(3HB) 50:50 blend films. The laser source delivered 10 ps pulses at 1064nm wavelength with energy of 12 μJ operating at a maximum repetition rate of 1 MHz. In addition to the fundamental mode, the laser emitted at second and third harmonic wavelengths of 532 and 355 nm, with maximum energies of approximately 22.5 and 17.5 μJ respectively and at a repetition rate of 200 kHz. The laser beam was focused over the sample by a focusing lens placed in the air that has a focal length of 100mm for light of 532 and 1064 nm wavelength, and of 103 mm for light of 355 nm wavelength. Spot sizes (beam radius at $1/e^2$) of 30 μm and 20.5 μm were obtained at energy of 0.2 μJ for wavelengths of 532 nm and 355 nm, respectively, by selecting optional fixed beam expanders. Sample position was selected by a XY stage with lateral resolution in the μm-range and a Z positioning system with a vertical resolution of roughly 10 nm. By means of pulse overlapping we obtained different microstructures, whose width and depth could be controlled by appropriately selecting the laser power, frequency and mark speed, making it possible to obtain almost any desired topography and geometry. After an optimization process of the laser ablation parameters, varying the wavelength (λ), frequency (f), speed (v) and power level (P), the suitable laser configuration to carry out the material micropatterning was obtained which is as follows:

$$\boldsymbol{\lambda = 355\ \text{nm}, f = 250\ \text{kHz}, v = 600\ \text{mm/s}}$$

P(3HO)/P(3HB) 50:50 blend films were micropatterned by creating grooves of width (w) = 12 μm (P = 30%), interline distance or the distance between the grooves = 10 μm and the depth of the groove (d) = 6 μm.

5.14 Characterization of the micropatterned (3HO)/P(3HB) 50:50 blend film

5.14.1 Scanning Electron Microscopy (SEM)

Microgrooves were created on the P(3HO)/P(3HB) 50:50 blend films using the Laser micropatterning method as described in **section 5.13**. This was done to guide the attachment and proliferation of the endothelial cells in an aligned manner. Microstructural properties of the micropatterned P(3HO)/P(3HB) 50:50 blend film were studied using SEM as described in **section 2.9.1.** The surface topography of the laser micropatterned P(3HO)/P(3HB) 50:50 blend film was compared to the topography of the plain P(3HO)/P(3HB) 50:50 blend film as shown in **Figure 5.12.**

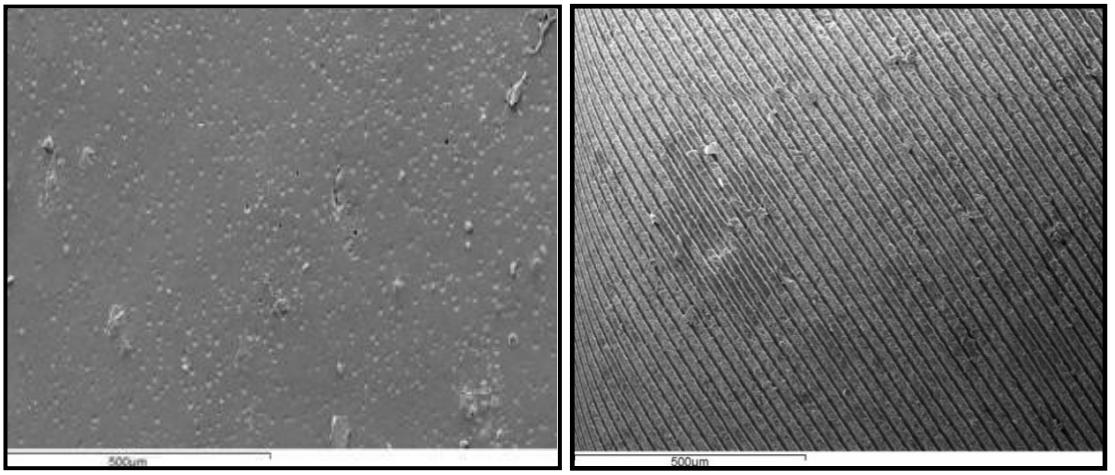

(a) **(b)**

Figure 5.12: SEM images of the (a) plain P(3HO)/P(3HB) 50:50 blend film (b) surface micropatterned P(3HO)/P(3HB) 50:50 blend film.

The microgrooves created on the blend films were of width (12μm) and depth (6 μm). The interline distance or the distance between the grooves was 10 μm. The SEM images confirmed that P(3HO)/P(3HB) 50:50 blend film with a new topography had been successfully created using the laser micropatterning technique. The fabricated blend films were further characterised using the Atomic force microscopy (AFM).

5.14.2 Atomic Force Microscopy (AFM)

In order to evaluate the effect of surface micropatterning on the surface roughness of the blend films, AFM was used to measure the surface roughness values of the fabricated blend films as described in **section 2.9.3.** Typical root mean square (rms) values were calculated to determine the roughness value of the micropatterned

blend films. As shown in **Figure 5.14**, the rms values of the plain blend film and micropatterned blend film were 0.59±0.02 and 1.87±0.2 µm respectively.

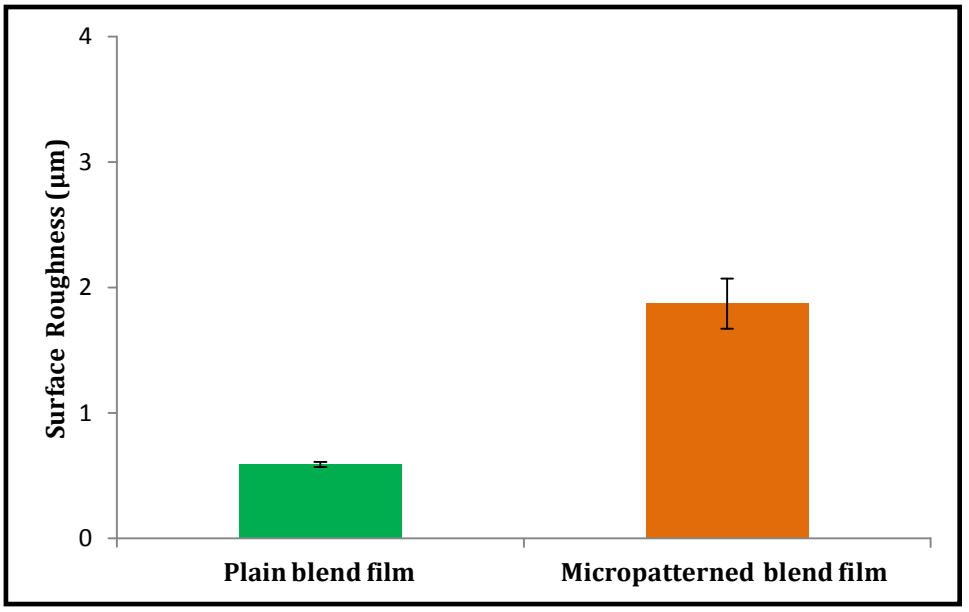

Figure 5.13: Surface roughness of the plain P(3HO)/P(3HB) 50:50 blend film and micropatterned blend film measured using AFM (n = 3).

The change in the topography of the P(3HO)/P(3HB) 50:50 blend films due to the micropatterning was confirmed by AFM. The laser micropatterned blend films had a 217% higher surface roughness value compared to the plain blend film indicating that laser micropatterning had increased the surface roughness of the blend films.

5.14.3 Contact Angle Study

Static contact angle experiments were carried out on the micropatterned blend film samples to study the effect of the surface micropatterning on the wettability of the fabricated blend films as described in **section 2.9.4.** Contact angle measurement of the micropatterned P(3HO)/P(3HB) 50:50 blend film was compared with the plain blend film as shown in **Figure 5.14**

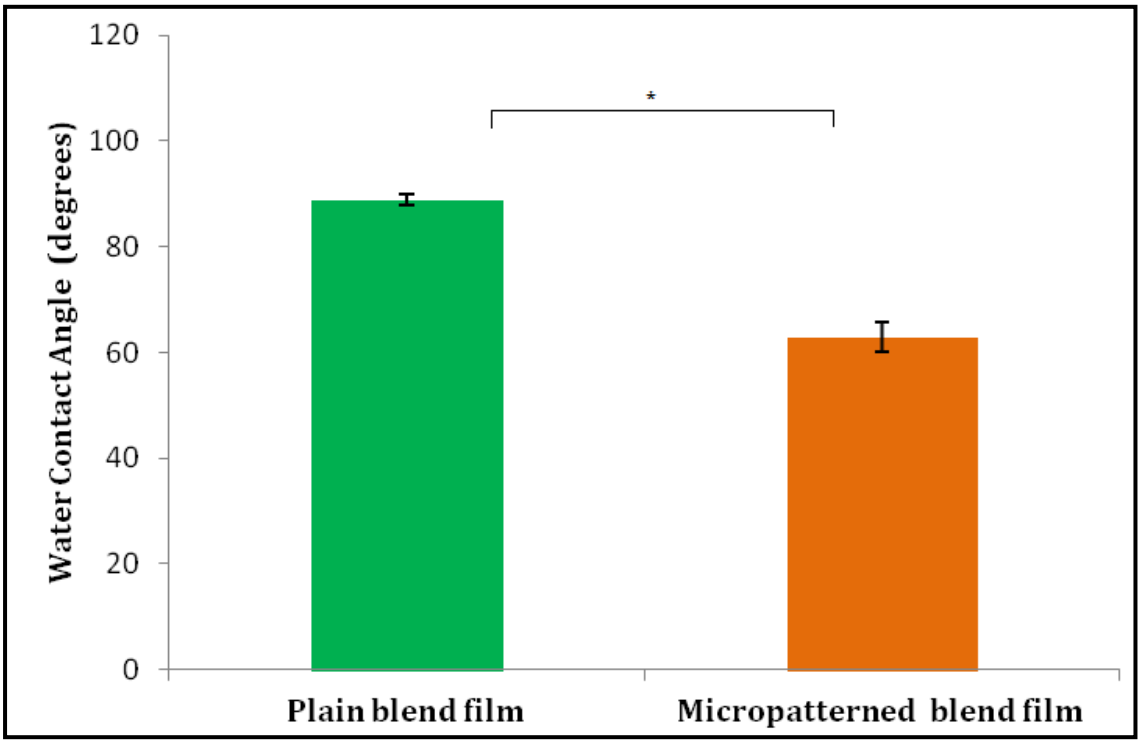

Figure 5.14: Static water contact angle measurements of the plain P(3HO)/P(3HB) 50:50 blend film and micropatterned blend film (n = 3; error bars = ± SD). The data were compared using t-test and the difference were considered significant when *p<0. 05.

The water contact angle of the micropatterned blend film was 62.9±2 that demonstrated hydrophilic characteristics compared to the plain blend film that had a contact angle of 88.8±1.0 (*p<0. 05). The surface micropatterning of the blend films by laser micropatterning lowered the water contact angle, making the films more hydrophilic compared to the plain blend film.

5.14.4 Protein Adsorption Test

The creation of the microgrooves on the blend films by laser micropatterning increased their surface area. Protein adsorption assay was done to quantify the total amount of Bovine serum albumin (BSA) adsorbed by the micropatterned blend film as described in **section 2.9.7.** The results were compared to the protein adsorption on the plain blend films as shown in **Figure 5.15.**

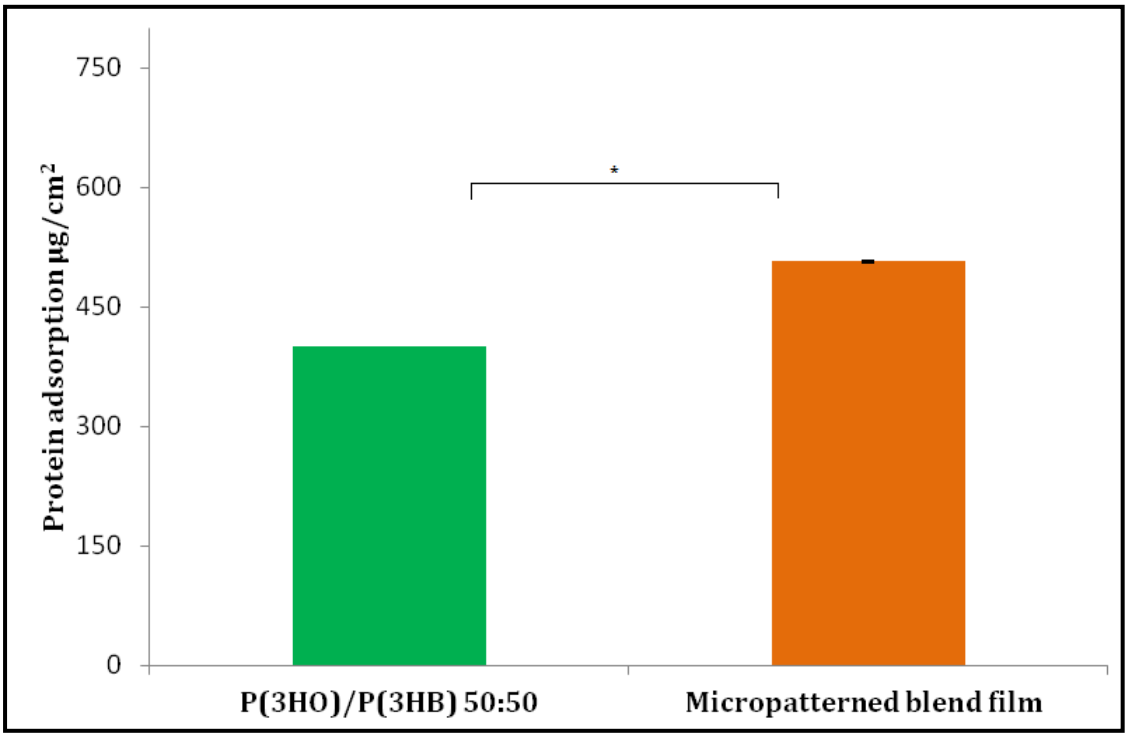

Figure 5.15: Total protein adsorption on the plain P(3HO)/P(3HB) 50:50 blend film and the micropatterned blend film (n = 3). The data were compared using t-test and the difference were considered significant when *p<0. 05.

The overall protein adsorbed by the plain blend film was 400±0.2 µg/cm^2 that was lower compared to the total protein adsorbed by the micropatterned blend film that was 507.3±0.9 µg/cm^2. This increase in the protein adsorption in the micropatterned blend film was significantly higher than the plain blend film (*p<0. 05).

5.14.5 Dynamic Mechanical Analysis

In order to evaluate the effect of the surface micropatterning on the blend film samples, detailed mechanical characterisation of the films were carried out as described in **section 2.9.5.** This was compared to the mechanical properties of the plain blend film. The results of the mechanical analyses are summarised in **Table 5.3.**

Samples	Young's Modulus (MPa) E values	Tensile strength (MPa)	Elongation at break (%)
Plain P(3HO)/P(3HB) 50:50	78.50 ± 0.01	7.80 ± 0.03	22.90 ± 0.05
Micropatterned blend film	74.50 ± 0.70	7.30 ± 0.30	25.40 ± 1.01

Table 5.3: Mechanical characterisation of the plain P(3HO)/P(3HB) 50:50 and the micropatterned blend films using Dynamic Mechanical Analysis (n = 3).

There was a decrease in the tensile strength and the Young's modulus (a measure of stiffness) of the micropatterned blend films compared to the plain blend films. However, there was an increase in the % elongation at break values.

5.14.6 *In vitro* biocompatibility studies

The effect of the surface micropatterning on the attachment and the proliferation of the Human microvascular endothelial cells (HMEC-1) cells was analysed by culturing the cells on the plain blend film as well as the micropatterned blend film samples. Preliminary *in vitro* cell culture studies were carried out as described in **section 2.10.2.** Neutral red (NR) assay was used for obtaining a quantitative measure of the cell adhesion and cell proliferation studies. Attachment and proliferation of HMEC-1 cells on the films were analysed over a period of 1, 4 and 7 days. The results of these biocompatibility tests have been summarised in **Figure 5.16.** There was better growth and proliferation of the cells on the micropatterned blend films compared to the plain blend film samples.

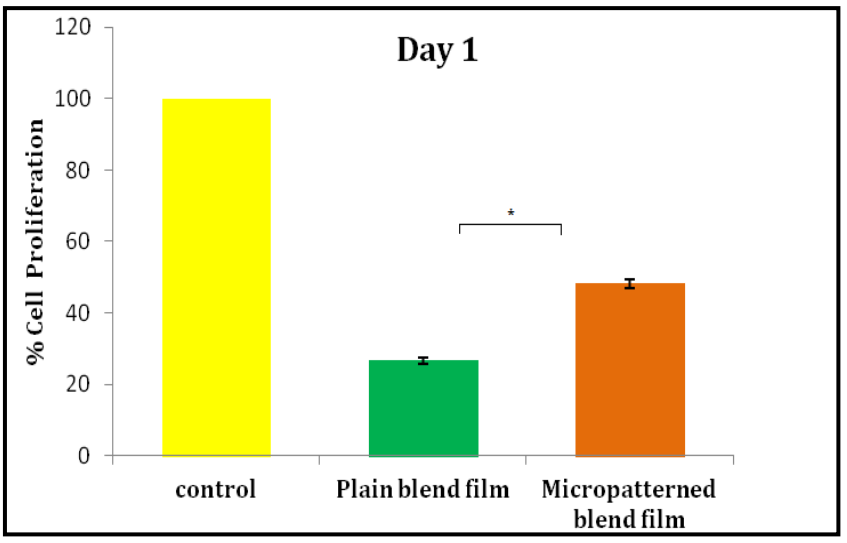

(a)

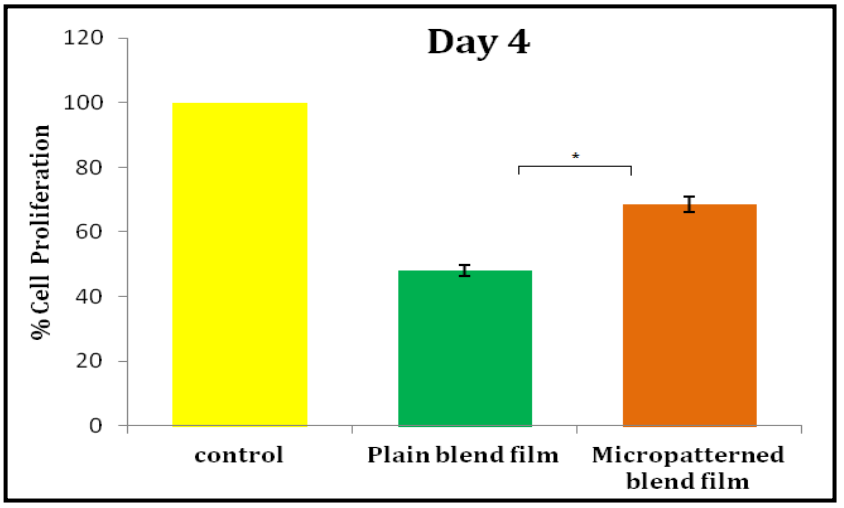

(b)

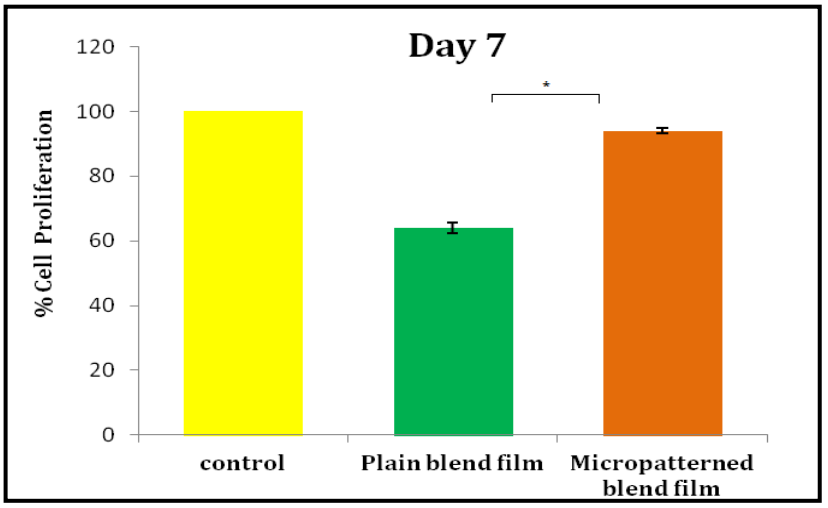

(c)

Figure 5.16: Cell proliferation study of the seeded HMEC-1 cells on the plain P(3HO)/P(3HB) 50:50 blend film and micropatterned blend film on (a) Day 1, (b) Day 4 and(c) Day 7. The data were compared using ANOVA and the difference were

considered significant when the *p<0. 05. All the tested samples were relative to the control and the control was set to 100%.

At the end of the 1st day, the growth of HMEC-1 cells on the plain blend film and the micropatterned film was 26.6±1% and 48.2±1% respectively, as compared to the tissue culture plastic. Cell attachment on the micropatterned films was much higher compared to the plain blend film. The cells continued to grow on all the samples. At the end of the 4th day, the growth of HMEC-1 cells on the micropatterned blend film was 68.5±2.3% as compared to the plain blend film which had 48.1±1.8% growth on the 4th day. At the end of the 7th day, there was a significant increase in the growth of the cells on the micropatterned blend film samples as opposed to the cells on the plain blend film samples (*p<0.05). The growth of HMEC-1 cells on the micropatterned blend film was 94.0±0.9% as compared to the 64.0±1.6% of cell growth on the plain blend film samples.

5.14.7 Scanning electron microscopy (SEM)

In this study, the HMEC-1 cells seeded onto the surface micropatterned blend film and the plain blend films were analysed using SEM as described in **section 2.9.1.** This was done to study the effect of micropatterning on the morphology and alignment of the HMEC-1 cells as shown in **Figure 5.17**.

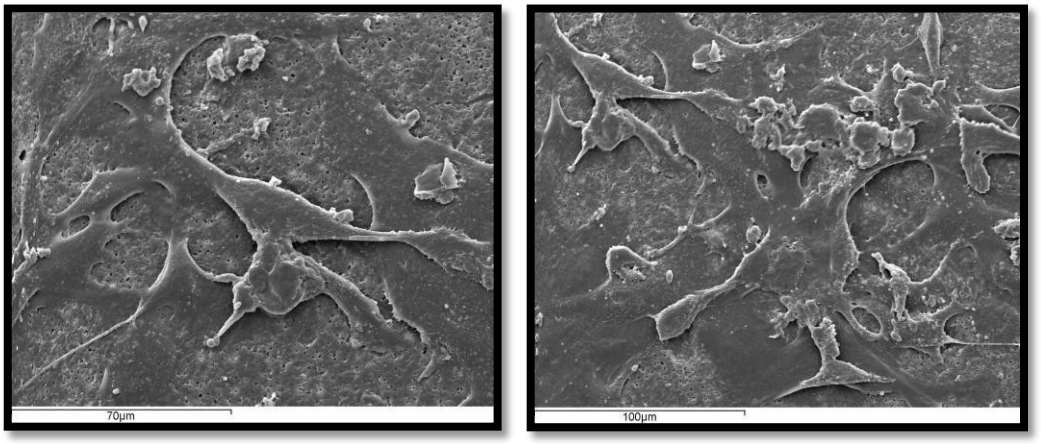

A1 **A2**

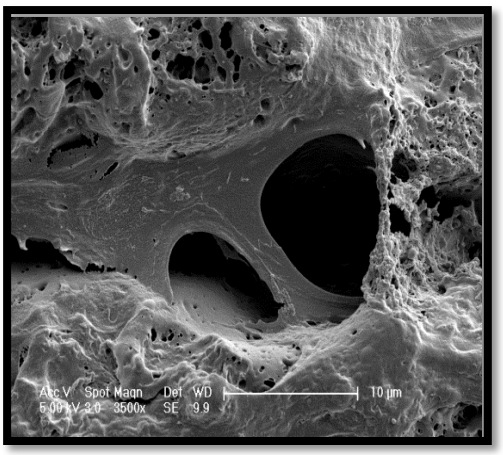

A3

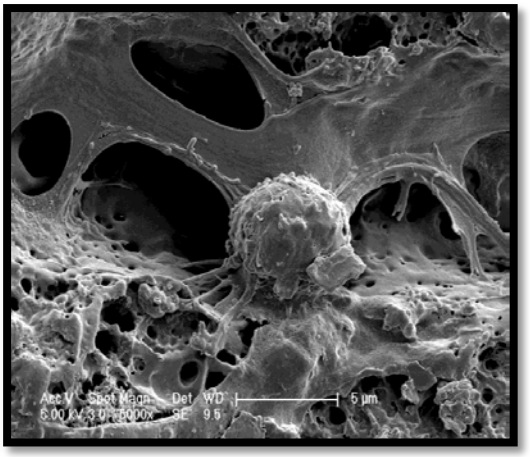

A4

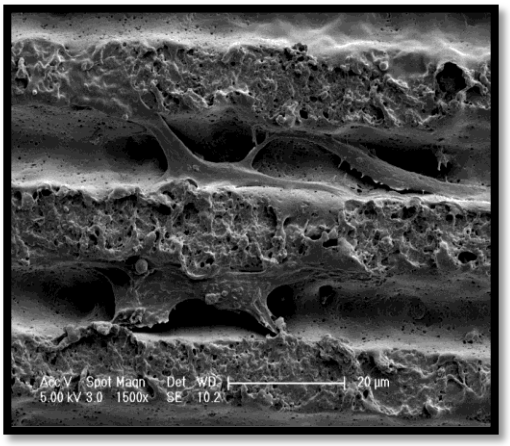

A5

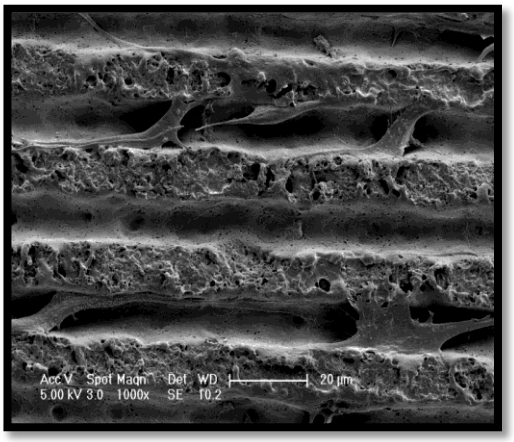

A6

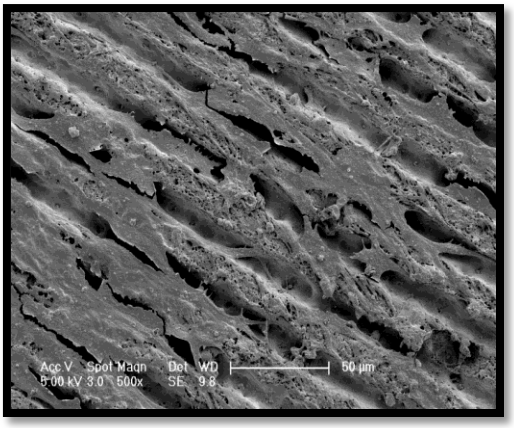

A7

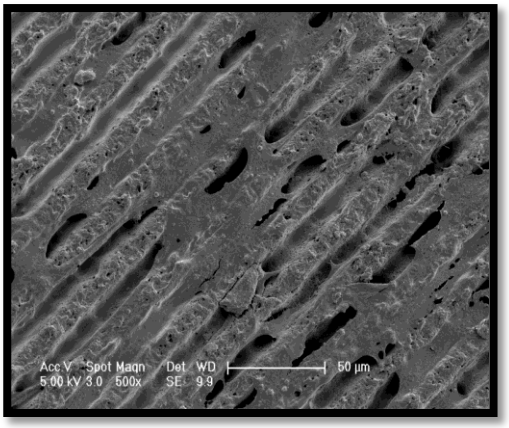

A8

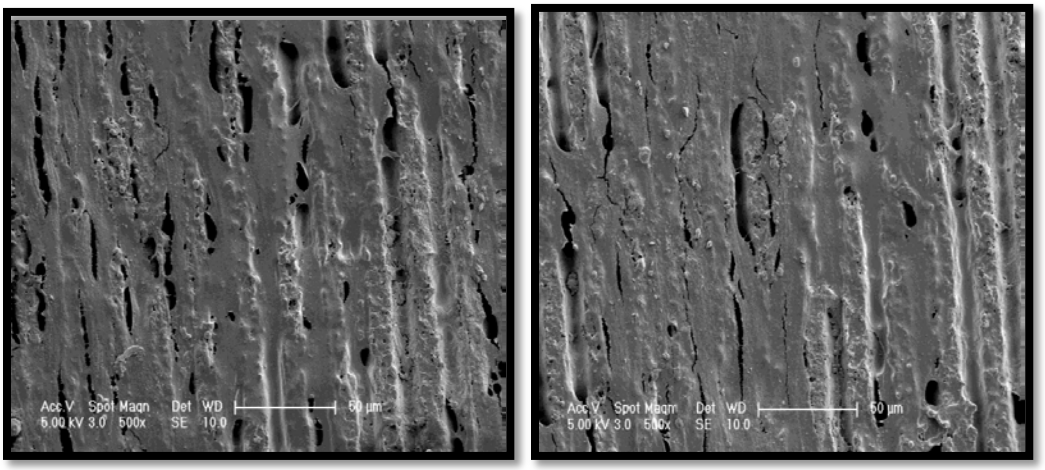

A9 **A10**

Figure 5.17: SEM images of the HMEC-1 cells on the (A1-A2) plain P(3HO)/P(3HB) 50:50 blend film on day 7. The SEM images of the HMEC-1 cells (A3-A4) dividing within the groove on the micropatterned blend film on day 1. The SEM image demonstrating the migration of the elongated HMEC-1 cells along the groove (A5-A6) on day 4. Images (A7-A10) showing HMEC-1 cells proliferating along the microgrooves in an aligned manner on day 7.

5.14.8 Development of stent prototype

The stent prototypes were made by laser microcutting the P(3HO)/P(3HB) 50:50 films. The dimensions of the stent prototype are shown in the **Figure 5.18**.

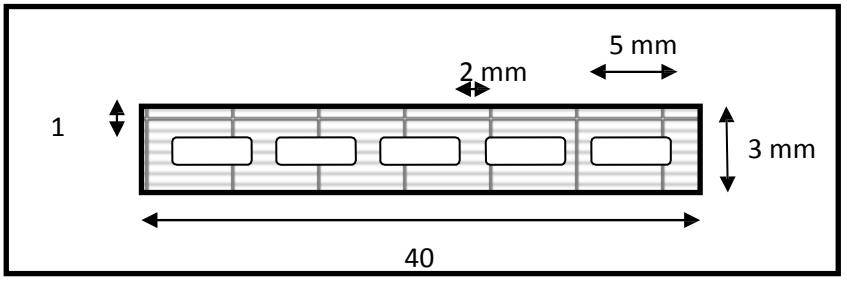

Figure 5.18: Dimensions of a laser cut film for stent prototype development

These laser cut films were wound to a mandrel to obtain a helical structure as shown in **Figure 5.19.**

Figure 5.19: A stent prototype made up of P(3HO)/P(3HB) 50:50 blend film.

The inner wall of these stent prototypes was micropatterned using laser to promote endothelialisation. Due to time constraint, the characterisation of these stent prototypes could not be completed and will be carried out in future. However, the stent prototypes were successfully developed.

PART III

Incorporation of aspirin within the P(3HO)/P(3HB) blend film and their characterisation

Preparation of P(3HO)/P(3HB) 50:50 blend film containing aspirin

The P(3HO)/P(3HB) 50:50 blend film containing aspirin was prepared using the solvent casting method. P(3HO) and P(3HB) were dissolved in dichloromethane with a polymer concentration of 5wt% in a ratio of 50:50. Aspirin was dissolved in dichloromethane and mixed with the polymer solution to achieve a drug loading of 15 wt%. The polymer solution containing aspirin was mixed well by sonication and then cast into a glass petri dish immediately to achieve a uniform distribution of aspirin within the polymer matrix. P(3HO)/P(3HB) 50:50 blend film without aspirin was also prepared to investigate the effect of drug loading on the properties of the blend film. The film was air dried for one week. Films of 0.18 mm thickness were produced.

Characterisation of the P(3HO)/P(3HB) 50:50 blend film with aspirin

5.14.9 Fourier Transform Infrared Spectroscopy (FTIR)

FTIR spectroscopy was performed on the blend film with aspirin as well as on the commercial aspirin sample using the method described in **section.** 2.6.1. This was done to establish that the aspirin had been absorbed within the matrix of the P(3HO)/P(3HB) 50:50 blend film. The IR Spectrum of (a) commercial aspirin (-) and (b) blend film with aspirin (-) is shown in **Figure 5.20**.

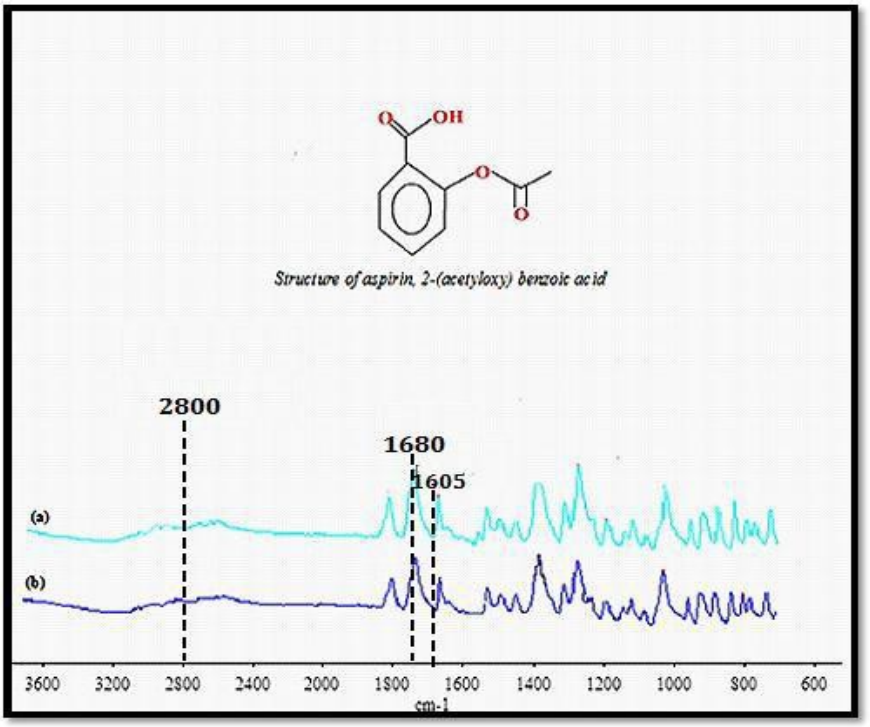

Figure 5.20: FTIR spectra of the (a) commericial aspirin (-) and (b) P(3HO)/P(3HB) 50:50 blend film with aspirin (-).

Three characteristic absorption peaks at 1680, 1605 and a broad peak in the range 2500 - 3500 cm^{-1} present in the commercial aspirin sample and were also present in the blend film with aspirin indicating that aspirin had been absorbed within the P(3HO)/P(3HB) 50:50 matrix. The broad absorption peak at 2800 cm^{-1} represented the carboxylic acid group present in aspirin. The peak at 1605 cm^{-1} occurred due to the benzene ring whereas the absorption peak at 1680cm^{-1} represented the two carbonyl groups found in aspirin (Li *et al.*, 1999).

5.14.10 Scanning electron microscopy (SEM)

Surface properties of P(3HO)/P(3HB) 50:50 blend film samples with aspirin were measured by SEM using the method described in **section 2.9.1.** The surface topography of the P(3HO)/P(3HB) 50:50 blend film with aspirin was compared to the topography of the blend film without aspirin as shown in **Figure 5.21**. This was done to examine the effect of aspirin loading on the surface properties of the film.

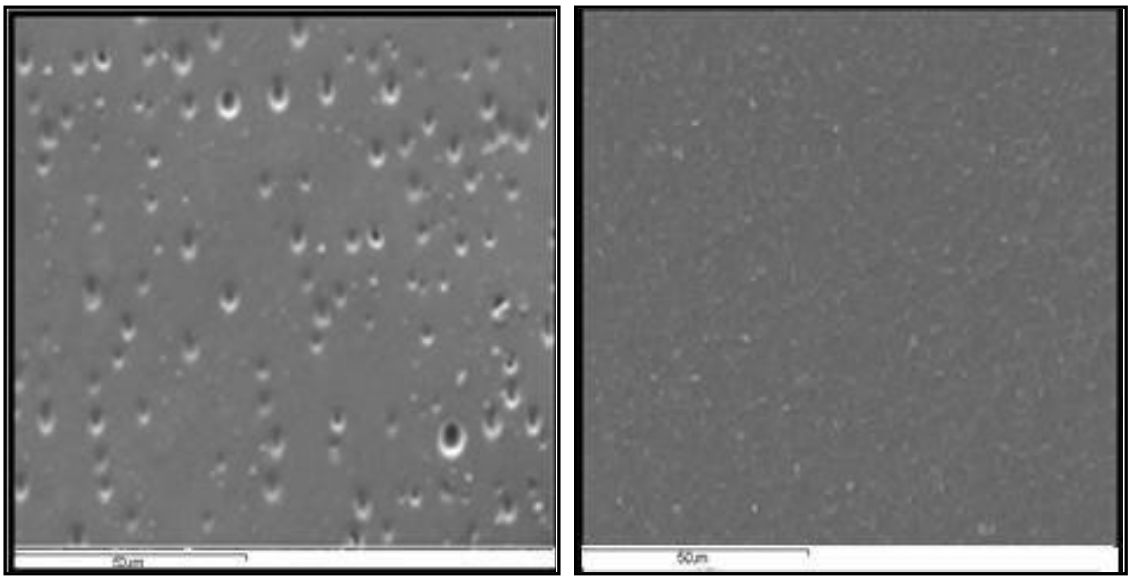

(a) **(b)**

Figure 5.21:.SEM images of the (a) P(3HO)/P(3HB) 50:50 blend film without aspirin and (b) P(3HO)/P(3HB) 50:50 blend film with aspirin. Scale bars = 50 µm.

The SEM results revealed that aspirin was uniformly distributed within the blend film. A new surface topography was introduced due to the incorporation of aspirin within the matrix of the P(3HO)/P(3HB) 50:50 blend film. The surface of the P(3HO)/P(3HB) 50:50 blend film with aspirin appeared to have a uniform roughness. The films were further characterised using the Atomic Force Microscopy (AFM).

5.14.11 Atomic Force Microscopy (AFM)

The change in surface properties of the blend film due to the incorporation of aspirin within their matrix was further investigated using AFM. This was done to compare the surface roughness of the P(3HO)/P(3HB) 50:50 blend film samples with and without aspirin. AFM analysis was carried out according to the method described in **section 2.9.3** and the results obtained are shown in **Figure 5.22**. From our previous studies, it was established that the rms values of the P(3HO)/P(3HB) 50:50 blend film was 0.59±0.02 µm.

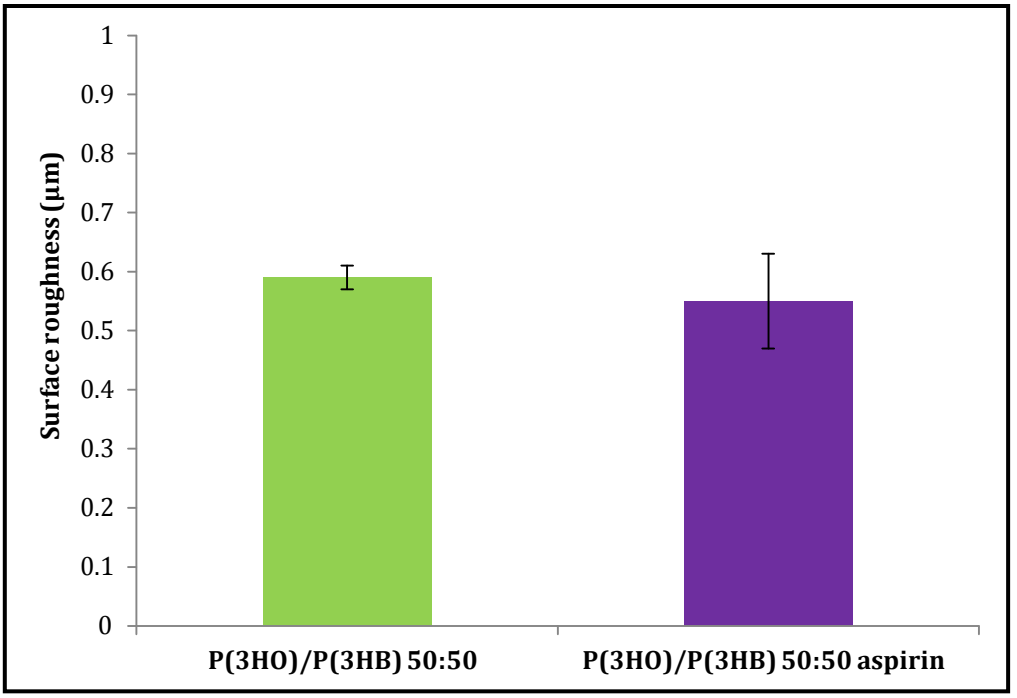

Figure 5.22: Surface roughness of P(3HO)/P(3HB) 50:50 blend film without aspirin (b) P(3HO)/P(3HB) 50:50 blend film with aspirin.

The surface roughness values of the P(3HO)/P(3HB) 50:50 blend film with aspirin was 6% lower compared to the P(3HO)/P(3HB) 50:50 blend film without aspirin. This confirmed that aspirin was homogeneously distributed within the matrix of the blend film making the surface of the blend film slightly smoother and more uniform compared to the P(3HO)/P(3HB) 50:50 blend film without aspirin (Zilberman and Persson, 2002).

5.14.12 Contact Angle Study

Static contact angle measurement were done to determine the hydrophilicity of the P(3HO)/P(3HB) 50:50 blend film samples with and without aspirin as described in **section 2.9.4.** Contact angle measurements of the P(3HO)/P(3HB) 50:50 blend film with and without aspirin is shown in **Figure 5.23**.

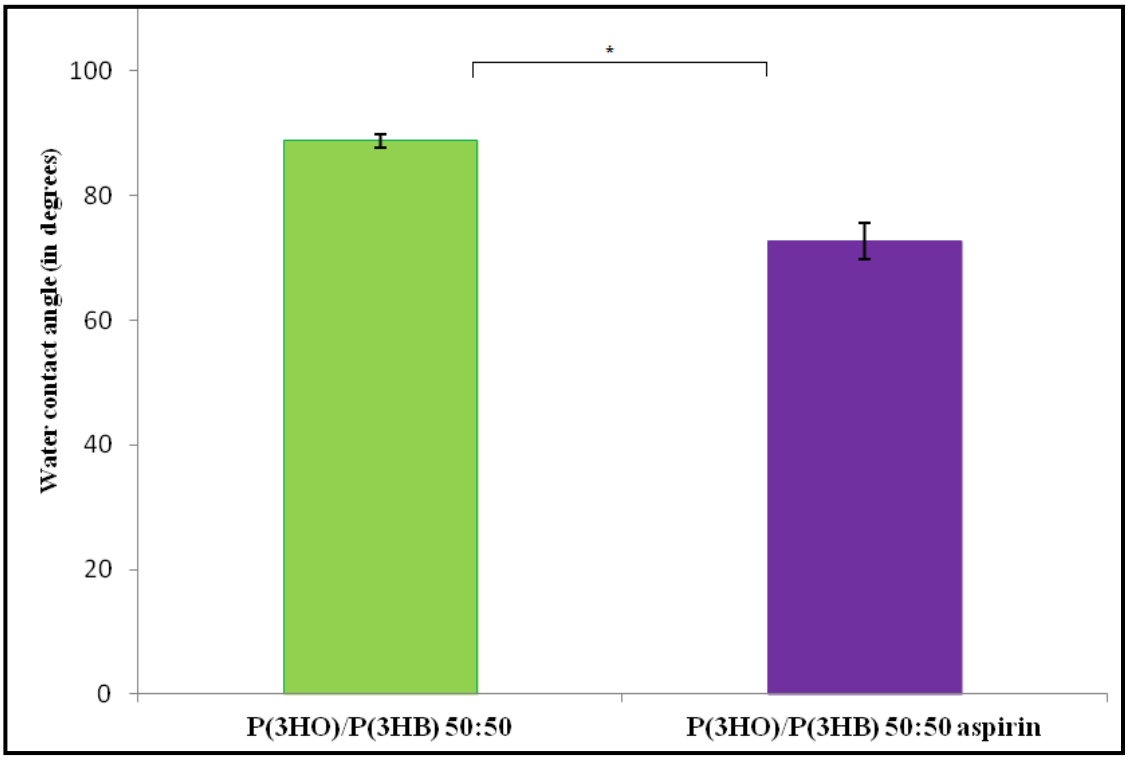

Figure 5.23: Static water contact angle measurements of the P(3HO)/P(3HB) 50:50 blend film samples with and without aspirin (n = 3). The data were compared using t-test and the difference were considered significant when *p<0. 05.

The water contact angle of the P(3HO)/P(3HB) 50:50 blend and the blend films with aspirin were 89.5 ± 0.8 and 72.7 ± 1.3 respectively. The results indicate that the water contact angle of the blend films with aspirin is significantly lower compared to the blend film without aspirin (*p<0. 05). Hence, the blend film containing aspirin was comparatively more hydrophilic in nature.

5.14.13 Protein adsorption Test

Protein adsorption assay was done to quantify the total amount of protein on the P(3HO)/P(3HB) 50:50 blend film samples with and without aspirin as described in **section 2.9.7**. The test was carried out to determine the effect of aspirin loading on the protein adsorption on the P(3HO)/P(3HB) 50:50 blend film. The results of the protein adsorption assays have been summarised in **Figure 5.24**.

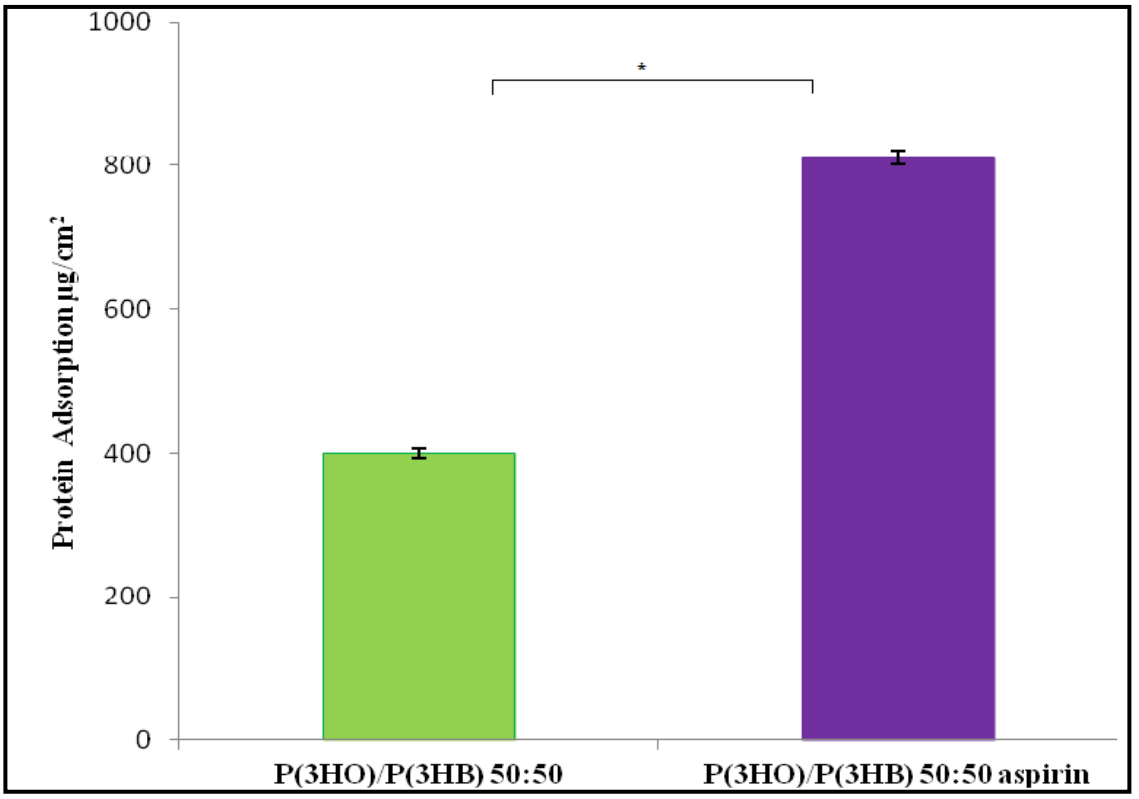

Figure 5.24: Protein adsorption on the P(3HO)/P(3HB) 50:50 blend film samples with and without aspirin (n = 3). The data were compared using t-test and the difference were considered significant when *p<0. 05.

Protein adsorption on the P(3HO)/P(3HB) 50:50 blend film samples with aspirin was 811 ± 1 µg/cm^2 while the protein adsorption on the P(3HO)/P(3HB) 50:50 blend film without aspirin was 400 ± 0.2 µg/cm^2. Hence, there was a significant increase of 102% in the P(3HO)/P(3HB) 50:50 blend films with aspirin compared to the P(3HO)/P(3HB) 50:50 blend film samples without aspirin due to the presence of hydrophilic aspirin within the matrix of the blend film (*p<0. 05).

5.14.14 Indirect cytoxicity testing

Indirect cytotoxicity testing was carried out as described in **section 2.9.8** to study the effect of the degradation products of the P(3HO)/P(3HB) 50:50 blend film samples with and without aspirin on the HMEC-1 cells. The results have been summarised in **Figure 5.25**.

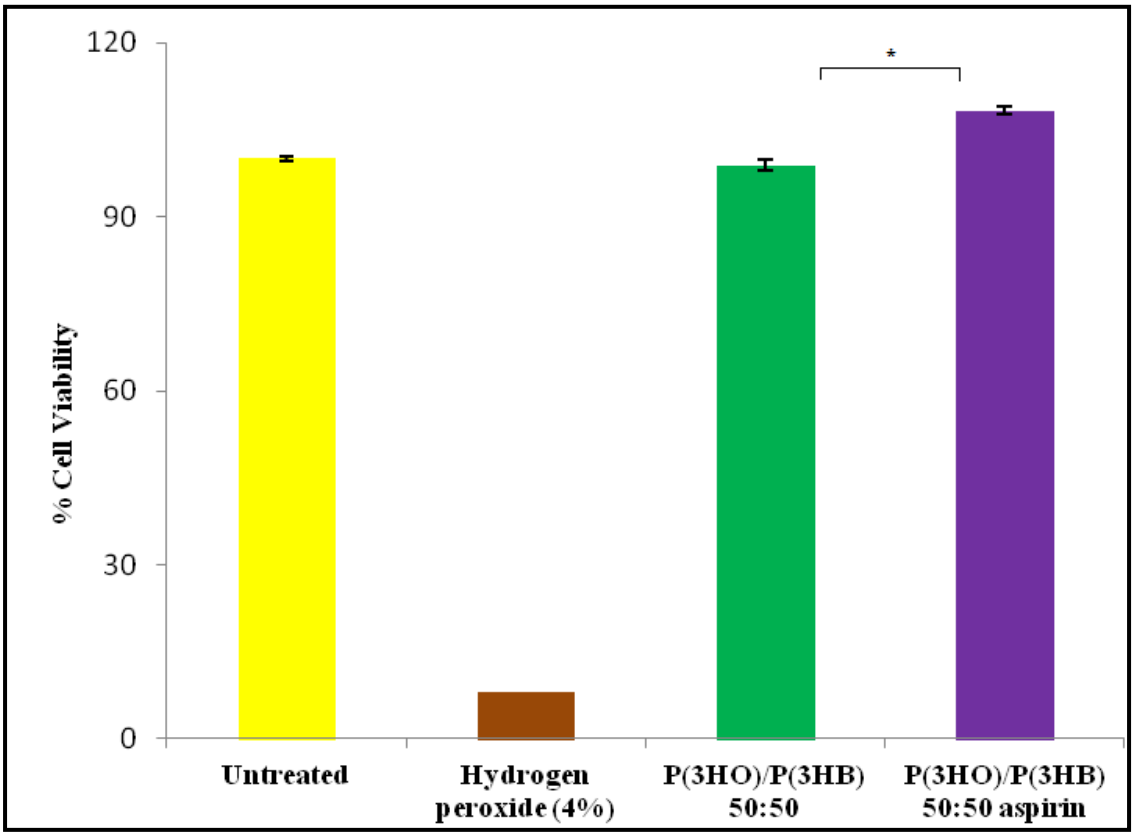

Figure 5.25: Indirect toxicity testing of the P(3HO)/P(3HB) 50:50 blend film samples with and without aspirin(n = 3). Cells grown in DMEM, in the absence of polymer were taken as untreated and the cells grown in the presence of 4% hydrogen peroxide were taken as the positive control. The data were compared using t-test and the difference were considered significant when *p<0. 05.

P(3HO)/P(3HB) 50:50 blend film samples with aspirin showed the highest cell viability percentage of 108.3 ± 0.6% followed by percentage cell viability of 100% when the HMEC-1 cells were grown in DMEM without any polymer. P(3HO)/P(3HB) 50:50 blend film samples without aspirin showed a percentage cell viability of 98.8 ± 1.0% while the lowest percentage cell viability of 8.0 ± 0.0% was observed when the HMEC-1 cells were grown in the presence of 4% hydrogen peroxide, a chemical that is known to induce cell death. These results, therefore, confirmed that no toxic by-products were released from the P(3HO)/P(3HB) 50:50 blend film samples with and without aspirin.

5.14.15 Thermal characterisation

Thermal properties such as the melting temperature (T_m), glass transition temperature (T_g) and the crystallization temperature(T_c) of P(3HO)/P(3HB) 50:50 blend film samples with and without aspirin were studied using DSC as described in **section 2.9.6.** The results have been summarised in **Table 5.4**.

Samples	T_m (°C)	T_g (°C)	T_c (°C)
P(3HO)/P(3HB) 50:50	159.5 ± 0.1	11.9 ± 0.1	98.5 ± 0.3
P(3HO)/P(3HB) 50:50 aspirin	152.4 ± 1.0, 123.1 ± 0.0	10.0 ± 0.1	71.1 ± 9.0

Table 5.4: Thermal properties of the P(3HO)/P(3HB) 50:50 blend film samples with and without aspirin (n = 3).

The melting temperature (T_m), glass transition temperature (T_g) and the crystallization temperature(T_c) of the P(3HO)/P(3HB) 50:50 blend film samples with aspirin were lower compared to the P(3HO)/P(3HB) 50:50 blend film samples without aspirin. A sharp peak at 123.1 °C was observed during the heating of the blend film with aspirin. It is known that the melting temperature of aspirin is 136°C. Hence, a shift in the melting temperature of aspirin to a lower value of 123.1°C was observed.

5.14.16 Dynamic Mechanical Analysis

Mechanical properties of the P(3HO)/P(3HB) 50:50 blend film samples with and without aspirin were carried out as described in **section 2.9.5.** The results of the mechanical analyses are summarised in **Table 5.5**

Samples	Young's Modulus (MPa) E values	Tensile strength (MPa)	Elongation at break (%)
P(3HO)/P(3HB) 50:50	78.50 ± 0.01	7.80 ± 0.03	22.90 ± 0.05
P(3HO)/P(3HB)50:50Aspirin	40.01 ± 0.70	3.03 ± 0.40	46.30 ± 5.10

Table 5.5: Mechanical characterisation of the P(3HO)/P(3HB) 50: 50 blend film samples with and without aspirin using Dynamic Mechanical Analysis (n = 3).

Incorporation of aspirin within the P(3HO)/P(3HB) 50:50 blend film led to a significant change in their mechanical properties. The tensile strength of the P(3HO)/P(3HB) 50:50 blend film samples with aspirin had decreased by 61% compared to the blend film without aspirin while the Young's modulus (a measure of stiffness) of the P(3HO)/P(3HB) 50:50 blend film samples with aspirin was 49% lower compared to the blend film without aspirin. However, there was an increase in the % elongation at break values.

5.15 *In vitro* degradation study in PBS

5.15.1 Water absorption and weight loss

The percentage of water absorbed (%WA) and weight loss (%WL) by the P(3HO)/P(3HB) 50:50 blend film samples with and without aspirin, when incubated in the PBS media for a period of 30 days were measured as described in **section 2.10** and presented in **Figure 5.26** (a)and (b).

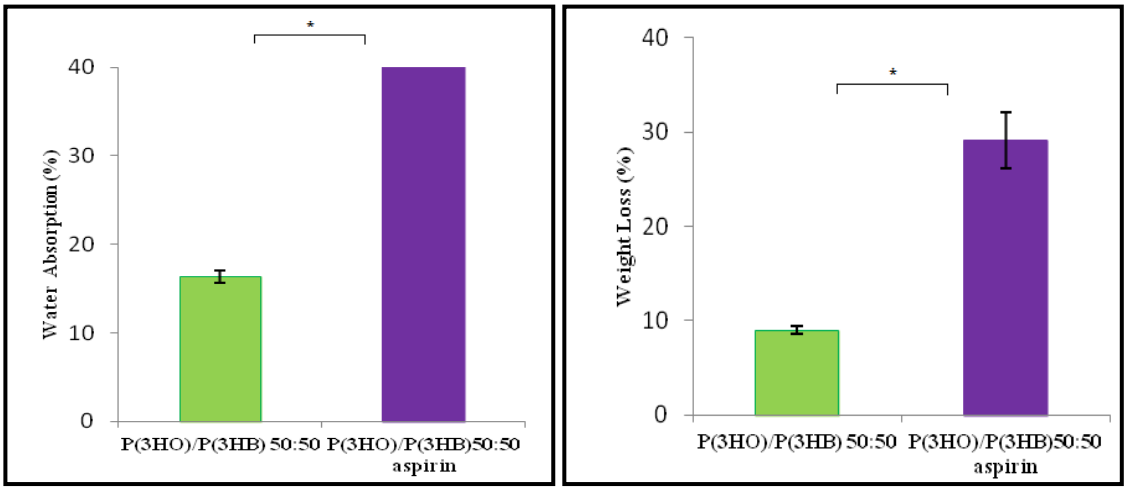

(a) **(b)**

Figure 5.26: (a) Water absorption (%WA) by the P(3HO)/P(3HB) 50:50 blend film samples with and without aspirin in PBS media **(b)** Weight loss (%WL) of the P(3HO)/P(3HB) 50:50 blend film samples with and without aspirin in PBS media (n=3). The data were compared using t-test and the difference were considered significant when *p<0. 05.

Water absorption in the P(3HO)/P(3HB) 50:50 blend film containing aspirin was 44.8±1% which was significantly higher compared to the water absorption in the P(3HO)/P(3HB) 50:50 blend film samples without aspirin which was 16.3±0.7% (*p<0. 05). Similarly, the weight loss in the P(3HO)/P(3HB) 50:50 blend film with aspirin was 29.1±10.4% which was significantly greater compared to the water absorption in the P(3HO)/P(3HB) 50:50 blend film samples without aspirin which was 9.0±0.3% (*p<0. 05).

5.15.2 Scanning Electron microscopy (SEM)

At the end of the degradation study, P(3HO)/P(3HB) 50:50 blend film samples with and without aspirin were rinsed in HPLC grade water . The degrading films were studied using SEM as described in **section 2.9.1.** This was done to study the microstructural properties of the degrading films. SEM images of the degrading films are shown in **Figure 5.27**.

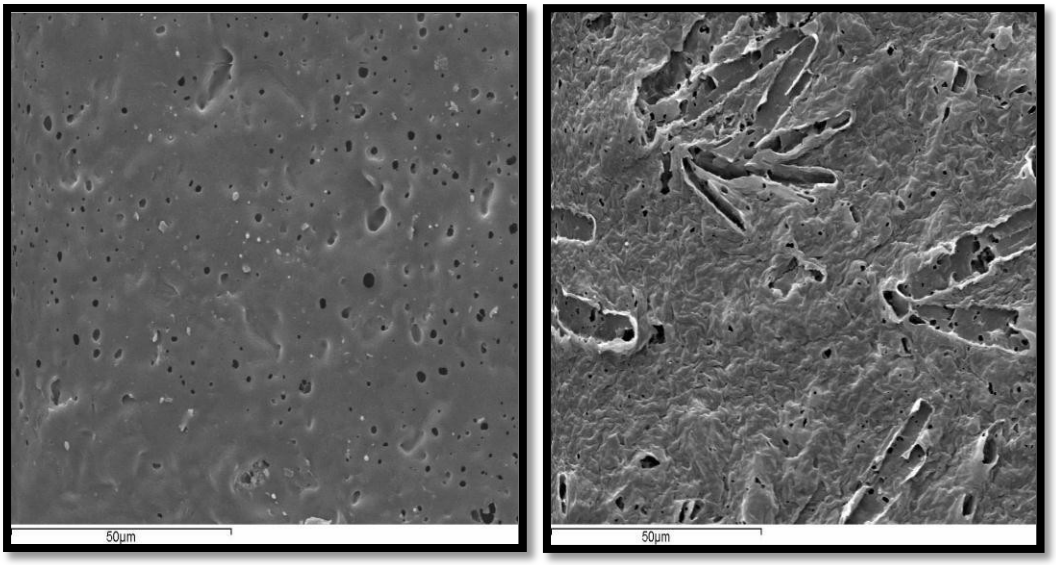

(a) **(b)**

Figure 5.27: SEM images of the (a) P(3HO)/P(3HB) 50:50 blend films and the (b) P(3HO)/P(3HB) 50:50 blend films with aspirin, after being immersed in PBS for one month.

The SEM images thus confirmed that there was an increased degradation of the P(3HO)/P(3HB) 50:50 blend film samples with aspirin as compared to the P(3HO)/P(3HB) 50:50 blend film samples. Surface properties of the P(3HO)/P(3HB) 50:50 blend film samples without aspirin after degradation indicated homogenous surface erosion where a rougher topography was observed. In the P(3HO)/P(3HB) 50:50 blend film samples with aspirin, a rough surface with a visible mass loss was observed suggesting an accelerated surface erosion due to the increased water uptake through the water channels formed by the diffused drug. Also, aspirin being hydrophilic would interact more with water than the blend film, hence enhancing the rate of hydrolytic degradation of the sample.

5.16 *In vitro* drug release studies

The release of aspirin from the P(3HO)/P(3HB) 50:50 blend film containing aspirin was carried out as described in **section 2.11** for a period of 30 days as shown in **Figure 5.28.**

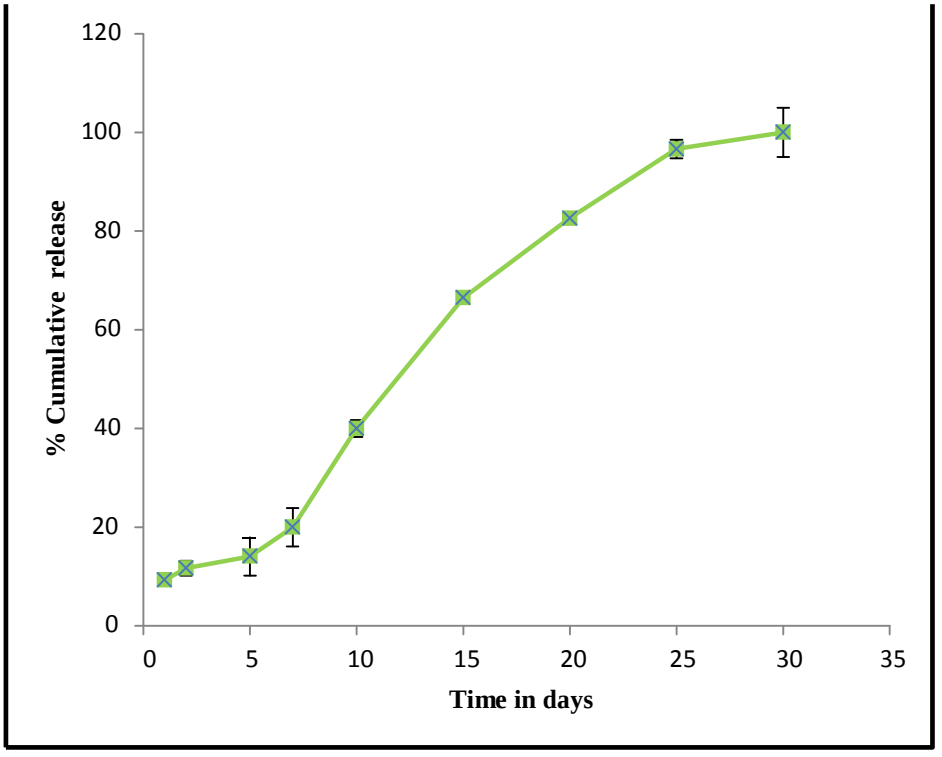

Figure 5.28: *In vitro* release profile of aspirin from P(3HO)/P(3HB) 50:50 blend film for a period of 30 days

Aspirin was released slowly at a constant rate throughout the period of release. There was a an initial burst release of only 9±1.5% on day 1. In this study, cumulative release of 96.6% occurred within a period of 25 days and aspirin was released in two stages. In the first stage, the aspirin was released slowly, this

occurred until the 7th day of release. In the second stage, the rate of drug release increased until the 25th day of release.

It is known that aspirin upon hydrolysis loses its therapeutic activity. Therefore, it is very crucial to release aspirin in its chemically stable form (Aubrey-Medendorp *et al.*, 2008). The amount of chemically stable aspirin in the released samples and in the control aspirin solution in PBS is shown in **Figure 5.29**

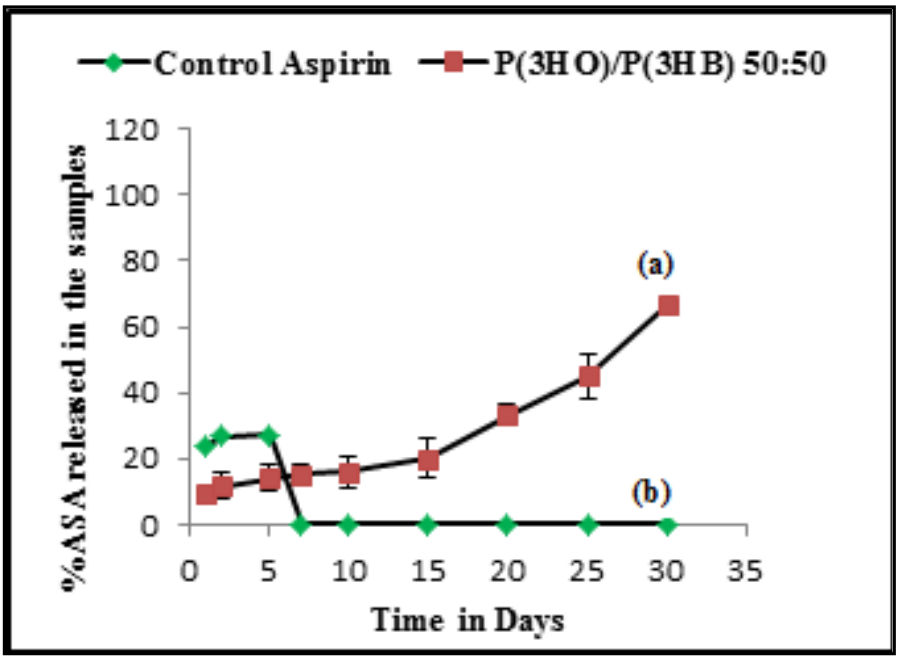

Figure 5.29: *In vitro* release profile of chemically stable aspirinP(3HB) 50:50 blend film(a) and control aspirin standard (b) for a period of 30 days.

The percentage of chemically stable aspirin released from the P(3HO)/P(3HB) 50:50 blend film containing aspirin was significantly higher compared to the control aspirin solution. This was in agreement with the results obtained by Tang and Singh, where the percentage of chemically stable aspirin was much higher in the PLGA based drug delivery compared to the free aspirin (Tang and Singh, 2008). Other studies on the controlled release of aspirin from polymer implants have not confirmed the release of chemically stable aspirin into the media.

Discussion
Part I

In this part of the study, P(3HB) was produced by *B. cereus* SPV using Kannan and Rehacek media, in a batch mode. The polymer produced was characterised using FTIR. The IR spectrum of the polymer showed the presence of two characteristic absorption peaks present in the SCL-PHAs, such as 1719 cm^{-1}, corresponding to the ester carbonyl group and the absorption peak at 1282 cm^{-1}, corresponding to the $-CH_2$ group (Valappil *et al.,* 2007). This confirmed that the polymer produced was a type of SCL-PHA. The polymer was further characterised using GC. This confirmed that the polymer produced by *B. cereus* SPV using Kannan and Rehacek media was P(3HB). P(3HO)/P(3HB) blend films were prepared using solvent casting method.

One of the potential applications of P(3HO)/P(3HB) blends developed in this work would possibly be in the area of biodegradable stents. According to the literature, the most desirable features of an ideal biodegradable stent include biocompatibility, tailorable biodegradability and excellent mechanical properties to provide support to the injured artery to facilitate its healing. Thermal stability is another characteristic which is essential for the processing of these blends. One of the major concerns regarding the implantation of these biodegradable stents within the artery is in stent restenosis. Therefore, a first requirement of the biodegradable polymers to be used in stent development is biocompatibility with the surrounding tissues to prevent any inflammatory response leading to neointimal thickening. Previous works have shown that other biodegradable polymers tested to be used in stent development have demonstrated tissue incompatibility leading to in stent restenosis (Regar *et al*., 2001). Thus, it is very crucial to establish the compatibility of the biomaterial with the endothelial cells which forms the inner lining of the blood vessel. The major advantage of the PHAs over the other biodegradable polymers such as Poly-L-Lactic acid (PLLA),Poly-D-Lactic acid (PDLA), Polylactic-co-glycolic acid (PLGA) is that it yields degradation products which are weaker acids compared to the highly acidic degradation products generated by the other biodegradable polymers (Mani *et al*., 2007; Liu *et al*., 2006; Cordewener *et al*., 2000).

In this study, P(3HO)/P(3HB) blend films of varying compositions were developed using solvent casting method. These blend films were characterised with respect to

their microstructural, mechanical and thermal characteristics. Degradation studies and biocompatibility studies were also carried out on the blend films.

Microstructural studies of these blend films were carried out using SEM. It is known from literature that the polymer blending leads to a change in their microstructural properties as well as their bulk properties (Zhang *et al.*, 1998). SEM images revealed a rough topography for all the blend films compared to the smooth surface of the neat P(3HO) film. However, the morphologies were different for all the blend films. The formation of spherulites on the surface of the blend film containing highest amount of P(3HB) represented a predominantly crystalline matrix with the highly crystalline P(3HB) at the air-polymer interface. A relatively smoother surface was observed for the blend P(3HO)/P(3HB) 20:80 which had the highest concentation of P(3HO) representing a predominantly amorphous matrix. This is possibly due to the presence of P(3HO) on the air-polymer interface which has a low crystallinity (Chen *et* al., 2002; Ha and Cho, 2002; Luo *et al.*, 2009). The surface of the P(3HO)/P(3HB) 50:50 blend film represented an intermediate morphology comprising of both crystalline and amorphous domains. The presence of tiny pores on the surface of this particular blend film could be due to the rapid evaporation of the solvent from the film during solvent casting. The solvent evaporation during the synthesis of the blend film is hugely affected by the arrangement of the amorphous and the crystallline regions of the film (Luo *et al.*, 2009). Kai *et al.*, observed that the surface of the P(3HB)/P(3HB-co-3HHx) blend films with increased concentration of P(3HB) revealed a rough topography with the formation of protusions. This was due to the high crystallization rate of P(3HB) causing it to crystallize simultaneously during solvent evaporation. The blend films with increased concentration of P(3HB-co-HHX) which has a low crystallinity revealed a smoother and continous surface without protusions. This was due to the low crystallization rate of P(3HB-co-3HHx) allowing the molecules to rearrange (Kai *et al.*, 2003).

Another study demonstrated that the surface topography of the hydrophobic poly(vinylidene) fluoride (PVDF) and hydrophilic poly(vinylpyrrolidone)(PVP) blend films varied depending on the concentrazhang

tion of PVP in the blend. With 10% PVP in the blend film, a spherulitic phase was revealed. This spherulitic phase was changed to an intermediate structure containing both spherulitic and plain domains, when the concentration of PVP was

50%. At 80% concentration of PVP, the surface of the blend film appeared to have no characteristic morphology (Chen and Hong, 2002).

Similar results were obtained when acetylated bacterial cellulose crystals were incorporated into P(3HO) matrix. SEM images revealed rougher surface topography of the composite films with the acetylated cellulose microcrystals compared to the neat P(3HO) matrix (Basnett *et al*., 2012). Another study demonstrated that the surface topography of the blend films of P(3HB-co-3HHx) and P(3HB-co-4HB) were much rougher compared to the neat P(3HB-co-4HB) and the P(3HB-co-HHx) films (Luo *et al*., 2009).

Surface roughness of these blend films were measured using AFM. The results were compared with the surface roughness values of the neat P(3HO) film to confirm the increase in the surface roughness of the blend film due to the presence of P(3HB). The increase in the surface roughness with the increase in the P(3HB) concentration is most likely due to the presence of the highly crystalline P(3HB) on the surface of the film. The AFM results were in agreement with the images produced by SEM which depicted the change in the surface topography of the blend films depending on the concentration of P(3HB) within the film. It is known that the arrangement of the amorphous and the crystallline regions at the polymer air interface affects the surface topography of the film (Luo *et al*., 2009). Surface roughness of a biomaterial plays a crucial role in its biocompatibility (Das *et al*., 2007).

Surface roughness has been asociated with the protein adsorption and cell adhesion behaviour. Chen *et al*., demonstrated that there was an increase in the adsorption of fibrinogen on the patterned surface of the poly(dimethylsiloxane) compared to flat, smooth surface (Chen *et al*., 2009). Previous studies have shown that surface roughness enhances the cell adhesion process by changing the surface energy of the biomaterial (Das *et al*., 2007; Lampin *et al*., 1997). Therefore, this increase in the surface roughness of the blend films was considered to be a encouraging result. In future, surface energy of the blend films could be measured to gain a better understanding.

Water contact angle studies were carried out to measure the hydrophilicity/hydrophobicity of the blend films. The results highlighted the role of P(3HB) in increasing the hydrophilicity of the blend films. It is a known fact that P(3HB) in which the monomer is composed of only four carbon atoms is more

hydrophilic in nature compared to P(3HO) in which the monomer is made up of eight carbon atoms (Rai *et al*., 2011). Hence, with the increase in the amount of P(3HB) incorporation, the resulting blends exhibited increased hydrophilicity compared to the neat P(3HO) films. Similar results were observed by Rai *et al.,* when the P(3HO) matrix was modified by the incorporation of hydrophilic n-BG (bioglass). There was a decrease in the water contact angle resulting in increased hydrophilicity of the composite film compared to neat P(3HO)(Rai *et al*., 2011). In another study, there was an increase in the hydrophilicity of the P(3HB)/PVA (Polyvinyl alcohol) blend films compared to the neat P(3HB) films due to the incorporation of hydrophilic PVA. The water contact angle values were very close to the water contact angle values of the hydrophilic PVA (Ikejima *et al*., 1998). Chen *et al*., demonstrated that the presence of hydrophilic PVP within the hydrophobic PVDF dominated film lowered the water contact angle of the resulting PVP/PVDF blend films (Chen and Hong, 2002).

Hydrophilicity is another important characteristic that plays a crucial role in the biocompatibility of the material. According to literature, a low water contact angle which means increased hydrophilicity results in an increase in the surface energy of the material. This results in increased cell adhesion, thereby improving the biocompatibility of the material (Das *et al*., 2007). It has been demonstrated by Bruil *et al*., that the number of cells adhering to the polyurethane surface increased with the increase in the surface hydrophilicity (Bruil *et al*., 1994). Another study demonstrated that there was an increase in the number of Human umbilical vein endothelial cells (HUVECs) adhering to the surface of the self assembled monolayers when there was a decrease in the water contact angle (Arima and Iwata, 2007). Previous studies have also shown that there is a strong correlation between the surface roughness, hydrophilicity and the total protein adsorption (Hao and Lawrence, 2006b).

Another characterisation that was done on these blend films was the total protein adsorption test. According to literature, it is known that the mammalian cells are anchorage dependent. They require a protein rich surface for their attachment and elongation. When a biological implant is placed within the body, water and a layer of adsorbed protein is formed on the surface of the biomaterial depending upon its

surface properties.. This is considered to be the initiation of the healing process (Kurella and Dahotre, 2005). The cells then adhere to these protein rich surfaces. Therefore, protein adsorption plays a key role in evaluating the biocompatibilty of the biomaterial for tissue engineering applications (Rai *et al*., 2011). In this study, there was an increase in the total protein adsorption on the blend films compared to the neat P(3HO) film. This increase in the protein adsorption in the P(3HO)/P(3HB) blends is most likely due to the incorporation of P(3HB) within the P(3HO) matrix which in turn has increased the surface roughness and hydrophilicity, hence changing the surface properties of the blend films (Hao and Lawrence, 2006a). Misra *et al*., demonstrated an increase in the total protein adsorption on the P(3HB)/Bioglass™ composite films compared to the neat P(3HB) film. The authors stated that this increase in the protein adsorption was due to the change in the surface topography and surface wettability of the composite films owing to the presence of hydrophilic bioglass within the P(3HB) matrix (Misra *et al*., 2010). In another study, there was an increase in the adsorption of fibrinogen and fibronectin adsorption on the patterned poly(dimethylsiloxane) film compared to the smooth, flat surface. This increase was due to the increase in the surface roughness of the patterned PDMS film (Chen *et al*., 2009). Hao and Lawrence in 2006, observed a strong corelation between surface roughness, surface hydrophilicity and protein adsorption on the material. They stated that surface roughness and hydrophilicity were predominant factors that dictated the total protein adsorption (Hao and Lawrence, 2006a). This increase in the protein adsorption in the blend films was an encouraging result, bearing in mind their potential medical applications. Another characterisation done on these blend films was the indirect cytoxicity assay. This was done to investigate the effect of the substances released from the blend films on the growth of Human dermal microvascular endothelial cells (HMEC-1) by MTT assay. It is a known fact that the endothelial cells form the lining of the blood vessel wall and therefore play a significant role in retaining the vascular homeostasis. During stent placement, the injury caused to the vessel wall or the incompatibility of the stent material with the blood components could lead to the development of neointimal hyperplasia causing stent restenosis. Therefore, accelerating the endothelialisation of the stent could speed up the natural healing process, thereby avoiding in stent restenosis (Ong *et al*., 2005). The assessment proved that no cytotoxic degradation products were

released from the blend as well as neat P(3HO) films, however % cell viability was higher for the blend films compared to the neat P(3HO) films. According to literature, P(3HB) and its derivatives are present in human blood and tissues as endogenous metabolites. They are non-toxic in nature (Volova and Volova, 2004). Also, P(3HB) used in this study was produced by *Bacillus cereus SPV*, a Gram positive bacteria which is free of lipopolysaccharides (LPS), a known endotoxin found in the Gram negative bacteria. However, the P(3HO) that was used in the synthesis of the blend films were produced by *Pseudomonas mendocina*, a Gram negative bacteria, which is known to have lipopolysaccharide (Rai *et al*., 2011). P(3HO) used in this study was thoroughly purified, however it might have contained traces of LPS leading to relatively lower cell viability. One of the major requirements of a successful stent implantation is its rapid endothelialisation to prevent inflammatory response. This aspect could be verified further using surface cell proliferation and animal studies.

Thermal characterisation of the blend films were carried out to investigate the effect of P(3HB) on the thermal stability of the blend films. There was an increase in the glass transition temperature (T_g) of the blend films with the increase in the amount of P(3HB) compared to the T_g of neat P(3HO) film. The increase in the T_g of the blend films with increasing P(3HB) content could be due to the presence of the crystalline P(3HB) within the P(3HO) matrix, hence restricting the mobility of the amorphous phase comprising mainly of P(3HO) (Qiu *et al*., 2005). As summarised in **Table 5.1**, only one T_g values was obtained for all the blends indicating that the blends were miscible (Kai *et al.*, 2003; Luo *et al*., 2009). Luo *et al*., demonstrated the increase in the T_g of the blend films of P(3HB-co-HHx) and P(3HB-co-4HB) compared to the T_g of the neat P(3HB-co-4HB). The authors also stated that only one T_g value was obtained indicating complete miscibility of the P(3HB-co-HHx) and P(3HB-co-4HB) blends (Luo *et al*., 2009). Similar results were obtained in another study, where there was an increase in the T_g value of polylactic acid (PLA) and polyurethane (PU) blend films compared to the T_g value of PU films with a low crystallinity compared to PLA (Li and Shimizu, 2007).

Similar trends were observed in the melting temperature (T_m) of the blend films. There was an increase in the T_m of the blend films with the increase in the amount of P(3HB) in the blend film compared to the neat P(3HO) film. The results indicated

that there was increase in the thermal stability of the blend films. This is due to the increase in the crystallinity of the blend film owing to the presence of the crystalline P(3HB) polymer. According to literature, the increase in melting temperature occurs when the mobility of the amorphous region is restricted due to presence of composites or fillers of crystalline nature (Qiu *et al*., 2005). The crystallization temperature (T_c) also increased with increasing P(3HB) content in the film. The crystallization of the polymer occurred during the cooling run from 200°C to -50°C. The blend films with the higher concentration of P(3HB) crystallized rapidly at a higher temperature during the cooling whereas the crystallization occurred at a slightly lower temperature in the blend films with increasing amount of P(3HO. This is possibly due to the positive effect of the presence of P(3HB) which accelerates the nucleation process of P(3HO) spherulites (Qiu *et al*., 2005). Similar results were obtained where there was a decrease in the crystallization rate of the P(3HB)/P(3HB-co-3HHx) blend films with the increase in the concentration of P(3HB-co-3HHx) which has a low crystallinity compared to the highly crystalline P(3HB) (Kai *et al*., 2003).

Mechanical characterisation of these blend films were carried out to understand the effect on the P(3HB) on the mechanical properties of the blend films. The Young's Modulus values (E values) which is the measure of the stiffness increased with the increase in the concentration of P(3HB) in the blend film. This increase in stiffness of the blends with increased P(3HB) content is most likely due to the increase in the crystallinity of the blend films with increased incorporation of crystalline P(3HB). From literature, it has been established that the increase in crystallinity enhances the stiffness of the material whereas their ductility is highly reduced (Rai *et al*., 2011). These DMA results were in agreement with the thermal characterisation results, demonstrating an increase in the crystallinity of the blend films. It has also been shown in our previous studies that the presence of bacterial cellulose microcrystals in the P(3HO) matrix increased the Young's modulus of the P(3HO)/bacterial cellulose composite film compared to the neat P(3HO). This was due to the presence of highly crystalline cellulose microcrystals within the P(3HO) matrix (Basnett *et al*., 2012). Another study demonstrated similar results where there was an increase in the E values of polylactic acid (PLA)/MCL-PHA blend films with an increase in the concentration of crystalline PLA within the film (Martelli *et al*., 2012).

The tensile strength of all blend films also increased compared to the neat P(3HO) film. However, the tensile strength of the P(3HO)/P(3HB) 20:80 blend film which has the highest concentration of the P(3HB) content was slightly lower compared to the P(3HO)/P(3HB) 50:50 blend film. Similar results were observed in our previous study when P(3HO) films were reinforced using bacterial cellulose. A low value of tensile strength was measured for the P(3HO) film containing the highest concentration of bacterial cellulose microcrystals. This could be due to the increase in the stiffness causing P(3HO)/P(3HB) 20:80 blend film to be brittle (Basnett *et al*., 2012). Kai *et al*., observed higher tensile strength values with higher concentration of P(3HB) within the P(3HB)/P(3HB-co-3HHx) blends. This increase in tensile strength was due to the higher crystallinity of P(3HB) compared to P(3HB-co-3HHx) (Kai *et al*., 2003). Li and Shimizu, 2007 also demonstrated high values of Young's modulus and tensile strength vlaues for PLA/PU blends observed with high concentrations of crystalline PLA within the film (Li and Shimizu, 2007).

The elongation at break values of the blend films were lower compared to the neat P(3HO) film. This is possibly due to the lack of adhesion of the two phases, i.e., P(3HO) and P(3HB) in certain regions form weak points in the films causing them to be brittle in nature. Similar results were obtained in a study where there was a decrease in the elongation at break values of the PLA/PU blends with the increase in the PLA concentration within the film. An investigation was carried out to understand the mechanism causing a change in the elongation at break values of the blend films. They observed the tensile tested specimen under the SEM to study the morphology of different necking regions. They concluded that the PLA/PU blend films were a partially miscible system bearing two different morphologies. This was in disagreement with their DSC results that showed only one T_g value for all the blends indicating complete miscibility (Li and Shimizu, 2007). However, the Young's modulus and tensile strength values need to be be further improved by reinforcing these blend films with fibres or fillers.

The standard reference for the mechanical properties desired for a stent development is SS316L stainless steel. It is the most commonly used material for the development of vascular stents. It has a tensile strength, Young's modulus value and % elongation at break value of 490 MPa, 193 GPa and 40% respectively. It has a radial strength value of 135 KPa. Radial strength is key in determining the success of the stent after its implantation within the body. In order to meet the clinical

requirements, the radial strength value should be in a range of 80-120 KPa (Feng *et al*., 2011). With significant improvement in mechanical properties, these novel blends could be used for the development of biodegradable stents. Feng *et al*.., demonstrated a significant increase in the radial strength of the poly-p-dioxane stent with a novel sliding lock architecture compared to the poly-p-dioxane stent with a basic net tube structure. They concluded that the stent architecture also plays an important role in improving the mechanical properties of the stents (Feng *et al*., 2011). These blend films developed in this study could also be used as scaffolds for tissue engineering applications.

Another important characterisation that was carried out on these blend films was the *in vitro* degradation study. Biodegradability is considered to be a significant feature of a biomaterial with potential medical application (Li and Shimizu, 2007). Previous studies have shown that biodegradability of a polymer blend system is dependent on factors such as the surface blend composition, phase structure or the miscibility of the blend components and the blend composition (Ikejima *et al*., 1998).

The blend film P(3HO)/P(3HB) 20:80 had the highest percentage of water absorption and highest percentage of weight loss in both DMEM and PBS media. It is known that P(3HB) is known to be more hydrophilic than P(3HO) due to the presence of a relatively shorter hydrophobic side chain, therefore, this was an expected result. Previous studies have also shown that there is an association between water uptake and progressive degradation and hence weight loss of the samples. Hydrophilicity of the biomaterial plays a very important role in the hydrolytic degradation of the biodegradable polymer (Renard *et* al., 2004). During this study, the film samples were incubated in enzyme free media and hence, degradation in the films would have occurred solely due to hydrolysis. Hydrolytic degradation would have occured in two stages. Initially, the water molecules would have begun to cleave the amorphous part of the polymer followed by the degradation of crystalline part of the polymer (Volova and Volova, 2004). The presence of P(3HB) on the surface of the blend films would have made the blend films more hydrophilic compared to the hydrophobic surface of the P(3HO) film. (Ikejima *et al*., 1998). This would have lead to an increased water uptake resulting in an increase in hydrolytic degradation.

Therefore, surface composition of the blend films plays a crucial role during the initial stages of degradation. It is a known fact that the degradation of the PHAs occurs via surface erosion as opposed to the bulk degradation observed in the case of PLA. This would lead to highly controlled degradation, maintaining the core structure, a highly desirable property in an ideal biodegradable stent. These blend films could also be used as the tissue engineering scaffolds. Due to their mechanical properties, especially their elastomeric nature, tailorable degradation property and biocompatibility, these blend materials could also be used for soft tissue engineering. Depending on the desired application, the degradation rate of the blend can be tailored and controlled by modifying the relative composition of the two types of PHAs (Rathbone *et al.*, 2010). Another potential application of these blend films could also be in the area of drug delivery. Due to the surface erosion degradation mechanism, the controlled release of drugs can be achieved (Gopferich, 1996).

In conclusion, this study led to the development of P(3HO)/P(3HB) blends with increased Young's modulus, tensile strength, thermal stability and tailorable biodegradability as compared to neat P(3HO) film. The results of the cytotoxicity assessment have demonstrated that these blend films are not toxic to the HMEC-1 cells. With further improvement in the tensile strength, these novel blends could also be used for the development of biodegradable stents.

Part II

Endothelial cells act as an interface between the blood and the vessel wall. In order to avoid a vascular dysfunction, it is imperative to maintain a healthy endothelial layer. In recent times, studies have been carried out to understand the function and the characteristics of the endothelial cells. The findings have suggested that the endothelial cells alter their morphology and function depending on their alignment (Uttayarat *et al.*, 2008; Anderson and Hinds, 2011). However, these studies were carried out in the presence of the blood flow. One of the techniques employed in understanding the behaviour of endothelial cells under static conditions is the micropatterning technique. Using this technique, micro topographical features are created on the surface of the substrate on which the cells are cultured under static

conditions. These topographical cues allow cells to adhere and proliferate in an aligned fashion (Thery, 2010). It is a known fact that surface topography determines the biocompatibility of a biomaterial by governing various important processes and properties such as protein adsorption, wettability, cell adhesion, proliferation and migration (Duncan *et al*., 2007).

In this study, P(3HO)/P(3HB) 50:50 blend films were surface micropatterned using the laser micropatterning technique to allow the cells to grow in an aligned manner or give a definite orientation to the cells. Bearing in mind the potential application of these micropatterned blend films as platform materials for the development of a biodegradable stent , their biocompatibilty with the endothelial cells is crucial. Previous studies have shown that the formation of an endothelial cell monolayer on the surface of artificial conduits have resulted in a decreased thrombus formation and intimal thickening (Kidd *et al*., 2003). Some of the biomaterials have been deemed incompatible and toxic due to their inability to integrate with the surrounding tissues. Therefore, it is extremely important for a biomaterial to be able to encourage the adhesion and proliferation of specific cells (Hallab *et al*., 2001)

As mentioned earlier, surface topography determines the biocompatibility of a biomaterial (Duncan *et al*., 2007). Microstructural studies of the micropatterned blend film samples were studied using SEM. The SEM images confirmed that microgrooves had been successfully created using the laser micropatterning technique. The surface roughness measurements of the micropatterned blend films were carried out using AFM. This was done to study the effect of micropatterning on the surface roughness of the blend films. Hence, there was a drastic increase in the surface roughness of the micropatterned surface due to the micropatterning. Increased surface roughness is an inevitable outcome of most surface micropatterning techniques. However, the extent depends on the type of the micropatterning technique and the material (Gogolides *et al*., 2006). As mentioned in part I, surface roughness is known to play a significant role in cell adhesion and proliferation, providing cells with adhesion points for migration (Hao and Lawrence, 2006a). Previous studies have shown that the cells prefer to attach to the rough surface of the implants compared to the smooth surface. Therefore, several investigations have been carried out on the micropatterning of the implants for better cell attachment (Hallab *et al*., 2001).

Water contact angle studies were carried out on the micropatterned blend films. Surface micropatterning of the blend films by laser micropatterning lowered their water contact angle, making them more hydrophilic compared to the plain blend film. In a similar experiment conducted by Yu *et al*., a polycarbonate (PC) film was surface micropatterned using Laser Interference Lithography (LIL) to study the *in vitro* cell response. They observed that surface micropatterning led to a decrease in the water contact angle by 10 degrees compared to the unfabricated PC film. They also found that this decrease in the water contact angle was advantageous for cell adhesion (Yu *et al*., 2005). In another experiment conducted by Li *et al*., a polyethylene terephthalate film was micropatterned using laser ablation. They studied the effect of the micropatterning on the equilibrium water contact angles. They found that the water contact angle of the laser modified surface was lower compared to the unmodified surface (Li *et al*., 2003). This decrease in the water contact angle of the micropatterned blend film could be due to the increased surface roughness previously seen in this study. Previous studies have shown that hydrophilic surfaces are favourable for cell attachment and proliferation (Li *et al*., 2003). Therefore, an increase in the hydrophilicity of the biomaterial is a desirable property

Another characterisation that was done on the fabricated blend film samples was the protein adsorption test. In this study, there was an increase in the total protein adsorption in the micropatterned blend film compared to the plain P(3HO)/P(3HB) 50:50 blend film. Therefore, this increase in the total protein adsorption was most likely due to the increase in the hydrophilicity and the increase in the surface roughness. The results in this study was in agreement with the results of previous studies stating that surface roughness, hydrophilicity and total protein adsorption are interrelated (Das *et al*., 2007). In a study carried out by Sato and Murahara in 2012, a poly(tetrafluroethylene)(PTFE) material was modified using excimer laser irradiation. They measured the total protein adsorption on the modified samples and compared it to the total protein adsorbed on to the unmodified samples. They stated that there was a marked increase in protein adsorption on the modified samples compared to the unmodified samples. They made an important observation that the higher amount of protein was attached to the modified samples with a lower water contact angle. This demonstrated that an increase in

hydrophilicity resulted in an increase in protein adsorption (Sato and Murahara, 2012). Several studies have been carried out in the past to surface fabricate various materials to enhance protein adsorption to improve the biocompatibility of the material (Hao and Lawrence, 2004).

Mechanical characterisation of the fabricated blend film samples was carried out to evaluate the effect of the surface modification on bulk properties such as Young's modulus, tensile strength and elongation at break. There was a decrease in the Young's modulus and the tensile strength values of the micropatterned blend films. However, there was an increase in the elongation at break values of the micropatterned blend films compared to the plain blend films. These values were statistically tested using t-test and the difference were considered significant when the $*p<0.05$. The decrease in the Young's modulus values of the micropatterned blend films were considered to be statistically significant. However, the decrease in the tensile strength and the increase in the % elongation at break value were considered to be statistically insignificant. This demonstrated that the bulk properties of the blend film remained intact while the surface characterisations have shown that there were drastic changes in the surface properties of the fabricated blend film. One of the major advantages of using laser micropatterning technique over the other chemical modification methods is that it does not affect the bulk properties of the biomaterial (Li *et al*., 2003*).* This was confirmed in this study where there was very little change in the mechanical properties post laser micropatterning.

Cell culture studies were carried out to determine the effect of the surface micropatterning on the adhesion and the proliferation of the HMEC-1 cells. There was an increased cell adhesion on the micropatterned blend film samples compared to the plain blend film samples. Apart from the obvious reason, i.e. surface micropatterning, this increased cell adhesion could also be due to factors such as increased hydrophilicity and protein adsorption. Hallab *et al*., demonstrated that the increased surface roughness due to the laser modification resulted in an increase in number of the 3T3 MC fibroblast cells adhering to the polymer surface (Hallab *et al*., 2001).

At the end of the 7th day, there was 47% increase in the percentage cell proliferation on the laser micropatterned surface compared to the plain blend films. In an experiment conducted by Dadsetan *et al*., in 2001, polyethylene terephthalate (PET) films were modified using laser irradiation. Microstructures of various dimensions were created on the surface of these PET films. In order to study the effect of surface micropatterning on cell response, they cultured L929 fibroblast cells on these PET films. They demonstrated increased cell proliferation on these micropatterned PET films. They concluded that this increase in cell proliferation was due to the change in surface topography and increased hydrophilicity (Dadsetan *et al*., 2001). Rebollar *et al*., conducted a study where a polystyrene foil was modified using laser irradiation. The surface topography of the polystyrene foils were modified and Human Embryonic Cells (HEK-293), Chinese hamster ovary (CHO-K1) cells and skeletal myoblasts were grown on this modified surface. They observed an increase in the cell attachment and the proliferation of all the cell types on the modified polystyrene foils compared to the untreated foils (Rebollar *et al*., 2008). Hence, the finding reported in this study is in agreement with the results obtained by several researchers in the past.

SEM studies were carried out to observe the alignment and morphology of the HMEC-1 cells on the micropatterned blend films compared to the plain blend films. It is known from the literature that the alignment and the morphology of the endothelial cells is determined by the blood flow. It is also known that aligned and elongated endothelial cells exhibit healthy characteristics. Several attempts have been made to obtain an aligned growth of endothelial cells with an elongated morphology under static conditions (Gray *et al*., 2002). The micropatterning technique has been used widely in recent times due to its ease of handling, time efficiency and its ability to produce various micropatterns with precision. They

have been used for surface fabrication of vascular grafts, stents and tissue engineering scaffolds (Thery, 2010; Anderson and Hinds, 2011).

When the cells are grown on the surface with grooves, they tend to align themselves along the direction of the groove and change their morphology. However, the alignment of the cells depends on the dimensions such as the width and the depth of the grooves present on the surface (Wilkinson *et al*., 2002). During cell migration on the flat surface, the cytoskeleton of the cells migrate from near the nucleus towards the periphery of the cells in different direction whereas on the micropatterned surface, the cell microfilaments responsible for the cell movement bundle together and migrate along the direction of the groove (Wilkinson *et al*., 2002). Therefore, cells cultured on the micropatterned surfaces seem to grow in an aligned fashion compared to the cells on the flat, smooth surface.

Several studies have been conducted to demonstrate the effect of micropatterning on the alignment and the morphology of the endothelial cells. In one of the studies, endothelial cells were cultured on silicon platforms patterned with microchannels of 25-220 μm width. The authors observed increased alignment of the endothelial cells on the micropatterned silicon platform compared to the unmodified surface. They also observed that the endothelial cells displayed an elongated morphology. They stated that the endothelial cells became increasingly elongated with decrease in the size of the microchannels on the surface of the silicon platform (Gray *et al*., 2002).

Li *et al.,* 2001 demonstrated that 80% of the cells seeded on the surface modified PET films were aligned in a definite direction. They made an observation that the width of the microgroove played a significant role in the orientation of the cells. They observed that the laser micropatterned surface affected the focal adhesion points as well as the cell migration (Li *et al.,* 2001). In a study conducted by Uttayarat *et al*., microgrooves of various dimensions were created on the surface of the silicon wafers. Human aortic endothelial cells (HAEC) were cultured on these surface modified silicon wafers in the absence of the flow. They observed that the 3D microgrooves on the surface provided an important stimulus that guided the cells to migrate in a definite direction. 90% of the HAEC cells were aligned parallel to the microgrooves. They made an important observation that the 3D microgrooves provided additional anchorage sites compared to the unmodified

surfaces, thereby increasing the cell adhesion followed by aligned growth (Uttayarat *et al*., 2008).

In another study, bovine aortic endothelial cells were cultured on a collagen strip micropatterned with the creation of parallel grooves of three different widths such as 15, 30 and 60 μm. The authors observed that the cell alignment and elongation was higher on the micropatterned surface of all widths compared to the unmodified surface. However, the cell alignment and the elongation were highest in the grooves with the smallest width (15 μm). The authors stated that this was due to the smaller area available for the endothelial cells to spread causing the morphology of the cells to become elongated and to migrate along the direction of the groove (Li *et al*., 2001).

The results in this part of the study were in agreement with the findings of the previous studies. In conclusion, surface micropatterning of the P(3HO)/P(3HB) 50:50 blend film using laser, increased their surface roughness, hydrophilicity and total protein adsorption. Mechanical characterisation confirmed that the bulk properties of the blend films were not drastically affected by surface micropatterning. Cell culture studies showed that there was increased cell adhesion and cell proliferation on the fabricated blend films compared to the unfabricated blend films. SEM imaging showed that the cells had proliferated in an aligned manner.

Part III

One of the most desirable characteristics of an ideal stent is its ability to deliver drugs at the site of injury to prevent in stent restenosis (Cantor *et al*., 2000). In this study, P(3HO)/P(3HB) 50:50 blend film were investigated for their ability to deliver aspirin in a controlled manner. The P(3HO)/P(3HB) 50:50 blend film containing aspirin was successfully prepared by using the solvent casting method.

The effect of aspirin loading on the surface, mechanical, thermal and degradation properties of these blend films were studied. *In vitro* drug release studies were carried out. The FTIR spectrum confirmed the presence of the aspirin within the P(3HO) matrix.

Detailed surface analysis was carried out to investigate the effect of drug loading on the surface topography of the blend films using SEM. A uniform surface of the blend film with aspirin was revealed compared to the rough surface of the blend film without aspirin using SEM. The results indicated that aspirin was homogenously dispersed within the matrix of the blend film.

Similar observation was made in a study where the surface of the aspirin loaded polyesterurethane network appeared to have a uniform surface. The authors attributed this to the homogenous dispersion of aspirin within the network in an amorphous form (Zhang *et al.*, 2010). Pang *et al.*, demonstrated a correlation between the % drug loading and the surface topography. The authors observed the formation of voids on the surface of the films with higher loading of ibuprofen compared to lower drug loading concentrations (Pang *et al.*, 2011). Similar observations were made where theophylline and salicylic acid crystals were visible on the surface of the chitosan films at a drug loading higher than 10% and 30% drug loading respectively. The authors concluded that this was due to the crystallization of the theophylline crystals during the film processing (Puttipipatkhachorn *et al.*, 2001). At 15% aspirin loading, no aspirin crystals were visible on the surface of the blend films. In future, different drug loading concentrations could be studied to have an indepth understanding of the effect of drug loading on the surface topography.

Surface roughness of these blend films with aspirin as well as the blend film samples without aspirin were measured using the AFM. AFM measurements were in agreement with the SEM results. This decrease in the surface roughness of the blend films with aspirin could be due to the homogenous dispersion of the aspirin within the matrix of the blend film. The absence of the aspirin crystals on the surface of the blend film also revealed that the aspirin was present in an amorphous form (Zhang *et al.*, 2010).

In order to evaluate the effect of the aspirin loading on the wettability properties of the blend film, water contact angle studies were carried out. This decrease in the water contact angle indicated that the presence of aspirin within the blend film had

increased its hydrophilic properties compared to the blend film without aspirin. It is a known fact that aspirin is a hydrophilic drug and has a water solubility of 3 mg/ml (Aubrey-Medendorp *et al*., 2008). It is known that wettability is generally related to the surface roughness of the biomaterial (Das *et al*., 2007). However, AFM results have shown that there was a decrease in the surface roughness of the blend film with aspirin. Therefore, in this particular study, the increase in the hydrophilicity of the blend film could be solely attributed to the presence of the hydrophilic aspirin within the blend film. Similar observations were made by Paul and Sharma in 1997, where there was an increase in the hydrophilicity of the aspirin loaded PVA membranes compared to the unloaded PVA membrane. A decrease in the water contact angle with the increase in the concentration of aspirin within the membrane was observed. This increase in the hydrophilicity was attributed to the presence of hydrophilic aspirin within the PVA membranes (Paul and Sharma, 1997). A similar effect was also observed when hydrophilic Bioglass™ particles were incorporated within the P(3HB) composite films (Misra *et al*., 2008).

The total protein adsorption test was also carried out on the blend film with aspirin to assess the effect of the presence of the aspirin within the blend film. As mentioned previously, protein adsorption is generally found to be higher on the hydrophilic surface (Hao and Lawrence, 2006b). This was in agreement with the results of this study. The increased protein adsorption on the blend film with aspirin compared to the blend film without aspirin is most likely due to the increase in the hydrophilicity owing to the presence of aspirin within the matrix. The model protein used in this study was Bovine serum albumin (BSA). Jeyachandran *et al*., demonstrated that 95% of Bovine BSA was adsorbed on the hydrophilic surface while the hydrophobic surface was saturated at 50%. The authors observed that the molecular confirmation and the adsorption strength of BSA varied on both the surfaces (Jeyachandran *et al*., 2010). This was in agreement with the results observed in this study. Another study demonstrated that there was an increase in the total protein adsorption on the gentamicin loaded polyvinyl alcohol/dextran hydrogel compared to the unloaded gel. The authors attributed this increase in the protein adsorption to the presence of the hydrophilic drug gentamicin (Hwang *et al.,* 2010). Similar observations were made where there was an increase in the total protein adsorption on the tetracyline loaded microsphere films compared to the unloaded film. This was due to the increase in the

hydrophilicity of the tetracycline loaded film compared to the unloaded film (Francis *et al*., 2010). This increase in the protein adsorption was considered to be an encouraging result.

Another characterisation that was done on these blend films with aspirin was the indirect cytotoxicity testing. This was carried out to determine the effect of the aspirin on the growth of HMEC-1 cells. Considering the potential application of these P(3HO)/P(3HB) 50:50 blend films with aspirin as the base material for the drug eluting stent development, it is very crucial that they demonstrate compatibility with the HMEC-1 cells. There was an increase in the % cell viability with the blend films with aspirin compared to the blend without aspirin. Podhaisky *et al*., conducted an experiment to study the effect of aspirin Bovine pulmonary artery endothelial cells (CCL 209) under oxidative stress conditions. They demonstrated that the presence of aspirin at an anti-thrombotic concentration helped maintain the endothelial integrity and preserved their function as compared to the endothelial cells incubated without the aspirin (Podhaisky *et al*., 1997). This finding was supported by another study that confirmed the anti-oxidative properties of aspirin on vascular tissues (Wu *et al*., 2002). Similar findings were reported where, aspirin at a therapeutic concentration prevented endothelial cells senescence or ageing by inducing the production of nitric oxide and by reducing the oxidative stress (Bode-Boger *et al*., 2005). This could be the reason for the increased viability of the HMEC-1 cells in the presence of blend films with aspirin. The results of this study were considered to be very encouraging and established the potential of these blend films with aspirin in the area of drug eluting biodegradable stents.

Thermal characterisation of these blend films with aspirin were carried out in order to investigate the effect of aspirin loading on the thermal properties of the blend films. There was a decrease in the glass transition temperature (T_g) of the blend films with aspirin compared to the blend films without aspirin. This result indicated that there was an increased mobility within the amorphous region of the polymer blend with aspirin compared to the blend film without aspirin causing a decrease in the T_g (Siepmann and Gopferich, 2001). Also, the decrease in the T_m of the blend film with aspirin confirmed the decrease in the overall crystallinity. This indicated that the aspirin was incorporated within the crystalline region of the polymer blend causing disruption within the crystalline arrangement, leading to

the decrease in T_m values. Renard *et al.*, observed a decrease in the melting temperature of the ibuprofen loaded within the PLGA film. The authors attributed this to the decrease in the crystallinity of ibuprofen (Renard *et al.*, 2004). Zhang *et al.*, observed the absence of the melting peak of aspirin when loaded within the polyesterurethane network. The authors concluded that the absence of the melting peak was due to the presence of the aspirin within the network in an amorphous form (Zhang *et al.*, 2010). In this study, heating scan from -50°C to 200°C , the polymer blend were subjected to the cooling scan from 200°C to -50°C during which the polymer blend crystallized. The P(3HO)/P(3HB) 50:50 blend film samples without aspirin crystallized at a lower temperature whereas the blend film with aspirin crystallized rapidly at a higher temperature. This result confirmed that there was a decrease in crystallinity due to the incorporation of the aspirin within the blend film. A similar observation was made where there was a decrease in the T_g, T_m and the T_c of the polyvinyl/dextran hydrogel loaded with gentamicin compared to the unloaded hydrogel (Hwang *et al.*, 2010). Another study similarly demonstrated a decrease in the overall crystallinity of the PLGA film loaded with ibuprofen compared to the unloaded PLGA film. The authors concluded that this decrease in the crystallinity of the films was confirmed using the X-ray diffraction technique (XRD) and was responsible for the decrease in their thermal properties (Pang *et al.*, 2011).

Mechanical characterisation of these blend films with aspirin were carried out to investigate the effect of drug loading on the mechanical properties of the blend films. Addition of aspirin in the blend films had a drastic effect on their mechanical properties. The tensile strength and the Young's modulus values of the blend films with aspirin were lower compared to the blend films without aspirin. However, the % elongation at break values was higher indicating an increase in the flexibility with the addition of aspirin. These results were in agreement with the DSC results that indicated a decrease in the overall crystallinity of the blend film with aspirin. Zilberman and Persson, 2002 observed a similar decrease in the tensile strength and the Young's modulus of the dexamethasone loaded Poly(L-Lactide) or PLLA film. The authors observed that this decrease was due to the incorporation of the dexamethasone molecules within the matrix of the film rather than on the surface. They also observed that this decrease in the tensile strength and the Young's modulus was due to the poor interaction between the dexamethasone molecules

with the polymer matrix (Zilberman and Persson, 2002). Another similar study demonstrated a decrease in the tensile strength of the aspirin loaded PVA membrane with the increase in the concentration of aspirin within the membrane. The % elongation at break values however increased with the increase in the concentration of aspirin. The authors concluded that the increase in the % elongation at break values was due to the decrease in the crystallinity of the aspirin loaded PVA membranes allowing less inhibited movement of the polymer chains within the membranes (Paul and Sharma, 1997). Hence, increase in the % elongation at break value of the blend film with aspirin in this study indicated an increase in the flexibility which is a direct consequence of a decrease in the crystallinity. The findings of this study suggested that the aspirin loading had a drastic effect on the mechanical properties of the blend film. One would need to significantly improve the mechanical properties of these films in order to make them suitable in biodegradable stent development.

Another important characterisation that was carried out on these blend films with aspirin was the *in vitro* degradation study. According to literature, it is known that polyhydroxyalkanoates degrade via surface erosion. Due to this, they are considered to be suitable for controlled drug delivery studies (Pouton and Akhtar, 1996). During surface erosion, degradation initiates on the surface of the polymer and proceed towards the core. The integrity of the polymer is maintained for a longer period of time (Siepmann and Gopferich, 2001). It is known that the water absorption is directly proportional to the progressive degradation of the material (Naraharisetti *et al*., 2005). This could explain the higher percentage of weight loss in the P(3HO)/P(3HB) 50:50 blend film with aspirin compared to the P(3HO)/P(3HB) 50:50 blend film samples without aspirin. Previously, it has been demonstrated that the presence of the aspirin molecules increased the hydrophilicity of the P(3HO)/P(3HB) 50:50 blend film. This would have led to the increased water uptake by the blend films during their incubation in PBS media. Increased water uptake, eventually increased the degradation rate. Frank *et al*., demonstrated a similar increase in the water uptake by the PLGA film loaded with lidocaine compared to the film without the drug. This increased water uptake resulted in a greater weight loss in the lidocaine loaded PLGA film. SEM images of the lidocaine loaded PLGA film after the drug release revealed a rough surface with the pores and blisters indicating visible mass loss (Frank *et al*., 2005). In another study carried out by Paul and Sharma, 1997, there was an increase in the water

uptake in the PVA membranes containing a higher concentration of aspirin molecules. They attributed this to the presence of the hydrophilic aspirin within the PVA membranes. Zhang *et al*., demonstrated a similar increase in the degradation rate of the polyesterurethane network loaded with the aspirin. They attributed this to the increase in the hydrophilicity of the polyesterurethane network due to the presence of aspirin. The authors concluded that upon water absorption, aspirin which is an acidic drug (pka= 3.49), dissociated within the polyesterurethane network, thus affecting the pH of the drug loaded polyesterurethane network thereby accelerating its degradation (Zhang *et al*., 2010).

Drug release kinetics is known to be dependent on a large number of different factors including the type of the polymer, geometry, thickness and the surface area of the drug delivery vehicle, mode of release, type of the drug, drug loading concentration and the pH of the release medium (Acharya and Park, 2006). In this study, aspirin was released from the blend film in a controlled manner and a very low burst release effect was observed. It is known that the burst release occurs due to surface associated drugs (Pouton and Akhtar, 1996). The low burst release observed in this study attributed to the presence of the aspirin within the blend matrix rather than on the surface. The burst release of 9±1.5% observed in this study was significantly lower compared to the PLGA based *in situ* gel containing the PEG400 delivery system containing aspirin that showed a burst release of 30.9±1.2% (Tang and Singh, 2008). Chen *et al*., demonstrated an aspirin burst release of 21% within 1 minute from the magnetic nano composites with 23% drug loading (Chen *et al*., 2012).

From the drug release pattern obtained in this study, it is evident that the drug release occurred in two stages. The drug release from the P(3HO)/P(3HB) 50:50 blend film during the first stage would have occurred due to surface erosion. The rate of the drug release was slow during this stage. The drug release in the second stage would have been accelerated due to the increase in water uptake by the blend film with the drug which resulted in increased degradation. The presence of aspirin which is hydrophilic in nature would have accelerated the penetration of water molecules, thereby having a significant effect on drug release. The finding of this study was in the agreement with drug release pattern of the aspirin loaded polyesterurethane film. The authors described the release of aspirin in three different stages. There was no burst release effect. This was due to the cross linking

network of the polyesterurethane that prevented degradation. Drug release rate increased during the second stage due to the increase in the water uptake which accelerated the diffusion of the drug from within the network. The drug release rate decreased during the third stage due to the low concentration of the drug within the network (Zhang *et al*., 2010).

In conclusion,the drug release pattern in this study demonstrated controlled release of aspirin throughout the release period. This suggested that the aspirin P(3HO)/P(3HB) 50:50 blend with aspirin would be suited for the drug delivery applications. In future,a further investigation into the antithrombotic effect of the released aspirin from the blend film could be carried out. Previous studies have shown that it is critical to maintain the therapeutic index (TI) of the drug. One of the studies demonstrated the anti-thrombotic effect of the aspirin by carrying out platelet adhesion test. The authors incubated the aspirin loaded PVA membranes in the platelet rich plasma. The SEM micrographs revealed the anti-thrombotic property of the aspirin loaded PVA membranes (Paul and Sharma, 1997). A similar experiment could be carried out in the future to investigate the anti-thrombotic property of the P(3HO)/P(3HB) 50:50 blend film containing aspirin .

CHAPTER 6

P(3HB) film and microspheres for controlled release of Aspirin

INTRODUCTION

Poly (3-hydroxybutyrate) or P(3HB) is a member of the polyhydroxyalkanoate (PHA) family which includes -R(3HA) monomer units (Sudesh *et al*., 2000). P(3HB) is one of the most commonly occurring SCL-PHAs (Huisman *et al*., 1989; Valappil *et al*., 2007). In 1926, Lemoigne identified lipid like inclusions within *Bacillus megaterium* to be P(3HB). Since its discovery in the 1920s, P(3HB) has been studied extensively. P(3HB) produced by a wild type bacteria generally has a molecular weight ranging from 1 x 10^4 to 3 x 10^6 g/mol and has a Polydispersity Index (PDI) of 2. However, this varies depending upon the type of organism and their culture conditions (Khanna and Srivastava, 2005). P(3HB) has a melting temperature (T_m) of around 180°C and a glass transition temperature (T_g) of around 4 °C and are hydrophobic in nature. Thermal properties of P(3HB) could also differ depending upon the type of extraction method and their molecular weight. The tensile strength, Young's modulus and the % elongation at break values of P(3HB) has been measured to be 43 MPa, 3.5 GPa and 5% respectively (Sudesh *et al*., 2000). P(3HB) is highly crystalline in nature which makes them very brittle (Ha and Cho, 2002). Due to their established mechanical and thermal properties as well as their commercial accessibility, P(3HB) was the first member of PHAs to be used in biomedical applications. Apart from its biodegradability and biocompatibility properties, P(3HB) has also demonstrated piezoelectric properties that promote bone growth and healing (Misra *et al.,* 2006, Knowles *et al.,* 1992). P(3HB) has been used for various biomedical applications such as bone and cartilage tissue engineering, composite fabrication, biodegradable sutures, wound dressing films and coronary stent development (Misra *et al.,* 2006). However, one of the most interesting applications of P(3HB) is its use as the drug delivery tool which is the main focus of this study.

Local drug delivery is an attempt to deliver an effective local drug concentration to elicit a pharmacological response and eliminate toxicity caused by systemic drug delivery (Basnett and Roy, 2010). Several polymers both of natural origin and synthetic have been used as a vehicle for controlled delivery of drugs. Surface and bulk properties of the polymers that affect the drug release include their hydrophobicity, surface porosity, crystallinity, molecular weight and their mode of

degradation. Poly(lactic acid) or PLA, Poly(glycolic acid) or PGA and their copolymer Poly(lactic acid-co-glycolic acid) or PLGA are the most commonly used polymers for drug delivery due to their adjustable physical and degradation properties. However, one of the main drawbacks of using these polymers is the local acidity caused during their degradation which leads to site inflammation and affects the drug stability. Apart from this, they degrade via bulk erosion which demonstrates complex erosion kinetics and is not considered ideal for controlled release (Pillai and Panchagnula, 2001; Liu *et al.,* 2006; Cordewener *et al.,* 2000).

The use of P(3HB) as a drug release system was reported by Korsatko *et al.,* for the first time in 1983 (Misra *et al.,* 2006). Previous studies have shown that P(3HB) is an excellent biomaterial for drug delivery applications. P(3HB) is degraded via surface erosion which is a physical process based on diffusion and a dissolution phenomenon and is considered ideal for controlled drug release. P(3HB) is degraded into less acidic by products compared to the PLA, PGA and PLGA and therefore has better biocompatibility. P(3HB) is hydrophobic in nature and therefore ideal for slow drug release. However, this could have a detrimental effect on the dissolution of hydrophilic drugs thereby affecting its encapsulation and drug release (Pillai and Panchagnula, 2001; Misra *et al.,* 2006; Liu *et al.,* 2005)

The main aim of this study was to develop P(3HB) microspheres and films to investigate their potential as a drug delivery tool for the controlled delivery of aspirin. Aspirin is one of the most frequently used drugs against fever and pain. However, studies have shown that aspirin has poor oral bioavailability and their prolonged use gives rise to side effects such as gastrointestinal (GI) mucosa ulcer and GI haemorrhage. Clinical trials have confirmed that a minimum dose parenteral administration of aspirin would increase its therapeutic efficacy (Tang and Singh, 2008).

SECTION I

6.0 Results

6.1 **Preparation of the P(3HB) solvent cast film with and without aspirin** and their characterisation.

P(3HB) produced was used to prepare a solvent cast film and aspirin was added to the P(3HB) film. P(3HB) film with and without aspirin were prepared using the solvent casting method. P(3HB) was dissolved in dichloromethane in order to obtain a polymer concentration of 5wt%. In order to prepare P(3HB) film with aspirin, aspirin was dissolved in dichloromethane and mixed with the polymer solution to achieve a drug loading of 15wt%. The polymer solution containing aspirin was mixed well by sonication and then cast into a glass petri dish immediately to achieve a uniform distribution of aspirin within the polymer matrix. P(3HB) film without aspirin was prepared to investigate the effect of drug loading on the properties of the film. The film was air dried for one week. Films of 0.18 mm thickness were produced as shown in **Figure 6.1.**

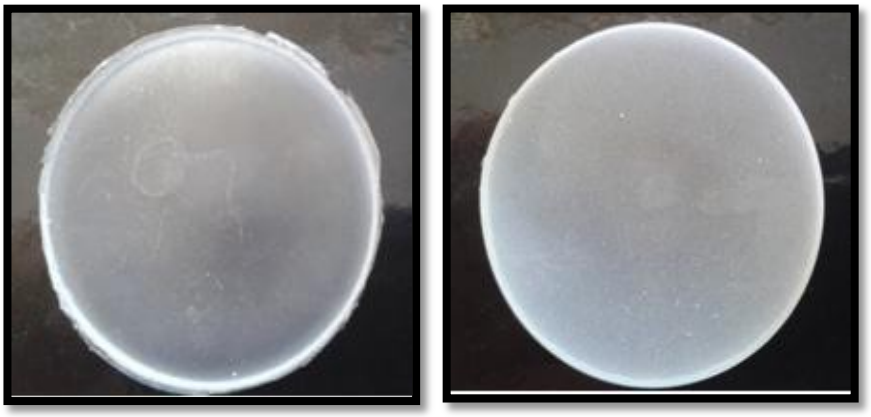

(a) **(b)**

Figure 6.1: Solvent cast (a) P(3HB) film and the (b) P(3HB) film with aspirin

The presence of the aspirin within the P(3HB) matrix was analysed using FTIR.

6.1.1 Fourier Transform Infrared Spectroscopy (FTIR):

FTIR analysis was carried out on the P(3HB) film with and without aspirin using the method described in **section 2.6.1.** This analysis was performed to confirm the presence of aspirin within the matrix of the P(3HB) film. The IR Spectrum of the (a) P(3HB) film with aspirin (-) and the (b) P(3HB) film (-) is shown in **Figure 6.2.**

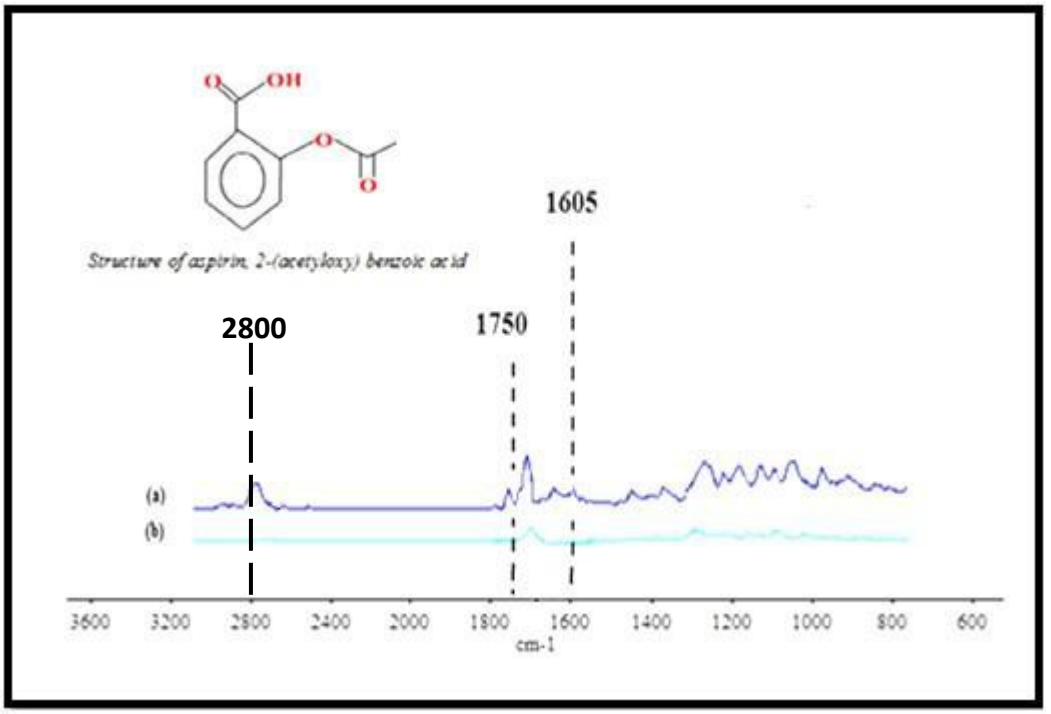

Figure 6.2: The FTIR spectra of the (a) P(3HB) film with aspirin and the (b) P(3HB) film.

The characteristic absorption peaks at 1750 cm^{-1} corresponding to the carbonyl group and an absorption peak at 1605 cm^{-1}, corresponding to the benzene ring and absorption peak at 2800 cm^{-1} corresponding to the carboxylic group present in the chemical structure of aspirin, were all observed in the P(3HB) film containing aspirin (Li *et al.*, 1999). This confirmed the presence of aspirin within the matrix of the P(3HB) film**.**

6.1.2 Scanning electron Microscopy

Microstructural studies of the P(3HB) film samples with and without aspirin were carried out using SEM as described in **section 2.9.1.** The surface topography of the P(3HB) film containing aspirin was compared to the topography of the P(3HB) film without aspirin as shown in **Figure 6.3.** The SEM images revealed that a new topography was introduced in the P(3HB) film with aspirin due to the addition of aspirin within the matrix of the P(3HB) film.

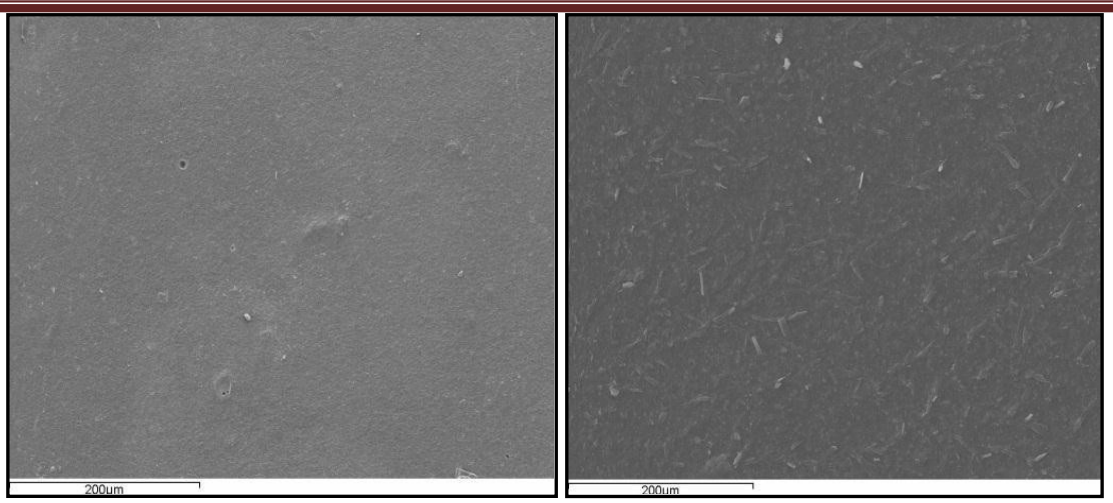

(a) **(b)**

Figure 6.3: SEM images of the **(a)** P(3HB) film **(b)** P(3HB) film containing aspirin.

The surface of the P(3HB) film with aspirin appeared to have a rough topography compared to the P(3HB) film without aspirin. At 15% drug loading, aspirin crystals were observed on the surface of the film, indicating that aspirin had crystallized during the synthesis of P(3HB) film. The films were further characterised using Atomic Force Microscopy (AFM).

6.1.3 Surface Roughness

In order to evaluate the effect of the aspirin incorporation on the surface roughness of the film, AFM analysis was carried out on the P(3HB) films with and without aspirin, as described in **section 2.9.3.** The AFM images of the surface of the P(3HB) film and the P(3HB) film with aspirin are shown in **Figure 6.4.** The surface roughness of the films was determined by calculating typical root mean square (rms) values as shown in **Figure 6.4.**

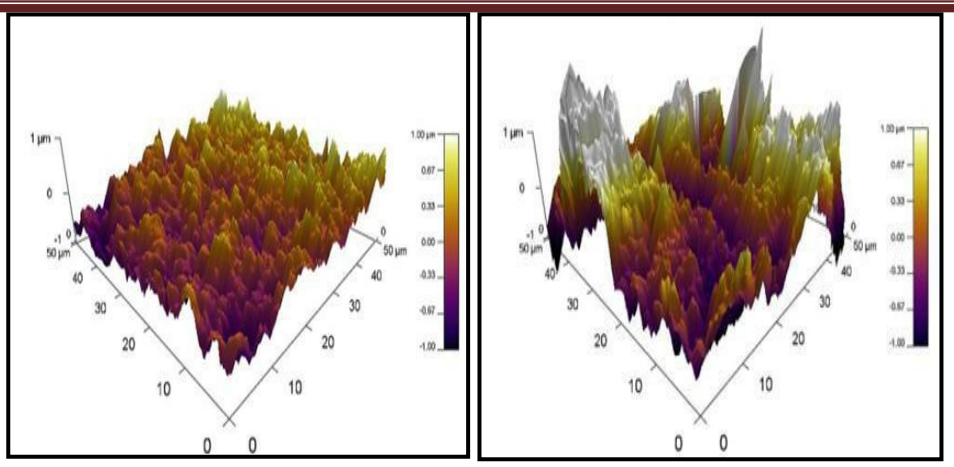

(a) **(b)**

Figure 6.4: The AFM images of the (a) P(3HB(film (b) P(3HB) film with aspirin.

The change in the topography of the P(3HB) film with aspirin was confirmed using AFM. The rms value of the P(3HB) film was calculated to be 0.24 ± 0.1 µm whereas the rms value of the P(3HB) film with aspirin was calculated to be 0.60 ± 0.3 µm. The surface roughness of the P(3HB) film with aspirin was 199% higher than the P(3HB) film without aspirin. This confirmed that the presence of aspirin increased the surface roughness of the film.

6.1.4 Water Contact Angle

Water contact angle measurements were carried out to study the effect of aspirin loading on the wettability of the P(3HB) films, as described in **section 2.9.4** . It is known from literature that polymer films with θ values less than 70° are considered to be hydrophilic in nature whereas θ values greater than 70° are considered to be hydrophobic in nature (Peschel *et al*., 2008). The results of the water contact angle measurements are shown in **Figure 6.5**.

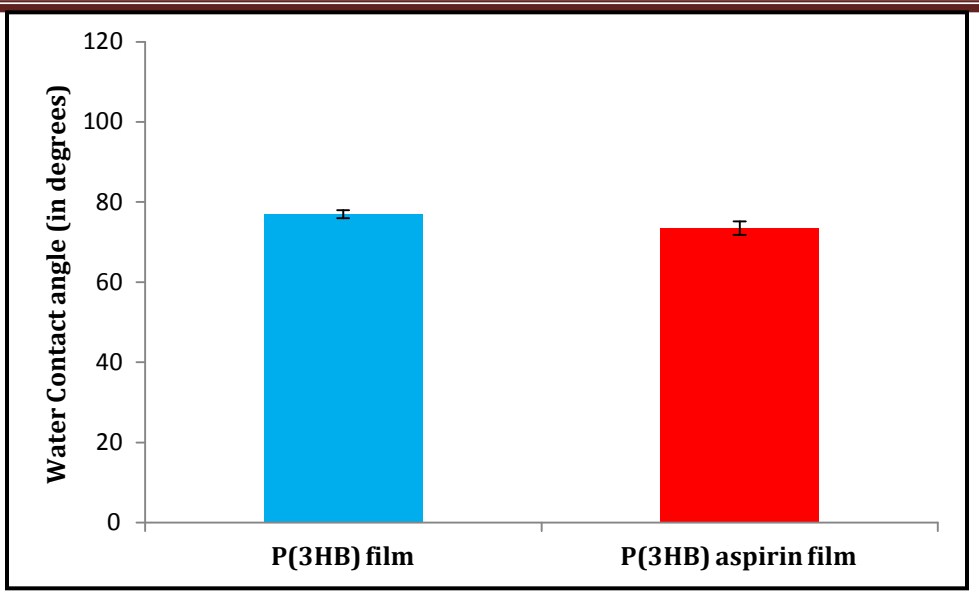

Figure 6.5: Static water contact angle measurements of the P(3HB) film and the P(3HB) film with aspirin. (n = 3). The data were compared using t-test and the difference were considered significant when *p<0. 05.

The water contact angle of the P(3HB) film with and without aspirin was 73.5° ± 1 and 77°±3 respectively which is higher than 70° and hence, they were both considered to be hydrophobic in nature. There was an increase in the hydrophilicity of the P(3HB) film due to the presence of aspirin, however this increase was not significant.

6.1.5 Protein Adsorption Test

The protein adsorption test was done to measure the overall protein adsorbed on the P(3HB) film with and without aspirin. This test was carried out to determine the effect of aspirin loading on protein adsorption on the P(3HB) film, as described in the **section 2.9.7**. The results of the protein adsorption tests have been summarised in **Figure 6.6**.

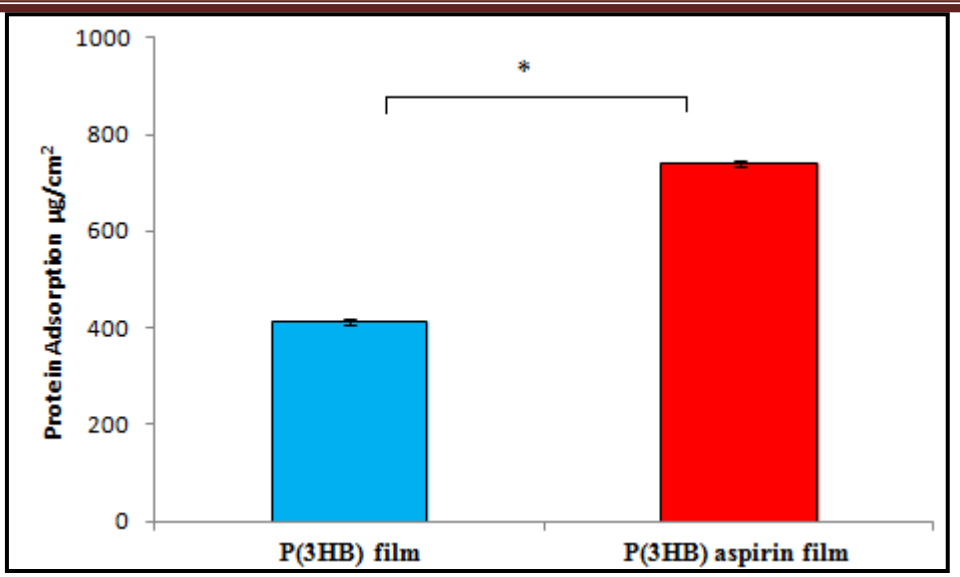

Figure 6.6: Protein adsorption on the P(3HB) film and the P(3HB) film with aspirin (n = 3). The data were compared using t-test and the difference were considered significant when *p<0. 05.

Protein adsorption on the P(3HB) film was 414±3 µg/cm^2 while that on the P(3HB) film with aspirin was 739±2 µg/cm^2. Hence, there was 78% increase in the amount of protein adsorbed on to the P(3HB) film due to the addition of aspirin compared to the P(3HB) film without aspirin. This increase in the protein adsorption was statistically significant (*p<0. 05).

6.1.6 Indirect Cytoxicity Testing

The samples of P(3HB) film and the P(3HB) film containing aspirin were incubated in the DMEM for 24 hours at 37^{0}C. Simultaneously, HMEC-1 cells were cultured for 24 hours in 24 well plates at a concentration of 1000,000 cells/ml. The DMEM medium from step 1 was then exposed to the cells and cultured for another 24 hours. This was done to study the effect of the degradation products of the samples on the HMEC-1 cells. These studies were carried out as described in **section 2.9.8 .** The results of the tests are shown in **Figure 6.7**.

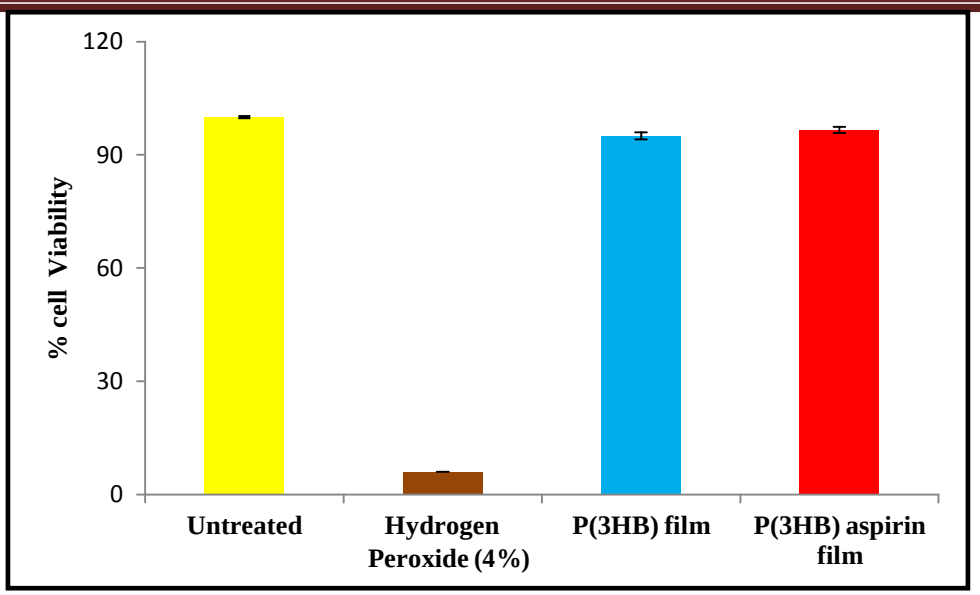

Figure 6.7: Indirect toxicity testing of the P(3HB) film with and without aspirin (n = 3). Cells grown in DMEM, in the absence of polymer were taken as untreated and the cells grown in the presence of 4% hydrogen peroxide were taken as the positive control. The data were compared using ANOVA and the difference were considered significant when *p<0. 05.

HMEC-1 cells grown in DMEM without any polymer showed a highest cell viability percentage of 100±0.3%, followed by the P(3HB) film with aspirin which showed a cell viability percentage of 96.6±0.8% . P(3HB) film samples without aspirin showed a cell viability percentage of 95.0±0.9% while the lowest percentage of cell viability of 6.2±0.0% was observed when the HMEC-1 cells were grown in 4% hydrogen peroxide, a chemical that is induces cell death. The increase in the % cell viability in the P(3HB) film with aspirin compared to the P(3HB) film samples were not statistically significant.

6.1.7 Differential Scanning Calorimetry

Thermal properties such as the melting temperature (T_m), glass transition temperature (T_g) and the crystallization temperature(T_c) of the P(3HB) films with and without aspirin were analysed using DSC, as described in **section 2.9.6.** This was done to study the effect of aspirin on the thermal properties of the P(3HB) film. The results are summarised in **Table 6.1.**

Samples	T_m (°C)	T_g (°C)	T_c (°C)
P(3HB) film	170.3 ± 0.0	10.0 ± 0.0	109.5 ± 0.0
P(3HB) film with aspirin	136.0 ± 0.5, 160.3 ± 0.7	9.0 ± 1.3	101.0 ± 0.2

Table 6.1: Thermal properties of the P(3HB) films with and without aspirin (n = 3).

The melting temperature (T_m) of the P(3HB) film with aspirin was lower compared to the T_m of the P(3HB) film without aspirin. A peak at 136.0°C was detected during the heating scan which corresponded to the T_m of commercial aspirin. The crystallization temperature (T_c) of the P(3HB) film with aspirin was also lower compared to the P(3HB) film without aspirin. During the cooling run (200°C to -50°C), the P(3HB) film crystallized rapidly at a higher temperature compared to the P(3HB) films with aspirin. The glass transition temperature (T_g) of the P(3HB) film with aspirin was also lower compared to the P(3HB) film without aspirin.

6.1.8 *In vitro* degradation study in PBS

6.1.8.1 Water absorption

In vitro degradation study was carried out on the P(3HB) film samples with and without aspirin to examine the effect of aspirin on the degradation properties of the P(3HB) films. The percentage of water absorbed (%WA) by the P(3HB) films with and without aspirin were measured by incubating the film samples in the PBS media for a period of 3, 15 and 30 days, as described in **section 2.10.**

The data obtained at the end of the incubation are presented in **Figure 6.8**.

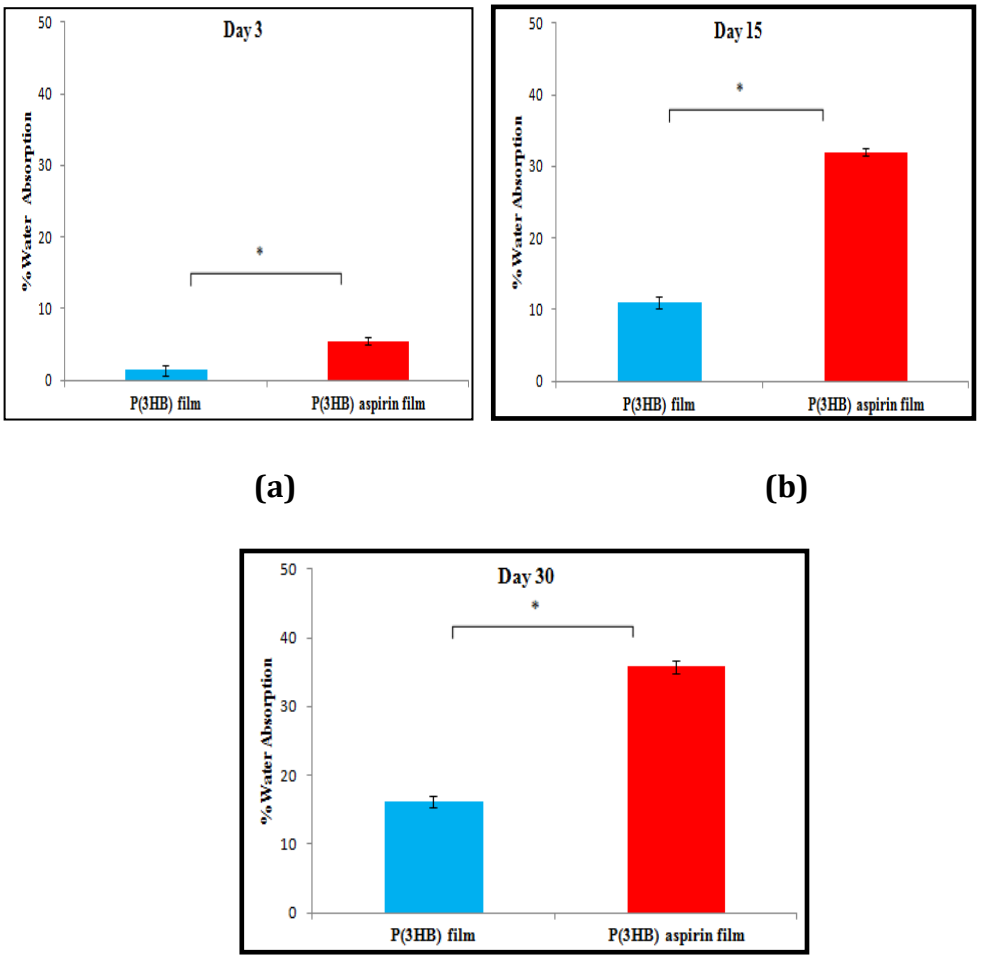

Figure 6.8: Water absorption (%WA) by the P(3HB) and P(3HB) film samples with aspirin for a period of (a) 3 days (b) 15 days and (c) 30 days (n=3). The data were compared using t-test and the difference were considered significant when *p<0. 05.

The % water absorbed by the P(3HB) film on day 3 was 1.4±0.3%. It increased progressively to 11.1±1% and 16.2±0.1% at day 15 and 30 respectively. Similarly, the % water absorbed by the P(3HB) film containing aspirin on day 3 was 5±0.4% which increased significantly to 31.9±0.9% and 35.8±0.6% on day 15 and day 30 respectively. The % water absorbed by the P(3HB) film with aspirin was significantly higher compared to the P(3HB) film without aspirin(*p<0. 05).

6.1.8.2 Weight Loss

Percentage weight loss (%WL) of the P(3HB) films with and without aspirin were measured by incubating the film samples in PBS media for a period of 3, 15 and 30 days, as described in **section 2.10.** The data obtained at the end of the incubation period is represented in **Figure 6.9**.

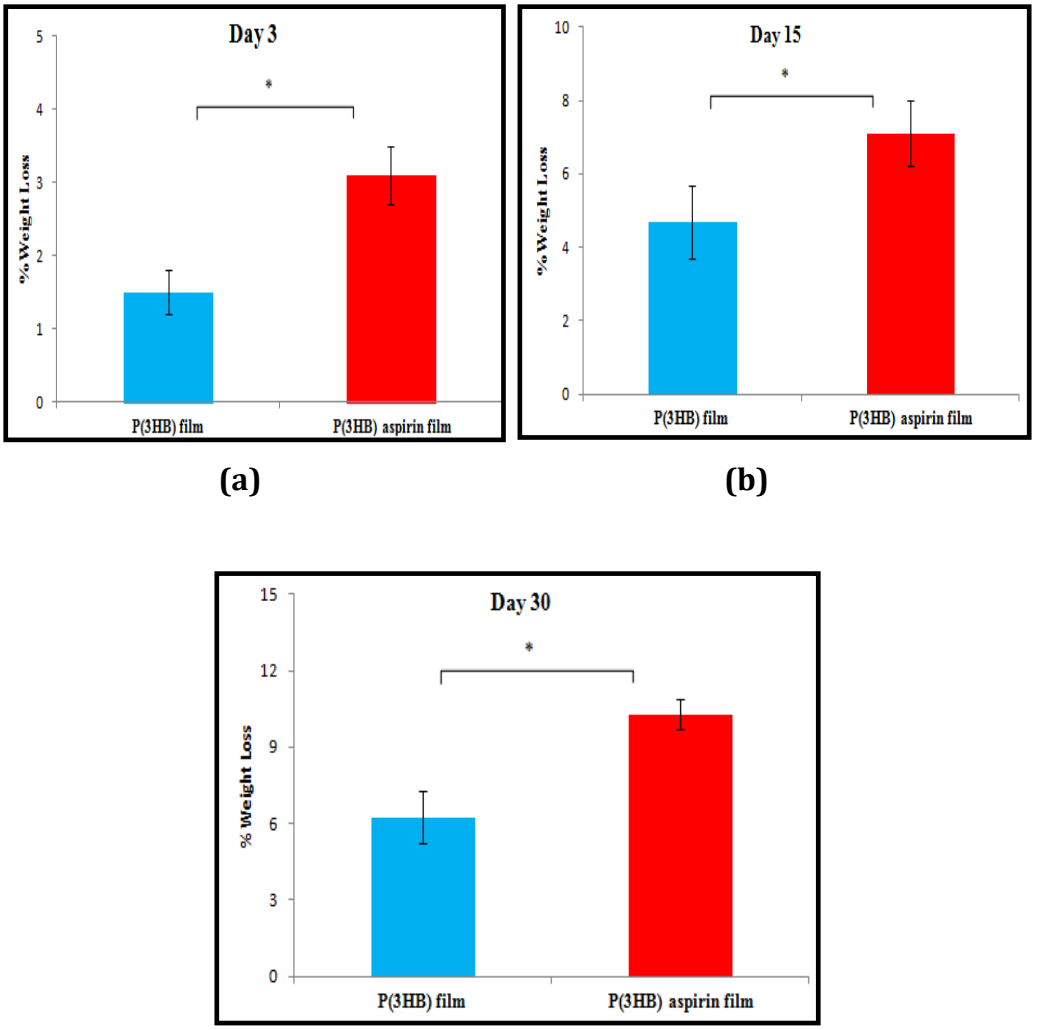

Figure 6.9: % Weight Loss (WL) in the P(3HB) film with and without aspirin at (a) day 3 (b) day 15 and (c) day 30 (n=3). The data were compared using t-test and the difference were considered significant when *p<0. 05.

The % weight loss (%WL) in the P(3HB) film on day 3 was 1.5±0.3% . It increased gradually to 4.7±1% on day 15, followed by 6.2±1.0% on day 30. A similar trend was observed in the P(3HB) film samples with aspirin where there was gradual increase in the % weight loss with time. On day 3, the % weight loss was 3.1±0.4%,

which increased to 7.1±0.9% on day 15. On day 30, the % weight loss was 10.2±0.6%. From the data, it was clear that the % weight loss was significantly higher in the P(3HB) film with aspirin compared to the P(3HB) film without aspirin (*p<0. 05).

6.1.9 *In vitro* drug release studies

1 cm^2 of the P(3HB) film samples with aspirin, in triplicates, were immersed in PBS release medium. Their drug release rates were measured as described in **section 2.11.** The cumulative release profile of aspirin from P(3HB) films with aspirin is shown in **Figure 6.10**.

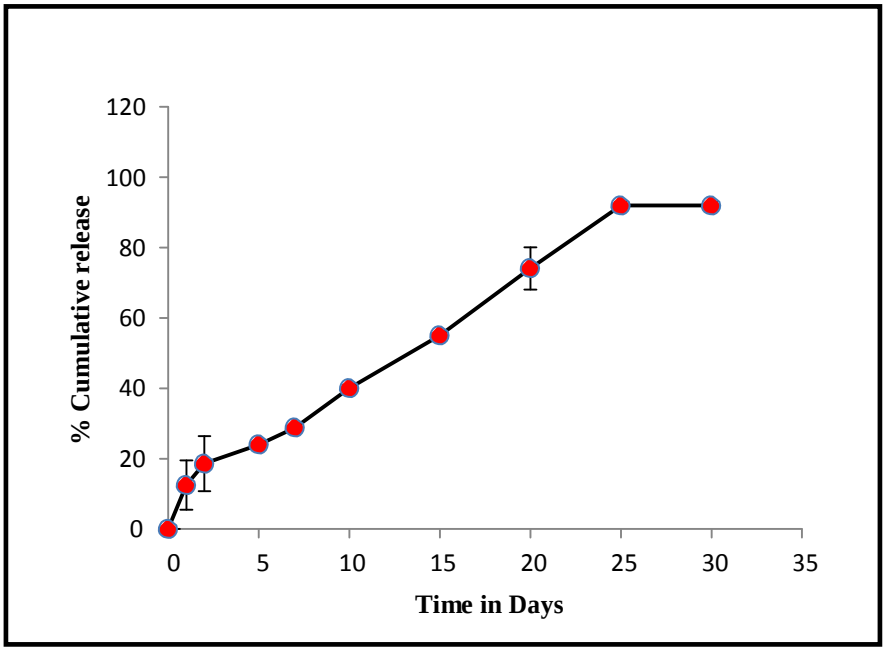

Figure 6.10: *In vitro* release profile of aspirin from the P(3HB) film with aspirin for a period of 30 days (n=3).

Aspirin was released throughout the period of 30 days. 92% of the total drug was released during this period. An initial burst release of 12.5± 7.0% was observed on day 1. After this initial burst, a controlled release of aspirin was obtained, where 28.8% of the total drug was released within the first 7 days. Finally, after 30 days, the cumulative aspirin release was 92%.

It is a known fact that aspirin upon hydrolysis loses its therapeutic activity. Therefore, it is very crucial to release aspirin in its chemically stable form (Aubrey-Medendorp *et al*., 2008). The amount of chemically stable aspirin in the released samples and in the control aspirin solution in PBS is shown in **Figure 6.11**.

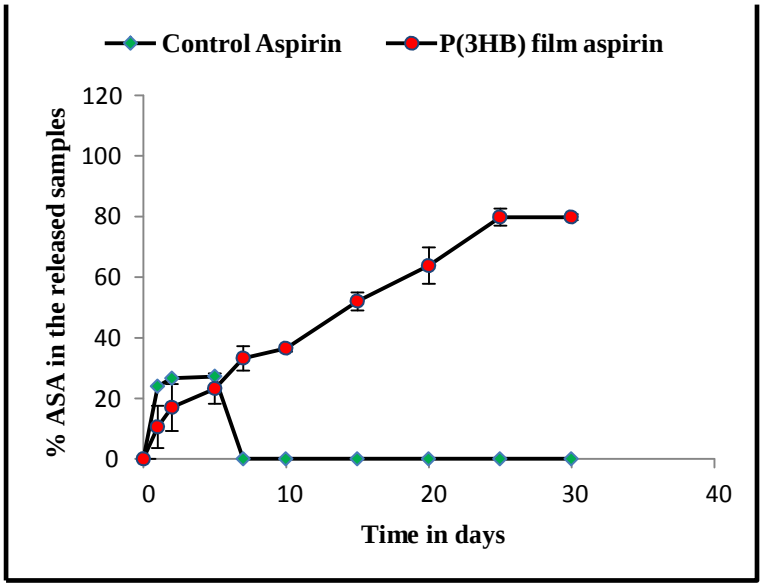

Figure 6.11: *In vitro* release profile of chemically stable aspirin in the released samples from the (a) P(3HB) film with aspirin and (b) control aspirin standard for a period of 30 days (n=3).

At the end of the release period, 79.8% of chemically stable aspirin was released from the P(3HB) film samples containing aspirin compared to the 27.2% of the chemically stable aspirin present in the control aspirin solution incubated under same conditions. The percentage of chemically stable aspirin released from the P(3HB) film with aspirin was higher compared to the control aspirin solution.

SECTION II

6.2 Synthesis of P(3HB) microspheres

P(3HB) microspheres were produced using a solid-in-oil-in-water emulsion technique. 0.3g of P(3HB) was dissolved in 6 mL of dichloromethane and agitated for 3 min. This mixture was then transferred into the first water-in-oil emulsion (w/o) of 48 mL of 0.8% w/v polyvinyl alcohol (PVA) solution, and stirred at 800 rpm for 5 min. This solution was transferred to a second water-in-oil-in water emulsion (w/o/w) of 120 mL of 0.1% w/v aqueous PVA solution, forming the second-oil-in-water emulsion. This emulsion was stirred at 800 rpm for 4 hours to form P(3HB) microspheres. The resulting microspheres were isolated by centrifugation and then washed three times with the distilled water and freeze dried. While preparing the microspheres containing aspirin, aspirin was added to 48 mL 0.8% PVA solution which was later added to the 120 mL of 0.1% PVA solution (Francis *et al.*, 2011). Aspirin was encapsulated within these microspheres. These P(3HB) microspheres and the P(3HB) microspheres with aspirin were characterised using FTIR.

6. 2.1 Characterisation of the P(3HB) microspheres

6.2.1.1 Fourier Transform Infrared Spectroscopy (FTIR)

P(3HB) microspheres with and without aspirin were analysed by FTIR as described in **section 2.6.1.** This was done to detect the presence of aspirin encapsulated within the P(3HB) microspheres. The IR Spectrum of the (a) P(3HB) microspheres (-) and the (b) P(3HB) microspheres with aspirin (-) is shown in **Figure 6.12.**

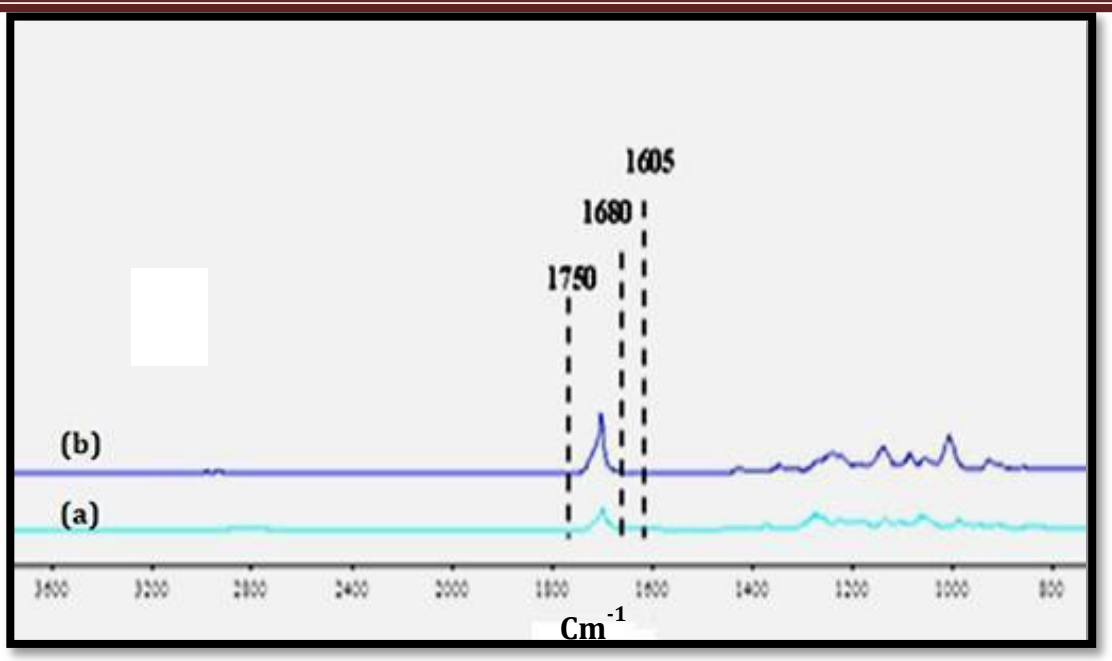

Figure 6.12: The FTIR spectra of the (a) P(3HB) microspheres with aspirin and the (b) P(3HB) microspheres without aspirin.

The signature absorption peaks at 1750 cm^{-1} and 1680 cm^{-1} corresponding to the presence of carbonyl groups and an absorption peak at 1605 cm^{-1} corresponding to the benzene ring present in the chemical structure of aspirin were not observed in the P(3HB) microspheres with aspirin (Li *et al.*,1999). This indicated that at 15% drug loading, it was not possible to detect the presence of the drug within the microspheres. The drug concentration was too low compared to the polymer concentration. Therefore, encapsulation efficiency test was carried out to detect the presence and quantify the presence of aspirin within the microspheres.

6.2.1.2 Encapsulation efficiency

The % encapsulation efficiency of the P(3HB) microspheres was calculated using the following equation (1)

EE% = Experimental drug loading/Actual drug loading x 100---------- (1)

Encapsulation efficiency was calculated by dissolving 5 mg of P(3HB) microspheres with aspirin in 1 mL of dichloromethane. After the microspheres had completely dissolved, 5 ml of water was added. Aspirin is hydrophilic in nature and hence would be found in the water phase which was later analysed using High performance Liquid Chromatography (HPLC) (Francis *et al.*, 2011).

In this study, the encapsulation efficiency of the P(3HB) microspheres with the average size of 30 µm was found to be 50%. This test confirmed the presence of aspirin within the microspheres.

6.2.1.3 Scanning electron Microscopy:

Microstructural studies of the P(3HB) microspheres with and without aspirin were carried out using SEM as described in **section 2.9.1.** This was done to examine the effect of the aspirin encapsulation on the surface topography of the P(3HB) microspheres. The SEM images of the microspheres are shown in **Figure 6.13.**

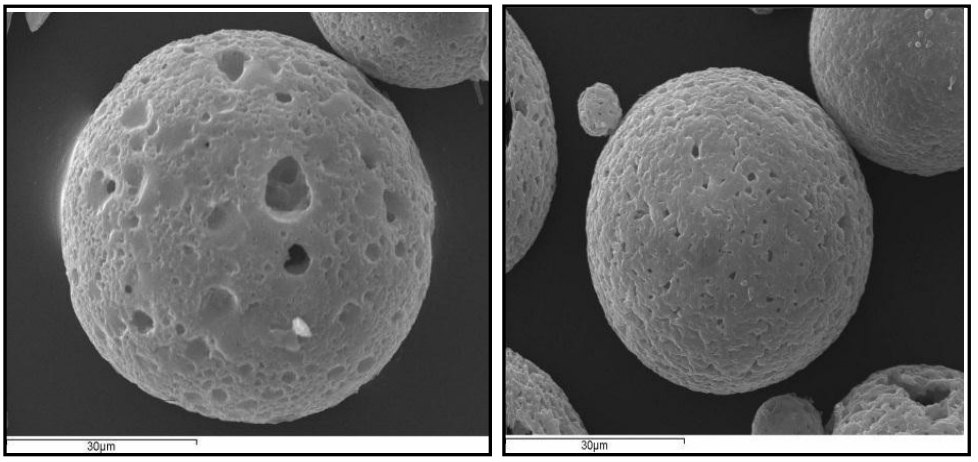

(a) **(b)**

Figure 6.13: SEM images of the (a) P(3HB) microspheres and the (b) P(3HB) microspheres containing aspirin aspirin. Scale bars = 30 µm.

The SEM images revealed that the surface morphology of the P(3HB) microspheres was rough and porous compared to the P(3HB) microspheres with aspirin. The SEM images also revealed that the encapsulation of aspirin within the P(3HB) microspheres reduced the porosity of the microspheres. This reduction in the porosity was further confirmed by carrying out porosity studies.

6.2.1.4 Porosity studies

The porosity (ε) of the P(3HB) microspheres with and without aspirin was determined using the liquid displacement method (Francis *et al.,* 2011). The porosity was calculated using the following equation (2):

V_p (Volume of the matrix pores) = $(W_2 - W_3 - W_s) / \rho_e$

V_s (Volume of the matrix polymer phase) = $(W_1 - W_2 \pm\pm W_s) / \rho_e$

$E = V_p / (V_{p+} V_s) = (W_2 - W_3 - W_s) / (W_1 - W_s)$ ---------- (2)

W_1 is the weight of the cylinder filled with ethanol before the immersion of the microspheres, W_2 is the weight of the cylinder, the ethanol and the sample after removing excess ethanol, W_3 is the weight of the cylinder and ethanol after removing the microspheres and W_s is the actual weight of the microsphere sample used in the porosity measurement (Francis *et al.*, 2011).

The average porosity of the P(3HB) microspheres was 51±2% compared to 39.0±1.3% of the P(3HB) microspheres with aspirin, as shown in **Figure 6.14**.

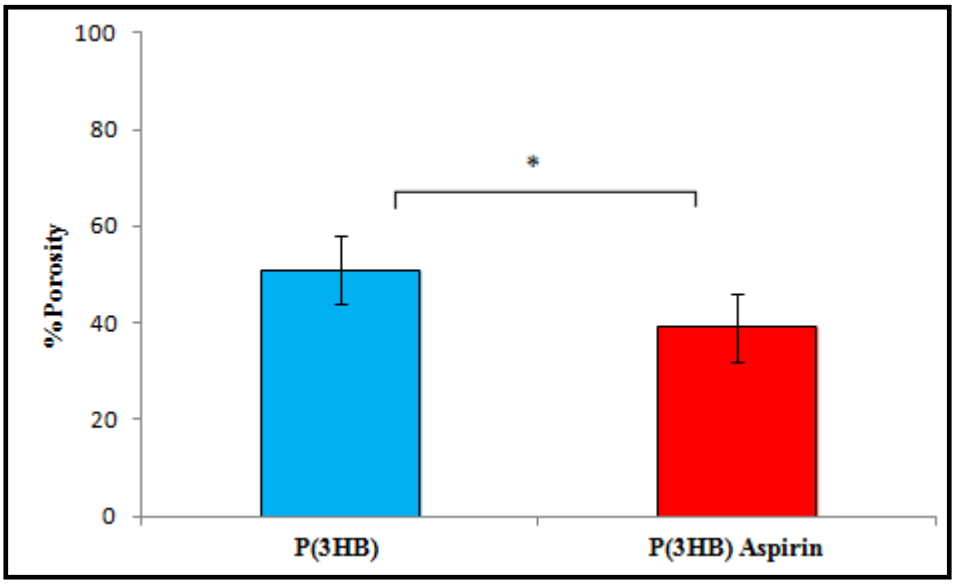

Figure 6.14: Porosity measurements of the P(3HB) microspheres and P(3HB) microspheres containing aspirin (n=3). The data were compared using t-test and the difference were considered significant when *p<0. 05.

The porosity studies confirmed that the encapsulation of aspirin within the P(3HB) microspheres reduced their porosity significantly (*p<0. 05). The entrapment of drug within the pores of the polymer could have led to this decrease in the porosity of the microspheres with aspirin (Chee *et al.,* 2008).

6.2.1.5 Surface Hydrophobicity

In order to evaluate the effect of the aspirin encapsulation on the surface properties of the P(3HB) microspheres, the surface hydrophobicity of the P(3HB) microspheres and P(3HB) microspheres containing aspirin were measured. 1 mg of P(3HB) microspheres with and without aspirin were incubated with four different concentration of Rose Bengal Dye (mg/mL) for 3 hours at room temperature. After incubation, the samples were centrifuged at 11,000g for 30 min. The absorbance of the supernatant was measured at 542.7 nm to determine the unbound dye. The dye solution without any microspheres was used as a control (Sahoo *et al.,* 2002; Francis *et al*., 2011).

The amount of Rose Bengal dye adsorbed per mg of the P(3HB) microspheres with and without aspirin is shown in **Figure 6.15.**

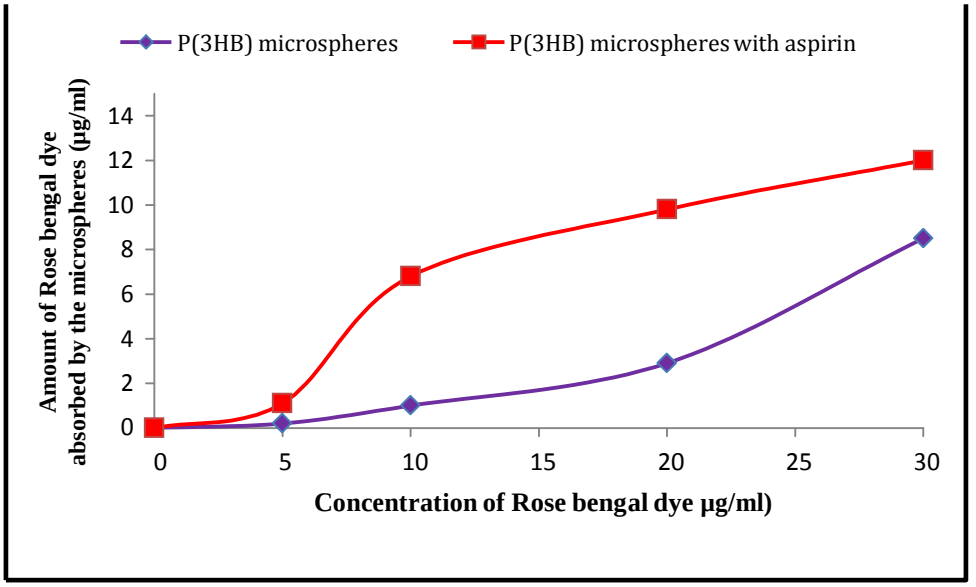

Figure 6.15: The amount of the Rose Bengal dye adsorbed onto the surface of the P(3HB) microspheres with and without aspirin, as a function of an increase in the Rose Bengal dye concentration.

The amount of the dye adsorbed onto the P(3HB) microspheres with aspirin was higher compared to the P(3HB) microspheres without aspirin. This is most likely due to the presence of a hydrophilic drug encapsulated within the P(3HB) microspheres. This showed that the presence of aspirin within the microspheres increased the hydrophilicity of the P(3HB) microspheres.

6.2.1.6 Protein adsorption

To determine the overall protein adsorbed on the surface of P(3HB) microspheres with and without aspirin, protein adsorption test was carried out as described in **section 2.9.7**. This was done to understand the effect of the encapsulated aspirin on protein adsorption. The results of the protein adsorption test have been summarised in **Figure 6.16.**

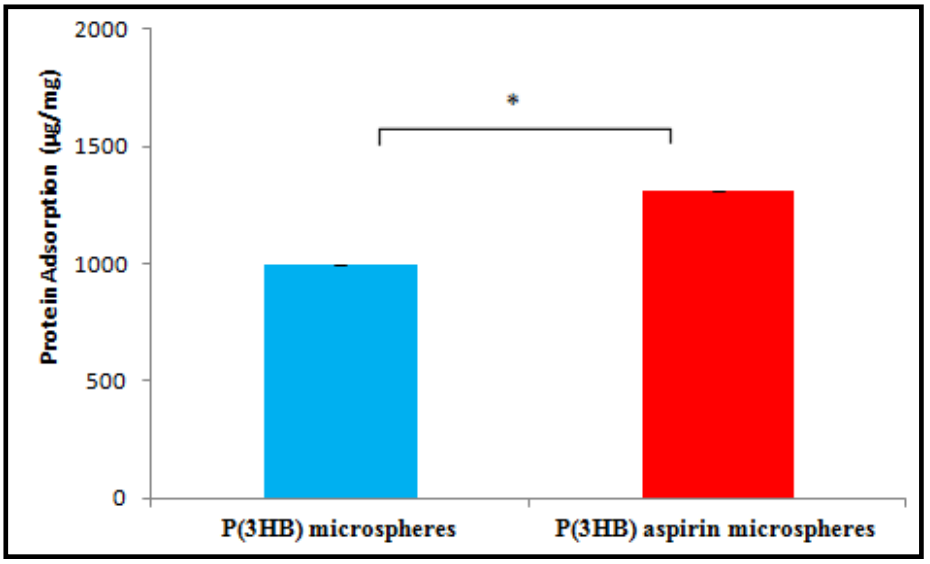

Figure 6.16: Protein adsorption on the P(3HB) microspheres with and without aspirin (n = 3). The data were compared using t-test and the difference were considered significant when *p<0. 05.

The total amount of protein adsorbed on to the P(3HB) microspheres with aspirin was 1313 ± 1µg/mg which was significantly higher than the total amount protein adsorbed on to the P(3HB) microspheres without aspirin which was 996± 2 µg/mg (*p<0. 05).

6.2.1.7 Differential Scanning Calorimetry

Thermal properties such as the melting temperature (T_m), glass transition temperature (T_g) and the crystallization temperature (T_c) of the P(3HB) microspheres with and without aspirin were analysed using DSC, as described in **section 2.9.6.** This was carried out to understand the effect of aspirin encapsulation on the thermal properties of the P(3HB) microspheres. The results have been summarised in **Table 6.2**.

Samples	T_m (°C)	T_g (°C)	T_c (°C)
P(3HB) microspheres	169.9 ± 0.9	9.8 ± 0.5	102.3 ± 0.6
P(3HB) aspirin	161.5 ± 0.9, 8 ± 0.3	9.1 ± 1.0	80.6 ± 1.5

Table 6.2: Thermal properties of the P(3HB) microspheres with and without aspirin (n = 3).

The T_m, T_c, and T_g of the P(3HB) microspheres with aspirin were lower compared to the P(3HB) microspheres. An additional peak at 81°C was observed in the DSC thermogram of the P(3HB) microspheres with aspirin. It is known that the melting temperature of aspirin is 136°C. Hence, a shift in the melting temperature of aspirin was observed.

6.2.2 *In vitro* degradation study in PBS

6.2.2.1 Water absorption

In vitro degradation study was carried out on the P(3HB) microsphere with and without aspirin samples to examine the effect of aspirin on the degradation properties of the P(3HB) microspheres. The percentage of water absorbed (%WA) by the P(3HB) microspheres with and without aspirin were measured by incubating the microsphere samples in the PBS media for a period of 3, 15 and 30 days, as described in **section 2.10**. The data obtained at the end of the incubation is presented in **Figure 6.17.**

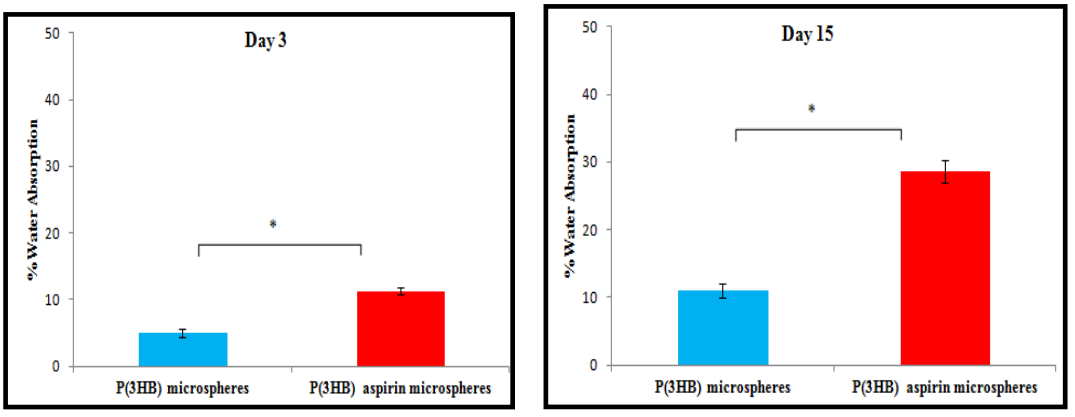

(a) **(b)**

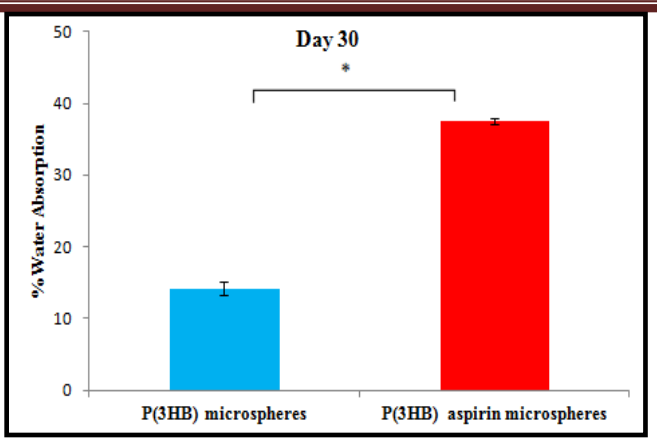

(c)

Figure 6.17: Water absorption (%WA) by the P(3HB) microspheres with and without aspirin for a period of (a) 3 days (b) 15 days and (c) 30 days (n=3). The data were compared using t-test and the difference were considered significant when *p<0. 05.

The % water absorbed by the P(3HB) microspheres on day 3 was 5±0.6%. It increased progressively to 11±0.5% and 14.2±0.9% on day 15 and 30 respectively. Similarly, the % water absorbed by the P(3HB) microspheres with aspirin on day 3 was 11.3±0.5%, which increased significantly to 28.6±1.7% and 37.6±0.4% on day 15 and day 30 respectively. The % water absorbed by the P(3HB) microspheres with aspirin was significantly higher compared to the P(3HB) microspheres without aspirin.

6.2.2.2 Weight Loss

Percentage weight loss (%WL) of the P(3HB) microspheres with and without aspirin were measured by incubating the microsphere samples in PBS media for a period of 3, 15 and 30 days, as described in **section 2.10**. The data obtained at the end of the incubation period is represented in **Figure 6.18.**

(a) (b)

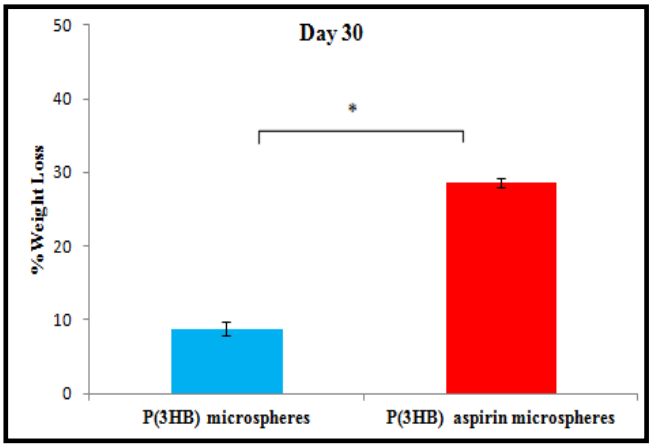

(c)

Figure 6.18: % Weight Loss (WL) in the P(3HB) microspheres with and without aspirin at (a) day 3 (b) day 15 and (c) day 30 (n=3). The data were compared using t-test and the difference were considered significant when *p<0. 05.

The % weight loss (%WL) in the P(3HB) microspheres on day 3 was 2±0.6% . It increased gradually to 6.1±0.9% on day 15, followed by 8.8±0.9% on day 30. A similar trend was observed in the P(3HB) microspheres with aspirin, where there was gradual increase in the % weight loss with time. On day 3, the % weight loss was 7.9±1% which increased to 15.3±0.4% on day 15. On day 30, the % weight loss was 28.6±0.7%. From the data, it was clear that the % weight loss was significantly higher in the P(3HB) microspheres with aspirin compared to the P(3HB) microspheres (*p<0. 05).

6.3 *In vitro* drug release studies

The drug elution studies from the P(3HB) microspheres with aspirin was carried out as described in **section 2.11.** The cumulative release profile of aspirin from P(3HB) microspheres with aspirin is shown in **Figure 6.19.**

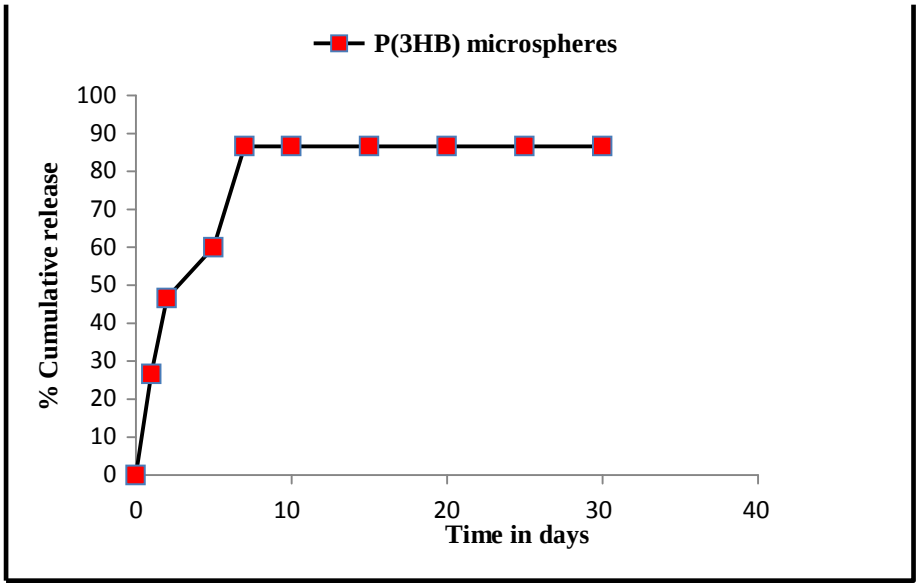

Figure 6.19: *In vitro* release profile of aspirin from the P(3HB) microspheres with aspirin for a period of 30 days (n=3).

86.6±5% of the total drug encapsulated within P(3HB) microspheres was released within 15 days of the release period. An initial burst release of 26.6±1% was observed on day 1. This could be due to the presence of aspirin on the surface of the microspheres (Kassab *et al.,* 1997). This burst release was higher compared to the burst release observed in the P(3HB) film with aspirin. However, it was lower compared to the PLGA based *in situ* gel delivery system for aspirin which showed a burst release of 30.9±1.2% (Tang and Singh, 2008).

From the drug release pattern, it appeared that the drug release occurred through the water channels created within the microspheres. Previous studies have shown that aspirin loses its therapeutic activity upon hydrolysis, therefore it is crucial to release aspirin in its stable form (Aubrey-Medendorp *et al.*, 2008).

The amount of chemically stable aspirin in the released samples and in the control aspirin solution in PBS is shown in **Figure 6.20.**

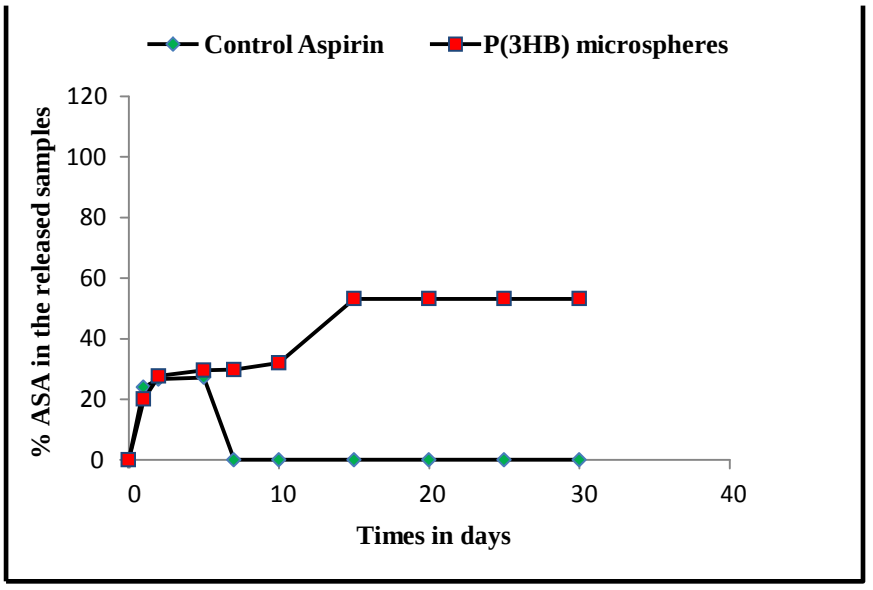

Figure 6.20: *In vitro* release profile of chemically stable aspirin in the released samples from the (a) P(3HB) microspheres with aspirin and (b) control aspirin standard for a period of 30 days (n=3).

At the end of the release period, 53.2% of chemically stable aspirin was released from P(3HB) microsphere samples with aspirin which was higher compared to the 27.2% of the chemically stable aspirin present in the control aspirin solution incubated under same conditions.

DISCUSSION

In this study, P(3HB) films and P(3HB) films containing aspirin were prepared using the solvent casting technique to investigate their potential as a drug delivery system for the controlled release of aspirin. Simultaneously, P(3HB) microspheres and P(3HB) microspheres containing aspirin were also produced using solid-in-oil-in water emulsion technique for the same purpose. The influence of aspirin loading on the microstructural, thermal and degradation properties of the P(3HB) films were studied. *In vitro* drug release rate were calculated. Similarly, the effect of aspirin loading on the surface, porosity, thermal and the degradation properties of the P(3HB) microspheres were also studied.

SECTION I

To detect the presence of aspirin within the P(3HB) matrix, FTIR analysis was carried out. The FTIR spectrum confirmed the presence of the aspirin within the P(3HB) matrix (Li *et al*., 1999).

Microstructural studies of the P(3HB) film with and without aspirin were studied using SEM. SEM images revealed that a new topography was introduced in the P(3HB) film with aspirin due to the addition of aspirin. Aspirin crystals were visible on the surface of the P(3HB) film. A similar observation was made where theophylline and salicylic acid crystals were visible on the surface of the chitosan films at a drug loading higher than 10% and 30% drug loading respectively. The authors stated that this was due to the crystallization of the theophylline crystals during the film processing (Puttipipatkhachorn *et al*., 2001). In a similar experiment carried out by Wang *et al*., bovine serum albumin (BSA) was added to the chitosan/poly-co-vinyl film. SEM images revealed that BSA loaded chitosan/poly-co-vinyl had a rough topography compared to the unloaded film (Wang *et al*., 2005). The results in this study indicated that aspirin crystals had crystallized during the processing of the film, thereby increasing the roughness of the film. This increase in the surface roughness of the P(3HB) film with aspirin was further analysed using AFM. AFM analysis confirmed that the presence of aspirin had increased the surface roughness of the film. Similar results were obtained when rifampicin was added to poly-co-vinyl film. There was an increase in the surface roughness of the poly-co-vinyl film compared to the unloaded film. The authors attributed this to the heterogenous dispersion of rifampicin within the

poly-co-vinyl matrix (Lee *et al*., 2007). Contrasting results were obtained in a study where the surface of the aspirin loaded polyesterurethane network appeared to have a smooth surface compared to the unloaded network. The authors attributed this to the homogenous dispersion of aspirin within the network. The authors also stated that the aspirin was present in an amorphous form within the network (Zhang *et al*., 2010). The results in this study indicated that the aspirin crystals were present in its crystalline form within the P(3HB) film.

Water contact angle measurements were carried out to study the effect of aspirin loading on the wettability of these P(3HB) films. The water contact angles of the P(3HB) film with and without aspirin were higher than 70° and hence, they were both considered to be hydrophobic in nature (Peschel *et al*., 2008). However, there was an increase in the hydrophilicity of the P(3HB) film due to the presence of aspirin. It is known that PHAs are hydrophobic in nature whereas aspirin is hydrophilic and has a water solubility of 3 mg/ml (Aubrey-Medendorp *et al*., 2008). Hence, we can conclude that the presence of aspirin within the P(3HB) film had increased the hydrophilic properties of the film. A similar observation was made where there was an increase in the hydrophilicity of the PVA membranes containing aspirin compared to the PVA membrane without aspirin. The authors also observed a decrease in the water contact angle with the increase in the concentration of aspirin within the membrane. They attributed this increase in the hydrophilicity to the presence of hydrophilic aspirin within the PVA membranes (Paul and Sharma, 1997). Similar findings were reported by Hwang *et al*., where the hydrophilic properties of the polyvinyl alcohol/dextran hydrogel was enhanced as a result of the addition of gentamicin which is hydrophilic in nature (Hwang *et al*., 2010). Addition of hydrophilic polyethylene glycol (PEG) to the hydrophobic PLLA film also enhanced the hydrophilic properties of the film (Lee *et al*., 2005). Studies in the past have shown that the increase in the surface roughness of the biomaterial leads to a decrease in the water contact angle (Elias *et al*., 2008). Therefore, in this particular study, the results indicated that the decrease in the water contact angle of the P(3HB) film with aspirin was due to the presence of the hydrophilic aspirin crystals on the surface of the film, causing an increase in the surface roughness.

Another characterisation that was done on the P(3HB) film samples with and without aspirin was the protein adsorption test. Total protein adsorbed on the P(3HB) film with aspirin was higher compared to the P(3HB) film without aspirin.

Several investigations have been made to understand the relationship between the surface roughness, wettability and protein adsorption (Elias *et al*., 2008). In an experiment conducted by Rechendorff *et al*., the surface of the tantalum samples were modified to increase their surface roughness. Due to the increase in the surface roughness, the surface area of the tantalum film samples also increased by around 20%. In order to study the effect of the surface roughness on the total protein adsorption, two different proteins such as fibrinogen and Bovine serum albumin (BSA) were adsorbed on to the tantalum films. The authors observed that there was 70% increase in the adsorption of the fibrinogen which was much higher compared to the increase in the surface area. In the case of BSA, there was 20% increase in the adsorption which corresponded to the increase in the surface area. The authors concluded that the increased fibrinogen adsorption was due to the protein anistropy caused due to the increase in the surface roughness. They attributed the low BSA adsorption to the post adsorption relaxation effects of BSA. The authors concluded that the total protein adsorption increased with the increase in the surface roughness when the roughness did not induce any confirmational changes on the structure of the protein (Rechendorff *et al*., 2006). Another study demonstrated an increase in the protein adsorption on the nanostructured titanium dioxide samples with the increase in the surface roughness. The authors observed that a rough topography led to protein aggregation within the pores, thereby creating protein nucleation sites. With the increase in the surface roughness, the number of the protein nucleation sites increased, thereby increasing the total protein adsorption (Scopelitti *et al*., 2010). Apart from the surface roughness, another reason for the increase in the protein adsorption could be the increase in the hydrophilicty of the P(3HB) films with aspirin compared to the films without aspirin. Misra *et al*., conducted an experiment where hydrophilic Bioglass™ particles were incorporated within P(3HB) composite films to improve the physical properties of the composite film. They observed a significant increase in protein adsorption on the P(3HB) composite films containing hydrophilic Bioglass™ particles compared to the plain P(3HB) films. They concluded that the increased protein adsorption was due to increased hydrophilicity and surface roughness of the P(3HB)/Bioglass™ particles composite films compared to the plain films (Misra *et al*., 2008). From these findings, we could conclude that the increase in the protein adsorption in the P(3HB) films with aspirin was due to the presence of hydrophilic aspirin crystals on

the surface of the film, thereby increasing its hydrophilicity and roughness. According to literature, it is known that protein adsoprtion regulates important processes such as cell adhesion, differentiation, *in vivo* inflammatory responses. Therefore, the results in this study indicating an increase in the total protein adsorption was considered to be an encouraging result. This would increase the biocompatibilty of these P(3HB) films with aspirin.

In order to study the effect of the degradation products of the P(3HB) film samples with and without aspirin on the HMEC-1 cells, indirect cytotoxicity testing was carried out. It is known that PHAs are bicompatible in nature and the degradation product of P(3HB) which is 3-hydroxybutyric acid is a natural metabolite present in the human blood at a concentration of 3-10 mg/100 mL of the blood (Hocking and Marchessault, 1998). The results of the cytoxicity tests confirmed that the degradation products of the P(3HB) films with and without aspirin were not toxic in nature. However, % cell viability was higher in the media containing aspirin. In an experiment conducted by Grosser and Schroder in 2003, vascular endothelial cells were grown in varying concentration of aspirin. They concluded that the presence of aspirin improved the integrity of the endothelial cells and also provided antioxidative protection by activating the nitric oxide-cGMP signalling pathway in the endothelial cells (Grosser and Schroder, 2003).

Thermal properties of the P(3HB) films with and without aspirin were analysed using DSC. The melting temperature (T_m) of the P(3HB) films with aspirin was lower compared to the P(3HB) films without aspirin. A peak at 136.0°C was detected during the heating scan which corresponded to the T_m of the commercial aspirin. A decrease in the T_m usually occurs when the crystalline region of the polymer is disrupted. This disruption could have occurred due to the presence of aspirin within the crystalline region of the film. The cold crystallization temperature (T_c) of the P(3HB) films with aspirin was lower compared to the P(3HB) films. The decrease in the T_c often occurs due to the decrease in the overall crystallinity of the film. This decrease in the T_c could be due to the presence of aspirin within the crystalline region of the polymer. The glass transition temperature (T_g) was lower compared to the P(3HB) films without aspirin. The decrease in T_g occurs due to the increased mobility within the amorphous region of the polymer. The decrease in the crystallinity causes an increase in the mobility of the amorphous region. This result is in agreement with an observation made by

Westedt *et al*., where the T_g of the PVA-g-PLGA film decreased with the addition of paclitaxel which is a hydrophilic drug. They explained that this decrease in the T_g was due to the drug being molecularly dispersed within the matrix of the polymer (Westedt *et al*., 2006). A similar observation was made by Glaessl *et al*., where there was a decrease in the T_g of the polymethylacrylate film with the increase in the loading percentage of metoprolol tartrate within the film (Glaessl *et al*., 2009). It is known that a weak interaction between the drug and the polymer could also lead to the the decrease in T_g of the drug loaded films (Alexis, 2005). There was a decrease in the melting temperature, glass transition and the crystallization temperature of the Poly(L-lactic acid) composites due to the addition of ibuprofen (Dagnon *et al*., 2009).

In vitro degradation study was carried out on the P(3HB) film samples with and without aspirin to examine the effect of aspirin on the degradation properties of the P(3HB) films. The percentage of water absorbed (%WA) by the P(3HB) films with and without aspirin were measured. Previously in this study, it was found that the addition of aspirin molecules within the P(3HB) films increased the hydrophilic properties of the film. The presence of the hydrophilic drug could have lead to the increased water uptake. This progressive increase in the water uptake, with time, by the P(3HB) films with aspirin could be due to the desorption of the aspirin crystals present on the surface of the film, creating pores and water channels (Bazzo *et al.,* 2009). Similar results were obtained when hydrophilic dexamethasone was incorporated within the chitosan films. The presence of dexamethasone improved the surface wettability of the chitosan films, thereby increasing the water uptake (Rodrigues *et al*., 2009). The addition of hydrophilic paclitaxel within the polyvinyl alcohol grafted poly(lactic-co-glycolactic) or (PVA-g-PLGA) film accelerated their water absorption when incubated in PBS media (Westedt *et al*., 2006). In this study, P(3HB) films with aspirin demonstrated increased water absorption compared to the P(3HB) films without aspirin. The percentage of water absorbed (%WA) by the P(3HB) films with and without aspirin were measured. From the data, it was clear that the % weight loss was higher in the P(3HB) film containing aspirin compared to the P(3HB) film without aspirin. This was in agreement with the finding reported by Naraharisetti *et al*., that the water absorption is directly proportional to the progressive degradation of the material (Naraharisetti *et al*., 2005). A similar observation was made by Giunchedi *et al*.,

where the rate of degradation of the PLGA microparticle accelerated with the incorporation of diazepam, compared to the unloaded PLGA microparticle (Giunchedi *et al*., 1998).

Zhang *et al*., demonstrated an increase in the degradation rate of the polyesterurethane network loaded with the aspirin. They attributed this to the increase in the hydrophilicity of the polyesterurethane network due to the presence of aspirin. The authors also stated that upon water absorption, aspirin which is an acidic drug (pka = 3.49) dissociated within the polyesterurethane network, affecting the pH of the drug loaded polyesterurethane network, thereby accelerating its degradation (Zhang *et al*., 2010). In this study, P(3HB) film samples with and without aspirin were incubated in the PBS media devoid of any enzymes, therefore degradation occurred via hydrolysis.

In vitro drug release studies were carried out to measure the drug release rates using HPLC. Burst release of 12.5± 7% was observed on day 1. This could be due to the presence of surface bound aspirin (Kassab *et al.,* 1997). This burst release was much lower compared to the PLGA based *in situ* gel delivery system for aspirin which showed a burst release of 30.9±1.2% (Tang and Singh, 2008). It is known that there are three main mechanisms of drug release from the biodegradable polymers. The first mechanism involves the release of drug which is covalently bound to the polymer backbone. The release occurs when the polymer backbone is hydrolytically cleaved. The second mechanism involves the release of drugs due to polymer degradation. The third mechanism involves the release of drugs from the polymer matrix via diffusion, combined with surface erosion (Dash and Suryanarayanan, 1992). The drug release rate is dependent on the type of encapsulated drug, the polymer used and the mode of release (Poletto *et al.,* 2007). In this study, sustained release of aspirin was obtained throughout the period of release. The drug release pattern demonstrated that the release of aspirin was slow until the 7th day. This was due to the release of drugs via surface erosion. The increase in the water uptake due to the presence of hydrophilic aspirin crystals would have most likely led to increased degradation causing an accelerated drug release after the 7th day.

SECTION II

In the second part of this study, P(3HB) microsphere with and without aspirin were synthesised. FTIR analysis was not able to detect the presence of aspirin within these microspheres. Therefore, encapsulation efficiency study was carried out to determine and quantify the amount of aspirin encapsulated within the microspheres. The encapsulation efficiency of the P(3HB) microspheres with the average size of 30 μm was found to be 50%. It is a known fact that the increase in the encapsulation efficiency prevents the loss of the drug and increases the dosage of the treatment (Freiberg and Zhu, 2004). One of the factors that affect the encapsulation efficiency is the microsphere size. Previous studies showed that with the decrease in the size of the microspheres, there was an increase in encapsulation efficiency. The encapsulation efficiency of the P(3HB-co-3HV) microspheres with an average size of 399 μm was 20.2% compared to 30.1% exhibited by the microspheres with the average size of 340 μm (Sendil *et al.,* 1999). Yang *et al*., demonstrated that the encapsulation efficiency was dependent on the microsphere preparation temperature. They observed 50% encapsulation at both high (38°C) and low temperature (4°C). They stated that the sphere and the water were immiscible at a low temperature causing drug encapsulation within the rapidly forming sphere wall during the evaporation process. They also observed that at a high temperature, solvent evaporation occurred rapidly, causing the hardening of the sphere wall (Yang *et al*., 2000). Another factor that influences the encapsulation efficiency is the concentration of the polymer within the organic phase. Previous studies have shown an increase in the encapsulation efficiency with the increase in polymer concentration within the organic phase (Ghaderi *et al*., 1996). One of the studies demonstrated that the encapsulation efficiency was dependent on the type of the polymer used for the synthesis of the microspheres. 46% and 21% encapsulation efficiency were obtained for the PGA and PLGA microspheres respectively. They were prepared under identical conditions. They explained that this could be due to the faster precipitation of PGA (Le Corre *et al*., 1994).

Microstructural studies of the P(3HB) microspheres with and without aspirin were carried out using SEM**.** The SEM images revealed that the surface morphology of the P(3HB) microspheres without aspirin were rough and porous compared to the P(3HB) microspheres with aspirin. The surface property of the microspheres is hugely influenced by the type of the solvent used. In this study, dichloromethane

was used as the solvent to dissolve P(3HB) during the preparation of the microspheres as aspirin as well as P(3HB) were soluble in dichloromethane. Dichloromethane has a miscibility of 1 in 50 parts in water compared to the other solvents such has chloroform, which has a miscibility of 1 in 200 parts (Sahoo *et al.,* 2002). Similar results were obtained by Yang *et al.,* when dichloromethane was used during the preparation of PCL and PLGA microspheres (Yang *et al.,* 2000). On the contrary, uniform spherical P(3HB) microspheres were obtained by Francis *et al.,* when chloroform was used as the solvent for the fabrication of P(3HB) microspheres (Francis *et al.,* 2011). Apart from the type of the solvent used, the volume of the solvent used during the synthesis of the microspheres is known to affect the surface morphology of the microspheres. If the volume of the solvent is lower than the optimal volume, the water molecules trapped on the surface, as well as within the microspheres, evaporate leaving a rough topography. The porosity studies confirmed that the encapsulation of aspirin within the P(3HB) microspheres reduced their porosity. The entrapment of drug within the pores of the polymer could have led to this decrease in the porosity of the P(3HB) microspheres with aspirin (Chee *et al.,* 2008). This could also explain the initial burst release of the encapsulated drug when the microspheres were immersed in the release medium. Previous studies have shown that porosity is an important factor in determining the rate of drug release. Rate of drug release is faster when the porosity is higher (Yang *et al*., 2000). Another study demonstrated a decrease in the porosity of the microspheres by replacing water with methanol in the first emulsion phase (Tuncay *et al*., 2000). Previous studies have shown that the rate of the solvent evaporation during the microsphere synthesis also directly affects the porosity of the spheres (Freiberg and Zhu, 2004).

The surface hydrophobicity of P(3HB) microspheres with aspirin were measured. Higher concentration of hydrophilic Rose Bengal dye was bound to the surface of the P(3HB) microspheres with aspirin compared to the P(3HB) microspheres without aspirin. This showed that the presence of aspirin, which is hydrophilic in nature, within the microspheres increased the wettability of the P(3HB) microspheres. Another reason for this increased hydrophilicity could also be the presence of residual PVA on the surface of the microspheres. PVA is hydrophilic in nature and it was used in this study as an emulsifier during the synthesis of the microspheres. Even though, the microspheres were prepared in 0.8% of PVA,

higher amount of residual PVA could have been present on the surface of the microspheres with aspirin. In future, determination of the residual PVA concentration on the P(3HB) microspheres with and without aspirin would explain the effect of aspirin loading on the residual PVA concentration. One study demonstrated an increased Rose Bengal dye binding on the surface of the PLGA microspheres with higher residual PVA concentration on the microspheres (Sahoo *et al*., 2002).

Another characterisation that was done on the P(3HB) microspheres with and without aspirin was the protein adsorption test. The total amount of protein adsorbed on to the P(3HB) microspheres with aspirin was higher compared to the protein adsorbed on to the microspheres without aspirin. Microspheres have a large surface area and therefore when injected within the human body, they come in contact with the extensive area within the body. Incompatibility of the microspheres would lead to a strong immune reaction (Shishatskaya *et al*., 2002). Previous studies have shown that protein adsorption enhances cellular processes such as cell adhesion and migration, thereby increasing the compatibility of the biomaterial with the mammalian cells which are anchorage dependent in nature (Keselowsky *et al*., 2003). One of the important factors that influence protein adsorption is surface hydrophilicity. Previously, in this study, we found that the P(3HB) microspheres with aspirin were more hydrophilic compared to the P(3HB) microspheres without aspirin. Therefore, this increase in the adsorption of the protein could have occurred due to the hydrophilic surface of the microspheres with aspirin. A similar observation was made by Francis *et al.,* when hydrophilic gentamicin was loaded within the P(3HB) microspheres. The protein adsorption was much higher in the presence of the drugs compared to the unloaded P(3HB) microspheres. This increase was thought to be due to the hydrophilic surface of the gentamicin loaded P(3HB) microspheres (Francis *et al.,* 2011). The increase in the protein adsorption by the P(3HB) microspheres containing aspirin was considered to be an encouraging result.

In order to examine the effect of aspirin encapsulation on the thermal properties of P(3HB) microspheres, properties such as the melting temperature (T_m), glass transition temperature (T_g) and the crystallization temperature(T_c) of the P(3HB) microspheres with and without aspirin were analysed using DSC. The T_m, T_c, and T_g of the microspheres with aspirin were lower compared to the microspheres.

Without aspirin. The decrease of 8.4°C in the T_m of the P(3HB) microspheres with aspirin indicated that the drug was encapsulated within the crystalline structure of the polymer, hence interrupting the crystal structure. Due to this disruption of the crystalline structure, there was a decrease in the overall crystallinity of the polymer, which led to the decrease in the T_c of the P(3HB) microspheres with aspirin. The T_g of the P(3HB) microspheres with aspirin were lower compared to the P(3HB) microspheres without aspirin. The decrease in the T_g usually occurs when there is an increased mobility within the amorphous region of the polymer. This decrease in the T_g indicated that the presence of aspirin within the crystalline region of the polymer and the overall decrease in the crystallinity of the polymer, led to an increased mobility of the amorphous region of the polymer. There was a decrease in the melting temperature of the aspirin. Previous studies have shown that the change in the thermal properties of the microspheres, due to the addition of any drug indicates an interaction between the polymer and the drug (Sahoo *et al*., 2005). This indicated an interaction between the aspirin and the P(3HB) polymer. Bidone *et al.,* demonstrated a decrease in the melting temperature of the ibuprofen when encapsulated within P(3HB) microspheres. The authors stated that this decrease in the melting temperature of the ibuprofen was due to the presence of ibuprofen within the microsphere in both amorphous and crystalline forms. The authors also reported the decrease in the T_g and T_c of the ibuprofen loaded microspheres compared to the unloaded P(3HB) microspheres. They explained that the presence of ibuprofen affected the crystalline structure of the P(3HB) (Bidone *et al.,* 2009). Another study demonstrated a decrease in the T_g and T_m of the PLLA-PLGA microspheres loaded with etanidazole compared to the unloaded microspheres (Lee *et al*., 2002). A similar observation was made by Francis *et al.,* when gentamicin was incorporated within the P(3HB) microspheres. There was a decrease in the crystallinity of the polymer causing a decrease in the T_m of the gentamicin loaded P(3HB) microspheres, compared to the unloaded microspheres (Francis *et al.,* 2011). Berthold *et al*., used DSC to detect the modification of drug within the chitosan microspheres. They observed a sharp peak at 341.9°C, indicating the T_m of the prednisolone which was encapsulated within the chitosan microspheres. The authors stated that there was no interaction between the drug and the chitosan. Therefore, in this study there was an interaction between the aspirin molecules and P(3HB) (Berthold *et al*., 1996).

In vitro degradation studies were carried out on the P(3HB) microsphere samples with and without aspirin to examine the effect of aspirin on the degradation properties of the P(3HB) microspheres. The percentage of water absorbed (%WA) by the P(3HB) microspheres with and without aspirin were measured**.** The % water absorbed by the P(3HB) microspheres with aspirin was much higher compared to the P(3HB) microspheres without aspirin. Aspirin is a hydrophillic drug and therefore, this could have lead to the increased water uptake. Previously in this study, it was found that the aspirin molecules were trapped within the pores of the polymer. After the dissolution of aspirin in the release media, water channels were created within the microspheres. This progressive increase in the water uptake with time could be due to the increase in the network of these water channels created during drug dissolution (Bazzo *et al.,* 2009). Similar results were obtained by Francis *et al.,* where there was an increase in the water uptake by the gentamicin loaded P(3HB) microspheres compared to the unloaded microspheres (Francis *et al.,* 2011). Bazzo *et al.,* stated that there was an increase in the water absorption by the piroxicam loaded P(3HB) microspheres compared to the unloaded microspheres. They concluded that this rapid uptake of water by the microspheres occurred when the drugs trapped within the pores of the microsphere created a network of water channels during its dissolution in the release media (Bazzo *et al.,* 2009). Percentage weight loss (%WL) of P(3HB) microspheres with and without aspirin were also measured**.** From the data, it was clear that the % weight loss was higher in the P(3HB) microspheres with aspirin compared to the P(3HB) microspheres without aspirin. In this study, the P(3HB) microsphere samples with and without aspirin were incubated in the PBS media. Previous studies have shown that water absorption is directly proportional to the progressive degradation of the material (Naraharisetti *et al*., 2005). The rapid ingress of water through the network of water channels created within the microspheres would have accelerated the hydrolytic degradation of the polymer (Bazzo *et al.,* 2009). In future, molecular weight analysis by gel permeation chromatography would confirm the effect of aspirin loading on the degradation of the P(3HB) microspheres .

According to literature, the drug release kinetics are affected by several factors such as the structure of the drug delivery vehicle, type of the drug and the properties of the polymer such as its molecular weight, crystallinity and its mode of

degradation. It is known that a drug release pattern demonstrating a constant release of drug with respect to time without any burst release effect is desirable (Freiberg and Zhu, 2004). *In vitro* drug release studies were carried out to measure the drug release rates from the P(3HB) microspheres using HPLC. 86.6% of the total drug encapsulated within the P(3HB) microspheres was released within 15 days of the release period. From the drug release pattern, it appeared that the drug dissolution occurred through the water channels created within the microspheres. It is known that P(3HB) is very crystalline in nature and the mode of drug release from the P(3HB) matrix usually depends upon the morphology of the drug delivery matrix (Bidone *et al*., 2009). According to the literature, it is known that the size of the particle is inversely proportional to the surface area available for the drug release. Therefore, faster drug release rate is obtained for the particles of smaller size offering a large surface area for the drug release (Sahoo *et al*., 2005). In one experiment, isosorbide dinitrate was encapsulated within the P(3HB) microspheres at 3% drug loading. The average diameter of the P(3HB) microspheres obtained was 0.85 μm which was exceptionally small compared to the avarage size of 30 μm obtained in this study. The porosity of 72% of the isosorbide dinitrate loaded P(3HB) microspheres was much higher compared to the 39% porosity of the P(3HB) microspheres with aspirin obtained in this study. The authors observed that the 80% of the encapsulated drug was released within the 12 hours of incubation. They concluded that these isosorbide dinitrate P(3HB) microspheres were unsuitable for parenteral applications due their fast drug release rate (Kim *et al*., 2000b). Another factor that plays a significant role in the drug release rate is the % porosity (Freiberg and Zhu, 2004). Previous studies have shown that the drug release rate is affected by the porosity of the microspheres. Several researchers have observed an increase in the drug release rates with the increase in the porosity of the drug delivery matrix (Ghaderi *et al*., 1996; Yang *et al*., 2000). In another study, ibuprofen encapsulated within the P(3HB) microspheres with 16% drug loading observed and with an average diameter of 22 μm showed a burst release of 21.63%, within 1 hour of the incubation. The total release of the drug was obtained within 33 hours of incubation. There was no mention of the porosity of the drug loaded microspheres, however, the SEM images revealed a highly porous surface with large pores (Bidone *et al*., 2009). The drug release observed in this study was much slower compared to the previous findings. However, in comparison to the aspirin release rates from the P(3HB) film, aspirin release was much faster from the

microspheres. This confirmed that the drug release rate depends on the morphology of the drug delivery vehicle.

From the results obtained, we could conclude that both P(3HB) films and microspheres could be used for the controlled drug release. However, P(3HB) film is more suitable for long term drug release studies. A further investigation into the antithrombotic effect of the released aspirin from the P(3HB) film and microspheres is crucial to establish their potential use as a controlled delivery system for aspirin.

Chapter 7

Conclusions and Future work

7.1 CONCLUSION

Polyhydroxyalkanoates have become one of the most attractive biomaterials in recent times. They are biodegradable, biocompatible and sustainable. There is a huge interest in the commercial exploitation of these PHAs (Hazer and Steinbuchel, 2007; Khanna and Srivastava, 2005). However, one of the major hindrances in the commercialization of these PHAs is its high price. Some of the most effective strategies to reduce the cost of the PHA production have been the use of cheap carbon sources, the use of metabolically engineered strains, efficient mode of fermentation and the use of statistical mode of optimisation (Lee *et al.,* 2005; Hong *et al*., 2009).

The first part of this project involved the economical production of MCL-PHAs using renewable and cheap carbon sources such as sugarcane molasses, biodiesel waste and pure glycerol. *Pseudomonas* spp have been known to produce MCL-PHAs. They utilize both structurally related and unrelated carbon sources and accumulate diverse MCL-PHA monomer units (Diard *et al.*, 2002). Therefore, in this study *P. mendocina* was the chosen organism. Using sugarcane molasses as the sole carbon source, a PHA yield of 20% dcw was obtained. The polymer was identified using FTIR and GC-MS. It was found to be a MCL-PHA copolymer containing 3HO and 3HD monomer units. The results demonstrated that sugarcane molasses was a promising carbon source for the production of MCL-PHAs. *P. mendocina* also utilized biodiesel waste rich in glycerol, fatty acids and fatty acid methyl esters to produce MCL-PHAs containing 3-hydroxydecanoate (3HD) monomer units. A PHA yield of 43.2% dcw was obtained. This was an encouraging result which confirmed that biodiesel waste could be used as a carbon source for the production of MCL-PHAs. In this study, *P. mendocina* was also cultivated in a medium containing pure glycerol for the production of PHAs. The results obtained were compared with that of the glycerol rich biodiesel waste. A PHA yield of 10.5% dcw was obtained, which was lower compared to the PHA yield in the biodiesel waste. However, the polymer produced was also identified to be MCL-PHA containing 3HD monomer units. These results demonstrated that *P. mendocina* was capable of utilising sugarcane molasses, biodiesel waste and pure glycerol as the feedstock for the production of PHAs. The use of these inexpensive carbon sources could effectively reduce the cost of the production of PHAs and hence enhance its utilisation in various applications.

One of the main objectives of this research project was to utilize the PHA produced for various biomedical applications. To fulfill this, multifunctional novel P(3HO)/bacterial cellulose 2D composite films were developed focusing on the potential use of these composite films as scaffolds for tissue engineering. Bacterial cellulose was used as a reinforcing agent to enhance the mechanical properties of P(3HO). It was produced successfully using *A. xylinum,* which was then subjected to an acetylation reaction in order to increase the miscibility of bacterial cellulose with the hydrophobic P(3HO) matrix. Neat P(3HO), P(3HO)/5% bacterial cellulose, P(3HO)/15% bacterial cellulose and P(3HO)/25% bacterial cellulose composite films were prepared by solvent casting. The composite films were characterised in order to evaluate the effect of these cellulose microcrystals on the properties of the polymer. The results obtained emphasized the role of these cellulose crystals in enhancing the mechanical properties of these composite films. Mechanical properties such as the Young's modulus or 'E' values of the bacterial cellulose films increased with the addition of the cellulose microcrystals in the composite films compared to the neat P(3HO) film. The tensile strength of all the bacterial cellulose microcrystal composite films were found to be higher compared to the neat P(3HO) film. According to the wettability studies, there was a decrease in the water contact angle of the composite films compared to the neat P(3HO) films, due to the incorporation of the cellulose microcrystals, indicating an increase in the hydrophilicity of the composite film. P(3HO)/25% bacterial cellulose composite films with the highest Young's modulus value and a relatively higher hydrophilicity, known to favour cell adhesion, was chosen for further characterisation. Microstructural studies revealed that the incorporation of cellulose microcrystals had added a new surface topography to P(3HO)/25% bacterial cellulose composite films. These results were also confirmed by White light interferometry which demonstrated that there was an increase in the surface roughness of the composite films compared to the neat P(3HO) film. From the *in vitro* degradation studies, it was found that the inclusion of the acetylated cellulose microcrystals in the P(3HO) films increased the degradation rate of the composite films in comparison to the neat P(3HO) films in both PBS and DMEM media. Finally, cell proliferation studies were carried out using the HMEC-1 cells over a period of 1, 4 and 7 days, which demonstrated the biocompatibility of the P(3HO)/bacterial cellulose composite and neat P(3HO) films. The cell growth and proliferation on the composite films was higher compared to the neat P(3HO) film at day 7. These results indicated that

these novel P(3HO)/bacterial cellulose composites would be well suited for tissue engineering applications. Biocompatibility is one of the most important features of an excellent tissue engineering scaffold. The cell culture data obtained from this study revealed promising results by demonstrating good cell growth and proliferation on the composites.

In this part of the study, P(3HB) was produced by *B. cereus* SPV using the Kannan and Rehacek media, in a batch mode. The polymer produced was identified as P(3HB) using FTIR and GC. In addition, novel, multifunctional 2D P(3HO)/P(3HB) blend films with varying percentages of P(3HO) and P(3HB) such as P(3HO)/P(3HB) 80:20, P(3HO)/P(3HB) 50:50 and P(3HO)/P(3HB) 20:80 were developed to assess their suitability in the development of biodegradable stents and scaffolds in tissue engineering. These blend films were characterised with respect to their mechanical, thermal and surface properties. They were also characterised for their bioactivity using HMEC-1 cells and their degradation properties. The results highlighted that the addition of P(3HB) within the P(3HO) matrix enhanced the mechanical and thermal properties of these blend films compared to the neat P(3HO) film. P(3HB) played a significant role in introducing a new surface topography thereby increasing the surface roughness compared to the neat P(3HO) film. The hydrophilicity of these blend films increased by lowering the water contact angle. The addition of P(3HB) also affected the total protein adsorption on the blend films. Protein adsorption plays an important role in cell adhesion and survival. Hence, protein adsorption is crucial in evaluating a biomaterial for tissue engineering applications (Rai *et al*., 2011). Protein adsorption was higher in the blend films containing P(3HB) compared to the neat P(3HO) film. Indirect cytotoxicity results showed that these blend films were not toxic to the HMEC-1 cells. The % cell viability on the blend films was higher compared to the neat P(3HO) film. From the *in vitro* degradation studies, it was found that the presence of P(3HB) increased the degradation rate of the blend films compared to the neat P(3HO) film. The results of the cytocompatibility assessment demonstrated increased biocompatibility of these blends with the HMEC-1 cells. Hence, these properties make these blends an attractive biomaterial for a range of medical applications. The standard reference for the mechanical properties desired for a stent development is SS316L stainless steel. It is the most commonly used material for the development of vascular stents. It has a tensile strength, Young's modulus value and % elongation at break value of

490 MPa, 193 GPa and 40% respectively. It has a radial strength value of 135 KPa. Radial strength is key in determining the success of the stent after its implantation within the body. In order to meet the clinical requirements, the radial strength value should be in a range of 80-120 KPa (Feng *et al*., 2011). With further improvement in mechanical properties, these novel blends could be used for the development of biodegradable stents. They could also be used as scaffolds for tissue engineering applications.

It is a known fact that surface topography determines the biocompatibility of a biomaterial by governing various important processes and properties such as the protein adsorption, wettability, cell adhesion, proliferation and migration (Duncan *et al*., 2007). To improve the biocompatibility of the P(3HO)/P(3HB) 50:50 blend film with the HMEC-1 cells, the blend films were surface functionalized using the laser micropatterning technique. In this study, HMEC-1 cells were grown on the micropatterned P(3HO)/P(3HB) 50:50 blend films to assess the influence of micropatterning on cell growth and proliferation. These micropatterned blend films were also characterised with respect to their mechanical and surface properties. The results highlighted the role of micropatterning towards the addition of a new topography, thereby increasing the surface roughness and also increasing hydrophilicity by lowering the water contact angle in the blend films compared to the unfabricated blend films. In this study, there was an increase in the total protein adsorption in the farbricated blend film compared to the unfabricated P(3HO)/P(3HB) 50:50 blend film. The effect of the laser surface micropatterning on the mechanical properties of the blend films was not drastic. This demonstrated that the bulk properties of the blend film remained intact. The cell viability assay using Neutral Red assay was carried out at the end of day 1, 4 and 7. There was an increased cell adhesion on the fabricated blend film samples compared to the unfabricated blend film samples. The SEM images demonstrated the oriented growth of the HMEC-1 cells along the microgrooves on the surface of the blend film. Hence, these results demonstrated that surface micro-patterning can be successfully used to enhance cell attachment and proliferation as well as cell alignment which is a highly desirable outcome.

Furthermore, investigation of the P(3HO)/P(3HB) 50:50 2D blend film as the base material for the development of a drug eluting biodegradable stent was carried out by incorporating aspirin within this blend film. This drug P(3HO)/P(3HB) 50:50

blend film with aspirin was characterised for its mechanical properties, thermal and surface properties, in order to investigate the effect of the drug loading on the properties of the blend film. The effect of aspirin loading on the biocompatibility and the degradation properties of the blend films were investigated. A drug release study to measure the release of aspirin was carried out using High performance Liquid Chromatography (HPLC). Microstructural studies revealed that the addition of aspirin within the blend films introduced a new surface topography. Water contact angle study of the blend films with aspirin showed increase in the hydrophilicity by lowering the water contact angle. This was followed by a significant increase in the total protein adsorption which was higher than the film without aspirin. Cytotoxicity assessment of the blend films with aspirin demonstrated higher cell viability compared to the blend films without aspirin. This increase in the biocompatibility of the blend films due to the incorporation of the aspirin is a huge step forward towards preventing in stent restenosis by accelerating the reendothelialisation process. Surprisingly, addition of aspirin in the blend films had a drastic effect on their mechanical properties. The tensile strength and the Young's modulus values of the films with aspirin were lower compared to blend films without aspirin. However, the % elongation at break values was higher, indicating an increase in the flexibility with the addition of aspirin. It is crucial for a stent to demonstrate excellent mechanical properties to provide support to the injured artery for a considerable amount of time, required for the complete healing of the artery. There was a decrease in the melting, glass transition and the crystallization temperature of the blend films with aspirin respectively compared to the blend films without aspirin. One of the most important features of the drug eluting biodegradable stent is the controlled release of the drugs. Drug release studies showed that there was a controlled release of chemically stable aspirin from the blend films, throughout the release period. On the basis of the outcome of this study, we can conclude that the P(3HO)/P(3HB) 50:50 blend films could be used for various applications such as a drug delivery vehicle for sustained drug release applications and as a biodegradable scaffold for tissue engineering. However, their potential application as a base material for the development of drug eluting biodegradable stents can only be achieved with a significant improvement in their mechanical properties.

Finally, a drug delivery system for the controlled delivery of aspirin was successfully developed. P(3HB) films with and without aspirin were prepared using the solvent casting technique to investigate their potential as a drug delivery system for the controlled release of aspirin. Simultaneously, P(3HB) microspheres with and without aspirin were also produced using solid-in-oil-in water emulsion technique for the same purpose. From the drug release pattern, we could conclude that the P(3HB) films could be used for the sustained long term drug release, whereas the P(3HB) microspheres were more suitable for fast release.

7.2 Future work

Based on the results of this particular study, there are several potential areas that could be investigated in the future.

7.2.1 Statistical optimisation of the MCL-PHA production using cheap carbon sources

Statistical method such as response surface analysis could be used to optimize the production of MCL-PHAs using the cheap carbon sources to achieve higher yield. Further, optimisation using different modes of fermentation such as fed batch would also be interesting.

7.2.2 P(3HO)/bacterial cellulose composites

The surface fabrication of these composite films using Laser micropatterning technique and culturing of different cell lines on these modified surfaces would be an interesting area of research. Apart from the 2D films, construction of 3D scaffolds for other biomedical applications such as cartilage tissue engineering would be of interest.

7.2.3 P(3HO)/P(3HB) blends

In this study, a stent prototype was successfully developed. However, due to lack of time it could not be fully characterised. Development of a stent prototype with a novel stent design and its complete characterisation would be very interesting and relevant. Incorporation of anti-mitotic drugs such as paclitaxel within the stent prototype and monitoring their drug release pattern would be the next step forward. Cell culture and degradation studies of these stent prototypes would be of interest. Finally, *in vivo* studies using these stent prototypes would be of great interest.

7.2.4 Development of controlled drug/gene/active factor delivery systems

In this study, P(3HB) films and microspheres were successfully produced for the controlled release of aspirin. In future, a wide range of geometries could be synthesized such as rods, capsules, compressed tablets and nanospheres for controlled drug delivery. Apart from drug delivery, they could also be used for gene transfer. Another interesting area of research would be the encapsulation of multiple drugs.

7.2.5 Development of drug loaded stents and their characterisation

In this study, P(3HO)/P(3HB) blend films were synthesized for their use in the development of biodegradable stents. In future, the mechanical properties of these blend films could be significantly improved with the addition of filler materials such as nano bioglass or by blending with other synthetic polymers such as PLLA. Stent design or architecture and their mechanical characterisation such as collapse pressure measurements is another important and a very interesting area of research. Addition of drugs such as Sirolimus, also known as rapamycin (immunosuppressant) within the stent structure and monitoring their release would be of great interest. *In vitro* as well as *in vivo* studies to assess the performance of these drug loaded stents could be carried out.

REFERENCES

Acharya, G. & Park, K. 2006. Mechanisms of controlled drug release from drug-eluting stents. *Advanced Drug Delivery Reviews,* 58**,** 387-401.

Agrawal, C. M. & Clark, H. G. 1992. Deformation Characteristics of a Bioabsorbable Intravascular Stent. *Investigative Radiology,* 27**,** 1020-1023.

Ahn, W. S., Park, S. J. & Lee, S. Y. 2000. Production of Poly(3-Hydroxybutyrate) by Fed-Batch Culture of Recombinant *Escherichia coli* with a Highly Concentrated Whey Solution. *Applied and Environmental Microbiology,* 66**,** 3624-3627.

Akaraonye, E., Moreno, C., Knowles, J. C., Keshavarz, T. & Roy, I. 2012. Poly (3-hydroxybutyrate) production by *Bacillus cereus* SPV using sugarcane molasses as the main carbon source. *Journal of Biotechnology,* 7**,** 293-303.

Akiyama, M., Tsuge, T. & Doi, Y. 2003. Environmental life cycle comparison of polyhydroxyalkanoates produced from renewable carbon resources by bacterial fermentation. *Polymer Degradation and Stability,* 80**,** 183-194.

Alexis, F. 2005. Factors affecting the degradation and drug-release mechanism of poly (lactic acid) and poly [(lactic acid)-co-(glycolic acid)]. *Polymer International,* 54**,** 36-46.

Alias, Z. & Tan, I. K. P. 2005. Isolation of palm oil-utilising, polyhydroxyalkanoate (PHA)-producing bacteria by an enrichment technique. *Bioresource Technology,* 96**,** 1229-1234.

Allen, T. M. & Cullis, P. R. 2004. Drug Delivery Systems: Entering the Mainstream. *Science,* 303**,** 1818-1822.

Al-Salihi, K. A. & Samsudin, A. R. 2004. Bone marrow mesenchymal stem cells differentiation and proliferation on the surface of coral implant. *The Medical Journal of Malaysia*, 59, 45-46.

Anderson, A. J. & Dawes, E. A. 1990. Occurrence, metabolism, metabolic role, and industrial uses of bacterial polyhydroxyalkanoates. *Microbiological Reviews,* 54**,** 450-472.

Anderson, D. E. J. & Hinds, M. T. 2011. Endothelial cell micropatterning: methods, effects and applications. *Annual Biomedical Engineering,* 39(9), 2329-2345.

Arima, Y. & Iwata, H. 2007. Effect of wettability and surface functional groups on protein adsorption and cell adhesion using well-defined mixed self-assembled monolayers. *Biomaterials,* 28**,** 3074-3082.

Ashby, R., Solaiman, D. Y. & Foglia, T. 2004. Bacterial Poly(Hydroxyalkanoate) Polymer Production from the Biodiesel Co-product Stream. *Journal of Polymers and the Environment,* 12**,** 105-112.

Ashby, R. D. & Foglia, T. A. 1998. Poly(hydroxyalkanoate) biosynthesis from triglyceride substrates. *Applied Microbiology and Biotechnology,* 49**,** 431-437.

Ashby, R. D., Nunez, A., Solaiman, D. K. & Foglia, T. A. 2005. Sophorolipid biosynthesis from a biodiesel co-product stream. *Journal of the American Oil Chemists' Society,* 82**,** 625-630.

Asrar, J., Valentin, H. E., Berger, P. A., Tran, M., Padgette, S. R. & Garbow, J. R. 2002. Biosynthesis and Properties of Poly(3-hydroxybutyrate-co-3 hydroxyhexanoate) Polymers. *Biomacromolecules,* 3**,** 1006-1012.

Athanasiadis, I., Boskou, D., Kanellaki, M., Kiosseoglou, V. & Koutinas, A. A. 2002. Whey Liquid Waste of the Dairy Industry as Raw Material for Potable Alcohol Production by Kefir Granules. *Journal of Agricultural and Food Chemistry,* 50**,** 7231-7234.

Aubrey-Medendorp, C., Parkin, S. & Li, T. 2008. The confusion of indexing aspirin crystals. *Journal of Pharmaceutical Sciences,* 97**,** 1361-1367.

Baptist, J. N. & Ziegler, J. B. 1965. Method of making absorbable surgical sutures from poly beta hydroxyl acids. *U. S. Patent No*. 3225766

Barud, H. S., de Araujo Junior, A. M., Santos, D. B., de Assuncao, R., Meireles, C. S., Cerqueira, D. A., Rodrigues Filho, G., Ribeiro, C. A., Messaddeq, Y. & Ribeiro, S. J. 2008. Thermal behavior of cellulose acetate produced from homogeneous acetylation of bacterial cellulose. *Thermochimica acta,* 471**,** 61-69.

Basnett, P. & Roy, I. 2010. Microbial production of biodegradable polymers and their role in cardiac stent development. *Current Research in Technology and Education Topics in Applied Microbiology and Microbial Biotechnology*, 1405-1415.

Basnett, P., Knowles, J. C., Pishbin, F., Smith, C. , Keshavarz, T., Boccaccini, A. R. & Roy I. 2012. Novel Poly(3-hydroxyoctanoate)/Bacterial Cellulose Composites as potential materials for biodegradable stent. *Advanced Biomaterials.* 14, 6 330–343.

Bazzo, G.,Lemos-Senna, E. & Pires, A. 2009. Poly(hydroxybutyrate)/chitosan/ketoprofen or piroxicam composite microparticles: Preparation and controlled drug release evaluation. *Carbohydrate Polymers,* 77**,** 839-844.

Berthold, A., Cremer, K. & Kreuter, J. 1996. Preparation and characterization of chitosan microspheres as drug carrier for prednisolone sodium phosphate as model for anti-inflammatory drugs. *Journal of Controlled Release,* 39**,** 17-25.

Bhatt, R., Shah, D., Patel, K. C. & Trivedi, U. 2008. PHA–rubber blends: Synthesis, characterization and biodegradation. *Bioresource Technology,* 99**,** 4615-4620.

Bidone, J., Melo, A. P. P., Bazzo, G. C., Carmignan, F., Soldi, M. S., Pires, A. T. N. & Lemos-Senna, E. 2009. Preparation and characterization of ibuprofen-loaded microspheres consisting of poly(3-hydroxybutyrate) and methoxy poly (ethylene glycol)-b-poly (D,L-lactide) blends or poly(3-hydroxybutyrate) and gelatin composites for controlled drug release. *Materials Science and Engineering,* 29**,** 588-593.

Bier, J. D., Zalesky, P., Li, S. T., Sasken, H. & Williams, D. O. 1992. A New Bioabsorbable Intravascular Stent: *In Vitro* Assessment of Hemodynamic and Morphometric Characteristics. *Journal of Interventional Cardiology,* 5**,** 187-194.

Bledzki, A. & Gassan, J. 1999. Composites reinforced with cellulose based fibres. *Progress in Polymer Science,* 24**,** 221-274.

Bledzki, A., Mamun, A., Lucka-Gabor, M. & Gutowski, V. 2008. The effects of acetylation on properties of flax fibre and its polypropylene composites. *Express Polymer Letters,* 2**,** 413-422.

Bode-Boger, S. M., Martens-Lobenhoffer, J., Tager, M., Schroder, H. & Scalera, F. 2005. Aspirin reduces endothelial cell senescence. *Biochemical and Biophysical Research Communications,* 334**,** 1226-1232.

Bogaert, J. & Dymarkowski, S. 2005. Delayed contrast-enhanced MRI: use in myocardial viability assessment and other cardiac pathology. *European Radiolog supplements*, 15, B52-B58.

Bonatto, D., Matias, F., Lisboa, M., Bogdawa, H. & Henriques, J. 2004. Production of Short Side Chain-Poly[Hydroxyalkanoate] by a Newly Isolated *Ralstonia Pickettii* Strain. *World Journal of Microbiology and Biotechnology,* 20**,** 395-403.

Bondeson, D., Mathew, A. & Oksman, K. 2006. Optimization of the isolation of nanocrystals from microcrystalline cellulose by acid hydrolysis. *Cellulose,* 13**,** 171-180.

Bormann, E. J. & Roth, M. 1999. The production of polyhydroxybutyrate by *Methylobacterium rhodesianum* and *Ralstonia eutropha* in media containing glycerol and casein hydrolysates. *Biotechnology Letters,* 21**,** 1059-1063.

Bostman, O., Vainionpaa, S., Hirvensalo, E., Makela, A., Vihtonen, K., Tormala, P. & Rokkanen, P. 1987. Biodegradable internal fixation for malleolar fractures. A prospective randomised trial. *Journal of Bone & Joint Surgery, British Volume,* 69**,** 615-619.

Bowald, S. F. & Johansson, E. G. 1990. A novel surgical material. *European Patent Application no*. 0349 505 A2.

Braunegg, G., Lefebvre, G. & Genser, K. F. 1998. Polyhydroxyalkanoates, biopolyesters from renewable resources: Physiological and engineering aspects. *Journal of Biotechnology,* 65**,** 127-161.

Browne, N. & Dowds, B. 2002. Acid stress in the food pathogen *Bacillus cereus*. *Journal of Applied microbiology,* 92**,** 404-414.

Bruil, A., Brenneisen, L. M., Terlingen, J. G., Beugeling, T., Aken, W. G. & Feijen, J. 1994. *In vitro* leukocyte adhesion to modified polyurethane surfaces. II. Effect of wettability. *Journal of Colloid and Interface Science*, 165(1), 72-81.

Byrom, D. 1987. Polymer synthesis by microorganisms: technology and economics. *Trends in Biotechnology,* 5**,** 246-250.

Cantor, W. J., Peterson, E. D., Popma, J. J., Zidar, J. P., Sketch, M. H., Tcheng, J. E. & Ohman, E. M. 2000. Provisional stenting strategies: systematic overview and implications for clinical decision-making. *Journal of the American College of Cardiology,* 36**,** 1142-1151.

Carlo, E. C., Borges, A. P. B., Pompermayer, L. G., Martinez, M. M. M., Eleotério, R. B., Nehme, R. C. & Morato, G. O. 2009. Composite for the fabrication of resorbable implants for osteosynthesis: biocompatibility evaluation in rabbits. *Ciencia Rural*, 39(1), 135-140.

Castilho, L. R., Mitchell, D. A. & Freire, D. M. 2009. Production of polyhydroxyalkanoates (PHAs) from waste materials and by-products by submerged and solid-state fermentation. *Bioresource Technology,* 100**,** 5996-6009.

Chasin, M. R. & Langer, Eds. 1990. Biodegradable Polymers. *Natural Polymers as Drug Systems*. New York, Marcel Dekker Inc.

Chaudhry, W. N., Jamil, N., Ali, I., Ayaz, M. H. & Hasnain, S. 2011. Screening for polyhydroxyalkanoate (PHA)-producing bacterial strains and comparison of PHA production from various inexpensive carbon sources. *Annals of Microbiology,* 61**,** 623-629.

Chee, J. W., Amirul, A., Majid, M. & Mansor, S. 2008. Factors influencing the release of Mitragyna speciosa crude extracts from biodegradable P(3HB-co-4HB). *International Journal of Pharmaceutics,* 361**,** 1-6.

Chen, C., Jiang, X., Kaneti, Y. V. & Yu, A. 2012. Design and construction of polymerized-glucose coated Fe magnetic nanoparticles for delivery of aspirin. *Powder Technology*, 157-163

Chen, H., Song, W., Zhou, F., Wu, Z., Huang, H., Zhang, J., Lin, Q. & Yang, B. 2009. The effect of surface microtopography of poly (dimethylsiloxane) on protein adsorption, platelet and cell adhesion. *Colloids and Surfaces B: Biointerfaces,* 71**,** 275-281.

Chen, J. Y., Liu, T., Zheng, Z., Chen, J. C. & Chen, G. Q. 2004. Polyhydroxyalkanoate synthases PhaC1 and PhaC2 from *Pseudomonas stutzeri* 1317 had different substrate specificities. *FEMS Microbiology Letters,* 234**,** 231-237.

Chen, K.-S., Ayon, A. A., Zhang, X. & Spearing, S. M. 2002. Effect of process parameters on the surface morphology and mechanical performance of silicon structures after deep reactive ion etching. *Journal of Microelectromechanical Systems,* 11**,** 264-275.

Chen, N. & Hong, L. 2002. Surface phase morphology and composition of the casting films of PVDF–PVP blend. *Polymer,* 43**,** 1429-1436.

Chen, G. Q. & Wu, Q. 2005. The application of polyhydroxyalkanoates as tissue engineering materials. *Biomaterials,* 26(33), 6565-6578.

Cheng, Q., Wang, S., Rials, T. G. & Lee, S. H. 2007. Physical and mechanical properties of polyvinyl alcohol and polypropylene composite materials reinforced with fibril aggregates isolated from regenerated cellulose fibers. *Cellulose,* 14**,** 593-602.

Cheng, S. T., Chen, Z. F. & Chen, G. Q. 2008. The expression of cross-linked elastin by rabbit blood vessel smooth muscle cells cultured in polyhydroxyalkanoate scaffolds. *Biomaterials,* 29**,** 4187-4194.

Choi, J. & Lee, S. Y. 1999. Factors affecting the economics of polyhydroxyalkanoate production by bacterial fermentation. *Applied Microbiology and Biotechnology,* 51**,** 13-21.

Ciechanska, D. 2004. Multifunctional bacterial cellulose/chitosan composite materials for medical applications. *Fibres & Textiles in Eastern Europe,* 12**,** 48.

Cordewener, F. W., Van Geffen, M. F., Joziasse, C. A., Schmitz, J. P., Bos, R. R., Rozema, F. R. & Pennings, A. J. 2000. Cytotoxicity of poly (96L/4D-lactide): the influence of degradation and sterilization. *Biomaterials,* 21**,** 2433-2442.

Cromwick, A. M., Foglia, T. & Lenz, R. W. 1996. The microbial production of poly(hydroxyalkanoates) from tallow. *Applied Microbiology and Biotechnology,* 46**,** 464-469.

Dadsetan, M., Mirzadeh, H., Sharifi-Sanjani, N. & Daliri, M. 2001. Cell behavior on laser surface-modified polyethylene terephthalate *in vitro*. *Journal of Biomedical Materials Research,* 57**,** 183-189.

Dagnon, K. L., Ambadapadi, S., Shaito, A., Ogbomo, S. M., DeLeon, V., Golden, T. D., Rahimi, M., Nguyen, K., Braterman, P. S. & D'Souza, N. A. 2009. Poly (L-lactic acid) nanocomposites with layered double hydroxides functionalized with ibuprofen. *Journal of Applied Polymer Science,* 113**,** 1905-1915.

Dalmas, F., Chazeau, L., Gauthier, C., Cavaille, J. Y. & Dendievel, R. 2006. Large deformation mechanical behavior of flexible nanofiber filled polymer nanocomposites. *Polymer,* 47**,** 2802-2812.

Das, K., Bose, S. & Bandyopadhyay, A. 2007. Surface modifications and cell–materials interactions with anodized Ti. *Acta Biomaterialia,* 3**,** 573-585.

Dash, A. & Suryanarayanan, R. 1992. An Implantable Dosage Form for the Treatment of Bone Infections. *Pharmaceutical Research,* 9**,** 993-1002.

Dawes, E. A. & Senior, P. J. 1973. The role and regulation of energy reserve polymers in micro-organisms. *Advances in Microbial Physiology,* 10**,** 135-266.

Deng, Y., Zhao, K., Zhang, X., Hu, P. & Chen, G. Q. 2002. Study on the three-dimensional proliferation of rabbit articular cartilage-derived chondrocytes on polyhydroxyalkanoate scaffolds. *Biomaterials,* 23**,** 4049-4056.

Dhanasekar, R. & Viruthagiri, T. 2005. Batch kinetics and modelling of poly-β-hydroxybutyrate synthesis from *Azotobacter vinelandii* using different carbon sources. *Indian Journal of Chemical Technology,* 12, 322-326.

Diard, S., Carlier, J. P., Ageron, E., Grimont, P. A., Langlois, V., Guerin, P. & Bouvet, O. M. 2002. Accumulation of poly (3-hydroxybutyrate) from octanoate in different Pseudomonas belonging to the rRNA homology group I. *Systematic and Applied Microbiology*, 25(2), 183-188.

Doyle, C., Tanner, E. T. & Bonfield, W. 1991. *In vitro* and i*n vivo* evaluation of polyhydroxybutyrate and of polyhydroxybutyrate reinforced with hydroxyapatite. *Biomaterials,* 12**,** 841-847.

Duarte, M. A. T., Hugen, R. G., Martins, E. S. A., Pezzin, A. P. T. & Pezzin, S. H. 2006. Thermal and mechanical behavior of injection molded Poly(3-hydroxybutyrate)/Poly(e-caprolactone) blends. *Materials Research,* 9**,** 25-28.

Duncan, A. C., Rouais, F., Lazare, S., Bordenave, L. & Baquey, C. 2007. Effect of laser modified surface microtopochemistry on endothelial cell growth. *Colloids and Surfaces B: Biointerfaces*, 54(2), 150-159.

Elbahloul, Y. & Steinbuchel, A. 2009. Large-scale production of poly (3-hydroxyoctanoic acid) by *Pseudomonas putida* GPo1 and a simplified downstream process. *Applied and Environmental Microbiology,* 75**,** 643-651.

Elias, C. N., Oshida, Y., Lima, J. H. C. & Muller, C. A. 2008. Relationship between surface properties (roughness, wettability and morphology) of titanium and dental implant removal torque. *Journal of the Mechanical Behavior of Biomedical Materials,* 1**,** 234-242.

Engelberg, I. & Kohn, J. 1991. Physico-mechanical properties of degradable polymers used in medical applications: A comparative study. *Biomaterials,* 12**,** 292-304.

Faxon, D. P. 2002. Systemic drug therapy for restenosis. *Circulation,* 106**,** 2296-2298.

Feng, Q., Jiang, W., Sun, K., Sun, K., Chen, S., Zhao, L. & Ma, N. 2011. Mechanical properties and in vivo performance of a novel sliding-lock bioabsorbable poly-p-dioxanone stent. *Journal of Materials Science: Materials in Medicine*, 22(10), 2319-2327.

Follonier, S., Panke, S. & Zinn, M. 2011. A reduction in growth rate of Pseudomonas putida KT2442 counteracts productivity advances in medium-chain-length polyhydroxyalkanoate production from gluconate. *Microbial Cell Factories*, 10(1), 25.

Findlay, R. H. & White, D. C. 1983. Polymeric Beta-Hydroxyalkanoates from Environmental Samples and *Bacillus megaterium*. *Applied and Environmental Microbiology,* 45**,** 71-78.

Francis, L., Meng, D., Knowles, J., Keshavarz, T., Boccaccini, A. R. & Roy, I. 2011. Controlled delivery of gentamicin using poly (3-hydroxybutyrate) microspheres. *International Journal of Molecular Sciences,* 12**,** 4294-4314.

Francis, L., Meng, D., Locke, I. C., Mordan, N., Salih, V., Knowles, J. C., Boccaccini, A. R. & Roy, I. 2010. The Influence of Tetracycline Loading on the Surface Morphology and Biocompatibility of Films Made from P(3HB) Microspheres. *Advanced Engineering Materials,* 12**,** B260-B268.

Frank, A., Rath, S. K. & Venkatraman, S. S. 2005. Controlled release from bioerodible polymers: effect of drug type and polymer composition. *Journal of Controlled Release,* 102**,** 333-344.

Freiberg, S. & Zhu, X. 2004. Polymer microspheres for controlled drug release. *International Journal of Pharmaceutics,* 282**,** 1-18.

Füchtenbusch, B., Wullbrandt, D. & Steinbüchel, A. 2000. Production of polyhydroxyalkanoic acids by *Ralstonia eutropha* and *Pseudomonas oleovorans* from an oil remaining from biotechnological rhamnose production. *Applied Microbiology and Biotechnology,* 53**,** 167-172.

Fukui, T. & Doi, Y. 1998. Efficient production of polyhydroxyalkanoates from plant oils by *Alcaligenes eutrophus* and its recombinant strain. *Applied Microbiology and Biotechnology,* 49**,** 333-336.

Furrer, P., Hany, R., Rentsch, D., Grubelnik, A., Ruth, K., Panke, S. & Zinn, M. 2007. Quantitative analysis of bacterial medium-chain-length poly ([R]-3-hydroxyalkanoates) by gas chromatography. *Journal of Chromatography,* 1143**,** 199-206.

Gabr, M. H., Elrahman, M. A., Okubo, K. & Fujii, T. 2010. A study on mechanical properties of bacterial cellulose/epoxy reinforced by plain woven carbon fiber modified with liquid rubber. *Composites Part A: Applied Science and Manufacturing,* 41**,** 1263-1271.

Gabriels, M. & Plaizier-Vercammen, J. 2004. Experimental designed optimisation and stability evaluation of dry suspensions with artemisinin derivatives for paediatric use. *International Journal of Pharmaceutics,* 283**,** 19-34.

Galego, N., Rozsa, C., Sánchez, R., Fung, J., Analıia, V. & Santo Tomas, J. 2000. Characterization and application of poly(β-hydroxyalkanoates) family as composite biomaterials. *Polymer Testing,* 19**,** 485-492.

Gentile, F., Tirinato, L., Battista, E., Causa, F., Liberale, C., di Fabrizio, E. M. & Decuzzi, P. 2010. Cells preferentially grow on rough substrates. *Biomaterials,* 31**,** 7205-7212.

Gerlier, D. & Thomasset, N. 1986. Use of MTT colorimetric assay to measure cell activation. *Journal of immunological methods*, 94(1), 57-63.

Ghaderi, R., Sturesson, C. & Carlfors, J. 1996. Effect of preparative parameters on the characteristics of poly d,l-lactide-co-glycolide) microspheres made by the double emulsion method. *International Journal of Pharmaceutics,* 141**,** 205-216.

Giunchedi, P., Conti, B., Scalia, S. & Conte, U. 1998. *In vitro* degradation study of polyester microspheres by a new HPLC method for monomer release determination. *Journal of Controlled Release,* 56**,** 53-62.

Glaessl, B., Siepmann, F., Tucker, I., Siepmann, J. & Rades, T. 2009. Characterisation of quaternary polymethacrylate films containing tartaric acid, metoprolol free base or metoprolol tartrate. *European Journal of Pharmaceutics and Biopharmaceutics,* 73**,** 366-372.

Gogolewski, S., Jovanovic, M., Perren, S. M., Dillon, J. G. & Hughes, M. K. 1993. Tissue response and in vivo degradation of selected polyhydroxyacids: Polylactides (PLA), poly(3-hydroxybutyrate) (PHB), and poly(3-hydroxybutyrate-co-3-hydroxyvalerate) (PHB/VA). *Journal of Biomedical Materials Research,* 27**,** 1135-1148.

Gogolides, E., Constantoudis, V., Patsis, G. P. & Tserepi, A. 2006. A review of line edge roughness and surface nanotexture resulting from patterning processes. *Microelectronic Engineering,* 83**,** 1067-1072.

Gopferich, A. 1996. Mechanisms of polymer degradation and erosion. *Biomaterials,* 17**,** 103-114.

Gouda, M. K., Swellam, A. E. & Omar, S. H. 2001. Production of PHB by a *Bacillus megaterium* strain using sugarcane molasses and corn steep liquor as sole carbon and nitrogen sources. *Microbiological Research,* 156**,** 201-207.

Grabow, N., Bunger, C., Schultze, C., Schmohl, K., Martin, D., Williams, S., Sternberg, K. & Schmitz, K.-P. 2007. A Biodegradable Slotted Tube Stent Based on Poly(l-lactide) and Poly(4-hydroxybutyrate) for Rapid Balloon-Expansion. *Annals of Biomedical Engineering,* 35**,** 2031-2038.

Gray, B. L., Lieu, D. K., Collins, S. D., Smith, R. L. & Barakat, A. I. 2002. Microchannel platform for the study of endothelial cell shape and function. *Biomedical Microdevices,* 4**,** 9-16.

Grosser, N. & Schroder, H. 2003. Aspirin protects endothelial cells from oxidant damage via the nitric oxide-cGMP pathway. *Arteriosclerosis, Thrombosis, and Vascular Biology,* 23**,** 1345-1351.

Grunert, M. & Winter, W. 2000. Progress in the development of cellulose reinforced nanocomposites. *Polymeric Material Science and Engineering. Washington,* 82**,** 232-232.

Ha, C. S. & Cho, W. J. 2002. Miscibility, properties, and biodegradability of microbial polyester containing blends. *Progress in Polymer Science,* 27**,** 759-809.

Haghighat, M., Zadhoush, A. & Khorasani, S. N. 2005. Physicomechanical properties of α-cellulose–filled styrene–butadiene rubber composites. *Journal of Applied Polymer Science,* 96**,** 2203-2211.

Hallab, N. J., Bundy, K. J., O'Connor, K., Moses, R. L. & Jacobs, J. J. 2001. Evaluation of metallic and polymeric biomaterial surface energy and surface roughness characteristics for directed cell adhesion. *Tissue Engineering,* 7**,** 55-71.

Hang, X., Lin, Z., Chen, J., Wang, G., Hong, K. & Chen, G.-Q. 2002. Polyhydroxyalkanoate biosynthesis in *Pseudomonas pseudoalcaligenes* YS1. *FEMS Microbiology Letters,* 212**,** 71-75.

Hao, L. & Lawrence, J. 2004. The adsorption of human serum albumin (HSA) on CO_2 laser modified magnesia partially stabilised zirconia (MgO-PSZ). *Colloids and Surfaces B: Biointerfaces,* 34**,** 87-94.

Hao, L. & Lawrence, J. 2006a. Albumin and fibronectin protein adsorption on CO2-laser-modified biograde stainless steel. *Proceedings of the Institution of Mechanical Engineers, Part H: Journal of Engineering in Medicine,* 220**,** 47-55.

Hao, L. & Lawrence, J. 2006b. Effects of Nd: YAG laser treatment on the wettability characteristics of a zirconia-based bioceramic. *Optics and Lasers in Engineering,* 44**,** 803-814.

Hazer, B. & Steinbuchel, A. 2007. Increased diversification of polyhydroxyalkanoates by modification reactions for industrial and medical applications. *Applied Microbiology and Biotechnology,* 74**,** 1-12.

He, W., Tian, W., Zhang, G., Chen, G. Q. & Zhang, Z. 1998. Production of novel polyhydroxyalkanoates by *Pseudomonas stutzeri* 1317 from glucose and soybean oil. *FEMS Microbiology Letters*, 169(1), 45-49.

Hocking, P. J. & Marchessault, R. H. 1998. Polyhydroxyalkanoates. *Biopolymers from Renewable Resources*, 220-248. Berlin Heidelberg, Springer.

Holland, S., Jolly, A., Yasin, M. & Tighe, B. 1987. Polymers for biodegradable medical devices: Hydroxybutyrate-hydroxyvalerate copolymers: hydrolytic degradation studies. *Biomaterials,* 8**,** 289-295.

Holmes, P. A. 1985. Applications of PHB-a microbially produced biodegradable thermoplastic. *Physics in Technology*, 16(1), 32.

Hong, C., Hao, H. & Haiyun, W. 2009. Process optimization for PHA production by activated sludge using response surface methodology. *Biomass and Bioenergy,* 33**,** 721-727.

Hopewell, J., Dvorak, R. & Kosior, E. 2009. Plastics recycling: challenges and opportunities. *Philosophical Transactions of the Royal Society B: Biological Sciences,* 364**,** 2115-2126.

Huang, H., Hu, Y., Zhang, J., Sato, H., Zhang, H., Noda, I. & Ozaki, Y. 2005. Miscibility and hydrogen-bonding interactions in biodegradable polymer blends of poly (3-hydroxybutyrate) and a partially hydrolyzed poly (vinyl alcohol). *The Journal of Physical Chemistry B,* 109**,** 19175-19183.

Hufenus, R., Reifler, F. A., Maniura-Weber, K., Spierings, A. & Zinn, M. 2012. Biodegradable Bicomponent Fibers from Renewable Sources: Melt-Spinning of Poly (lactic acid) and Poly [(3-hydroxybutyrate)-co-(3-hydroxyvalerate)]. *Macromolecular Materials and Engineering,* 297**,** 75-84.

Huisman, G. W., de Leeuw, O., Eggink, G. & Witholt, B. 1989. Synthesis of poly-3-hydroxyalkanoates is a common feature of fluorescent pseudomonads. *Applied and Environmental Microbiology,* 55**,** 1949-1954.

Hutchinson, J. M. 1995. Physical ageing of polymers. *Progress in polymer science,* 20**,** 703-760.

Hwang, M.-R., Kim, J. O., Lee, J. H., Kim, Y. I., Kim, J. H., Chang, S. W., Jin, S. G., Kim, J. A., Lyoo, W. S. & Han, S. S. 2010. Gentamicin-loaded wound dressing with polyvinyl alcohol/dextran hydrogel: gel characterization and in vivo healing evaluation. *American Association of Pharmaceutical Scientists,* 11**,** 1092-1103.

Ikejima, T., Cao, A., Yoshie, N. & Inoue, Y. 1998. Surface composition and biodegradability of poly(3-hydroxybutyric acid)/poly(vinyl alcohol) blend films. *Polymer Degradation and Stability,* 62**,** 463-469.

Isenberg, B. C., Tsuda, Y., Williams, C., Shimizu, T., Yamato, M., Okano, T. & Wong, J. Y. 2008. A thermoresponsive, microtextured substrate for cell sheet engineering with defined structural organization. *Biomaterials*, 29(17), 2565-2572.

Jeyachandran, Y., Mielczarski, J., Mielczarski, E. & Rai, B. 2010. Efficiency of blocking of non-specific interaction of different proteins by BSA adsorbed on hydrophobic and hydrophilic surfaces. *Journal of Colloid and Interface Science,* 341**,** 136-142.

Jiang, Y., Song, X., Gong, L., Li, P., Dai, C. & Shao, W. 2008a. High poly (β-hydroxybutyrate) production by *Pseudomonas fluorescens* A2a5 from inexpensive substrates. *Enzyme and Microbial Technology,* 42**,** 167-172.

Jiang, L., Morelius, E., Zhang, J., Wolcott, M. & Holbery, J. 2008b. Study of the poly (3-hydroxybutyrate-co-3-hydroxyvalerate)/cellulose nanowhisker composites prepared by solution casting and melt processing. *Journal of Composite Materials*, 42(24), 2629-2645.

Jonoobi, M., Harun, J., Mathew, A. P., Hussein, M. Z. B. & Oksman, K. 2010. Preparation of cellulose nanofibers with hydrophobic surface characteristics. *Cellulose*, 17(2), 299-307.

Kahar, P., Tsuge, T., Taguchi, K. & Doi, Y. 2004. High yield production of polyhydroxyalkanoates from soybean oil by *Ralstonia eutropha* and its recombinant strain. *Polymer Degradation and Stability,* 83**,** 79-86.

Kai, Z., Ying, D. & Guo-Qiang, C. 2003. Effects of surface morphology on the biocompatibility of polyhydroxyalkanoates. *Biochemical Engineering Journal,* 16**,** 115-123.

Kashiwaya, Y., Takeshima, T., Mori, N., Nakashima, K., Clarke, K. & Veech, R. L. 2000. D-β-Hydroxybutyrate protects neurons in models of Alzheimer's and Parkinson's disease. *Proceedings of the National Academy of Sciences*, 97(10), 5440-5444.

Kassab, A. C., Xu, K., Denkbas, E., Dou, Y., Zhao, S. & Piskin, E. 1997. Rifampicin carrying polyhydroxybutyrate microspheres as a potential chemoembolization agent. *Journal of Biomaterials Science, Polymer Edition,* 8**,** 947-961.

Kastrati, A., Hall, D. & Schomig, A. 2000. Long-term outcome after coronary stenting. *Curr Control Trials Cardiovascular Medicine,* 1**,** 48-54.

Kato, M., Fukui, T. & Doi, Y. 1996. Biosynthesis of Polyester Blends by *Pseudomonas* sp. from Alkanoic Acids. *Bulletin of the Chemical Society of Japan,* 69**,** 515-520.

Kawaguchi, Y. & Doi, Y. 1992. Kinetics and mechanism of synthesis and degradation of poly(3-hydroxybutyrate) in *Alcaligenes eutrophus*. *Macromolecules,* 25**,** 2324-2329.

Kenar, H., Kose, G. T. & Hasirci, V. 2010. Design of a 3D aligned myocardial tissue construct from biodegradable polyesters. *Journal of Materials Science: Materials in Medicine,* 21**,** 989-997.

Keselowsky, B. G., Collard, D. M. & García, A. J. 2003. Surface chemistry modulates fibronectin conformation and directs integrin binding and specificity to control cell adhesion. *Journal of Biomedical Materials Research Part A,* 66**,** 247-259.

Khanna, S. & Srivastava, A. K. 2005. Recent advances in microbial polyhydroxyalkanoates. *Process Biochemistry,* 40**,** 607-619.

Kidd, K. R., Patula, V. B. & Williams, S. K. 2003. Accelerated endothelialization of interpositional 1-mm vascular grafts. *Journal of Surgical Research,* 113**,** 234-242.

Kim, B. S., Lee, S. C., Lee, S. Y., Chang, H. N., Chang, Y. K. & Woo, S. I. 1994. Production of poly (3-hydroxybutyric acid) by fed-batch culture of *Alcaligenes eutrophus* with glucose concentration control. *Biotechnology and Bioengineering,* 43**,** 892-898.

Kim, D. Y., Nishiyama, Y., & Kuga, S. 2002. Surface acetylation of bacterial cellulose. *Cellulose*, 9(3-4), 361-367.

Kim do, Y., Kim, H. W., Chung, M. G. & Rhee, Y. H. 2007. Biosynthesis, modification, and biodegradation of bacterial medium-chain-length polyhydroxyalkanoates. *J Microbiol,* 45**,** 87-97.

Kim, D. Y., Kim, Y. B. & Rhee, Y. H. 2000a. Evaluation of various carbon substrates for the biosynthesis of polyhydroxyalkanoates bearing functional groups by *Pseudomonas putida. International Journal of Biological Macromolecules,* 28**,** 23-29.

Kim, G., Bang, K., Kim, Y. & Rhee, Y. 2000b. Preparation and characterization of native poly (3-hydroxybutyrate) microspheres from *Ralstonia eutropha. Biotechnology letters,* 22**,** 1487-1492.

Klemm, D., Schumann, D., Udhardt, U. & Marsch, S. 2001. Bacterial synthesized cellulose artificial blood vessels for microsurgery. *Progress in Polymer Science,* 26**,** 1561-1603.

Knowles, J. C., Hastings, G. W., Ohta, H., Niwa, S. & Boeree, N. 1992. Development of a degradable composite for orthopaedic use: *in vivo* biomechanical and histological evaluation of two bioactive degradable composites based on the polyhydroxybutyrate polymer. *Biomaterials,* 13**,** 491-496.

Koller, M., Bona, R., Braunegg, G., Hermann, C., Horvat, P., Kroutil, M., Martinz, J., Neto, J., Pereira, L. & Varila, P. 2005. Production of Polyhydroxyalkanoates from Agricultural Waste and Surplus Materials. *Biomacromolecules,* 6**,** 561-565.

Kominek, L. A. & Halvorson, H. O. 1965. Metabolism of Poly-β-Hydroxybutyrate and Acetoin in *Bacillus cereus*. *Journal of Bacteriology,* 90**,** 1251-1259.

Kurella, A. & Dahotre, N. B. 2005. Review paper: surface modification for bioimplants: the role of laser surface engineering. *Journal of Biomaterials Applications,* 20**,** 5-50.

Kurowska-Nouyrigat, W. & Szumbarski, J. 2009. Numerical Simulation of Restenosis in a Stented Coronary Artery. *World Academy of Science, Engineering and Technology,* 58, 42-45.

Lafferty, R.M., Korsatko, B. & Korsatko, W. 1988. Microbial production of poly-3-hydroxybutyric acid. Biotechnology: A Comprehensive Treatise, Special Microbial Processes. VCH Verlagsgesellschaft, Weinhheim.

Lageveen, R. G., Huisman, G. W., Preusting, H., Ketelaar, P., Eggink, G. & Witholt, B. 1988. Formation of polyesters by *Pseudomonas oleovorans*: effect of substrates on formation and composition of poly-(R)-3-hydroxyalkanoates and poly-(R)-3-hydroxyalkenoates. *Applied and Environmental Microbiology,* 54**,** 2924-2932.

Lampin, M., Warocquier-Clérout, R., Legris, C., Degrange, M. & Sigot-Luizard, M. 1997. Correlation between substratum roughness and wettability, cell adhesion, and cell migration. *Journal of Biomedical Materials Research,* 36**,** 99-108.

Langille, B. L. & Adamson, S. L. 1981. Relationship between blood flow direction and endothelial cell orientation at arterial branch sites in rabbits and mice. *Circulation Research,* 48**,** 481-488.

Law, J. H. & Slepecky, R. A. 1961. Assay of poly-β-hydroxybutyric acid. *Journal of Bacteriology*, 82(1), 33-36.

Le Corre, P., Le Guevello, P., Gajan, V., Chevanne, F. & Le Verge, R. 1994. Preparation and characterization of bupivacaine-loaded polylactide and polylactide-co-glycolide microspheres. *International Journal of Pharmaceutics,* 107**,** 41-49.

Lee, J. H., Go, A. K., Oh, S. H., Lee, K. E. & Yuk, S. H. 2005. Tissue anti-adhesion potential of ibuprofen-loaded PLLA–PEG diblock copolymer films. *Biomaterials,* 26**,** 671-678.

Lee, K. M. &, Gilmore, D. F. 2005. Formulation and process modeling of biopolymer (polyhydroxyalkanoates: PHAs) production from industrial wastes by novel crossed experimental design. *Process Biochemistry,* 40**,** 229-246.

Lee, S., Zhang, Z., Feng, S., Fischbach, C., Mooney, D., Coleman, R., Case, N., Guldberg, R., Rowlands, A. & Lim, S. 2007. Polymer contents. *Biomaterials,* 28**,** 11.

Lee, S. Y. 1996. Bacterial polyhydroxyalkanoates. *Biotechnology and Bioengineering,* 49**,** 1-14.

Lee, S. Y., Middelberg, A. P. J. & Lee, Y. K. 1997. Poly(3-hydroxybutyrate) production from whey using recombinant *Escherichia coli*. *Biotechnology Letters,* 19**,** 1033-1035.

Lee, T. H., Wang, J. & Wang, C. H. 2002. Double-walled microspheres for the sustained release of a highly water soluble drug: characterization and irradiation studies. *Journal of Controlled Release,* 83**,** 437-452.

Li, H., Schut, H. A., Conran, P., Kramer, P. M., Lubet, R. A., Steele, V. E. & Pereira, M. A. 1999. Prevention by aspirin and its combination with α-difluoromethylornithine of azoxymethane-induced tumors, aberrant crypt foci and prostaglandin E2 levels in rat colon. *Carcinogenesis*, 20(3), 425-430.

Li, P., Bakowsky, U., Yu, F., Loehbach, C., Muecklich, F. & Lehr, C.-M. 2003. Laser ablation patterning by interference induces directional cell growth. *NanoBioscience, IEEE Transactions on,* 2**,** 138-145.

Li, S., Bhatia, S., Hu, Y. L., Shiu, Y.-T., Li, Y.-S., Usami, S. & Chien, S. 2001. Effects of morphological patterning on endothelial cell migration. *Biorheology,* 38**,** 101-108.

Li, Y. & Shimizu, H. 2007. Toughening of polylactide by melt blending with a biodegradable poly (ether) urethane elastomer. *Macromolecular Bioscience,* 7**,** 921-928.

Libby, P., Ridker, P. M. & Maseri, A. 2002. Inflammation and Atherosclerosis. *Circulation,* 105**,** 1135-1143.

Liu, H., Slamovich, E. B. & Webster, T. J. 2006. Less harmful acidic degradation of poly (lactic-co-glycolic acid) bone tissue engineering scaffolds through titania nanoparticle addition. *International Journal of Nanomedicine,* 1**,** 541.

Liu, X., Gao, C., Shen, J. & Möhwald, H. 2005. Multilayer Microcapsules as Anti-Cancer Drug Delivery Vehicle: Deposition, Sustained Release, and *in vitro* Bioactivity. *Macromolecular Bioscience,* 5**,** 1209-1219.

Loo, C.-Y., Lee, W.-H., Tsuge, T., Doi, Y. & Sudesh, K. 2005. Biosynthesis and Characterization of Poly(3-hydroxybutyrate-co-3-hydroxyhexanoate) from Palm Oil Products in a *Wautersia eutropha* Mutant. *Biotechnology Letters,* 27**,** 1405-1410.

Luo, L., Wei, X. & Chen, G.-Q. 2009. Physical Properties and Biocompatibility of Poly (3-hydroxybutyrate-co-3-hydroxyhexanoate) blended with Poly (3-hydroxybutyrate-co-4-hydroxybutyrate). *Journal of Biomaterials Science, Polymer Edition,* 20**,** 1537-1553.

Macrae, R. M. & Wilkinson, J. F. 1958. Poly-β-hyroxybutyrate Metabolism in Washed Suspensions of *Bacillus cereus* and *Bacillus megaterium*. *Journal of General Microbiology,* 19**,** 210-222

Mani, G., Feldman, M. D., Patel, D. & Agrawal, C. 2007. Coronary stents: a materials perspective. *Biomaterials,* 28**,** 1689-1710.

Marangoni, C., Furigo Jr, A. & de Aragao, G. M. F. 2002. Production of poly(3-hydroxybutyrate-co-3-hydroxyvalerate) by *Ralstonia eutropha* in whey and inverted sugar with propionic acid feeding. *Process Biochemistry,* 38**,** 137-141.

Marangoni, C., Furigo Jr., A. & Aragao, G. M. F. 2001. The influence of substrate source on the growth of *Ralstonia eutropha,* aiming at the production of polyhydroxyalkanoate. *Brazilian Journal of Chemical Engineering,* 18**,** 175-180.

Martelli, S. M., Sabirova, J., Fakhoury, F. M., Dyzma, A., de Meyer, B. & Soetaert, W. 2012. Obtention and characterization of poly(3-hydroxybutyricacid-co-hydroxyvaleric acid)/MCL-PHA based blends. *Food Science and Technology,* 47**,** 386-392.

Martin, D. P. & Williams, S. F. 2003. Medical applications of poly-4-hydroxybutyrate: a strong flexible absorbable biomaterial. *Biochemical Engineering Journal,* 16**,** 97-105.

Martina, M. & Hutmacher, D. W. 2007. Biodegradable polymers applied in tissue engineering research: a review. *Polymer International,* 56**,** 145-157.

Massieu, L., Haces, M. L., Montiel, T. & Hernandez-Fonseca, K. 2003. Acetoacetate protects hippocampal neurons against glutamate-mediated neuronal damage during glycolysis inhibition. *Neuroscience,* 120**,** 365-378.

McCool, G. J. & Cannon, M. C. 2001. PhaC and PhaR Are Required for Polyhydroxyalkanoic Acid Synthase Activity in *Bacillus megaterium*. *Journal of Bacteriology,* 183**,** 4235-4243.

McLafferty, F. W. 1956. Mass spectrometric analysis broad applicability to chemical research. *Analytical Chemistry,* 28**,** 306-316.

Mikulikova, R., Moritz, S., Gumpenberger, T., Olbrich, M., Romanin, C., Bacakova, L. & Heitz, J. 2005. Cell microarrays on photochemically modified polytetrafluoroethylene. *Biomaterials,* 26(27), 5572-5580.

Misra, S. K., Ansari, T. I., Valappil, S. P., Mohn, D., Philip, S. E., Stark, W. J., Roy, I., Knowles, J. C., Salih, V. & Boccaccini, A. R. 2010. Poly (3-hydroxybutyrate) multifunctional composite scaffolds for tissue engineering applications. *Biomaterials,* 31**,** 2806-2815.

Misra, S. K., Mohn, D., Brunner, T. J., Stark, W. J., Philip, S. E., Roy, I., Salih, V., Knowles, J. C. & Boccaccini, A. R. 2008. Comparison of nanoscale and microscale bioactive glass on the properties of P(3HB)/Bioglass composites. *Biomaterials,* 29**,** 1750-1761.

Misra, S. K., Valappil, S. P., Roy, I. & Boccaccini, A. R. 2006. Polyhydroxyalkanoate (PHA)/Inorganic Phase Composites for Tissue Engineering Applications. *Biomacromolecules,* 7**,** 2249-2258.

Moore, J., Soares, J. & Rajagopal, K. 2010. Biodegradable Stents: Biomechanical Modeling Challenges and Opportunities. *Cardiovascular Engineering and Technology,* 1**,** 52-65.

Naraharisetti, P. K., Ning Lew, M. D., Fu, Y. C., Lee, D. J. & Wang, C.-H. 2005. Gentamicin-loaded discs and microspheres and their modifications: characterization and *in vitro* release. *Journal of Controlled Release,* 102**,** 345-359.

Nerem, R. M. & Seliktar, D. 2001. Vascular tissue engineering. *Annual Review of Biomedical Engineering,* 3**,** 225-43.

Nugent, H. M. & Edelman, E. R. 2003. Tissue engineering therapy for cardiovascular disease. *Circulation Research*, 92(10), 1068-1078.

Olbrich, H. 1963. The molasses. *Fermentation Technologist, Institut für Zuckerindustrie, Berlin, Germany*.

Ong, A., Aoki, J., Kutryk, M. & Serruys, P. 2005. How to accelerate the endothelialization of stents. *Archives des maladies du coeur et des vaisseaux,* 98**,** 123.

Page, W. J. 1992. Production of polyhydroxyalkanoates by *Azotobacter vinelandii* UWD in beet molasses culture. *FEMS Microbiology Letters,* 103**,** 149-157.

Palleroni, N., Doudoroff, M., Stanier, R., Solanes, R. & Mandel, M. 1970. Taxonomy of the aerobic pseudomonads: the properties of the *Pseudomonas stutzeri* group. *Journal of General Microbiology,* 60**,** 215-231.

Pang, J., Luan, Y., Li, F., Cai, X., Du, J. & Li, Z. 2011. Ibuprofen-loaded poly (lactic-co-glycolic acid) films for controlled drug release. *International Journal of Nanomedicine,* 6**,** 659.

Park, S. H., Lim, S. T., Shin, T. K., Choi, H. J. & Jhon, M. S. 2001. Viscoelasticity of biodegradable polymer blends of poly(3-hydroxybutyrate) and poly(ethylene oxide). *Polymer,* 42**,** 5737-5742.

Parulekar, Y. & Mohanty, A. K. 2007. Extruded Biodegradable Cast Films from Polyhydroxyalkanoate and Thermoplastic Starch Blends: Fabrication and Characterization. *Macromolecular Materials and Engineering,* 292**,** 1218-1228.

Paul, W. & Sharma, C. P. 1997. Acetylsalicylic acid loaded poly (vinyl alcohol) hemodialysis membranes: effect of drug release on blood compatibility and permeability. *Journal of Biomaterials Science, Polymer Edition,* 8**,** 755-764.

Peoples, O. P. & Sinskey, A. J. 1989. Poly-beta-hydroxybutyrate (PHB) biosynthesis in *Alcaligenes eutrophus* H16. Identification and characterization of the PHB polymerase gene (phbC). *Journal of Biological Chemistry,* 264**,** 15298-303.

Peschel, G., Dahse, H. M., Konrad, A., Wieland, G. D., Mueller, P. J., Martin, D. P. & Roth, M. 2008. Growth of keratinocytes on porous films of poly (3-hydroxybutyrate) and poly (4-hydroxybutyrate) blended with hyaluronic acid and chitosan. *Journal of Biomedical Materials Research Part A,* 85**,** 1072-1081.

Philip, S., Keshavarz, T. & Roy, I. 2007. Polyhydroxyalkanoates: biodegradable polymers with a range of applications. *Journal of Chemical Technology and Biotechnology,* 82**,** 233-247.

Pillai, O. & Panchagnula, R. 2001. Polymers in drug delivery. *Current Opinion in Chemical Biology*, 5(4), 447-451.

Podhaisky, H.-P., Abate, A., Polte, T., Oberle, S. & Schroder, H. 1997. Aspirin protects endothelial cells from oxidative stress–possible synergism with vitamin E. *FEBS letters,* 417**,** 349-351.

Poletto, F. S., Jager, E., Re, M. I., Guterres, S. S. & Pohlmann, A. R. 2007. Rate-modulating PHBHV/PCL microparticles containing weak acid model drugs. *International Journal of Pharmaceutics,* 345**,** 70-80.

Pouton, C. W. & Akhtar, S. 1996. Biosynthetic polyhydroxyalkanoates and their potential in drug delivery. *Advanced Drug Delivery Reviews,* 18**,** 133-162.

Povolo, S. & Casella, S. 2003. Bacterial production of PHA from lactose and cheese whey permeate. *Macromolecular Symposia,* 197**,** 1-10.

Puttipipatkhachorn, S., Nunthanid, J., Yamamoto, K. & Peck, G. 2001. Drug physical state and drug–polymer interaction on drug release from chitosan matrix films. *Journal of Controlled Release,* 75**,** 143-153.

Qi, Q. & Rehm, B. H. A. 2001. Polyhydroxybutyrate biosynthesis in *Caulobacter crescentus*: molecular characterization of the polyhydroxybutyrate synthase. *Microbiology,* 147**,** 3353-3358.

Qiu, Z., Yang, W., Ikehara, T. & Nishi, T. 2005. Miscibility and crystallization behavior of biodegradable blends of two aliphatic polyesters. Poly(3-hydroxybutyrate-co-hydroxyvalerate) and poly(ε-caprolactone). *Polymer,* 46**,** 11814-11819.

Rai, R., Yunos, D. M., Boccaccini, A. R., Knowles, J. C., Barker, I. A., Howdle, S. M., Tredwell, G. D., Keshavarz, T. & Roy, I. 2011. Poly-3-hydroxyoctanoate P (3HO), a medium chain length polyhydroxyalkanoate homopolymer from *Pseudomonas mendocina. Biomacromolecules,* 12**,** 2126-2136.

Rambo, C. R., Costa, C. M., Carminatti, C. A., Recouvreux, D. O. S., d'Acampora, A. J. & Porto, L. M. 2012. Osteointegration of poly-(3-hydroxybutyrate-co-3-hydroxyvalerate) scaffolds incorporated with violacein. *Materials Science and Engineering: C,* 32**,** 385-389.

Randriamahefa, S., Renard, E., Guérin, P. & Langlois, V. 2003. Fourier transform infrared spectroscopy for screening and quantifying production of PHAs by Pseudomonas grown on sodium octanoate. *Biomacromolecules,* 4**,** 1092-1097.

Rathbone, S., Furrer, P., Lübben, J., Zinn, M. & Cartmell, S. 2010. Biocompatibility of polyhydroxyalkanoate as a potential material for ligament and tendon scaffold material. *Journal of Biomedical Materials Research Part A,* 93**,** 1391-1403.

Ravichandran, R., Sundarrajan, S., Venugopal, J. R., Mukherjee, S. & Ramakrishna, S. 2012. Advances in Polymeric Systems for Tissue Engineering and Biomedical Applications. *Macromolecular Bioscience,* 12**,** 286-311.

Rebollar, E., Frischauf, I., Olbrich, M., Peterbauer, T., Hering, S., Preiner, J., Hinterdorfer, P., Romanin, C. & Heitz, J. 2008. Proliferation of aligned mammalian cells on laser-nanostructured polystyrene. *Biomaterials,* 29**,** 1796-1806.

Rechendorff, K., Hovgaard, M. B., Foss, M., Zhdanov, V. & Besenbacher, F. 2006. Enhancement of protein adsorption induced by surface roughness. *Langmuir,* 22**,** 10885-10888.

Reddy, C. S. K., Ghai, R., Rashmi & Kalia, V. C. 2003. Polyhydroxyalkanoates: an overview. *Bioresource Technology,* 87**,** 137-146.

Regar, E., Sianos, G. & Serruys, P. W. 2001. Stent development and local drug delivery. *British Medical Bulletin,* 59**,** 227-248.

Rehm, B. H. A. 2003. Polyester synthases: natural catalysts for plastics. *Biochemical Journal,* 376**,** 15-33.

Reis, K. C., Pereira, J., Smith, A. C., Carvalho, C. W. P., Wellner, N. & Yakimets, I. 2008. Characterization of polyhydroxybutyrate-hydroxyvalerate (PHB-HV)/maize starch blend films. *Journal of Food Engineering,* 89**,** 361-369.

Ren, Q., Roo, G., Beilen, J., Zinn, M., Kessler, B. & Witholt, B. 2005. Poly(3-hydroxyalkanoate) polymerase synthesis and *in vitro* activity in recombinant *Escherichia coli* and *Pseudomonas putida*. *Applied Microbiology and Biotechnology,* 69**,** 286-292.

Renard, E., Walls, M., Guérin, P. & Langlois, V. 2004. Hydrolytic degradation of blends of polyhydroxyalkanoates and functionalized polyhydroxyalkanoates. *Polymer Degradation and Stability,* 85**,** 779-787.

Rodrigues, L. B., Leite, H. F., Yoshida, M. I., Saliba, J. B., Junior, A. S. C. & Faraco, A. A. 2009. *In vitro* release and characterization of chitosan films as dexamethasone carrier. *International Journal of Pharmaceutics,* 368**,** 1-6.

Ruth, K., Grubelnik, A., Hartmann, R., Egli, T., Zinn, M. & Ren, Q. 2007. Efficient Production of (R)-3-Hydroxycarboxylic Acids by Biotechnological Conversion of Polyhydroxyalkanoates and Their Purification. *Biomacromolecules,* 8**,** 279-286.

Ryu, H. W., Hahn, S. K., Chang, Y. K. & Chang, H. N. 1997. Production of poly(3-hydroxybutyrate) by high cell density fed-batch culture of *Alcaligenes eutrophus* with phospate limitation. *Biotechnology and Bioengineering,* 55**,** 28-32.

Sahoo, S. K., Mallick, A. A., Barik, B. & Senapati, P. C. 2005. Formulation and *in vitro* Evaluation of Eudragit® Microspheres of Stavudine. *Tropical Journal of Pharmaceutical Research,* 4**,** 369-375.

Sahoo, S. K., Panyam, J., Prabha, S. & Labhasetwar, V. 2002. Residual polyvinyl alcohol associated with poly (D, L-lactide-co-glycolide) nanoparticles affects their physical properties and cellular uptake. *Journal of Controlled Release,* 82**,** 105-114.

Sandoval, A., Arias-Barrau, E., Bermejo, F., Canedo, L., Naharro, G., Olivera, E. R. & Luengo, J. M. (2005). Production of 3-hydroxy-n-phenylalkanoic acids by a genetically engineered strain of *Pseudomonas putida*. *Applied Microbiology and Biotechnology*, 67(1), 97-105.

Sato, Y. & Murahara, M. 2004. Protein adsorption on PTFE surface modified by ArF excimer laser treatment. *Journal of Adhesion Science and Technology,* 18**,** 1545-1555.

Satoh, H., Yoshie, N. & Inoue, Y. 1994. Hydrolytic degradation of blends of poly (3-hydroxybutyrate) with poly (3-hydroxybutyrate-co- 3-hydroxyvalerate). *Polymer*, *35*(2), 286-290.

Scopelliti, P. E., Borgonovo, A., Indrieri, M., Giorgetti, L., Bongiorno, G., Carbone, R., Podesta, A. & Milani, P. 2010. The effect of surface nanometre-scale morphology on protein adsorption. *Public Library of Science,* 5**,** e11862.

Sendil, D., Gursel, I., L Wise, D. & Hasırcı, V. 1999. Antibiotic release from biodegradable PHBV microparticles. *Journal of Controlled Release,* 59**,** 207-217.

Senior, P. & Dawes, E. 1971. Poly-β-hydroxybutyrate biosynthesis and the regulation of glucose metabolism in *Azotobacter beijerinckii. Biochemical Journal,* 125**,** 55.

Shieh, S. J. & Vacanti, J. P. 2005. Surgical research review State-of-the-art tissue engineering: From tissue engineering to organ building. *Surgery,* 137**,** 1-7.

Shimamura, E., Kasuya, K., Kobayashi, G., Shiotani, T., Shima, Y. & Doi, Y. 1994. Physical Properties and Biodegradability of Microbial Poly(3-hydroxybutyrate-co-3-hydroxyhexanoate). *Macromolecules,* 27**,** 878-880.

Shiraki, M., Endo, T. & Saito, T. 2006. Fermentative production of (R)-(−)-3-hydroxybutyrate using 3-hydroxybutyrate dehydrogenase null mutant of *Ralstonia eutropha* and recombinant *Escherichia coli*. *Journal of Bioscience and Bioengineering*, 102(6), 529-534.

Shishatskaya, E. I., Volova, T. G., Efremov, S. N., Puzyr, A. P. & Mogil'naya, O. A. 2002. Tissue Response to Biodegradable Suture Threads Made of Polyhydroxyalkanoates. *Biomedical Engineering,* 36**,** 210-217.

Shumigin, D., TarasovaA, E., Krumme, A. & Meier, P. 2011. Rheological and Mechanical Properties of Poly (lactic) Acid/Cellulose and LDPE/Cellulose Composites. *Materials Science,* 17**,** 32-37.

Siepmann, J. & Gopferich, A. 2001. Mathematical modeling of bioerodible, polymeric drug delivery systems. *Advanced Drug Delivery Reviews,* 48**,** 229-247.

Siqueira, G., Bras, J. & Dufresne, A. 2010. Cellulosic bionanocomposites: a review of preparation, properties and applications. *Polymers,* 2**,** 728-765.

Sodian, R., Sperling, J. S., Martin, D. P., Egozy, A., Stock, U., Mayer, J. E., Jr. & Vacanti, J. P. 2000. Fabrication of a trileaflet heart valve scaffold from a polyhydroxyalkanoate biopolyester for use in tissue engineering. *Tissue Engineering,* 6**,** 183-8.

Solaiman, D. Y., Ashby, R., Hotchkiss, A., Jr. & Foglia, T. 2006. Biosynthesis of Medium-chain-length Poly(hydroxyalkanoates) from Soy Molasses. *Biotechnology Letters,* 28**,** 157-162.

Soykeabkaew, N., Sian, C., Gea, S., Nishino, T. & Peijs, T. 2009. All-cellulose nanocomposites by surface selective dissolution of bacterial cellulose. *Cellulose,* 16**,** 435-444.

Stack, R. S., Califf, R. M., Phillips, H. R., Pryor, D. B., Quigley, P. J., Bauman, R. P., Tcheng, J. E. & Greenfield, J. C., Jr. 1988. Interventional cardiac catheterization at Duke Medical Center. *American Journal of Cardiology,* 62**,** 3F-24F.

Stock, U. A., Nagashima, M., Khalil, P. N., Nollert, G. D., Herdena, T., Sperling, J. S., Moran, A., Lien, J., Martin, D. P., Schoen, F. J., Vacanti, J. P. & Mayer Jr, J. E. 2000. Tissue-engineered valved conduits in the pulmonary circulation. *The Journal of Thoracic and Cardiovascular Surgery,* 119**,** 732-740.

Stubbe, J. & Tian, J. 2003. Polyhydroxyalkanoate (PHA) homeostasis: the role of the PHA synthase. *Natural Product Reports,* 20**,** 445-457.

Sudesh, K., Abe, H. & Doi, Y. 2000. Synthesis, structure and properties of polyhydroxyalkanoates: biological polyesters. *Progress in Polymer Science,* 25**,** 1503-1555.

Taguchi, K., Aoyagi, Y., Matsusaki, H., Fukui, T. & Doi, Y. 1999. Co-expression of 3-ketoacyl-ACP reductase and polyhydroxyalkanoate synthase genes induces PHA production in *Escherichia coli* HB101 strain. *FEMS Microbiology Letters,* 176**,** 183-190.

Tajima, K., Igari, T., Nishimura, D., Nakamura, M., Satoh, Y. & Munekata, M. 2003. Isolation and characterization of *Bacillus* sp. INT005 accumulating polyhydroxyalkanoate (PHA) from gas field soil. *Journal of Bioscience and Bioengineering,* 95**,** 77-81.

Takagi, Y., Yasuda, R., Yamaoka, M. & Yamane, T. 2004. Morphologies and mechanical properties of polylactide blends with medium chain length poly(3-hydroxyalkanoate) and chemically modified poly(3-hydroxyalkanoate). *Journal of Applied Polymer Science,* 93**,** 2363-2369.

Tamai, H., Igaki, K., Kyo, E., Kosuga, K., Kawashima, A., Matsui, S., Komori, H., Tsuji, T., Motohara, S. & Uehata, H. 2000. Initial and 6-Month Results of Biodegradable Poly-l-Lactic Acid Coronary Stents in Humans. *Circulation,* 102**,** 399-404.

Tang, Y. & Singh, J. 2008. Controlled delivery of aspirin: Effect of aspirin on polymer degradation and *in vitro* release from PLGA based phase sensitive systems. *International Journal of Pharmaceutics,* 357**,** 119-125.

Taniguchi, I., Kagotani, K. & Kimura, Y. 2003. Microbial production of poly(hydroxyalkanoate)s from waste edible oils. *Green Chemistry,* 5**,** 545-548.

Tasaki, O., Hiraide, A., Shiozaki, T., Yamamura, H., Ninomiya, N. & Sugimoto, H. 1999. The dimer and trimer of 3-hydroxybutyrate oligomer as a precursor of ketone bodies for nutritional care. *Journal of Parenteral and Enteral Nutrition*, 23(6), 321-325.

Thery, M. 2010. Micropatterning as a tool to decipher cell morphogenesis and functions. *Journal of Cell Science,* 123**,** 4201-4213.

Thomson, R. C., Moore, C. J., vom Saal, F. S. & Swan, S. H. 2009. Plastics, the environment and human health: current consensus and future trends. *Philosophical Transactions of the Royal Society: Biological Sciences,* 364**,** 2153-2166.

Tian, W., Hong, K., Chen, G.-Q., Wu, Q., Zhang, R. & Huang, W. 2000. Production of polyesters consisting of medium chain length 3-hydroxyalkanoic acids by *Pseudomonas mendocina* 0806 from various carbon sources. *Antonie van Leeuwenhoek,* 77**,** 31-36.

Tobin, K. M. & O'Connor, K. E. 2005. Polyhydroxyalkanoate accumulating diversity of *Pseudomonas* species utilising aromatic hydrocarbons. *FEMS Microbiology Letters,* 253**,** 111-118.

Tsuge, T. 2002. Metabolic improvements and use of inexpensive carbon sources in microbial production of polyhydroxyalkanoates. *Journal of Bioscience and Bioengineering,* 94**,** 579-584.

Tuncay, M., Calis, S., Kas, H., Ercan, M., Peksoy, I. & Hincal, A. 2000. Diclofenac sodium incorporated PLGA (50: 50) microspheres: formulation considerations and *in vitro/in vivo* evaluation. *International Journal of Pharmaceutics,* 195**,** 179-188.

Unverdorben, M., Spielberger, A., Schywalsky, M., Labahn, D., Hartwig, S., Schneider, M., Lootz, D., Behrend, D., Schmitz, K., Degenhardt, R., Schaldach, M. & Vallbracht, C. 2002. A Polyhydroxybutyrate Biodegradable Stent: Preliminary Experience in the Rabbit. *CardioVascular and Interventional Radiology,* 25**,** 127-132.

Uttayarat, P., Chen, M., Li, M., Allen, F. D., Composto, R. J. & Lelkes, P. I. 2008. Microtopography and flow modulate the direction of endothelial cell migration. *American Journal of Physiology-Heart and Circulatory Physiology*, 294(2), H1027-H1035.

Vainionpaa, S., Myllynen, P., Pätiälä, H. & Rokkanen, P. 1986. Outcome of clavicular fracture in 89 patients. *Archives of Orthopaedic and Traumatic Surgery*, 105(6), 337-338.

Valappil, S., Boccaccini, A., Bucke, C. & Roy, I. 2007. Polyhydroxyalkanoates in Gram-positive bacteria: insights from the genera *Bacillus* and *Streptomyces*. *Antonie van Leeuwenhoek,* 91**,** 1-17.

Vara, D. S., Salacinski, H. J., Kannan, R. Y., Bordenave, L., Hamilton, G. & Seifalian, A. M. 2005. Cardiovascular tissue engineering: state of the art. *Pathologie Biologie,* 53**,** 599-612.

Volova, T. A. G. & Volova, T. 2004. *Polyhydroxyalkanoates-Plastic Materials of the 21st Century: Production, Properties, Applications*, Nova Publishers.

Wallen, L. L. & Rohwedder, W. K. 1974. Poly-.β.-hydroxyalkanoate from activated sludge. *Environmental Science & Technology,* 8**,** 576-579.

Walker, J. M. 2009. The bicinchoninic acid (BCA) assay for protein quantitation. *The protein protocols handbook*, 11-15. Humana Press.

Wang, F. & Lee, S. Y. 1997. Poly(3-Hydroxybutyrate) Production with High Productivity and High Polymer Content by a Fed-Batch Culture of *Alcaligenes latus* under Nitrogen Limitation. *Applied and Environmental Microbiology,* 63**,** 3703-6.

Wang, Q., Du, Y. M. & Fan, L. H. 2005. Properties of chitosan/poly (vinyl alcohol) films for drug-controlled release. *Journal of Applied Polymer Science,* 96**,** 808-813.Wang, Y. W., Wu, Q. & Chen, G. Q. 2004. Attachment, proliferation and differentiation of osteoblasts on random biopolyester poly(3-hydroxybutyrate-co-3-hydroxyhexanoate) scaffolds. *Biomaterials,* 25**,** 669-675.

Wang, Y., Ameer, G. A., Sheppard, B. J. & Langer, R. 2002. A tough biodegradable elastomer. *Nature Biotechnology,* 20**,** 602-606.

Wang, Z., Itoh, Y., Hosaka, Y., Kobayashi, I., Nakano, Y., Maeda, I., Umeda, F., Yamakawa, J., Nishimine, M., Suenobu, T., Fukuzumi, S., Kawase, M. & Yagi, K. 2003. Mechanism of enhancement effect of dendrimer on transdermal drug permeation through polyhydroxyalkanoate matrix. *Journal of Bioscience and Bioengineering,* 96**,** 537-540.

Westedt, U., Wittmar, M., Hellwig, M., Hanefeld, P., Greiner, A., Schaper, A. K. & Kissel, T. 2006. Paclitaxel releasing films consisting of poly (vinyl alcohol)-graft-poly (lactide-co-glycolide) and their potential as biodegradable stent coatings. *Journal of Controlled Release,* 111**,** 235-246.

Wilkinson, C. D. W., Riehle, M., Wood, M., Gallagher, J. & Curtis, A. S. G. 2002. The use of materials patterned on a nano-and micro-metric scale in cellular engineering. *Materials Science and Engineering,* 19(1), 263-269.

Williams, S. F., Martin, D. P. & Skraly, F. A. 2003. *U.S. Patent No. 6,548,569*. Washington, DC: U.S. Patent and Trademark Office.

Wu, R., Lamontagne, D. & de Champlain, J. 2002. Antioxidative properties of acetylsalicylic acid on vascular tissues from normotensive and spontaneously hypertensive rats. *Circulation,* 105**,** 387-392.

Yang, D. Z. & Hu, P. 2008. Miscibility, crystallization, and mechanical properties of poly(3-hydroxybutyrate) and poly(propylene carbonate) biodegradable blends. *Journal of Applied Polymer Science,* 109**,** 1635-1642.

Yang, Y.Y., Chung, T.S., Bai, X.L. & Chan, W.K. 2000. Effect of preparation conditions on morphology and release profiles of biodegradable polymeric microspheres containing protein fabricated by double-emulsion method. *Chemical Engineering Science,* 55**,** 2223-2236.

Yao, Y.C., Zhan, X.Y., Zhang, J., Zou, X.H., Wang, Z.H., Xiong, Y.C., Chen, J. & Chen, G.Q. 2008. A specific drug targeting system based on polyhydroxyalkanoate granule binding protein PhaP fused with targeted cell ligands. *Biomaterials,* 29**,** 4823-4830.

Yasotha, K., Aroua, M., Ramachandran, K. & Tan, I. 2006. Recovery of medium-chain-length polyhydroxyalkanoates (PHAs) through enzymatic digestion treatments and ultrafiltration. *Biochemical Engineering Journal,* 30**,** 260-268.

Yellore, V., & Desai, A. 1998. Production of poly-3-hydroxybutyrate from lactose and whey by *Methylobacterium* sp. ZP24. *Letters in Applied Microbiology,* 26**,** 391-394.

Yoon, J. S., Lee, W. S., Jin, H. J., Chin, I. J., Kim, M. N. & Go, J. H. 1999. Toughening of poly(3-hydroxybutyrate) with poly(cis-1,4-isoprene). *European Polymer Journal,* 35**,** 781-788.

Yu, F., Mücklich, F., Li, P., Shen, H., Mathur, S., Lehr, C.M. & Bakowsky, U. 2005. *In Vitro* cell response to a polymer surface micropatterned by Laser Interference Lithography. *Biomacromolecules,* 6**,** 1160-1167.

Yu, F., Nakayama, T., Nakamura, N., Katsumata, K., Pan, P. & Inoue, Y. 2009. Miscibility and physical properties of Poly(3-hydroxybutyrate-co-hydroxyhexanoate)/Poly(ethylene oxide) binary blends. *Macromolecular Materials and Engineering,* 294**,** 868-876.

Yu, L., Dean, K. & Li, L. 2006. Polymer blends and composites from renewable resources. *Progress in Polymer Science*, 31(6), 576-602.

Zhang, D., Gracias, D., Ward, R., Gauckler, M., Tian, Y., Shen, Y. & Somorjai, G. 1998. Surface studies of polymer blends by sum frequency vibrational spectroscopy, atomic force microscopy, and contact angle goniometry. *The Journal of Physical Chemistry B,* 102**,** 6225-6230.

Zhang, L. M. 1999. Synergistic blends from aqueous solutions of two cellulose derivatives. *Colloid and Polymer Science,* 277**,** 886-890.

Zhang, L., Xiong, C. & Deng, X. 1996. Miscibility, crystallization and morphology of poly(β-hydroxybutyrate)/poly(d,l-lactide) blends. *Polymer,* 37**,** 235-241.

Zhang, S., Feng, Y., Zhang, L., Guo, J. & Xu, Y. 2010. Biodegradable polyesterurethane networks for controlled release of aspirin. *Journal of Applied Polymer Science,* 116**,** 861-867.

Zheng Y.D., Wang, Y.J., Chen, X.F., Ren, Y.B. & Wu G. 2003. Chemical Reaction of PHBV/Sol-gel Bioglass Foams for Born Tissue Engineering in Simulated Body Fluid. *Chemical Research In Chinese Universities,* 24(7), 1328.

Zilberman, S. & Persson, B. N. J. 2002. Adhesion between elastic bodies with rough surfaces. *Solid State Communications,* 123**,** 173-177.

Zinn, M., Witholt, B. & Egli, T. 2001. Occurrence, synthesis and medical application of bacterial polyhydroxyalkanoate. *Advanced Drug Delivery Reviews,* 53**,** 5-21.